THE UNIVERSITY
of EDINBURGH

Modelling the Structural Response of Reinforced Concrete Slabs Exposed to Fire: Validation, Sensitivity, and Consequences for Analysis and Design

Mohamad Emran Baharudin

Doctor of Philosophy

The University of Edinburgh

2017

Abstract

Structural fire design represents one important aspect of the design of reinforced concrete buildings. The work presented in this thesis seeks to elucidate the structural behaviour of reinforced concrete slabs during exposure to heating from below, as would occur in the case of a building fire, with a particular focus on structural fire modelling using finite element analysis. The focus in on validating finite element models against experimental results and quantifying the sensitivity of model outputs to relevant thermal and mechanical input parameters.

A primary goal of the work is to provide recommendations to structural fire engineering analysts and designers considering the performance-based design of reinforced concrete slabs for structural fire resistance using available finite element software. A critical review of the available knowledge of the structural fire response of reinforced concrete structures in general and concrete slabs in particular is presented, along with an awareness as to the importance of understanding structural response of concrete structures exposed to fires. Current techniques for structural fire design of concrete structures are reviewed, and shortcomings highlighted. Available experimental data are presented, and various finite element models of these slabs are developed and interrogated to identify important aspects for understanding, as well as for future improvement of similar studies (both experimental and numerical) with the intention of supporting future progress in structural fire engineering, in particular as regards performance based structural fire design of concrete slabs.

A range of thermal and mechanical parameters that are potentially important and influential in the structural fire design of reinforced concrete slabs is then studied, including: fire scenario, thermal properties of materials (thermal conductivity and specific heat), heat transfer parameters (coefficient of convection and emissivity) and assumptions, restraint conditions at the supports, variations of span-to-depth ratio, reinforcement detailing, as well as plan aspect ratio are all investigated; their influence on the structural fire response of reinforced concrete slabs is studied and discussed.

A key issue in validating finite element models against experimental results lies in defining the temperature inputs to the structural finite element models correctly. Variation of available thermal and mechanical input parameters, as recommended in Eurocodes, influences the predictive performance of thermal and structural finite element models, however these are not the main contributing factors in obtaining a credible prediction of response from the finite element models. The most challenging aspect in performing heat transfer analysis for fire furnace tested reinforced concrete slabs lies in defining the correct thermal boundary condition.

For simply supported one-way spanning and two-way spanning slabs, increasing slab's thickness (lowering span-depth ratio) does not improve fire resistance rating for the slabs when both limiting deflection criteria and limiting tensile plastic strain are set as acceptance criteria. Two-way slabs with higher span-depth ratio have better fire resistance ratings, judging from the overall trends and magnitudes of mid-span deflections. The formation of plastic hinges is likely to occur for one-way spanning slabs modelled with finite rotational spring stiffness at supports, but not for two-way spanning slabs. A yield line mechanism in two-way slabs means that the behaviour is more complex as compared to the simple flexural mechanism for one-way slabs. In one-way slabs, plastic hinges potentially occur at the location where top reinforcement is curtailed, highlighting the importance of properly understanding the nuances in response of concrete slabs in fire.

Investigation of the influence of aspect ratio in two-way spanning slabs confirms that slabs with lower aspect ratios have better structural fire resistance than slabs with higher aspect ratios when both limiting deflection criteria and limiting tensile strain in reinforcing steel were used as the performance indicators.

A combination of both limiting mid-span deflection criteria as well as limiting tensile plastic strain is recommended for specifying acceptance criteria for both one-way and two-way slabs, since it gives more accurate and comprehensive assessment on the structural response of the slabs under exposure to severe heating from below.

Acknowledgement

This research would have had not been smooth without the guidance from my supervisor, Luke Bisby. Thanks for helping me put everything in perspective. Thanks also goes to my co-supervisor, Tim for the supports either directly or indirectly throughout the course of the research.

My wife, Ayu and daughters Areesya, and Adelia for being there whenever I needed them the most. This journey would have had been really difficult without your patience and understanding. Special thanks to my parents for your understanding and encouragement for me to pursue my dream.

To all friends in John Muir, in particular Xu, Jamie, Ieuan, Daryan, Mohamed, Zaid, Farian and Zafiris who have made my time here in Edinburgh full of joy and happiness.

All fellow Malaysian friends, Anas, Aiman, Adib, Sofwan and Aizi who made me feel like close to ‘home’.

Last and not least, the government of Malaysia for providing the sponsorship.

Declaration

This thesis and the research described within have been completed solely by Mohamad Emran Baharudin under the supervision of Prof Luke A. Bisby and Dr Tim J. Stratford. Where others have contributed or other sources are quoted, references are given.

Mohamad Emran Baharudin

September, 2017

Publications

JOURNAL PAPERS

Wang, Y., Bisby, L.A., Wang, T.Y., Yuan, G., and Baharudin, E., (2018). Fire Behaviour of Reinforced Concrete Slabs under Combined Bi-axial In-plane and Out-of-plane Loads. *Fire Safety Journals*.

CONFERENCE PAPERS

Baharudin, E., Bisby, L.A., and Stratford.,(2016). Modelling The Response of Simply-Supported Two-Way Reinforced Concrete Slabs Exposed to Fire. *Key Engineering Materials*, (711), 588-595.

Baharudin, E., Rickard, I., Bisby, L.A., and Stratford,T.,(2017). Modelling Reinforced Concrete Slabs in Furnace Tests: Validation and Sensitivity to Input Parameters. *Proceedings of 2nd International Fire Safety Symposium*, Naples, Italy, 695-702.

Table of Contents

Table of Figures

Table of Tables

Chapter 1:
Introduction

1.1 Background to the project

Performance based structural fire engineering analysis and design has advanced by leaps and bounds in the past two decades (Buchanan and Abu, 2017). The development of advanced finite element models for both heat transfer analysis and full structural response, combined with ever increasing computing power, has made structural fire modelling a realistic opportunity in structural design offices (Gillie et al., 2012). This has been particularly evident in the structural fire design of steel-framed structures, thanks to a large amount of research (both experimental and computational) on this topic. Major improvements in understanding have been achieved for the fire performance of steel structures in both standard (Cooke and Latham, 1987; Lange and Boström, 2017) and non-standard (British Steel, 1998; Kotsovinos, 2013) heating conditions. However, similar achievements and advancements are not as clear for the case of concrete elements and concrete structures.

The behaviour of reinforced concrete elements under exposure to fire is highly non-linear. In that regard, finite element methods have become an indispensable tool in studying the behaviour of concrete elements (and structures) at elevated temperature. Understanding the capabilities and limitations of the available finite element packages with respect to their element formulations and constitutive material model formulations is crucial for analysts and designers, since individual packages have their own advantages and disadvantages, material models, and specific analysis approaches. In the current thesis, ABAQUS (both implicit and explicit dynamic) is selected as the primary finite element analysis package for assessment of the capability, variability, and sensitivity of finite element methods at predicting behaviour of reinforced concrete slabs under exposure to fires. Finite element packages LS-Dyna and SAFIR are also sparingly used herein for comparisons.

The level of confidence in the use of finite element model predictions is typically gauged by the capability of the model to predict experimental results, normally with a focus on reproducing the load versus deflection paths observed under sustained loads during a standard furnace test. The process is typically termed as validation, which is

normally carried out to claim that the developed finite element model is producing a reasonable prediction and is capable of predicting the same behaviour as was witnessed during the furnace tests. Therefore, the availability of high fidelity experimental test data is crucial to the development of better understanding of the structural behaviour of reinforced concrete slabs under exposure to both standard and realistic fires. The study presented in this thesis was initiated to explore the available experimental test data from tests on full scale reinforced concrete slabs (both one-way and two-way spanning) within the research and testing literature, and consequently to develop and assess finite element models of these slabs and their results and compare their predictions against those from the experiments. In this way, the goal of this thesis is to provide guidance to structural fire analysts and designers in the application of advanced finite element models to the structural fire design and assessment of reinforced concrete structures, with an emphasis herein on horizontal slabs in bending (or membrane) action.

Besides comparing the finite element model results against the available experimental test data, current codes of practice i.e. The *Structural Eurocodes* (CEN, 2005a, 2005b, 2004, 2002a, 2002b) and design manuals, for instance *Structural Fire Protection: Manual of Practice by American Society of Civil Engineers* (ASCE, 1992), recommend a range of possible material thermal and mechanical input properties for implementation in finite element models. However, to the knowledge of the author, no exhaustive studies have yet been conducted or presented methodically examining the sensitivity of these variations of model input material parameters on the predictive performance of available structural fire finite element models. It is also acknowledged that concrete in particular poses complex material properties both for thermal and mechanical (both in tension and compression) properties. Available numerical studies, for instance Huang et al. (2003, 2001); Lim et al. (2004) have only presented results from using *presumed as validated* finite element models, with no further details or justification on the selected material properties or their sensitivity for the predictive performance of the models. Quantification of model sensitivity is a necessary first step towards the widespread use of finite element modelling for performance-based assessment and design of reinforced concrete slabs in the future.

In the context of preparing structural designs of reinforced concrete slabs for fire performance, available knowledge to guide designers in providing an optimum and efficient design is still lacking. As the design of cast in-situ reinforced concrete buildings typically involved varying the geometrical configuration of the element under consideration i.e. thickness, width, and span, detailed studies looking at the consequences of varying these parameters for the output fire resistance rating (and real structural response) is potentially important to aid structural fire engineers in providing the best possible (optimum and economical) design solution conforming to the performance-based structural fire engineering design code.

Against the above background, the research presented in this thesis aims to investigate aspects of validation of finite element models of reinforced concrete slabs, together with sensitivity studies on thermal and mechanical input parameters, on the predictive performance of the models. In addition to these aspects, the structural behaviour of fire exposed reinforced concrete slabs under various configurations, designed to the relevant Eurocode (CEN, 2005a, 2004, 2002a) is studied and presented.

1.2 Objectives

The primary objectives of the research presented in this thesis are to aid further understanding on structural behaviour of both one-way and two-way reinforced concrete slabs under exposure to fires. By using the finite element approach, implemented via a range of commercially available finite element software packages, the specific goals of the research are:

a) to identify the key aspects that are important in validating finite element models against results from furnace tests on reinforced concrete slabs, and to highlight problems with furnace testing in terms of its usefulness for validating models of full structure reinforced concrete response to fire;
b) to study the sensitivity of model predictions to variation of recommended material thermal and mechanical properties that are given within relevant codes of practice and design manuals for the predictive performance of available finite element modelling software, and therefore to provide best practice

guidance to designers regarding material thermal and mechanical input parameters (for both one-way and two-way spanning reinforced concrete slabs);

c) to assess effects of varying design input configurations (i.e. restraint, span-to-depth ratio, etc.) on the structural fire response and performance of concrete slabs designed in accordance with Eurocode recommendations; and
d) to provide guidance to designers on suitable acceptance criteria to be applied when undertaking performance based design, using finite element modelling, of reinforced concrete slabs for fire, in light of approaches currently used to assess the structural 'fire resistance' of reinforced concrete slabs in practice.

1.3 Novelty and research significance

Outcomes from the current study provide information on a range of issues that are relevant to validating finite element models against experimental fire furnace tests of reinforced concrete slabs exposed to severe heating from below. Reasons as to why the low level of confidence on the predictive performance of finite element models, sensitivity of varying the available concrete material mechanical and thermal properties to the response predictions, as well as acceptance criteria are among issues that limits the wider application of finite element models for the analysis and design of reinforced concrete slabs under exposure to fires. Such detailed studies are very limited (thanks to in-depth studies presented by Khazaeinejad (2015)), and the resulting research outcomes provide crucial guidance to designers seeking to undertake performance based structural fire design of reinforced concrete structures (particularly cast-in-place concrete). Instead of showing the validated finite element models, without further justification as regards the selected both thermal and mechanical input parameters available within both code of practice and design manual (as is normally the case in the available literature), the current study presents and explores the sensitivity of the range of possible thermal and structural material input parameters on the predictive performance of the finite element models. In addition, the performance of the slabs under specific ranges of possible conditions that the slabs might be designed and constructed for are further investigated so as to elucidate best

practice for structural fire modellers. The conditions, such as the restraint condition at the supports, the steel reinforcements' curtailment length, and the slab span-to-depth ratio and aspect ratio, are investigated.

The intention is to generate practical information and guidance to structural fire engineering practitioners in general, as well as guidance for researchers to a certain extent in performing analysis and design work. Since an in-depth study with the depth and breadth presented here is not typically feasible (due to time and financial constraints) within practical structural fire engineering consultancy practices, it is intended that the information provided in this thesis can aid fire engineers to speed up the design process and tackle more critical issues in providing the best possible engineering design solutions, conforming to performance-based structural fire engineering design functional objectives.

1.4 Outline of thesis chapters and appendices

The above objectives are accomplished via research work presented over the following 5 chapters. An outline of this thesis is as follows:

Chapter 1 – Introduction

Chapter 1 provides a brief description of the research work presented in this thesis. An explanation of the research novelty and significance, aims, methodology, and finally thesis structure are presented to give an overview of the work.

Chapter 2- Reinforced concrete structures design for fire: an overview

Chapter 2 presents a literature review, beginning with a review of the objectives of structural fire engineering within the design of the built environment. Consequences and damage cause by fire events in reinforced concrete buildings around the world are reviewed. Current knowledge in implementing the structural fire design of reinforced concrete buildings as well as slabs are discussed. Performance criteria specified by the relevant codes of practice are compared against each other and discussed. Available studies, both experimental and numerical, aimed at understanding the full structure and

concrete slab's behaviour are reviewed. The final section presents constitutive formulations of material properties for implementation into finite element models, as well as analytical models. The chapter ends by summarising the research gaps identified by this review of the literature, and hence motivating the research presented in this thesis.

Chapter 3 – Finite element modelling of one-way reinforced concrete slabs exposed to severe heating from below

Chapter 3 presents computational studies aimed at validating finite element models against experimental tests available in the research literature for the case of one-way spanning, simply supported reinforced concrete slabs. Important aspects that need to be considered in order to make future studies beneficial are presented. The sensitivity of model predictions to variation of heat transfer parameters (e.g. coefficient of convection and emissivity), material thermal input properties (conductivity and specific heat), as well as mechanical input parameters (concrete tensile strength, fracture energy, and coefficient of thermal expansion) is also presented and discussed.

Chapter 4 – Parametric studies on one-way reinforced concrete slabs exposed to severe heating from below

In Chapter 4, the studies presented in Chapter 3 are extended. The structural behaviour of one-way slabs under different configurations is investigated and presented. Effects of different fire scenarios, restraint conditions at supports, reinforcement curtailments, and span-to-depth ratios on the structural behaviour of the slabs under exposure to severe heating from below are investigated and presented.

Chapter 5 – Finite element modelling of two-way reinforced concrete slabs exposed to severe heating from below

Chapter 5 presents similar studies as presented in Chapter 3, however two-way reinforced concrete slabs are considered rather than on-way slabs. Parameters studied include concrete tensile strength, fracture energy, as well as coefficient of thermal expansion.

Chapter 6 – Parametric studies on two-way reinforced concrete slabs exposed to severe heating from below

Chapter 6 presents an extension of the studies given in Chapter 5, wherein the structural behaviour of two-way slabs under exposure to fires under different fire scenario, restraint condition at support, reinforcement curtailment's length, span-to-depth ratio, and aspect ratio is investigated and discussed. Contrary to the studies presented for the case of one-way slabs in Chapter 4, additional parameters, which are relevant to the design of two-way slabs i.e. aspect ratio, are included for investigation.

Chapter 7 – Conclusions and further work

Chapter 7 summarises key findings from the work presented in this thesis, and conclusions are drawn. Key recommendations for structural fire analysts and designers are proposed. Finally, further work to enhance knowledge in the field of structural fire engineering of reinforced concrete structures, and concrete slabs specifically, is suggested.

Chapter 2:
Reinforced concrete structure design for fire: an overview

2.1 Structural fire engineering

Structural fire engineering is a discipline of knowledge that deals with an understanding of how elements response structurally under exposure to fires. Within the context of built environment, this understanding is important in ensuring structural designers produce a design that can provide adequate fire resistance for a specified period of fires, thus ensuring safe evacuation of people from the building under consideration.

Structural fire resistance of a building is generally defined within temperature domain (ASTM, 2015; International Code Council, 2009). Fire resistance of structural elements or frames is defined with the temperature as the controlling parameter i.e. as long as temperatures at the location under consideration does not exceed the limiting temperatures, the structural element or frame is said to have adequate fire resistance. On the other hand, understanding the structural response is very limited and research in this is still ongoing. Holistic understanding, that takes into consideration both temperature domain and structural response in prescribing structural fire resistance of reinforced concrete buildings is important so that the flexibilities in performance-based structural design codes can be explored.

Most design guides are formulated such that evolution of temperatures in concrete elements and/or reinforcing steels are limited to certain magnitude and if these temperatures are not exceeded, the concrete elements are considered as having adequate fire resistance. This method (limiting temperature, for instance critical temperature of 593 ℃ (ASTM, 2015)) is correct, founded on sound technical knowledge available within structural fire engineering community and performs satisfactorily. From a different perspective, these guides are recommended since available knowledge is not sufficient to provide suggestions beyond these criteria. As the design of reinforced concrete building structures is becoming more complicated i.e. more complex shapes, thinner structural elements, and using high strength material, better understanding on how concrete elements behave structurally at elevated temperatures is becoming more crucial (Gales, 2013). In other words, it is of the author's opinion that prescribing certain limit on maximum temperatures might not be

a desirable criteria as obviously thinner elements are heated quicker thus having less fire resistance rating.

As compared to other disciplines of knowledge, structural fire engineering is considered relatively young, thus more knowledge and understanding are required. Significant progress, however has been achieved in the past two decades. In addition, structural fire engineering has gained popularity more than ever since the introduction of performance-based codes. Rather than setting out a prescriptive guidance for a design exercise, performance-based code sets out pre-set objectives thus offering flexibilities in the method or approach in preparing the design.

In the event of fire in a building, slabs are exposed directly to fires. The ability of concrete slabs to retain their integrity is very crucial in ensuring fire resistance of the whole building. Numerous literature (Gillie et al., 2004; Huang, 2010; Huang et al., 2003a; Lim et al., 2004b) which studied the behaviour of reinforced concrete slabs have shown that reinforced concrete slabs have better fire resistance than estimated using conventional yield line theory. This is achieved through the slabs behaving as tensile membrane action. Initial studies by author and reported in Baharudin et al. (2016) also explicitly demonstrated that the two-way reinforced concrete slab was able to sustain imposed load even the criteria of critical rebar temperature by ASTM (2015) i.e. 593°C has been well exceeded.

2.1.1 Design for life safety

Main objective in structural design for fire is to ensure life safety of the people. This should be treated at the utmost importance with respect to structural performance of a building among other criteria. Unfortunately, current knowledge available within structural fire engineering community is not matured enough to be able to predict collapse of concrete building structures. More often than not, fires in concrete buildings can last for several hours without collapse; Andraus Building and Joelma Building (Crefisul Bank), both in Sao Paolo Brazil (Beitel and Iwankiw, 2005) but in some occasion, collapse of a building occurred very quickly, for instance, the fire occurrence at the 19-storey Apartment Block in St. Petersburg, Russia. The building suffered collapse in just 1 hour of a fire event (Lakhani et al., 2016).

These fire events demonstrate the lack of understanding on how concrete buildings response structurally under fire load. In the design, focus was given to controlling fire spread with compartmentation method, and protecting steel reinforcement against certain temperatures, which then were thought to be sufficient. With collapse being unpredictable, it further highlights the lack of holistic understanding on behaviour of reinforced concrete structures during fire events. Apparently, more studies are required to better understand the structural fire response of reinforced concrete buildings under fire exposure.

2.1.2 Design for property protection

In addition to ensuring life safety of the people, the objective for structural fire design of a building is also to protect properties against irreparable damage to ensure the building can still serve its design purpose. In contrast to the design for life safety, design for property protection attracts stakeholders to invest money for the studies and research related to structural fire engineering. For instance, insurance company seems to benefit the most with the advancement in the knowledge of fire safety engineering of building structures. Critical and credible evaluation of structural integrity of concrete buildings during post-fire events is very important in the decision making within an insurance company. Either the building is still fit for occupancy or no longer safe, it is a decision that a structural fire engineer must make and consequently advising the insurance company on the issue.

Even though research on residual strength of concrete elements is still ongoing, it is believed that current available knowledge is not mature enough to provide an accurate assessment on the integrity of buildings during post-fire events. It is true given the nature of damages resulting from fire events, which are sometimes not physical in nature. Spalling and cracking for instance, are physical damages to the concrete elements and are slightly easier to be assessed whereas if the concrete is still intact, it is extremely difficult to assess what would be the residual strength left in the concrete after a certain period of fire events. This is important for structural fire engineers to evaluate whether the residual strength is enough for the building to continue its design life.

Buchanan and Abu (2017) described the importance of structural fire design for property protection as being the possibility of business losses, irreplaceable of heritage values. With all the above statements, it is acknowledged that even though fire is considered as a rare occurrence, losses due to fire events might potentially be the one that is irreplaceable, and therefore initial investment (financial) on the appropriate fire protection studies and strategy is a worth investment.

2.2 Fire events on concrete buildings

The level of importance in specifying fire safety design strategy typically depends on the purpose and usage of the buildings. For example, in a small occupancy type of buildings e.g. residential-type buildings, fire escape route and preventive measures so that fires will not spread to neighbouring houses are always thought as sufficient fire safety design strategy. Structural performance of the buildings during fire is thought to be of secondary importance.

In contrast, for commercial, multi-storey buildings, fire occurrence is an important issue for many. Obviously, potential losses, in terms of life and economic are tremendous as compared to fires in small residential buildings. A historical survey conducted by Beitel and Iwankiw (2005) that listed a total of 9 cases of multi-storey concrete buildings engulfed in fires found that out of all nine (9) cases, seven (7) are categorised as fire-induced collapse. The survey covers events from 1970 to 2002. Malhotra (1978) also conducted a survey and listed several noteworthy fire events on concrete buildings from 1968 to 1974.

Table 2.1 lists fire events compiled from several sources (Beitel and Iwankiw, 2005; Lakhani et al., 2016; Malhotra, 1978; Meacham et al., 2010; Papaioannou, 1986). Some of the buildings suffered total collapse and partial collapse while the rest suffered severe damage without collapse. Following the events mentioned, lack of comprehensive understanding on the behaviour of concrete structures in fire is obvious.

Table 2.1: Some notable fire events on concrete buildings from 1967-2008 compiled from Beitel and Iwankiw, (2005); Lakhani et al. (2016); Malhotra (1978); Meacham et al. (2010); Papaioannou (1986)

No.	Date	Building name	Location	Notes on extent of damage, collapse
1	13-Mar-08	Faculty of Architecture Building, TU Delft	Delft, Netherlands	Partial collapse. Building destroyed by fire
2	12-Feb-05	The Windsor Tower	Madrid, Spain	Partial collapse with extensive slab collapse above the 17th floor. Building destroyed by fire
3	27-Nov-04	Underground car park, Gretzenbach	Gretzenbach, Switzerland	Collapse of ceiling slab and seven firefighters died
4	June, 2002	Apartment block	St. Petersburg, Rusia	Total collapse
5	February, 2002	Jackson Street Apartments	Hamilton, Ontario, Kanada	Partial collapse of concrete floor-ceilings
6	Sept, 2001	Pentagon	Washington, DC, USA	Partial collapses of floors and members
7	July, 2000	Textile factory	Alexandria, Egypt	Total collapse
8	May, 1987	CESP, Sede 2	Sao Paolo, Brazil	Partial, full height interior core collapse
9	Dec, 1980	Katrantzos Sport Department Store	Athens, Greece	Partial collapse of 5 to 8th floor, together with various other members, during a 2-3-hour fire
10	Feb, 1974	Joelma Building (Crefisul Bank)	Sao Paolo, Brazil	Minor damage to load bearing members, 12th floor concrete badly spalled. After repair, building was declared structurally safe
11	July, 1973	Military Personnel Record Centre	Overland, MO, USA	Roof and supporting columns partially collapse 12 hours after fire began
12	Feb, 1972	Andraus Building	Sao Paolo, Brazil	Spalling of exterior walls, joists and columns, exposing reinforcing
13	23-Jan-71	Linde Factory	Mainz, Germany	Three connected buildings. Progressive collapse of Building 2 and half of Building 1 was destroyed by the fire. Failure of columns: (1) Buckling due to extra load from next floor (2) Thermal expansion of beams caused shear failure
14	11-Feb-69	Co-op Store	Lincoln, UK	Extensive repair after the fire. 60% of floor slabs replaced. Building back in use in 1970
15	23-Feb-68	Avianca	Bogota, Colombia	Spalling on slab's soffit and columns. Large deflection on one way slab. 10% of floors need replacement
16	19-Oct-67	Kellogg Factory	Manchester, UK	Not sufficient shear reinforcement in beams caused beam disintegrated due to the fire. Shear crack in columns witnessed. Repair carried out after the fire

From the events listed in Table 2.1, numeral casualties (no exact figure reported) reported during fire events at Joelma Building, Sao Paolo in 1972. Besides casualties, all fire events listed above suffer significant fire damages and consequently property losses.

2.3 Fire scenario for structural design

2.3.1 Standard fire

Standard fire commonly refers to ISO 834 (ISO, 1999) fire. Similar temperature-time curve is specified in Eurocode 1 (CEN, 2002a), denoted as 'standard temperature-time curve' in clause 3.2.1. Also relatively similar fire environment specified in the US, which refers to ASTM E119 (ASTM, 2015).

'Standard temperature-time curve' is the control of temperatures adopted while performing 'standard fire test'. During the test, samples are loaded to their anticipated designed service load and subsequently heated to furnace environment where temperatures in the furnace are controlled in accordance to the 'standard temperature-time curve'.

Even though the whole idea of standard fire test is to attempt to produce the worst fire environment that an element might experience during its design life, its reliability is questioned in recent years by a few researchers, for instance, Maluk et al. (2016); Rickard et al. (2015); Bisby et al. (2013) and Law (1981). The argument relies on the lack of quantification, repeatability and more importantly, uncertainty within different furnace environment that is difficult to characterise. However, researchers are generally in agreement that standard fire is useful for comparative testing and benchmarking (Bisby et al., 2013).

Simple fire curves, that do not take into account factors such as fuel load, ventilation, and other relevant factors are for example ISO 834 (ISO, 1999), ASTM E119 (ASTM, 2015), and Hydrocarbon (CEN, 2002a). A rather more rational approach, that takes into consideration factors such as fuel load, ventilation, and other relevant factors is Parametric Fire (CEN, 2002a). In general, design fire scenario for structural design

can be categorised into three (3) broad categories namely compartment fires, localised fires, and travelling fires. Travelling fire is the latest introduction to the fire 'family' and research on this topic is actively ongoing within research community.

2.3.2 Non-standard fires

A comprehensive review of large scale, non-standard structural fire tests has been published by Bisby et al. (2013). Non-standard fire tests conducted globally for the past three decades have been reviewed by the authors. Emphasis has been put on the issues that have been studied and general conclusion drawn from the tests. The motivation behind the review is the fact that structural fire engineering community is in agreement that elementary test of samples exposed to standard fire (ASTM, 1985; ISO, 1999) does not represent realistic condition in buildings. In addition, fire environment provided by the standard gas temperature in a furnace is merely far from replicating the actual fire exposure experienced in buildings.

2.4 Method for design

Discussion on the design of concrete structures for fire can be broadly focused into two; (1) full frame response, and (2) single element response. Full frame design is relatively complex in nature. The complexities ranging from defining appropriate fire scenario or fire environment to performing structural analysis. In addition, performing design for full frame structures requires huge computational resources. Currently, studies on full frame behaviour (either computational or experimental method) are very limited, which then limits the progress of performing full frame design of reinforced concrete structures among practicing fire engineers. More studies are required to improve understanding and raise the level of confidence in the design within structural fire engineering community.

In general, approaches in the design (applicable to both full frame and elemental design) are; (1) temperature as the domain (2) structural response as another domain or as performance indicator.

2.4.1 Temperatures

It is well documented in literatures that concrete and steel reinforcement lose strength as temperature increases. Within temperature domain, the designed element is said to have sufficient fire resistance as long as the elements are protected against certain value of temperatures. For concrete slabs, temperature at the surface unexposed to fires is limited to 139 °C (ASTM, 2015) and steel reinforcement temperature at 593 °C (ASTM, 2015).

In addition, simplified calculation method based on reduced cross-section recommended in Eurocode 2 (CEN, 2004) suggests that sections where temperature is more than 500 °C will not be considered in the calculation for load-bearing capacity.

Evolution of temperatures within concrete element can be obtained either through heat transfer analysis or simply using tabulated temperature data available within the respective design codes or reported within literatures. These temperatures are normally compiled from available and credible experimental results.

2.4.2 Structural response

Designing with structural response as the performance indicator is slightly more complicated than only concentrating on temperatures as the domain. When heated, concrete and steel reinforcement expand and this expansion introduces additional load to be resisted at support whenever this expansion is restrained. In continuous elements, redistribution of moment occurs as the heated slab at mid-span deflects due to fire exposure from below. All of these require better understanding on how elements response when heated and good knowledge in structural mechanics.

Unfortunately, progress in the understanding of structural response of continuous concrete element is rather slow. The main reason being lack of motivation to pursue studies in structural behaviour of concrete structures as compared to steel or steel composite structures. Being a non-combustible material and low thermal conductance have made people to believe that concrete has superior fire resistance. Economic driver

is also lacking with respect to pursuing studies on reinforced concrete structures as opposed to steel or steel composite structures.

More than four (4) decades ago, significant works have been conducted by a few researchers (Gustaferro, 1976; Issen et al., 1970; Salse and Gustaferro, 1971; Selvaggio and Carlson, 1967) in the attempt to understand how continuous concrete elements behave during fires, with regard to existence of restraint at support. Since then, the direction has shifted and focus was given more on understanding membrane action in concrete slabs. On the other side, focus was also given towards steel or steel composite structures, with economic reason being the driver.

Level of confidence in the design of full frame reinforced concrete structures under fire exposure is still low. Several reasons contributing to this; (1) lack of comprehensive understanding on concrete material behaviour at elevated temperatures, (2) requires advanced computational method thus demanding huge amount of computational resources and (3) relatively less studies conducted so far to understand structural behaviour of reinforced concrete structures as compared to steel and composite structures.

2.5 Design for flexure

This work will only concentrate on the design of elements resisting load (gravity load) normal to the plane or specifically slabs. Design of members resisting axial load i.e. columns will not be covered as it is outside of the scope of the current work.

2.5.1 One-way slabs

Some of the studies reviewed in this section are about designing reinforced concrete beams. Since the design approach for one-way slabs is in general similar to reinforced concrete beams, the presented information is assumed also applicable to one-way slabs.

For simply-supported slabs, flexural capacity of a member is evaluated as reduced when strength in tension reinforcement decreases as temperature increases. Sectional analysis typically focuses on positive moment (sagging) capacity only as there is no

moment redistribution. Contribution of compressive strength capacity in the top of slab section also reduces as temperature increases. Selection of reduction factor for material strength can be either following recommendation from Eurocode (CEN, 2005, 2004) or from Structural Fire Protection Manual by American Society of Civil Engineers (ASCE) (ASCE, 1992). Designing simply-supported members is relatively straightforward as compared to continuous members where the supports are restrained against translational and/or rotational displacements.

During fire exposure, redistribution of moment occurs in multiple-span slabs (continuous). As the bottom of slab is heated, positive moment (sagging) at mid-span reduces and negative moment (hogging) at support increases. This shifting of moments generally improves fire resistance of the slabs, which also explains why continuous reinforced concrete slabs or beams are thought to have better fire-resistance rating. Note that this behaviour is a result of hotter section at the slab's bottom and relatively colder section at its top.

Continuity introduces thrust or axial restraint at slab's support and the existence of this thermal thrust, which acts similarly to pre-stressing forces in a pre-stress concrete slab increases positive moment (sagging) capacity (ASCE, 1992). Structural Fire Protection Manual by ASCE (ASCE, 1992) lists step-by-step procedures to calculate structural fire capacity of continuous slabs. The approach can be briefly described as determining the magnitude and location of this thrust and thereafter performing check whether the surrounding colder elements able to provide the required thrust, both in terms of magnitude and location. The relationship between thrust, strain, and *Z'* are represented by a nomogram proposed by Issen et al. (1970), reproduced and shown in Figure 2.1 below. $Z' = A/s$ where *A* is the cross section and *s* is the 'heated perimeter' of the portion of the perimeter of the cross section resisting the thrust exposed to fire (ASCE, 1992).

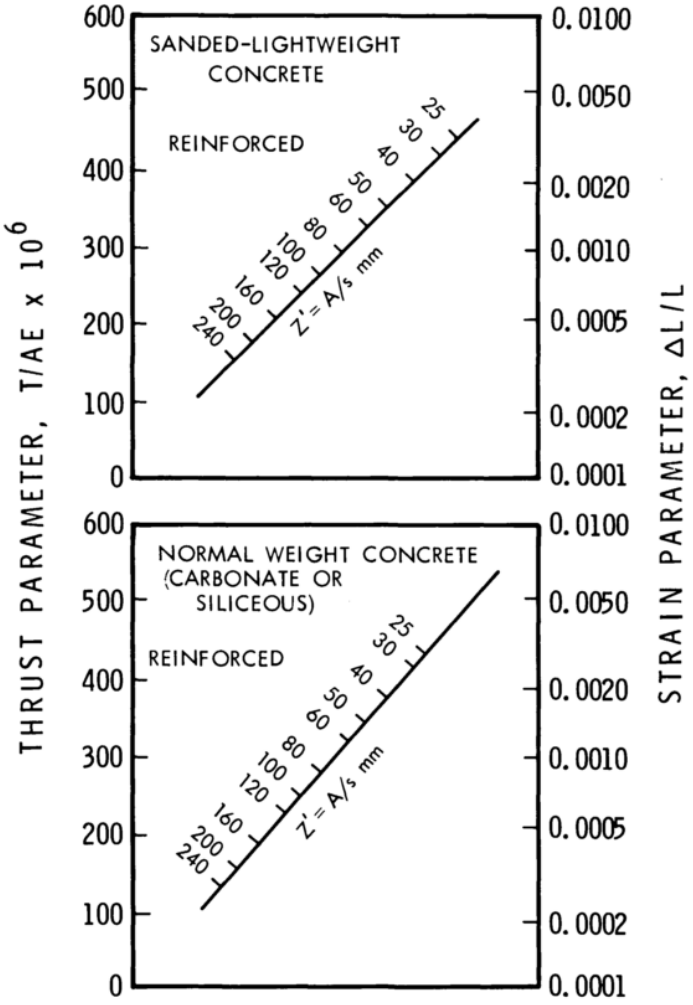

Figure 2.1: Nomogram relating thrust, strain, and Z' ratio, reproduced from Issen et al. (1970)

Method of calculation described above lies on the concept of axial thrust provision, acting at different location within the slab's depth, which in turn is thought as improving structural fire capacity of reinforced concrete slabs. This concept has become the motivation and led to the extensive studies by Lim (2003). The effect of axial spring stiffness acting at different depths at support on the performance of one-way reinforced concrete slabs has been studied by the author (Lim, 2003). However, it was found that the influence of rotational spring stiffness at support has not been investigated so far. The research at hand will attempt to look at this aspect and this will be presented in a later chapter of the thesis.

Salse and Gustaferro (1971) proposed an analytical solution to predict structural capacity of concrete beams both for the case of simply-supported and continuous. Collapse was thought to occur with three (3) locations of plastic hinges for the case of continuous beam and one (1) location for the case of simply supported. Two (2) at each support and one (1) at mid-span for the case of continuous beams. For simply supported case, plastic hinge would only occur at mid-span. In this method, the authors (Salse and Gustaferro, 1971) approached the problem by pre-determining the axial forces resulting from restraint thermal expansion. This axial forces can be obtained from readily available data during that time with regard to thermal expansion, concrete strength, as well as temperature distribution within concrete (Salse and Gustaferro, 1971). Although not realistic, the main intention was to explain the collapse mechanism of both simply-supported and continuous beam construction and thereafter calculating the flexural capacity of concrete beams exposed to fires.

Derivation of the above method also neglects the contribution of compressive reinforcement at top. To further complicate the problem, provision of top reinforcement in an actual practice typically curtailed at certain length for economic reason. This in turn, will affect the location of possible plastic hinges. Length of top reinforcement is estimated to provide enough bonding strength required so that the load is smoothly transferred and the designed capacity for both flexure and shear can be achieved. These aspects will be examined in the current study and presented in a later chapter of this thesis.

2.5.2 Two-way slabs

While design for one-way slabs is based on the simple flexural theory, design for the case of two-way slabs is in general based on plate theory. The classical yield line theory used for ambient design is extended for application in the design at elevated temperatures. The only difference is the degradation of material strength is taken into consideration. Throughout duration of fire exposure, flexural capacity of slabs is reduced due to the degradation of steel reinforcement strength.

Over time, as mechanism of membrane action is found to have significant influence on the structural response of two-way concrete slabs, considerable amount of research

has taken place. It is thought that application of the only yield line theory for the design of slabs at elevated temperature is not accurate, as the membrane behaviour of slabs is not taken into consideration. Some notable studies with regard to this area are Abu et al. (2013); Bailey (2004); Usmani and Cameron (2004); Wang et al. (2015). Membrane action in concrete slab is not new. It has been studied by Vecchio and Tang (1990) for the case of slab at ambient temperature.

Research on this area is still actively ongoing. Predicting limit load carrying capacity of two-way reinforced concrete slabs under exposure to fire remains a challenge. Most studies demonstrate that the inclusion of membrane action (specifically tensile membrane action) produce better prediction than the classical yield line theory. However, more experimental results are needed for validation purposes.

2.6 Criteria for evaluating structural performance of concrete slabs

Within structural fire engineering community, there is still an open discussion among the community on how to define failure for structural elements under consideration. There is no definite answer to this yet. As has been a common discussion among the community, Law (2010) in his studies explains failure with the following parameters, (1) deflection, (2) temperature and (3) excessive steel rebar strain. Deflection in general is referred to as runaway type of deflection. It is extremely important to have a clear agreement on what can be termed as 'failure' for concrete elements before one can claim his/her design has satisfied the structural fire resistance criteria.

Fire resistance rating in accordance to ASTM E119 (ASTM, 2015), BS 476-20: 1987 (BSI, 1987), and Eurocode 2 (CEN, 2004) are discussed in the following Section 2.6.1, Section 2.6.2, and Section 2.6.3 respectively. In general, the specifications are based on limiting temperature criteria as well as deflection criteria. Findings from the current body of work (presented in Chapter 3, Chapter 4, Chapter 5, and Chapter 6) have suggested that limiting deflection criteria of $L/20$ (BSI, 1987) does not give any physical meaning with regard to fire resistance rating of both one-way and two-way reinforced concrete slabs exposed to fires from below. In other words, the limiting deflection i.e. $L/20$ (BSI, 1987) does not indicate structural failure of the slabs. Instead, runaway type of deflection provides more realistic structural fire resistance

rating as it indicates the lack of equilibrium for the slabs under consideration. Results presented later in Chapter 3, Chapter 4, Chapter 5, and Chapter 6 will discuss more about both limiting deflection criteria i.e. $L/20$ (BSI, 1987) and runaway type of deflection whenever discussion about failure is made.

2.6.1 ASTM E119 (ASTM, 2015)

Fire resistance test of concrete slabs in accordance to ASTM E119 (ASTM, 2015) specifies two (2) criteria in defining performance of the slabs under fire exposure. These are based on critical steel temperatures, being 593°C (1100°F) and the temperature at the surface unexposed to fires not exceeding 139°C. Both conditions shall be met to fulfil condition of acceptance in the code.

2.6.2 BS 476-20:1987 (BSI, 1987)

BS 476-20:1987: Fire tests on building materials and structures- Part 20: Method for determination of the fire resistance of elements of construction (general principles), specifies the assessment of fire resistance is divided into three (3) criteria; (1) load bearing capacity, (2) integrity, and (3) insulation. With regard to insulation criteria, the element is said to have failed insulation criteria if the mean temperature at the unexposed surface has increased more than 140°C above its initial temperature.

Load-bearing capacity is reflected by the deflection behaviour of the slabs. The code specifies that the limiting deflection criteria of horizontal elements to be either $L/20$ or the rate of deflection (in mm/min) exceeds $L^2/9000d$, whichever comes first. However, the rate of deflection $L^2/9000d$ shall only apply after the deflection criteria of $L/30$ was exceeded. L is the clear span while d is the distance from the top of the structural section to the bottom of the design tension zone (in mm).

For the case of one-way slab tested by Cooke (2001), $L/20$ translates to 225 mm deflection while slab tested by Rickard et al. (2015) is 204 mm. If the rate of deflection is to be taken as limiting deflection criteria, $L^2/9000d$ gives deflection rate of 18.6 mm/min and 8.5 mm/min for the case slab tested by Cooke (2001) and Rickard et al. (2015) respectively.

Assuming these criteria are also applicable to two-way slabs, $L/20$ translates to 44.7 mm for the case of Lim et al. (2004), 44.6 mm for Zhang et al. (2014) and 36.2 mm for the case by Wang et al. (2016) slab. With regard to rate of deflection, 15.7 mm/min applicable to Lim et al. (2004) slab, 22.3 mm/min for Zhang et al. (2014), and 11.8 mm/min for the case of Wang et al. (2016) slab.

In contrast to the first two criteria described above, integrity criteria simply mean collapse or the flames are found to appear on the surface unexposed to fire or simply the slab is no longer 'impermeable'.

2.6.3 Eurocode 2 (CEN, 2004)

General design rules in Eurocode 2 (CEN, 2004), clause 5.2(4) specifies certain axis distance in tension zone within an element, where this axis distance has to be provided for the beams and slabs in order for the design to be considered as safe. For the case of simply-supported beams and one-way slabs, this translates to ensuring the tension steel is heated below 500 °C. This temperature is also termed as critical steel temperature. However, no clear criteria are explained for the case of two-way simply supported slabs. This is because it is relatively more difficult to define failure for two-way slabs.

Several studies (Gillie et al., 2004; Huang, 2010; Lim et al., 2004b) have shown that two-way concrete slabs have excellent structural fire resistance. Tensile membrane behaviour is claimed to be contributing to this enhancement of structural fire resistance. Preliminary studies presented in Baharudin et al. (2016) have also specifically demonstrated that two-way concrete slabs have far better fire resistance such that if the above criteria (500°C critical steel temperatures) are to be used to define the structural performance of the slab, the final design might not be an economical one. It is however worth to mention that constitutive formulation of steel rebar based on Eurocode 2 (CEN, 2004) reflects that a steel rebar will lose 50% of its yield strength at temperature of 550°C.

2.7 Studies on the structural behaviour of concrete buildings exposed to fires

2.7.1 Experimental studies

Fire tests on concrete buildings are scarce and relatively non-existent. With the exception of reinforced concrete frame test at Cardington (Bailey, 2002), the author is unaware of any reinforced concrete building specially designed and constructed for the purpose of testing the performance against fire, albeit it must be acknowledged that the building was not only designed and constructed solely for fire tests. It was also constructed for other purposes such as studying elasticity, shrinkage, and creep (Forth et al., 2003) and deflection of cast in-situ flat slab constructions (Vollum et al., 2002), both at ambient temperature.

Fire test on existing concrete buildings has been reported by Gillie et al. (2012). This test has been set out on the 4th floor of 23-storey residential apartment at Dalmarnock, Scotland. Throughout the discussion in the following sections, the former test will be referred as *Cardington Reinforced Concrete Frame Test* while the latter will be referred as *Dalmarnock Tower Block Test*.

2.7.1.1 Cardington Reinforced Concrete Frame Test

The building was designed as flat slab construction type using high strength concrete and was designed to have 60 minutes fire resistance in accordance to prescriptive guidance in BS 8110: Part 1 (BSI, 1997). It is unfortunate that some of the important data could not be recorded because the instrumentation cables were destroyed by fires. Severe spalling had caused the ceramic blanket and plasterboard covering the instruments detached from their original position.

The main goal of the test was to study a realistic, whole building behaviour during fire events. It was also to understand the beneficial and detrimental effects that the fire has on a full frame reinforced concrete building and how the results are compared to standard fire tests i.e. single element tests. However, as mentioned previously, it must be acknowledged that fire test was not the sole purpose the building was constructed. It was also designed to look at optimization of the execution process, which explains

why the design of the building was slightly unusual. The building was designed and constructed as flat slab construction throughout with diagonal steel flats fitted to provide lateral stiffness to the frame (Purkiss and Li, 2013). In addition, the use of high strength concrete, known to be susceptible to spalling should have had not been used if the initial intention for the test was to provide useful data for future modelling validation of structural fire response.

Purkiss and Li (2013) cited the cause of severe spalling of concrete slab was due to high strength concrete used in the construction i.e. 67MPa, while Bailey (2002) described the cause was due to compressive membrane action. The compressive membrane action was because the slab was restrained against thermal expansion (Bailey, 2002). Due to this spalling behaviour, the availability of this test for numerical model validation is hindered, thus limiting the progress on understanding a full frame behaviour of reinforced concrete building under exposure to fires. Bailey (2002) reported lateral movement of external columns, far from the fire exposure area, which further highlights the inadequate knowledge within fire engineering community and level of importance in understanding structural fire behaviour of this type of building construction.

Although in general, structural fire engineering community is in agreement that continuity and restraint have somehow enhanced fire resistance of a concrete element, no knowledge available at present to understand the extent at which this restraint improves fire resistance of concrete elements. Characterising the degree of fixity at elements' end/support is not easy as the behaviour of concrete elements under elevated temperature is highly non-linear, coupled with structural behaviour not fully understood, for instance, the moment redistribution.

2.7.1.2 Dalmarnock Residential Tower Block Test

Fire test on existing cast in-situ reinforced concrete building has been carried out at 4 Millerfield Place, Dalmarnock, Scotland on 25th July 2006 (Gillie et al., 2012). What distinguished this test from the previous *Cardington Reinforced Concrete Frame Test* is that it has been performed on existing concrete frame building (building not

specifically constructed for the purpose of fire test), and fire load used were real office furniture rather than wooden cribs or gas (Gillie et al., 2012).

Similar with the motivation of *Cardington Reinforced Concrete Frame Test*, this test had been planned and set up with the intention to make further progress and understanding on structural behaviour of realistic concrete structures. This is in part due to general consensus that testing of an individual, isolated concrete elements heated to standard ISO 834 (ISO, 1999) fire was not enough to study the performance of concrete structures under exposure to fires.

One of the main findings from the test was it demonstrated that evolution of gas temperatures within room compartment is slightly different from those represented by the standard ISO 834 (ISO, 1999) fire curve although it is acknowledged by the authors that the measured peak temperature is comparable to those that would be expected from the standard fire test. But more importantly, spatial distribution of gas temperatures within the fire compartment area is very considerable. These findings suggest that the assumption of uniform temperature in a compartment space following either ISO 834 (ISO, 1999) or Parametric Fire (CEN, 2002a) curve does not hold, even for small compartments (Gillie et al., 2012).

There was no concrete spalling reported in the test. This is potentially due to the age of concrete and relatively low strength concrete grade used as compared to most modern concrete construction nowadays. In addition, the authors also claimed that there was a layer of plaster on the fire exposed surface that might potentially affect the direct exposure of flames on the surface during the early stage of heating (Gillie et al., 2012).

After the test completed, lines of cracks were visible at the surface unexposed to fire. These cracks were found at the location where top reinforcements are curtailed. These cracks formed perpendicular to hogging reinforcement spanning on the slab's shorter span. This result suggests that the curtailment of top reinforcement for slab design under fire condition might need different treatment as compared to slab design at ambient temperature. This area needs further assessment both in numerical and experimental methods.

In terms of structural performance, it was concluded in the paper that the consequence of localised nature of fire to the performance of the structures is something not covered in the current design method. In other words, there is no knowledge available in predicting whether this localised nature of fire would have detrimental or beneficial effect to the structural performance of a concrete frame building.

2.7.2 Numerical studies

This section reviews available studies on modelling full frame response of concrete structures under exposure to fire. Note that, the term 'full frame' refers to numerical studies other than isolated, single element, in looking at the response under fire exposure. In other words, the presence of adjacent elements is physically modelled and their interaction was modelled explicitly and taken into consideration.

Significant amount of studies have been carried out for steel-concrete composite buildings for instance (Bailey et al., 1996; Elghazouli et al., 2000; Gillie, 2009). The studies were conducted partly motivated by the available experimental test results for validation. This referred to the full scale eight-storey composite test frame at Cardington. Unfortunately, similar opportunities do not exist for the case of reinforced concrete frame. While the test on reinforced concrete frame was also conducted on full-scale seven storey concrete building (referred as *Cardington Reinforced Concrete Frame Test* in the previous section) constructed at BRE Laboratories in Cardington, which has been described by Bailey (2002), the availability of important data are very limited due to equipment failures.

Huang (2010), Law (2010), and Wang (2006) have attempted to investigate the response of realistic concrete structures under exposure to fires. Huang (2010) in his studies concentrated on the influence of spalling to the behaviour of isolated slabs and beams (single element) elements and then proceeded to model similar subject for the case of slabs and beams within a generic reinforced concrete building frame. Critical spalling temperatures was defined at 350°C. Whenever temperatures reached this critical spalling temperatures, the section was assumed to lose its mechanical strength and does not influence heat transfer process. The author concludes that the behaviour of elements (both slabs and beams) act as an individual (isolated) is totally different

when acting within a frame and thus stressed on the importance of modelling full frame behaviour of concrete structures. However, it is not mentioned explicitly whether the performance of either isolated members or frame is better under the exposure to fires. The author suggests that this issue depends on many factors that need further investigations.

Law (2010) presents in-depth studies looking at the assessment method on the performance of reinforced concrete elements under exposure to fires. The studies then proceeded to investigating the performance of full frame behaviour of reinforced concrete structures which take into consideration a realistic, dynamic behaviour of fire occurring in a building. The influence of travelling fire to the structural behaviour of a generic reinforced concrete building was investigated. The method in assessing the structural performance of the building with respect to column structural response, and rebar temperatures were examined in detail.

In contrast to the previous works by Huang (2010) and Law (2010), Wang (2006) centred his discussion on the structural fire performance of reinforced concrete slabs only. The study focused on the behaviour of slabs with different complexities ranging from single slab (one-bay) to multiple-span slabs (up to nine-bays) and included fire decaying stage in the model. Although most of his discussion highlighted the importance of the performance of the slabs under fire decaying stage, more validation is required on the robustness of concrete material model during cooling stage as characterising material mechanical model under cooling stage remains a challenging topic within structural fire engineering community.

2.8 Studies on structural behaviour of concrete slabs exposed to fires

2.8.1 Experimental studies

Several researchers have performed individual element tests on instrumented reinforced concrete slabs, typically in furnaces. One-way slabs have been tested by Ali et al. (2009); Cooke (2001); Rickard et al. (2015). Cooke (2001) tested 14 samples of reinforced concrete slab to investigate several parameters such as concrete type (normal weight and lightweight), fire exposure (ISO 834 (ISO, 1999) and Hydrocarbon

(CEN, 2002a)), as well as slab thicknesses to the behaviour of the slab. It was concluded in the study that influence of thermal bowing is considerable while the imposed load has little influence on the magnitude of mid-span deflection. In addition, magnitude of deflection is found to double for the case of slabs exposed to Hydrocarbon (CEN, 2002a) fire as compared to ISO 834 (ISO, 1999) fire.

Rickard et al. (2015) experimental investigation is more oriented to material testing rather than structural testing. Of all the 75 samples tested, one (1) sample with a dimension of 4380×1450×250 was tested with its deflection measured and recorded with the intention to provide data for structural FEM model validation. While slab testing scheme by Ali et al. (2009) was designed for both material and structural investigation, the availability of the test for FEM validation is still limited. This is due to severe spalling and small number of temperature points (within slab's thickness) measured and recorded during the test.

Zhang et al. (2014) and Lim and Wade (2002) tested simply-supported two-way slabs, and these tests provide valuable information for studying full-scale, single span concrete slab behaviour under exposure to standard fires (ISO, 1999). Both tests provide insights into the behaviour of two-way simply-supported concrete slabs under realistic thermal gradients through the thickness of the slab.

Earlier in 1989, Lin et al. (1989) tested full-scale two-way reinforced concrete slabs. The slab was reinforced with epoxy-coated bars. Some degree of restraint was introduced to simulate moderate in-plane restraining force of an edge bay in a 3×3 bay floors system. Similar slab configuration with uncoated bars was also tested by Lin and Abrams (1981). One of the clear motivations behind testing two-way concrete slabs either simply-supported or with restrained support is the enhancement of structural fire resistance of the slabs due to tensile membrane action. For a composite steel-concrete construction, this membrane behaviour not only prolongs the fire resistance of the slab itself but it also provides fire protection to the unprotected steel beams. This finding has made interests in studying structural fire performance of steel-concrete composite structures significantly gaining its popularity especially from the steel industry.

More recently Wang et al. (2016) tested two-way reinforced concrete slabs also exposed to ISO 834 (ISO, 1999) fires to investigate the slab's behaviour under combined uniaxial in-plane and out of plane load. Both in-plane and out-plane load were introduced and thereafter maintained throughout fire exposure. It was found that the application of uniaxial in-plane load has significant effect on the number and direction of crack at the surface of slab unexposed to fire. In addition, slab with uniaxial in-plane load (uniaxial restraint) has more deflection and lower deflection recovery ratio as compared to slab with simple support.

Bailey and Toh (2007) tested forty-eight (48) small-scale two-way concrete slabs. These tests provide valuable information on the effect of various parameters to the behaviour of slabs that are useful for numerical validation in understanding the behaviour of fire-exposed concrete slabs. The notable disadvantage of testing small scale slabs is the fact that temperature gradient experienced by the slab is not representing the actual gradient in a realistic concrete slab. For example, testing of 40mm thickness small-scale slab by Fox (2013) might not be providing idealistic condition for the slab where temperature at the unexposed face of the slab could easily reach temperatures of more than 200°C. However, qualitative studies with the intention of investigating several parameters to the fire performance of the slabs are more than enough to justify the idea of testing small-scale slabs.

Fire test of small scale reinforced concrete slab by Fox (2013) is unique as compared to other tests described above in a sense that the setup of the test provides both translational and rotational restraint at supports. This aspect has not been considered in other tests mentioned above.

In general, all studies mentioned above show that two-way reinforced concrete slabs can carry greater loads than calculated using conventional yield-line theory. This is achieved by mobilising tensile membrane action, irrespective of whether the slabs are restrained or simply supported.

2.8.2 Numerical studies

Numerical study of concrete slabs is a broad term used in describing any work that utilises computational method to understand behaviour of the slabs under exposure to fire. This section will review and present selected studies on the application of finite element method to investigate the structural response of concrete slabs, both one-way and two-way. Studies concerning development of computational method and material model will not be discussed.

Two-way slabs have been modelled by (Deeny, 2010; Huang et al., 2003a, 2003b; Lim et al., 2004b; Wang, 2006). Huang et al. (2003a) and Huang et al. (2003b) modelled and validated concrete slab tested by Lin et al. (1989) while Lim et al. (2004b) modelled the slab tested by Lim and Wade (2002). A number of concrete slabs in a composite steel-concrete construction have also been modelled by a few researchers for instance (Elghazouli et al., 2000; Gillie et al., 2004, 2001).

Motivation behind most of the studies mentioned above was to understand membrane behaviour of the slabs under exposure to fire. Slabs were found to have better fire resistance than estimated using the conventional yield-line theory. General findings from all the studies above concur with this where slabs (in the model) sustaining large vertical deflection without collapse. Mobilisation of tensile membrane action occurs for both slabs with simple support and with restraint support conditions.

From all the studies, investigation on the slab's behaviour under finite restraint condition has not been the core of the investigation. This is partly due to the limited available experimental data for validation. Modelling the slab tested by Lin et al. (1989) by Huang et al. (2003a, 2003b) involves defining axial forces at slab's edges with the intention to simulate axial restraint in a real building. Application of the restraining forces follows the time-axial force relationship determined from the earlier studies described by Lin and Abrams (1981) where the thermal expansion-time reading was measured. Relatively similar motivation led to the experimental studies performed recently by Wang et al. (2016).

It is unaware of any numerical studies conducted so far, looking at the influence of degree of rotational stiffness. The motivation to pursue this kind of investigation is low due to unavailability of experimental data for validation. To the author's knowledge, no studies conducted so far to understand the influence of degree of rotational stiffness to the structural behaviour of two-way reinforced concrete slabs under exposure to fire. Similar shortcomings are found for the case of one-way span reinforced concrete slabs.

Extensive investigation on the behaviour of one-way reinforced concrete slabs under exposure to fire has been carried out by Lim et al. (2004a) and Lim (2003). Slabs with different degree of axial restraint, at different depth at slab's edge were investigated. The behaviour of slab with full rotational restraint was also investigated. No variation of degree of rotational stiffness was investigated. It was found that location of axial restraint has significant effect on the structural response of the slabs.

Ali et al. (2009) has also performed experimental and numerical studies on the behaviour of one-way reinforced concrete slabs exposed to fire. However, it was reported that severe spalling occurred during the fire test and discussion has been focused on the spalling rather than the structural behaviour.

2.9 Concrete material thermal properties

As compared to steel material, thermal properties of concrete are relatively more complex. Concrete is a mixture of several constituents of material forming it, namely sand, aggregates, the cement paste as well as water. Each of them has its own thermal properties and behaviour. When combined as a concrete, their thermal characteristics become more complex. In contrast, steel is a homogeneous material thus its thermal behaviour is rather simpler.

In performing heat transfer analysis, a relatively simplified technique utilises concrete material thermal properties that is temperature-independent. However, this assumption is very crude given the nature of concrete materials. For instance, the existence of moisture within concrete pores requires analysis to take proper consideration on its presence. When concrete elements are heated on one surface, moisture tends to shy

away from the heat sources. This movement causes pore pressure developed in the concrete as water reaches its boiling temperatures.

2.9.1 Density

The density of concrete reduces with the increase in temperature. This is mainly due to the reduction of moisture in concrete. For limestone aggregate however, concrete also loses its density due to the decomposition of limestone at 800°C (Buchanan and Abu, 2017) and this can be seen in Figure 2.2. Eurocode 2 (CEN, 2004) gives the recommendations on the density-temperature relationship and this is shown in Figure 2.2 and plotted together with values reported by Schneider (1988). The relationship suggests that concrete density starts to decrease from temperature 115 °C and above. It's hard to explain why the density degrades from temperature of 115 °C onwards instead of 100 °C as it is known that water boiling temperatures is at 100°C although it must be acknowledged that the presence of water/moisture in concrete is not only as free moisture, but also chemically bound moisture, which might explain this relationship.

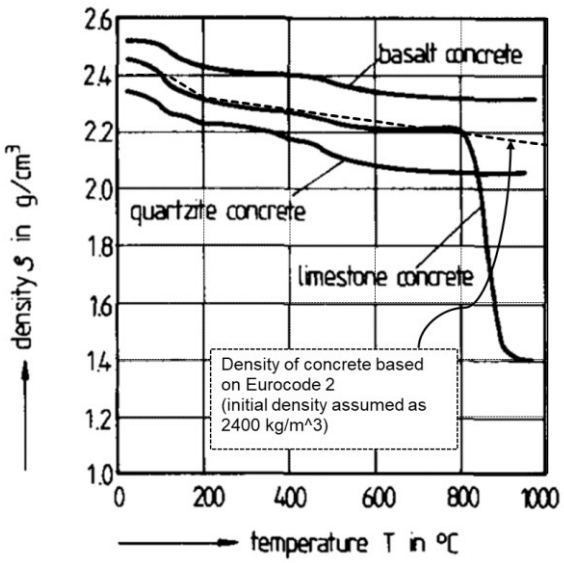

Figure 2.2: Temperature-dependent concrete density properties from Eurocode 2 (CEN, 2004) **plotted with values reported by** Schneider (1988)

2.9.2 Specific heat

Specific heat is the amount of heat per unit mass required to raise the temperature by one degree Celsius. Figure 2.3 shows the temperature-dependent specific heat for concrete with different types of aggregates compiled by Schneider (1988). Relationship from Eurocode 2 (CEN, 2004) with moisture content considered as 1.5% is included for comparison.

Change in specific heat properties in concrete occurs typically at temperature between 100 - 200°C. This is due to the loss of moisture as water reaches its boiling temperature.

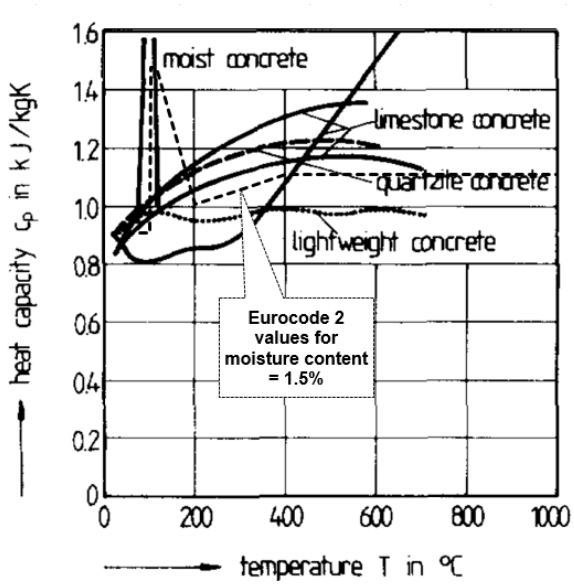

Figure 2.3: Temperature dependent specific heat properties from Eurocode 2 (CEN, 2004) **plotted with values reported by** Schneider (1988)

2.9.3 Conductivity

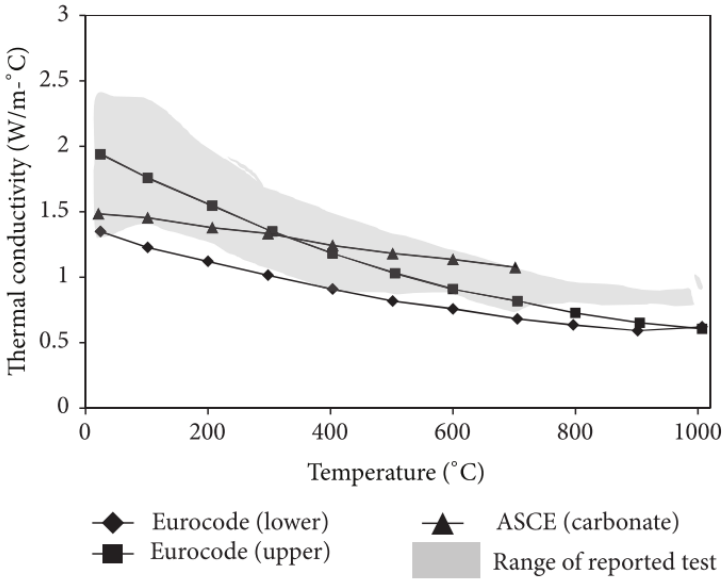

Figure 2.4: Temperature-dependent thermal conductivity properties of concrete reproduced from Kodur (2014)

Thermal conductivity of concrete varies significantly for different aggregates. A range of reported values compiled by Kodur (2014) is shown in Figure 2.4. Eurocode 2 (CEN, 2004) specifies lower and upper limits of thermal conductivity for normal weight concrete. These temperature-dependent values are defined not based on aggregate type, but rather an upper and lower bound limit. This is also shown in Figure 2.4 above.

2.10 Steel material thermal properties

2.10.1 Density

Reduction of mass for steel is hardly reported within literatures. Steel maintains its density at elevated temperature irrespective of the grade and strength. The density is typically 7850 kg/m^3.

2.10.2 Specific heat

Relatively less variation of temperature-dependent specific heat properties for steel with different grade and strength as compared to concrete. A large and sudden spike of specific heat value at approximately 730°C recommended in the Eurocode 3 (CEN, 2001) and Eurocode 4 (CEN, 2005). It is thought that this is due to metallurgical change in the steel at this temperature (Buchanan and Abu, 2017). In addition, for performing simple calculation, a constant value of 600 J/kg.K is suggested by Buchanan and Abu (2017). Relationship of Eurocode 3 (CEN, 2001) and Eurocode 4 (CEN, 2005) is plotted and shown in Figure 2.5 below.

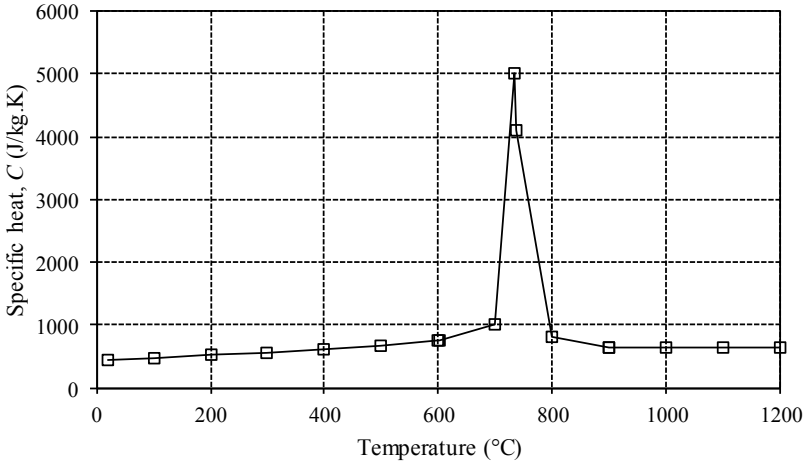

Figure 2.5: Temperature-dependent specific heat of steel in accordance to Eurocode 3 and Eurocode 4 (CEN, 2005, 2001)

2.10.3 Conductivity

Conductivity values of steel reduces linearly from 54 W/m.K at ambient temperature to 27.3 W/m.K at 800°C as recommended in Eurocode 3 (CEN, 2001) and Eurocode 4 (CEN, 2005). This relationship is plotted and shown in Figure 2.6 below.

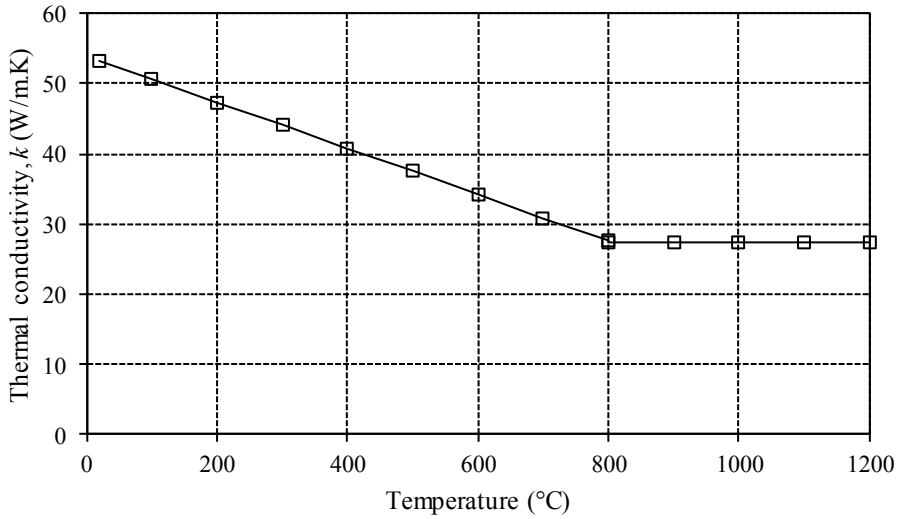

Figure 2.6: Temperature-dependent thermal conductivity of steel in accordance to Eurocode 3 and Eurocode 4 (CEN, 2005, 2001)

2.11 Concrete material mechanical properties

2.11.1 Compressive behaviour

Mechanical properties of concrete at elevated temperatures is a complex problem to understand. Compressive strength of concrete is higher than its tensile strength, roughly in the order of ten (10) times. When heated, peak strength of concrete degrades with the increase in temperature. However, failure strain is typically greater for a heated concrete as compared to concrete at ambient temperature. With peak strength significantly reduced, failure strain is projected further away, resulting slightly more ductile behaviour. Concrete compressive stress-strain-temperature relationship suggested in Eurocode 2 (CEN, 2004) plotted with characteristic compressive strength (F_c) at ambient assumed as 30MPa is plotted and shown in Figure 2.7 below.

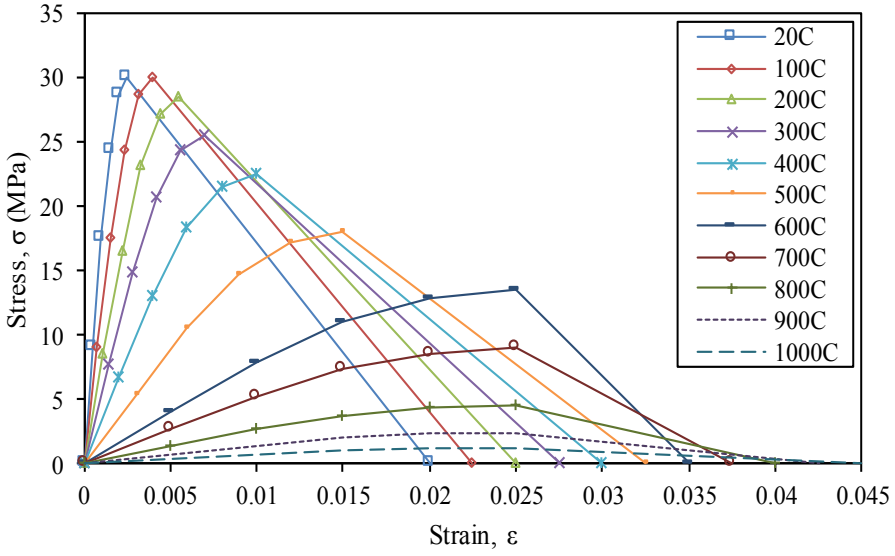

Figure 2.7: Stress-strain-temperature relationship for concrete at elevated temperature in accordance to Eurocode 2 (CEN, 2004) **with F_c = 30MPa**

2.11.2 Tensile behaviour

Flexural design of reinforced concrete elements generally ignores contribution of concrete tensile strength. Although concrete does have strength in tension but it is typically very low and ignoring it in the design is thought to be conservative and on the safe side. This assumption performs satisfactorily for the design based on the limit state approach at ambient temperature as both steel reinforcement and concrete are not anticipated to reach their plastic state while serving their design purpose.

Similarly, the design of reinforced concrete elements at elevated temperatures in general ignores contribution of concrete tensile strength. For simply-supported members, assessment of structural fire response only considers the strength reduction of steel reinforcement at the fire exposed surface (Buchanan and Abu, 2017). The existence of concrete in tension zone is neglected. The compression zone near the unexposed surface is assumed not yet heated thus the strength is not degraded. For continuous members, where some of the fire-exposed surfaces are in compression, degradation of concrete material need to be considered. This clearly demonstrates that tensile strength available in concrete is typically ignored in the design.

However, the design routine of reinforced concrete elements at elevated temperatures relies heavily on more complex computer program as a tool. This is due to the available knowledge and understanding on how concrete elements respond under exposure to a fire that is still relatively low. Therefore, characterising concrete material behaviour in tension is more crucial at elevated temperatures than at ambient temperature.

During fire, enough evacuation time must be provided to enable building occupants to leave the building within reasonable period of time. As fire engulfs in a building (assuming compartment fires), reinforced concrete members tend to behave in a non-elastic behaviour very quickly. This is due to the complex thermal bowing behaviour as a result of high temperature gradient within the concrete element's depth. Due to the thermal bowing behaviour, tensile cracking in section at mid-span will typically initiate at the elements' mid-depth (Deeny, 2010) and initial study by author has proved this behaviour in a two-way simply-supported reinforced concrete slab exposed to fires (Baharudin et al., 2016).

In addition, complex coupled strain behaviour i.e. free thermal, stress-related, and transient strain occurring either simultaneously or independently requires the designer to properly consider tensile strength behaviour in the concrete. Within practical limit, if only simple hand calculation is required in assessing fire resistance of a concrete element, ignoring contribution of concrete tensile strength might be sufficient, however in most situations, rigorous analysis (e.g. FEM) is always required for the analysis of concrete elements exposed to fire and therefore proper consideration of concrete tensile strength is thought to be crucial. Several range of reported values on the reduction of concrete tensile strength at elevated temperatures as compiled by Kodur (2014) is shown in Figure 2.8(a) while values reported in the Structural Fire Protection Manual by ASCE (ASCE, 1992) is shown in Figure 2.8(b). Note that the value recommended in Eurocode 2 (CEN, 2004) is also included in both figures for comparison.

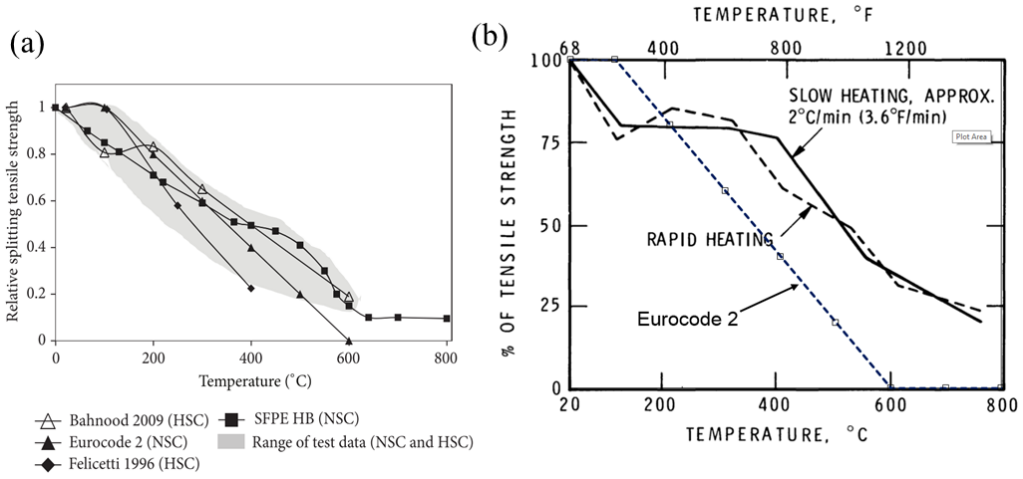

Figure 2.8: Reduction of concrete tensile strength at elevated temperature (a) review of available data by Kodur (2014) **and (b) as described in Structural Fire Protection Manual by ASCE** (ASCE, 1992) **plotted together with Eurocode 2** (CEN, 2004) **recommendation**

2.11.3 Strain decomposition

A few researchers believe that the inclusion of explicitly transient strain (ε_{tr}) has significant influence on the performance of numerical model in predicting structural fire response of concrete elements for instance Gernay (2012) and Wang et al. (2013). In general, total strain of a heated concrete can be summarised as:

$$\varepsilon_{total} = \varepsilon_{th} + (\varepsilon_{\sigma} + \varepsilon_{tr} + \varepsilon_{cr})_{mech} \qquad \text{Equation 2.1}$$

ε_{th} is the free thermal strain while ε_{mech} is the mechanical strain. Several free thermal strains, available and reported in literatures are presented in Figure 2.9. Mechanical strain typically composed of instantaneous stress-related strain (ε_{σ}), transient creep strain (ε_{tr}), and basic creep strain (ε_{cr}). Component of transient creep strain is believed to be included implicitly in the total strain components in Eurocode 2 (CEN, 2004) constitutive formulation of concrete.

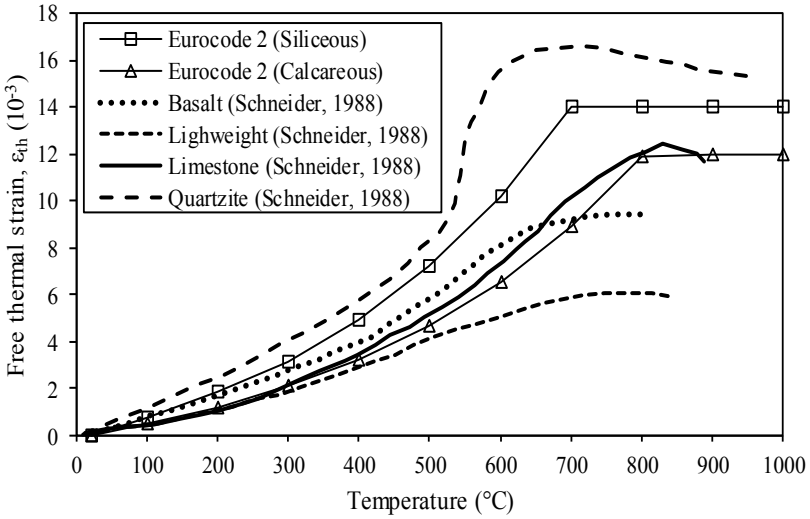

Figure 2.9: Thermal elongation of concrete with different aggregates

Other researchers explained the strain decomposition in a different approach for instance Khoury et al. (1985) introduced the term *Load Induced Thermal Strain* (LITS). *LITS* is the difference between the free thermal expansion of a concrete element without load and the net thermal expansion of the element when it is heated under load (Khoury et al., 1985). *LITS* is literally all the strain components of a heated concrete other than thermal strain (ε_{th}) and instantaneous stress related strain (ε_{σ}). The strain decomposition is shown below where ε_{th} is the free thermal strain while $\varepsilon_{\sigma}^{20°C}$ is the instantaneous stress related strain:

$$\varepsilon_{total} = \varepsilon_{th} + \varepsilon_{\sigma}^{20°C} + LITS \qquad \text{Equation 2.2}$$

There has been an active research topic on how to treat this different strain components in numerical modelling and it is believed that this has significant influence on how the concrete elements behave either during early stage of heating or later stage of heating and even during cooling stage. However, it is beyond the scope of the current study and will not be further discussed.

2.11.4 Concrete Damage Plasticity Model – ABAQUS

Implementation of material model properties in finite element beyond elastic region requires definition of yield criteria. Under realistic loading condition, the resulting stresses in concrete elements generally do not act as 1-dimensional problem thus requiring the introduction of yield surface to identify the limit of elastic behaviour or yielding condition of the materials in the principal stress space. Under biaxial condition, the typical yielding shape is shown in Figure 2.10. Note that the figure shows yield criteria of concrete proposed by Lubliner et al. (1989) with modifications by Lee and Fenves (1998) and described in ABAQUS user manual (ABAQUS, 2012) to account for different evolutions of strength under tension and compression.

As opposed to steel, concrete poses more complex behaviour. This is because high ratio of compressive strength to tensile strength, typically in the order of tenth times. This complexity makes formulating plasticity behaviour of concrete slightly more complex than defining the same for steel. Several criterion proposed for concrete available within literatures are for instance (Dahlblom and Ottosen, 1990; Feenstra and De Borst, 1996; Hoek and Brown, 1980; Lee and Fenves, 1998; Lin et al., 1987; Lubliner et al., 1989). Mohr-Coulomb and Drucker-Prager criterion are commonly adopted in most studies.

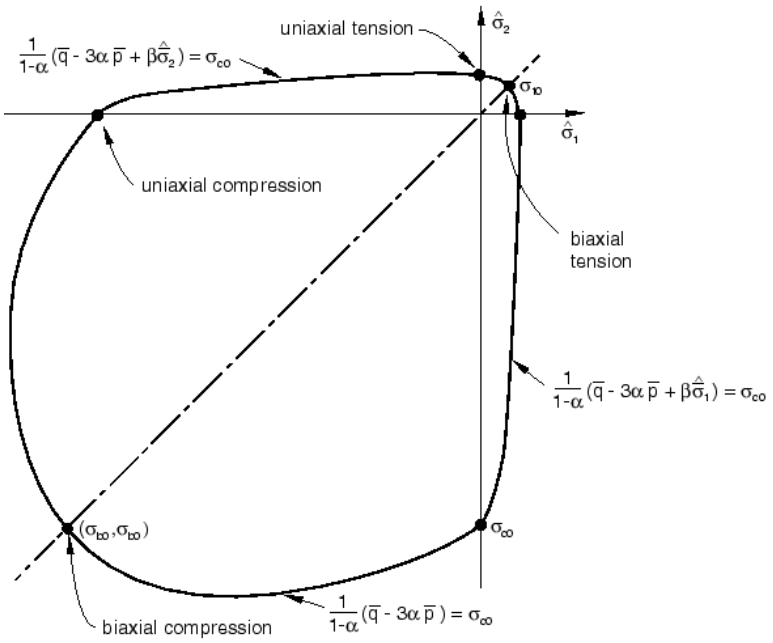

Figure 2.10: Yield surface in plane stress (ABAQUS, 2012)

In tension, post-peak properties can be modelled in three (3) ways in ABAQUS (ABAQUS, 2012):

a) Stress-strain
b) Stress-displacement
c) Fracture energy

Irrespective of any type of input provided by the modeller, ABAQUS will convert the relationship into stress-strain relationship. For (b) and (c) above, characteristic length is used in ABAQUS to convert the displacement into strain. With fracture energy inputted (as in (c) above), cracking displacement is calculated within ABAQUS based on the work of Hillerborg et al. (1976). This fracture energy – cracking displacement relationship will be discussed more in details in Section 3.4.3 in Chapter 3.

2.12 Steel material mechanical properties

2.12.1 Modulus of elasticity

The framework for characterising steel material mechanical behaviour is established by performing tensile test. Reduction factor for elastic modulus is shown in Figure

2.11 while the review on some of data available within literatures and plotted together with the recommended reduction factor from Eurocode 3 (CEN, 2001) is shown in Figure 2.12 by Kodur et al. (2010).

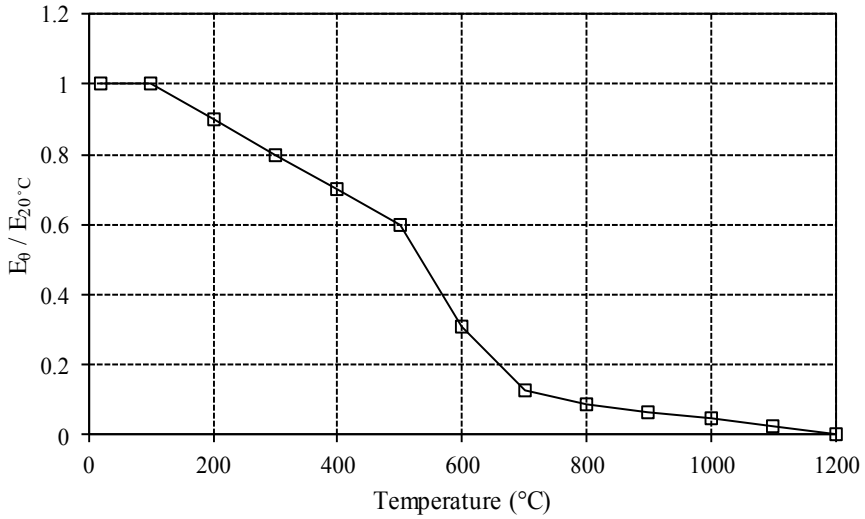

Figure 2.11: Reduction of elastic modulus at elevated temperature in accordance to Eurocode 2 (CEN, 2004)

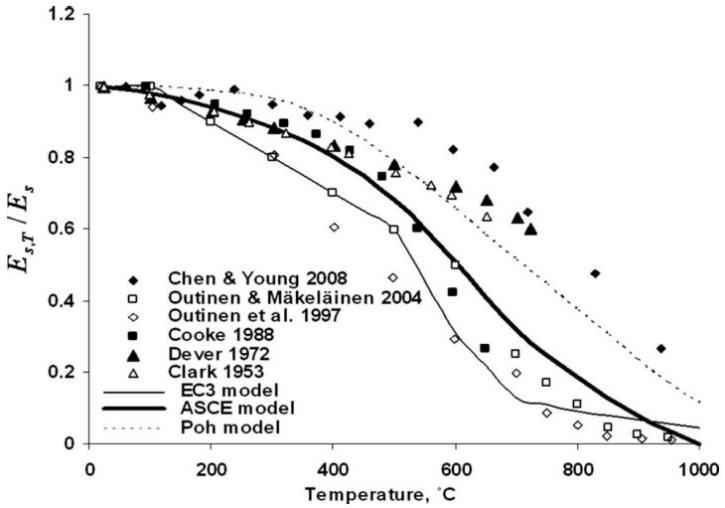

Figure 2.12: Reduction of elastic modulus at elevated temperature reproduced from Kodur et al. (2010)

2.12.2 Strength

Review on the constitutive formulation of steel material properties against available experimental results for steel material strength at elevated temperature has been carried out by Kodur et al. (2010). The authors list out reported mechanical and thermal properties of steel at high temperature and compared them with the constitutive formulation of the material model based on Eurocode 3 (CEN, 2001) and Structural Fire Protection Manual by ASCE (ASCE, 1992). Findings from the case study in the paper suggest no significant variation from either constitutive material suggested from both Eurocode (CEN, 2005, 2004, 2001) and Structural Fire Protection Manual by ASCE (ASCE, 1992) to the modelled simply-supported and restrained beam response when they were exposed to temperatures below 700°C. In contrast to Structural Fire Protection Manual by ASCE (ASCE, 1992) constitutive material model, formulation from Eurocode (CEN, 2005, 2004, 2001) includes consideration for creep behaviour thus suggesting that the Eurocode (CEN, 2005, 2004, 2001) material model predicts more realistic response (Kodur et al., 2010).

Other established work characterising steel material properties at elevated temperatures are (Anderberg, 1986; Chen et al., 2006; K.W.Poh, 2001; Outinen, 2006). These works generally provide significant amount of experimental results data that shape the current constitutive steel material model for the application in finite element modelling.

Degradation of steel strength with temperatures as given in Eurocode 2 (CEN, 2004) and Eurocode 3 (CEN, 2001) for hot-rolled steel is plotted and shown in Figure 2.13 below as a ratio to the strength of steel at ambient temperature. Slightly different reduction factors for cold-formed steel section are also given in the code but not shown here. Both Eurocode 2 (CEN, 2004) and Eurocode 3 (CEN, 2001) suggest no reduction of strength for steel up to 400°C. Trend in the scattered data from experimental tests also seem to agree with this recommendation. The plot for these experimental data together with recommendation from Eurocode 3 (CEN, 2001) is reproduced from Kodur et al. (2010) and shown in Figure 2.14 below. Note that both Eurocode 3 (CEN, 2001) and Eurocode 2 (CEN, 2004) give similar reduction factor. Both codes are

referred in this section interchangeably as where they are referred, but they are essentially the same.

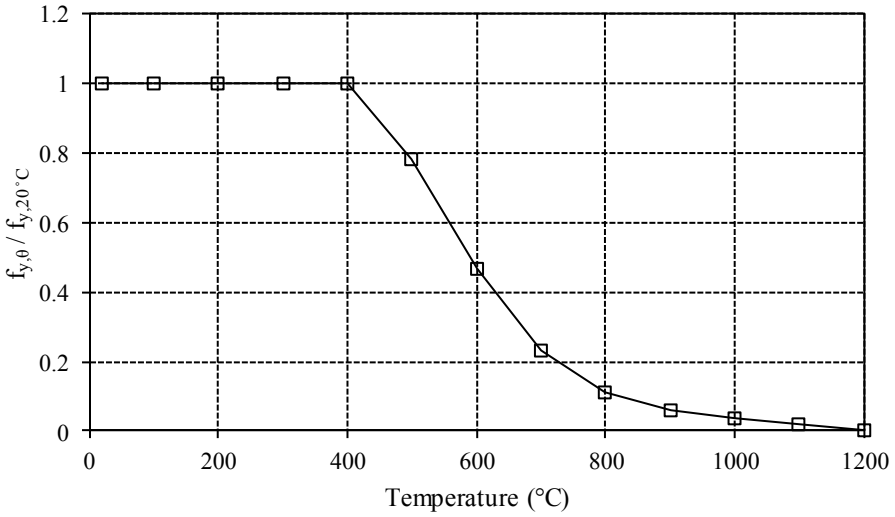

Figure 2.13: Reduction of yield strength for hot rolled steel at elevated temperature in accordance to Eurocode 2 and Eurocode 3 (CEN, 2004, 2001)

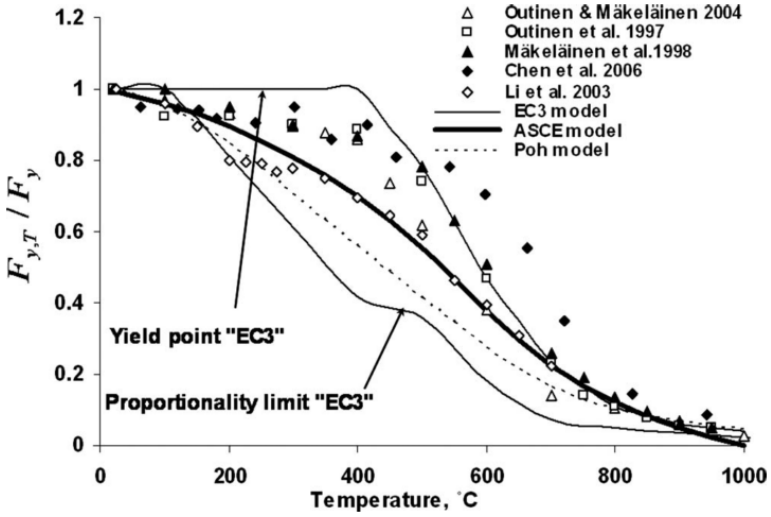

Figure 2.14: Reduction of yield strength at elevated temperatures: compilation of data from several sources, reproduced from Kodur et al. (2010)

2.12.3 Strain decomposition

As compared to strain decomposition of concrete, discussed in section 2.11.3 of this chapter, decomposition of strain in steel is relatively simpler. Components of strain in steel are as shown below:

$$\varepsilon_{total} = \varepsilon_{\sigma} + \varepsilon_{thermal} + \varepsilon_{creep} \qquad \text{Equation 2.3}$$

Where:

ε_{total} = total strain

ε_{σ} = instantaneous stress-related strain

$\varepsilon_{thermal}$ = thermal strain

ε_{creep} = creep strain (time-dependent strain)

Instantaneous stress-related strain is an elongation of steel material due to mechanical loading. It is the strain when an element is loaded for the first time. Thermal strain is the free thermal expansion in a steel when it is heated while creep is in general the time dependent strain. In the constitutive formulation of steel material model in accordance to Eurocode (CEN, 2005, 2004, 2001), the allowance for creep strain is included in the proposed formulation of stress-strain curve.

Creep strain can become significant at temperatures over 400°C or 500°C (Buchanan and Abu, 2017). Transient test by Kirby and Preston (1988) has demonstrated that creep is highly dependent on temperature and stress level (refer Figure 2.15). Researchers have different opinions on the level of importance on explicitly including creep strain to the predicted response for steel behaviour at elevated temperatures. Creep is implicitly included in stress-strain relationship based on Eurocode (CEN, 2005, 2004, 2001) formulation and is thought to perform satisfactorily. On the other hand, other researchers have shown that creep can be included explicitly in a computational model for instance Anderberg et al. (1986) and demonstrated that creep

and the nature of strain hardening can have significant influence on the predicted response.

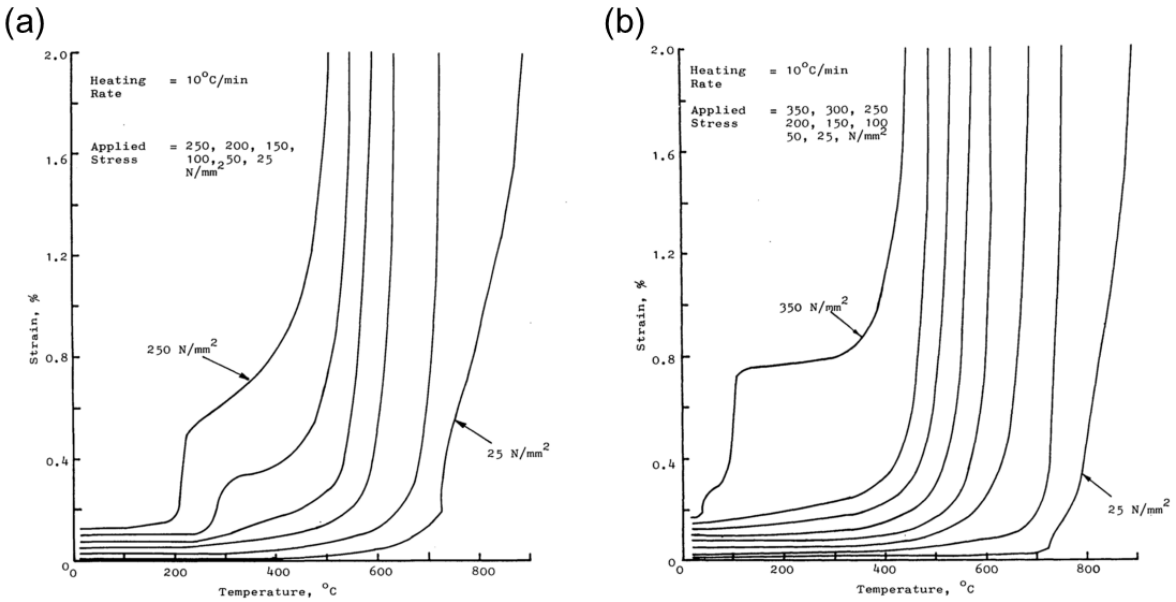

Figure 2.15: Creep of steel tested in tension (reproduced from (Kirby and Preston, 1988)**) for (a) grade 43A steel and (b) grade 50B**

2.12.4 Mathematical model at elevated temperature

When loaded in tension, initially steel elongates within elastic region followed by proportionate region. In this proportionate region, the behaviour is somewhere between purely elastic and purely plastic. Characterising the behaviour within this region is known to be the most challenging aspect in formulating steel constitutive material model not only at elevated temperature, but also at ambient temperature. This explains why finite element modellers tend to simplify their material model definition by simply defining the steel behaviour as perfectly elastic-plastic behaviour. This is done by simply defining linear ascending branch representing elastic state and thereafter straight horizontal line representing plastic state of the steel.

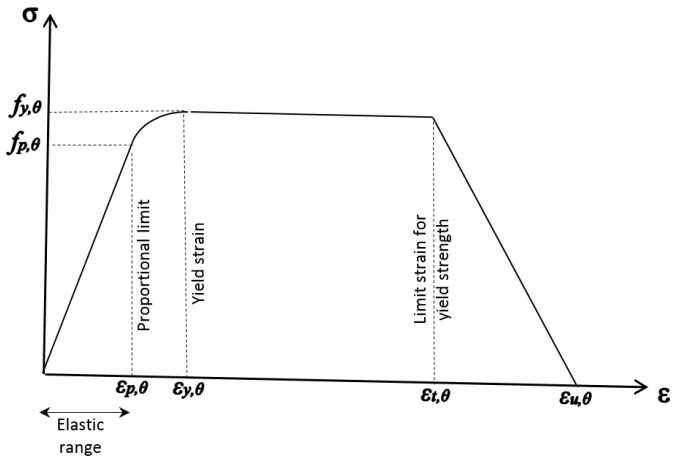

Figure 2.16: Stress-strain characterisation for steel reinforcement based on Eurocode 2 (CEN, 2004)

As the understanding for structural steel element behaviour at elevated temperatures is demanding over the recent years, together with the introduction of performance based code design, the push to minimize simplification and assumption has made the need for proper modelling of steel behaviour within elastic-plastic (proportional region) unavoidable. In addition, the advancement of computational method and capabilities have also accelerated improvement in proper modelling of material behaviour at elevated temperatures. Eurocode (CEN, 2005, 2004, 2001) proposed a mathematical model for steel material as shown above in Figure 2.16. The evolution of stress-strain behaviour under loading is as described above. An example of stress-strain behaviour at different temperature plotted with initial steel strength at ambient as 460 MPa is shown in Figure 2.17 below.

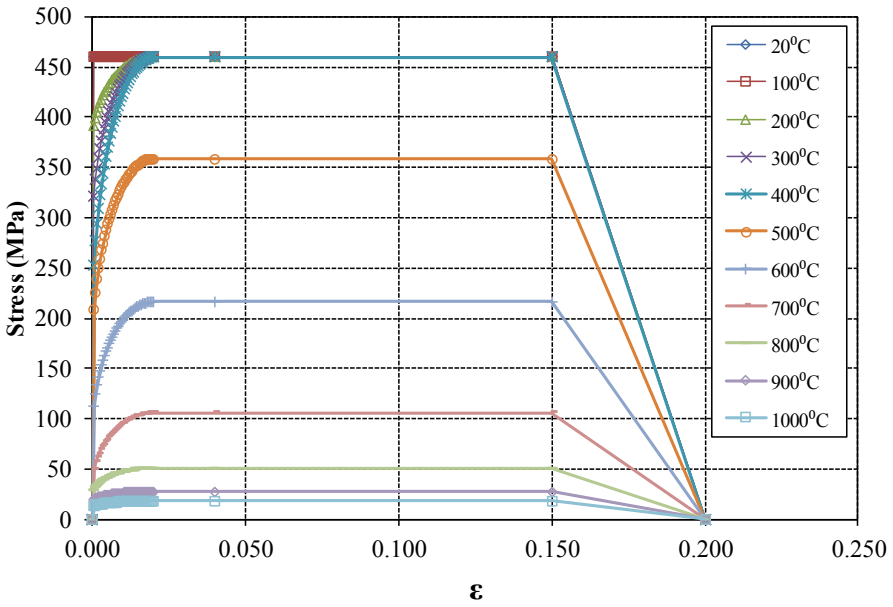

Figure 2.17: Stress-strain behaviour based on Eurocode 2 (CEN, 2004) **relationship plotted for steel with initial strength at ambient as 460 MPa**

2.13 Summary and conclusion

2.13.1 Fire scenario for structural design

Replicating a realistic fire environment for fire testing of structural elements remains a challenging topic within the research community. There is a considerable number of arguments on the applicability of standard fire test in representing realistic fire environment to the tested elements. This further questions the applicability of standard fire for performing structural design for fire resistance.

Fire scenario for structural design can be broadly divided into three categories: (1) compartment fire (2) localised fires (3) travelling fires. Significant amount of research is ongoing on the latter two categories as they are thought to be more representative of realistic fire behaviour in buildings amongst others.

2.13.2 Experimental and numerical studies

The need for more experimental studies are crucial, both at the scale of frame and elemental. This is important for providing the most needed data for validation purposes. More experimental data are required for FE model validation to increase the level of confidence on the response predicted by the model.

With respect to experimental testing of reinforced concrete slabs, instead of testing simply-supported slab, setting up restraint support condition in the test would provide the most crucial data needed within structural fire engineering community particularly for the FE model validation. It is also acknowledged that this task is relatively difficult to realise in the context of experimental setup. A few works replicating axial restraint have been carried out. However, similar works for rotational restraint are still relatively non-existent. With the exception of a small-scale test by Fox (2013), it is unaware of any test available within literatures.

2.13.3 Material model for FEM

Modelling elongation behaviour of concrete at elevated temperature remains a topic of high uncertainty. Characterising strain behaviour at different stress levels (or loadings)

during transient fire test is a complex problem to understand. Although different researchers have different ways of interpreting this strain, inserting this into formulation of finite element model is another challenge within structural fire engineering community. A considerable amount of research are still ongoing while significant improvement has been achieved in the past two decades.

2.13.4 Structural behaviour of reinforced concrete slabs exposed to fires

Under exposure to fires, two-way slab mobilises the membrane action and performs reasonably better than the capacity estimated using the conventional yield-line theory. This membrane action occurs for two-way slabs even there is no restraining at supports (simply-supported). This behaviour is now utilised in the design as providing structural capacity to the unprotected steel beams in a composite steel-concrete construction.

For the case of similar slabs in a cast in-situ reinforced concrete construction (concrete beam-slab construction), the knowledge is still limited, and studies on this is not gaining much interest within researchers. Among other factors, low thermal conductivity of concrete, which believed to provide good fire resistance rating has made studies on this aspect less attractive.

The aspect of continuity at support has not been given enough attention so far. There are relatively fewer numerical studies looking at the aspect of continuity to the structural performance of reinforced concrete slab, both for one-way and two-way slabs. This is partly due to the lack of data for validation besides complexities of defining realistic support condition in finite element model. Failure mechanism of beams (also applicable to one-way slab) as described by Salse and Gustaferro (1971) and explained in Buchanan and Abu (2017) is the formation of plastic hinges. Three (3) points of plastic hinges for the case of continuous slab and one (1) point at the slab's mid-span for the case of simply supported slab. For continuous slab, plastic hinges occur near both end supports and at the mid-span.

With respect to the structural design of reinforced concrete slabs for fire resistance, currently there is no information on the best design practice available to structural fire engineers in performing their design task. It is unknown to the designers whether

varying parameters such as span-to-depth ratio, configuration of steel reinforcement, restraint stiffness (both translational and rotational) would have given beneficial or detrimental effect to the performance of reinforced concrete slabs under exposure to fire.

Chapter 3:

Finite element modelling of one-way reinforced concrete slabs exposed to severe heating from below

3.1 Introduction

This chapter presents the studies aimed at validating finite element models against the results from furnace testing of one-way reinforced concrete slabs exposed to fires. To be considered as credible and realistic, results from the finite element models of concrete slabs exposed to furnace fires are compared and validated against available experimental results. Parametric studies are subsequently performed once the models are validated. Parametric studies are performed to investigate the influences of various thermal and mechanical parameters unable to be studied via experimental testing due to limitations such as cost, time, and complexity of full scale furnace testing.

Studies on the response to fire of one-way concrete slabs have received rather less attention in the research literature compared to two-way slabs. Research on two-way reinforced concrete slabs is more widespread, as such slabs are more representative of the typical floor slabs in conventional reinforced concrete and composite steel-concrete building structures. One-way slab more commonly represents a precast floor slab construction and it is usually in the form of pre-stress construction rather than conventional steel reinforced construction. Structural behaviour of one-way reinforced concrete slabs has been extensively investigated by Lim (2003). Specifically, Lim (2003) studied the membrane behaviour of this type of slab under different boundary conditions and whether those different boundary conditions enhance or reduce the structural fire resistance of the slab. 2-D beam element was used in the study.

Fundamental understanding on how reinforced concrete elements respond under exposure to fires remains low despite the advancement in the knowledge of thermo-mechanical properties of concrete at elevated temperatures. This is true even for a relatively simple element such as a single span beam or slab. In performing a structural fire design based on the performance-based code, there are no definite criteria on how structural failure is defined to fulfil the pre-set performance objective. Obviously, a better understanding on how concrete elements respond when exposed to fires is required to make further progress in the field.

With the above points in mind, the following section presents numerical studies on the behaviour of single span, simply supported one-way reinforced concrete slabs exposed to ISO 834 (ISO, 1999).

3.2 Analysis methodology

Two (2) experimental tests of one-way reinforced concrete slabs tested by Cooke (2001) and Rickard et al. (2015) are selected for numerical model assessment. Using experimental results from these two (2) - furnace fire test reinforced concrete slabs, the aspect of validating finite element model against experimental results is thoroughly investigated. The capability of finite element approach to predict the behaviour of these two slabs using the available constitutive material model, element formulation, and sensitivity of different input parameters is carefully examined.

Definition of structural failure is still not clear for a concrete element under exposure to fires. Collapse of a concrete slab cannot be predicted, as the knowledge in the field of structural performance of a concrete slab is relatively young as compared to the slab's performance at ambient temperature. A few experimental studies (Bailey and Toh, 2007; Cooke, 2001; Lim and Wade, 2002; Zhang et al., 2014) reported that their concrete slabs did not collapse at their anticipated time or period. It is also not clear with no available knowledge to support the claim that the slabs had longer fire resistance against collapsing.

3.3 Scope of study and limitations

The study focuses on the structural behaviour of one-way reinforced concrete slabs subjected to elevated temperatures. No attempt is made to study structural fire response of the slabs during cooling stage, since no experimental data are available for validation. The slabs, both in the tests and finite element models, were assumed to be heated in standard fire testing furnaces following the ISO 834 (ISO, 1999) standard time-temperature curve.

3.4 Available furnace tests on one-way reinforced concrete slabs

3.4.1 Slab 1 - (Cooke, 2001)

4700×925×150 mm one-way spanning reinforced concrete slabs under exposure to ISO 834 fire (ISO, 1999) were tested by Cooke (2001). Specimen 2 (Cooke, 2001) was selected for the current study. The slab was simply supported at 4500 mm centres. The length of exposure to fires from below was 4000 mm. Normal-weight concrete with siliceous aggregate was used in the concrete mix. 1.5 kN/m^2 imposed mechanical load was introduced during the test. Characteristics of cube strength of concrete was reported at 30 N/mm^2 and reinforcing steels were of high-yield ribbed bar having a nominal yield strength of 460 N/mm^2 (Cooke, 2001). Figure 3.1 below shows the geometrical configuration of the slab and reinforcement used in the slab.

Linear displacement transducers (LDT's) were used to measure vertical mid-span deflection and quarter-span position and all deflection measurements were made relative to the ends of a slab using two purpose-made hollow steel frames which rested on the ends of the slab (Cooke, 2001). Continuous flow of water was done into the frame so that it would not itself deflect due to a change in temperature. Mechanical load of 1.5 kN/m^2 was applied using A-frames, two hydraulic jacks and a system of load spreader to approximately and uniformly distributed load; this is shown in Figure 3.1.

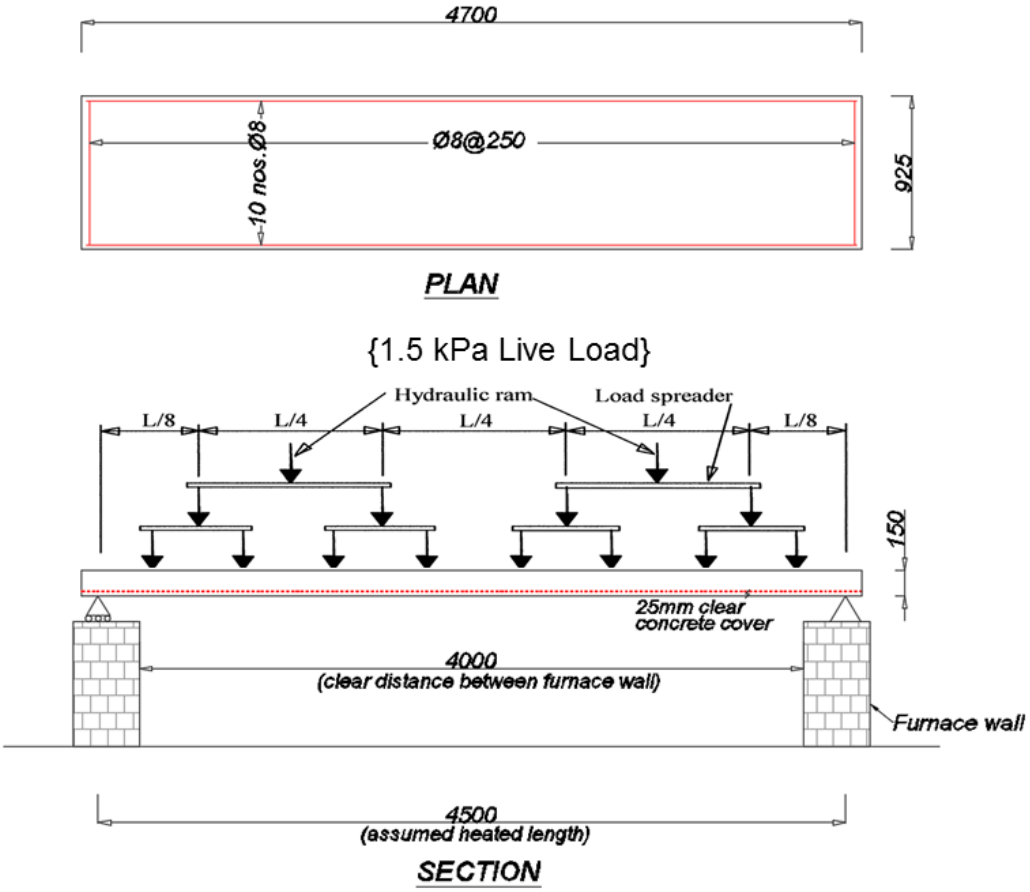

Figure 3.1: Configuration of slab tested by Cooke (2001)

3.4.2 Slab 2 - (Rickard et al., 2015)

Rickard et al. (2015) studied the practical predictive test method for the heat induced spalling of concrete. The experimental investigation involves 75 samples tested in the furnace at the Laboratory of CERIB, France, using a novel testing apparatus namely, Heat-Transfer-Rate Inducing System (H-TRIS) previously developed at The University of Edinburgh. One sample with a dimension of 4380×1450×250 denoted as P6 (Rickard et al., 2015) was selected for the study. The slab was reinforced with Ø7 bar spaced at 150 mm c/c in both longitudinal and transverse direction at the bottom and simply supported at both ends, giving a clear span of 4080 mm. No compression reinforcement was provided. 30 mm clear concrete cover was provided and the slab was exposed to ISO 834 (ISO, 1999) fires for 62 minutes. The slab was designed and tested to investigate its spalling behaviour. It was not designed for structural testing.

As a result, the only available results for comparison are in-depth temperature histories and vertical mid-span deflection. Vertical mid-span deflection measurement was done using string potentiometer gauges. No imposed mechanical applied on the slab except for the slab self-weight, making it a simple test available for modelling validation purposes. Figure 3.2 below shows the graphical configuration of the slab.

There was some light concrete spalling during the test which is not considered in the model. Consequently, there might be some inconsistency in comparing the results from the test and finite element model. However, only a qualitative assessment will be made with the objective to interrogate the capability of the model to predict the slab response.

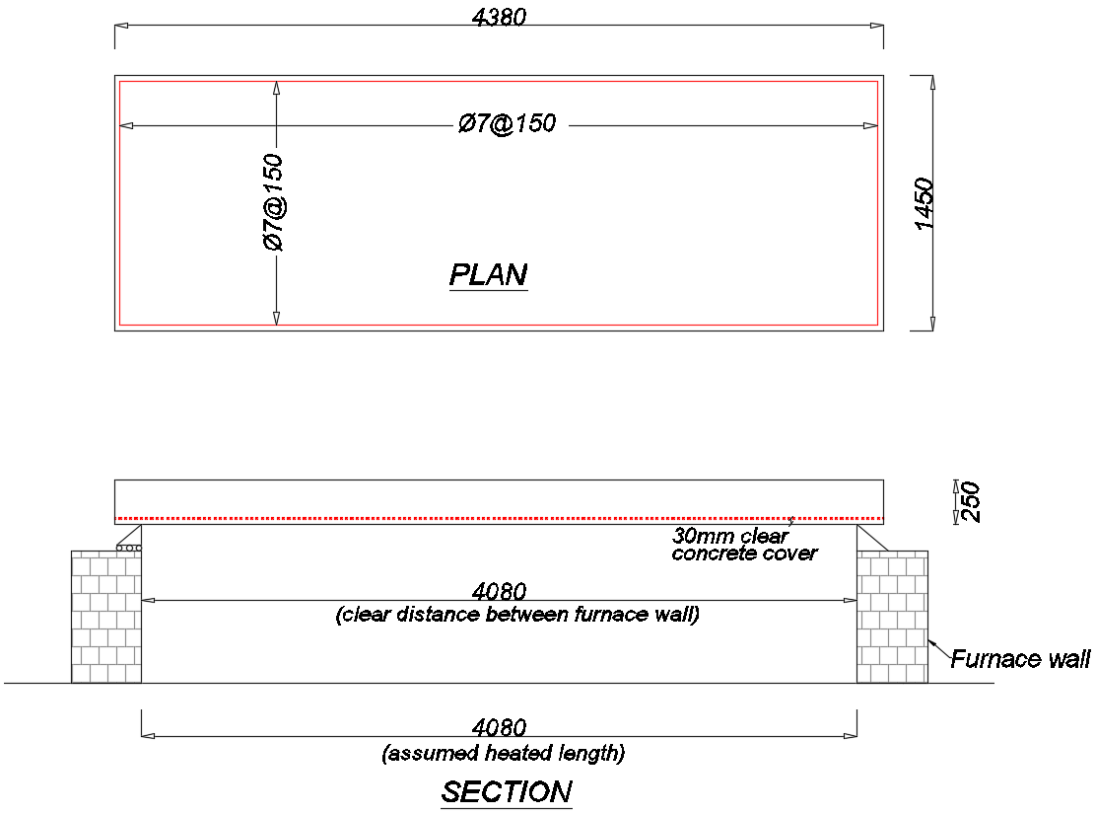

Figure 3.2: Configuration of slab tested by Rickard et al. (2015)

3.5 Material Properties

3.5.1 Concrete thermal properties

This section explains the material properties recommended by Eurocode 2 (CEN, 2004) used in the current study to carry out the heat transfer analysis.

Temperature dependent concrete density (ρ), thermal conductivity (k), and specific heat (C_p) follow the recommendations of Eurocode 2 (CEN, 2004). The influence of moisture migration during heat transfer process was not explicitly modelled in the current study. Instead, this was implicitly taken into consideration by modifying the temperature dependent properties of specific heat following recommendations from Eurocode 2 (CEN, 2004). The temperature dependent concrete density (ρ), thermal conductivity (k), and specific heat (C_p) defined in modelling Slab 1 (Cooke, 2001) and Slab 2 (Rickard et al., 2015) are shown in Figure 3.3, Figure 3.4, and Figure 3.5 respectively.

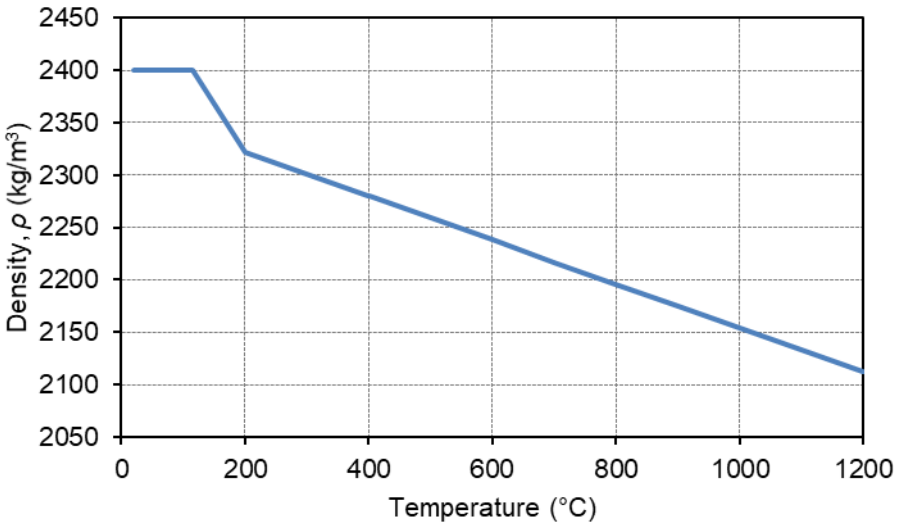

Figure 3.3: Evolution of concrete density, ρ with temperature defined for modelling Slab 1 (Cooke, 2001) **and Slab 2** (Rickard et al., 2015)

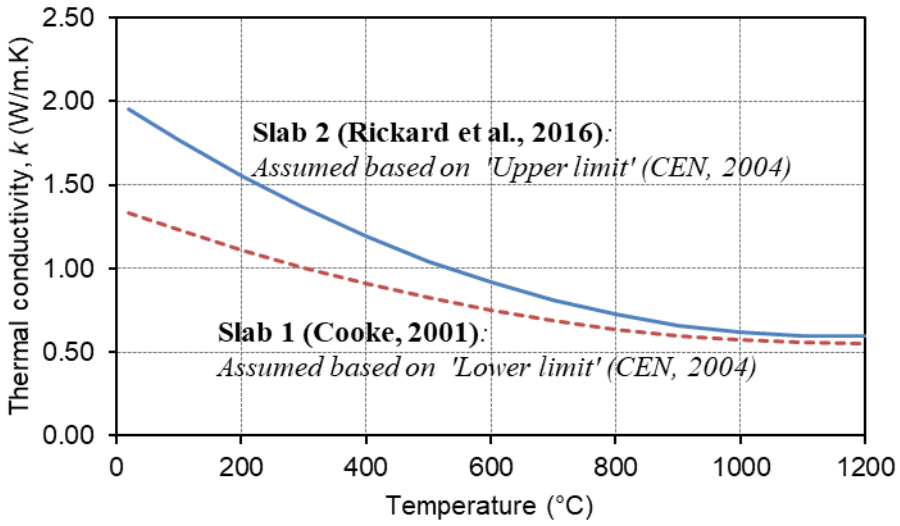

Figure 3.4: Evolution of concrete thermal conductivity, *k* with temperature defined for modelling Slab 1 (Cooke, 2001) **and Slab 2** (Rickard et al., 2015)

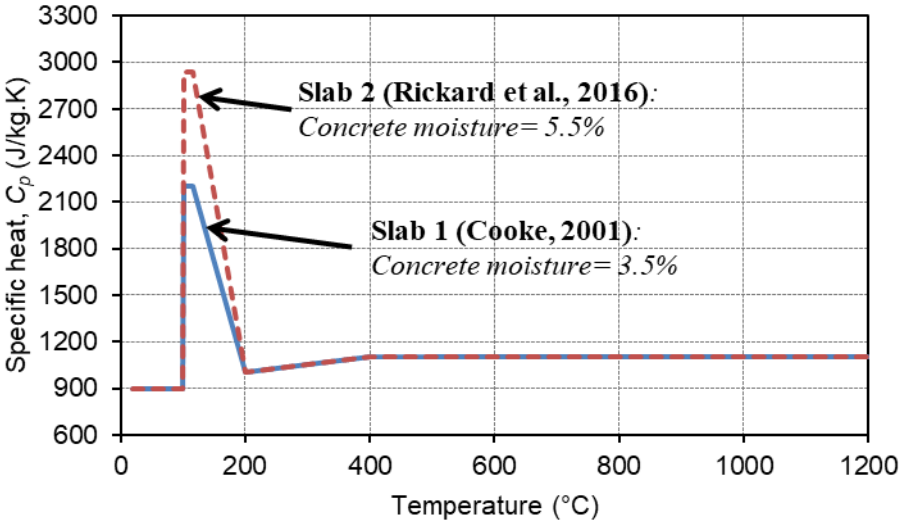

Figure 3.5: Evolution of concrete specific heat, C_p with temperature defined for modelling Slab 1 (Cooke, 2001) **and Slab 2** (Rickard et al., 2015)

3.5.2 Mechanical properties for concrete and reinforcing steels

Mechanical properties for both concrete and steel follow the recommendations from Eurocode 2 (CEN, 2004). Strain hardening was not considered in the constitutive formulation of the steel material model.

Table 3.1 shows the summary of the input mechanical properties for the models. An analysis based on these material properties will represent the base case analysis for comparison against other analysis, which will be presented in the later section of this chapter, where sensitivity of different input parameters to the predicted performance of FE model is investigated. Concrete tensile strength, F_t was defined based on the recommendations of CEB-FIP (2010).

Table 3.1: Mechanical input properties at ambient temperature assumed for 'base case' model

Parameters	Slab 1	Slab 2
Concrete compressive strength, F_c	30 MPa	50 MPa
Concrete tensile strength, F_t*	2.90 MPa	4.07 MPa
Thermal expansion (both concrete and steel)	EC 2	EC 2
Fracture energy, G_f*	135 N/m	148 N/m
Type of steel reinforcement	Hot rolled	Hot rolled
Steel reinforcement yield strength, F_y	460 MPa	450 MPa
Steel reinforcement elastic modulus, E	210 GPa	210 GPa

**Based on the recommendations from CEB-FIP (2010)*

3.5.3 Modelling tensile behaviour of concrete

In tension, concrete responses linearly up to a defined strength. When the defined strength (yield strength) is reached, cracking is triggered. This happens at integration points in the elements. Beyond this stage, cracking strain increases with the increase in tensile stress and will continue until the crack is fully opened (termed as stress-free crack opening/displacement). There are several methods available to treat this post-cracking behaviour of concrete.

Modelling post-cracking behaviour of concrete can be performed using either (1) discrete cracking, (2) embedded finite element method (EFEM of XFEM) and (3) smeared cracking approach. Smeared cracking approach is generally implemented due to its ease of application and efficient way of modelling the post-cracking behaviour. In this study, the author implemented the smeared cracking approach where the post-cracking behaviour was defined using simple linear stress-displacement relationship.

Implementation of post-cracking behaviour in finite element models using smeared cracking approach lends itself to a number of arguments regarding its accuracy to the response prediction. For instance, defining the post-cracking behaviour based on stress-strain relationship produces solution that is sensitive to the mesh size or a solution that is mesh dependent. Whereas, defining the post-cracking behaviour based on stress-displacement approach is claimed to be mesh independent (Gao et al., 2013). However, 'characteristic length' needs to be defined whenever one wants to adopt the stress-displacement approach so that the cracking strain can be calculated by the model. A report by CEB (1996) provides some recommendations on how to define the 'characteristic length' based on element sizes for both shell and solid finite elements. For instance, CEB (1996) recommends the length as square root of area for a 2-D element and cubic root of the volume for a 3-D element. In ABAQUS, for shell element, this is approximately equal to the length across an element (or simply the diagonal line based on the plan view of shell element) (ABAQUS, 2012).

Another method to estimate the crack displacement width for concrete under tensile stress is based on the work from Hillerborg et al. (1976). A fictitious crack model was proposed to define the crack displacement (width). This crack displacement approximation is based on the fracture energy theory. Fictitious crack width is a collected deformation of a band of micro cracks. In this approach, stress-free crack displacement width is defined based on the following relationship:

$$w_1 = 2\frac{G_f}{F_t} \qquad \text{Equation 3.1}$$

Where:

w_1 = stress-free crack displacement width

G_f = fracture energy

F_t = concrete tensile strength

Studies on the subject of fracture energy are widely available. Regarding fracture energy at elevated temperatures, the information is very limited. In addition, the available data for fracture energy at elevated temperatures were gathered from different testing methods and different types of test specimens. Research on fracture energy at elevated temperatures have been conducted in several studies previously (Baker, 1996; Bazant and Prat, 1988; Nielsen and Bicanic, 2003; Yu et al., 2012; Zhang and Bicanic, 2001). Indeed, tensile behaviour of concrete material at elevated temperature is a difficult problem to deal with both in the aspects of performing experimental test (for data collection) as well as implementing the behaviour into finite element models. The advent of high-performance, high-strength concrete has made the problems more difficult to understand and results from experimental tests available throughout many studies for the past 50 years have become difficult to be generalized (Bamonte and Felicetti, 2012).

In this study, the author did not consider the influence of high temperature to fracture energy values. The fracture energy was assumed as constant throughout the fire exposure. Concrete material behaviours implemented in the current study are shown in Figure 3.6 to Figure 3.10 below. The temperature dependent modulus of elasticity assumed in modelling for both Slab 1 (Cooke, 2001) and Slab 2 (Rickard et al., 2015) are shown in Figure 3.6 below. Stress versus strain (plastic) for concrete in compression is shown in Figure 3.7 for Slab 1 (Cooke, 2001) and Figure 3.9 for Slab 2 (Rickard et al., 2015). On the other hand, tensile behaviours for both modelling Slab 1(Cooke, 2001) and Slab 2 (Rickard et al., 2015) are shown in Figure 3.8 and Figure 3.10 respectively. Note that post-cracking behaviour of concrete was defined based on the work of Hillerborg et al. (1976), shown as tensile stress versus crack displacement in both Figure 3.8 and Figure 3.10.

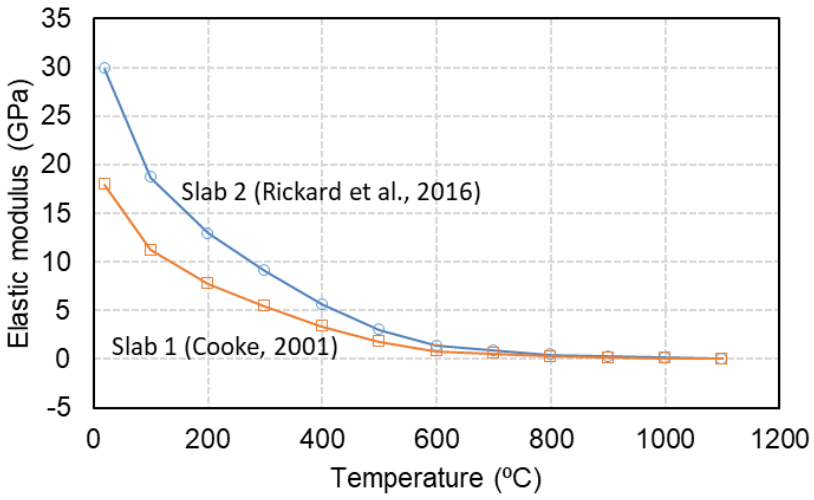

Figure 3.6: Temperature dependent elastic modulus assumed for Slab 1 (Cooke, 2001) **and Slab 2** (Rickard et al., 2015)

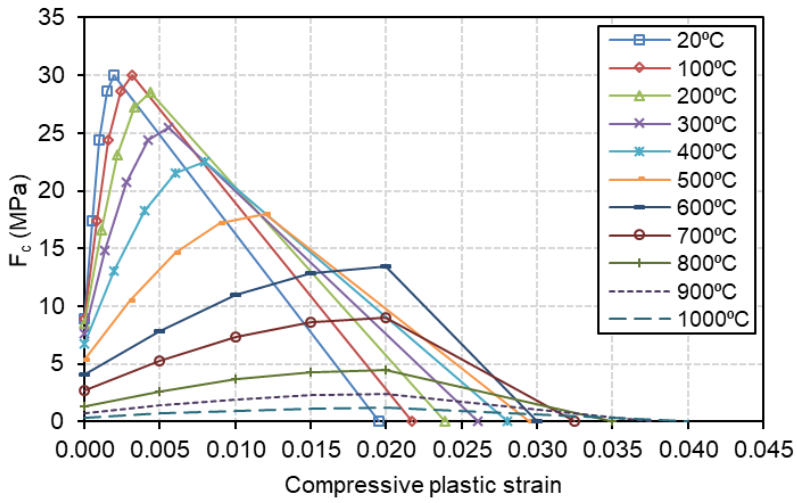

Figure 3.7: Compressive stress versus compressive plastic strain assumed and defined in modelling Slab 1 (Cooke, 2001)

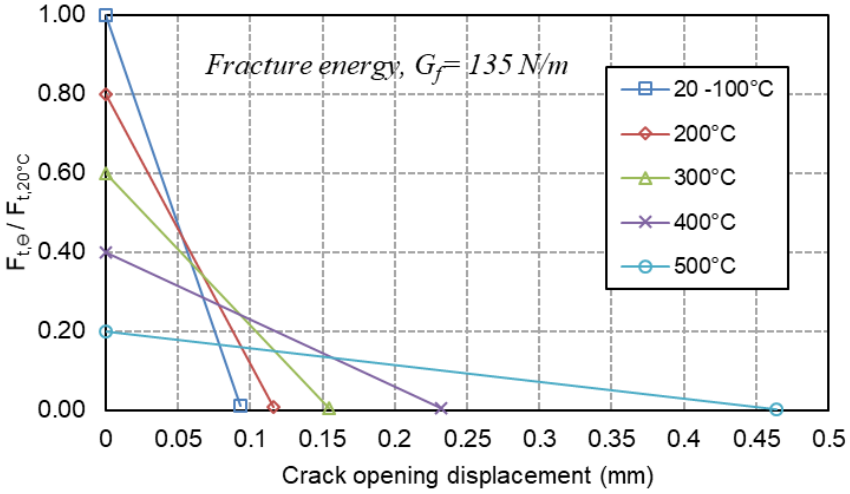

Figure 3.8: Tensile behaviour of concrete at elevated temperature assumed for Slab 1 (Cooke, 2001)**: tensile stress vs crack opening displacement**

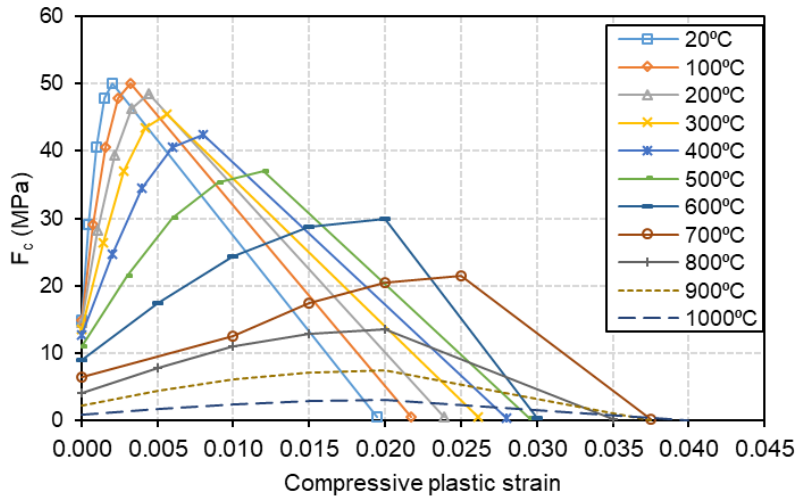

Figure 3.9: Compressive stress versus compressive plastic strain assumed and defined in modelling Slab 2 (Rickard et al., 2015)

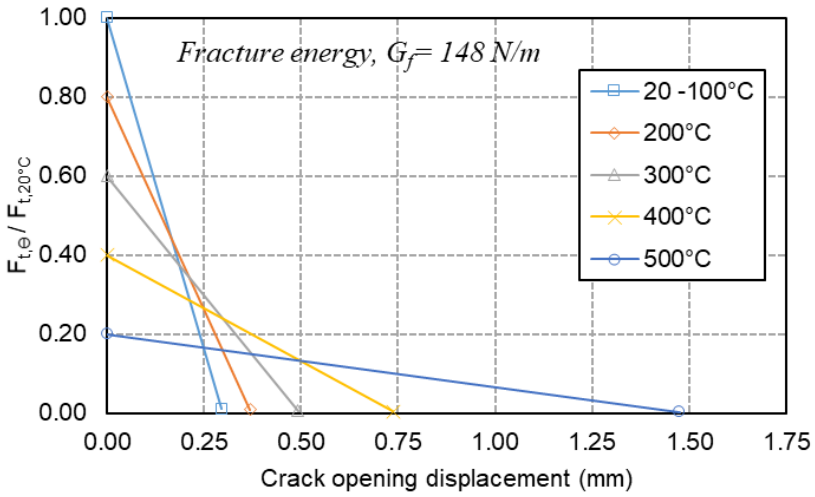

Figure 3.10: Tensile behaviour of concrete at elevated temperature assumed for Slab 2 (Rickard et al., 2015)**: tensile stress vs crack opening displacement**

3.5.4 Mesh sensitivity analysis

The previous section provides some discussion regarding the sensitivity of model prediction due to the way concrete tension behaviour is modelled. In this section, mesh sensitivity analysis is presented. Note that two (2) slabs were studied in the current chapter, Cooke (2001) and Rickard et al. (2015). However, only finite element model for the slab tested by Cooke (2001) is selected and presented here as a representative case (note that mesh sensitivity studies were carried out for all slabs in the current work) for the mesh sensitivity analysis results. This is because, slab tested by Cooke (2001) is used extensively in the thesis and will also be used later in Chapter 4. Five (5) sets of mesh sizes were selected and their corresponding predictions for mid-span deflection are shown in Figure 3.11.

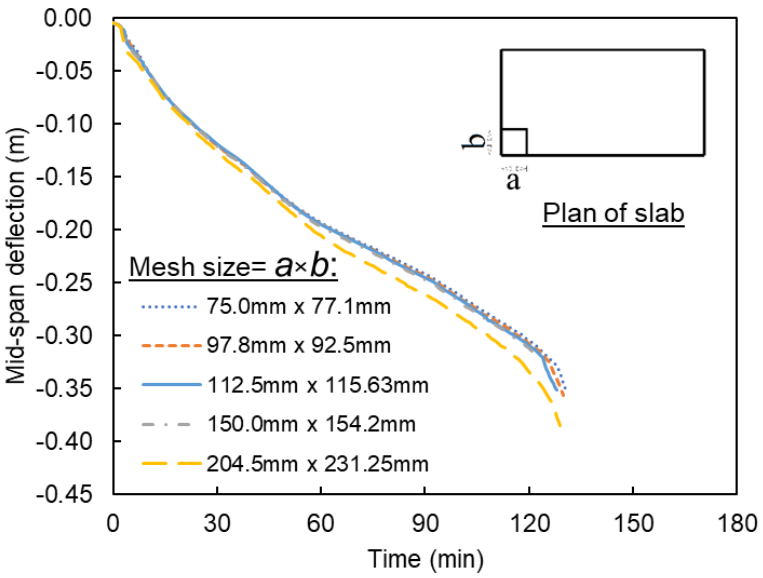

Figure 3.11: Sensitivity of selection of mesh size to the predicted mid-span deflection

With an exception of 204.5 × 231.25 mm mesh size (see Figure 3.11), all other mesh sizes selected demonstrated a converging prediction for mid-span deflection. In other words, the selection of mesh sizes (except 204.5 × 231.25 mm) produced a converge response prediction. Throughout the study presented in the current chapter and later in Chapter 4, mesh size of 112.5 × 115.63 mm was selected, as it provided almost the same mid-span deflection as the finer meshes.

3.6 Thermal analysis

1-D heat transfer analysis was performed and the temperature at every 5 mm interval was evaluated. A 4-node linear heat transfer quadrilateral (DC2D4) element available in ABAQUS (ABAQUS, 2012) was selected for the heat transfer analysis. It is a plane strain/stress element, also available for thermal analysis. As the name implies, the element has infinite thickness in the longitudinal dimension. There is no heat transfer occurring in the plane of the element. This formulation of element is capable of modelling a 2-D heat transfer analysis but for the current heat transfer analysis, only 1-D heat transfer was assumed.

Within the slab depth, the heat transfer process was done via conduction. Fourier's Law describes time dependent temperature distribution in the slab. Heat exchange at boundary surface between gas temperatures or ambient and the concrete surface occurs via convection and radiation. This is approximated by the means of the Robin boundary condition (Purkiss and Li, 2013):

$$-k\frac{\partial T}{\partial n} = h_c\left(T - T_f\right) + \sigma \varepsilon_m \varepsilon_f [(T - T_z)^4 - \left(T_f - T_z\right)^4] \qquad \text{Equation 3.2}$$

Where h_c is convective coefficient, σ is the *Stefan Boltzmann* constant equals to 5.67×10^{-8} W/m^{2}K^4. $\mathcal{E}_m$ and $\mathcal{E}_f$ are the concrete member surface emissivity and fire emissivity respectively. T_f and T_z are fire (gas) temperature and absolute zero temperature respectively. n is the outward normal direction of the slab's surface. Coefficient of convection at the exposed surface and unexposed surface were defined as 25 W/m^2.K and 9 W/m^2.K respectively. The radiative heat flux was calculated using a concrete emissivity, $\mathcal{E}_m$ value of 0.8. Emissivity of fire was assumed as 1.0 as recommended by Eurocode 1 (CEN, 2002a). The existence of steel reinforcement was neglected during the heat transfer analysis.

3.6.1 Slab 1

For the current base case analysis, moisture content was defined as 3.5%, and a lower limit of thermal conductivity value specified in Eurocode 2 (CEN, 2004) was adopted. The lower limit thermal conductivity value was selected because the preliminary analysis suggested that the predicted temperatures were far greater than the reported measured temperatures by Cooke (2001). Therefore, adopting a lower thermal conductivity value was decided for the current base case analysis.

Figure 3.12 shows the comparison between the predicted temperatures and reported temperature histories from Cooke (2001) while Figure 3.13 shows the comparison of temperature profiles in the slab's depth between the model and test results. In Figure 3.12, *Test 0*, *Test 50*, *Test 100*, and *Test 150* denote the reported temperatures (Cooke, 2001) at 0 mm (exposed surface), 50 mm, 100 mm, and 150 mm from the surfaces of

exposures respectively. Predicted temperatures at similar locations are denoted as *Model 0*, *Model 50*, *Model 100*, and *Model 150* respectively. Significant differences between the predicted temperatures and measured temperatures especially at the exposed surface and 50 mm from the exposed face were observed. Reasonably good agreements were found at 100 mm and 150 mm (unexposed surface).

Table 3.2 presents the difference between temperature prediction and measured temperatures. Temperature difference at the fire exposed surface between the model prediction and test results were calculated as 458 °C, 427 °C, 416 °C, and 358 °C at 30 mins, 60 mins, 90 mins, and 120 mins respectively. As the temperature difference between model prediction and test results is huge, it is therefore not appropriate to only input these temperatures into a structural model later in the Section 3.7.1. As such, two (2) models were developed in the section. First slab model will be heated using temperatures calculated from the heat transfer analysis presented here while in the second model, measured and reported temperatures (Cooke, 2001) were directly inputted into the model.

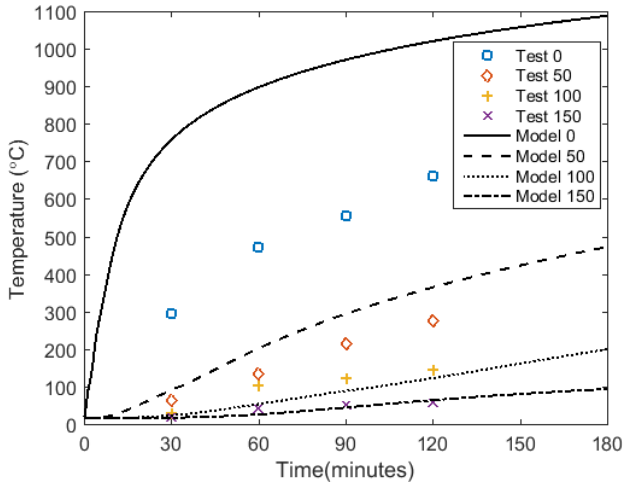

Figure 3.12: Comparison of predicted temperatures and measured temperatures (Cooke, 2001)

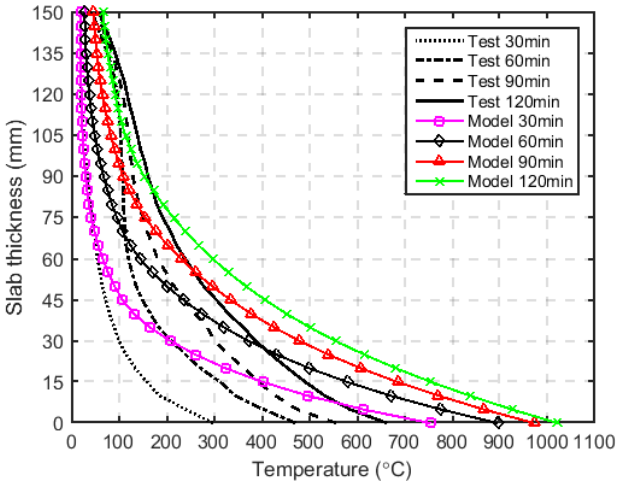

Figure 3.13: Temperature profile at 30 mins, 60 mins, 90 mins, and 120 minutes exposure (Prediction VS Test)

Table 3.2: Comparison of predicted temperatures against test results (Cooke, 2001) **at selected duration of fire exposures**

Duration	Distance from fire exposure surface	Temperatures		
		Test (°C)	Model (°C)	Difference (°C)
30 minutes	0 mm	299	757	458
	50 mm	66	92	26
	100 mm	29	26	-3
	150 mm	20	20	0
60 minutes	0 mm	473	900	427
	50 mm	137	205	68
	100 mm	106	56	-50
	150 mm	44	29	-15
90 minutes	0 mm	558	974	416
	50 mm	217	297	80
	100 mm	123	92	-31
	150 mm	53	47	-6
120 minutes	0 mm	665	1023	358
	50 mm	279	368	89
	100 mm	146	126	-20
	150 mm	58	67	9

Performing heat transfer analysis for concrete elements is not a straightforward task. Concrete is a mixture of cements, aggregates, sand and water. Each of them has different thermal properties and behaviour. Water evaporates when heated beyond its boiling temperatures. During exposure to fires, water tends to shy away from fires, introducing pressure in the concrete pores.

Most commonly, the disagreement between model predictions and measured temperatures occurs at the boundary surface i.e. the exposed and unexposed surface of the concrete elements. This is where the concrete surface interacts with fires and/or ambient air. Interaction between flames and the concrete surfaces of an element is influenced by uncertainties that are not easily characterised.

Lie and Williams-Leir (1979) claimed that heat transfer process in furnace is generally less intense than the one in large real fires. According to them, this is because, in furnace, fire is less luminous with less thickness than in real fires, making the heat transfer process significantly influenced by the radiation from furnace walls cooler than the gases. They also attempted to eliminate this effect in their studies by installing electrically heated heat resistance steel plates where these plates were kept at temperatures equal to the gas temperatures. Simultaneously, these steel plates provided heat and followed the defined fire curve to load the specimens.

The tested 800 mm × 900 mm slab with 150 mm thickness (similar to the slab's thickness considered in the current study) yielded temperatures in excess of 900 °C during 120 minutes of exposure, occurring at the exposed surface. This contradicts the furnace test specimen by Cooke (2001), which was selected for the current study where the measured and reported temperature is approximately 665 °C also at the same time and location. Note that the plan dimension of the two samples are different, however, this is not relevant as the heat transfer was assumed as a 1-D process. Also, fire curve for Lie and Williams-Leir (1979) samples followed the ASTM E119 standard curve (ASTM, 1985) while Cooke (2001) followed those of ISO 834 (ISO, 1999) fires. Table 3.3 shows some comparison of measured temperatures at the exposed surface of furnace tested concrete slabs exposed to ISO 834 (ISO, 1999) reported by different authors.

It is also worth mentioning that installing and placing thermocouples exactly at the exposed surface is not an easy task. As concrete has low thermal conductivity value, a difference of 5 mm in placing the thermocouples would result in significant variation in measured temperatures from the thermocouples (at the exposed surface). Therefore, it is extremely important to know exactly whether the thermocouples are placed

correctly at their intended location and whether the concrete casting process has potentially dislocated the thermocouples due to poor workability of the concrete and excessive vibrating. If the thermocouples are dislocated, this should be properly addressed and reported in the documents/paper. However, it must be acknowledged that this task is far from easy. 5 mm difference cannot be easily visualised with the naked eye and human error factors always play a part in the process.

Table 3.3: Some comparison of temperature at the exposed surface for furnace tested concrete slabs

Author(s)	Slab's dimension (l) × (w) × (h)	Reported temperature at exposed surface for the 120 minute exposure to standard ISO 834 fire (°C)
(Cooke, 2001)	4700×925×150	665*
(Lim and Wade, 2002)	4300×3300×100	≥ 900
(Zhang et al., 2014)	6660×5000×120	672*
(Wang et al., 2016)	3300×3300×100	658-737(4 samples)

**Values are traced from graphs in the original paper*

Eurocode 1 (CEN, 2002a), Eurocode 2 (CEN, 2004), and Eurocode 4 (CEN, 2005) provide recommendations on the selection of the appropriate range of parameters so that the heat transfer analysis can be performed as simple as possible. This is important especially in practising structural fire engineers as well as researchers to some extent. However, no studies conducted so far to gauge the sensitivity of the range of recommended thermal properties recommended in the code (CEN, 2005, 2004, 2002a) in order for the user to get a sense of confidence in choosing a reasonable range of parameters. Section 3.7.1.4 presents sensitivity studies on how the selection of these values influence the predicted temperatures.

3.6.2 Slab 2

A similar analysis method in Section 3.6.1 is repeated here to model the heat transfer analysis for the case slab tested by Rickard et al. (2015). Therefore, a detailed explanation on the procedures will not be repeated.

Figure 3.14 presents a comparison of predicted temperatures against the measured and reported temperatures from the test. The comparison herein was made at 1 mm, 10

mm, 20 mm, and 50 mm from exposed surface. The gas temperature measured during the test was also plotted and compared against the gas temperature calculated from ISO 834 (ISO, 1999) fire curve.

The predicted temperatures compared well with the measured temperatures. Therefore, these temperatures will be used as input temperature loads in the subsequent mechanical analysis for Slab 2.

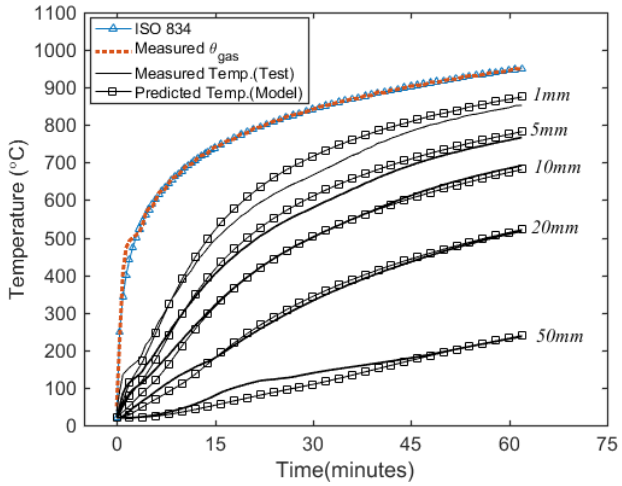

Figure 3.14: Comparison of predicted temperatures against test results

3.6.3 Sensitivity studies

The sensitivity of model prediction to input parameters is studied in this section using Slab 1, since this slab is more representative of the one-way spanning slabs designed in real buildings; it was specifically designed for the structural fire testing to have 90 minutes of 'fire resistance' based on the UK guidance (Morris et al., 1988). In addition, results from the heat transfer analysis for this slab was found to differ significantly from the measured temperatures (Cooke, 2001).

A total of 16 cases were investigated. The purpose of the analysis is to show the sensitivity of varying input parameters such as thermal conductivity, moisture content, and heat transfer parameters (convective coefficient and emissivity) to the predicted temperatures. Table 3.4 shows the selected properties together with their corresponding notes in the last column.

Additional cases (No. 15 and No. 16 in Table 3.4) are included to demonstrate the highest and lowest possible temperature predictions, judging from the earlier 14 cases. In these two analyses, parameters were simply selected and stacked up with the intention to predict the highest and lowest possible temperatures.

In all the analyses, their corresponding mid-span deflection was included whenever relevant. This was done to demonstrate the extent at which these temperature prediction variation has to the structural behaviour of the slab.

Table 3.4: Summary of selection of material and heat transfer thermal input properties

No.	Material thermal properties		Heat transfer parameters				Notes
	k	Moisture (%) - C_p	h_{exp}	$h_{un\text{-}exp}$	$\mathcal{E}_{exp}$	$\mathcal{E}_{un\text{-}exp}$	
	Lower	**3.5**	**25**	**9**	**0.8**	**0.8**	Base case
1	**Upper**	*Base*	*Base*	*Base*	*Base*	*Base*	Influence of k
2	*Base*	**0**	*Base*	*Base*	*Base*	*Base*	Sensitivity of moisture content
3	*Base*	**2**	*Base*	*Base*	*Base*	*Base*	
4	*Base*	**4**	*Base*	*Base*	*Base*	*Base*	
5	*Base*	**6**	*Base*	*Base*	*Base*	*Base*	
6	*Base*	*Base*	**10**	*Base*	*Base*	*Base*	Sensitivity of convective coefficient, h
7	*Base*	*Base*	**20**	*Base*	*Base*	*Base*	
8	*Base*	*Base*	**30**	*Base*	*Base*	*Base*	
9	*Base*	*Base*	**40**	*Base*	*Base*	*Base*	
10	*Base*	*Base*	**50**	*Base*	*Base*	*Base*	
11	*Base*	*Base*	*Base*	*Base*	**0.6**	*Base*	Sensitivity of emissivity, $\mathcal{E}$
12	*Base*	*Base*	*Base*	*Base*	**0.7**	*Base*	
13	*Base*	*Base*	*Base*	*Base*	**0.9**	*Base*	
14	*Base*	*Base*	*Base*	*Base*	**1.0**	*Base*	
15	***Upper***	***0***	***50***	*Base*	**1.0**	*Base*	Hottest
16	*Base*	***6***	***10***	*Base*	**0.6**	*Base*	Coolest

**Base – identical properties as in 'base case' analysis were selected*

Figure 3.15 shows the temperature predictions for all cases specified in Table 3.4. Note that the curve for the highest and lowest (case No. 15 and No. 16) temperatures were plotted with slightly thicker lines for clarity purposes. Measured temperatures from the test (Cooke, 2001) were also included for comparison.

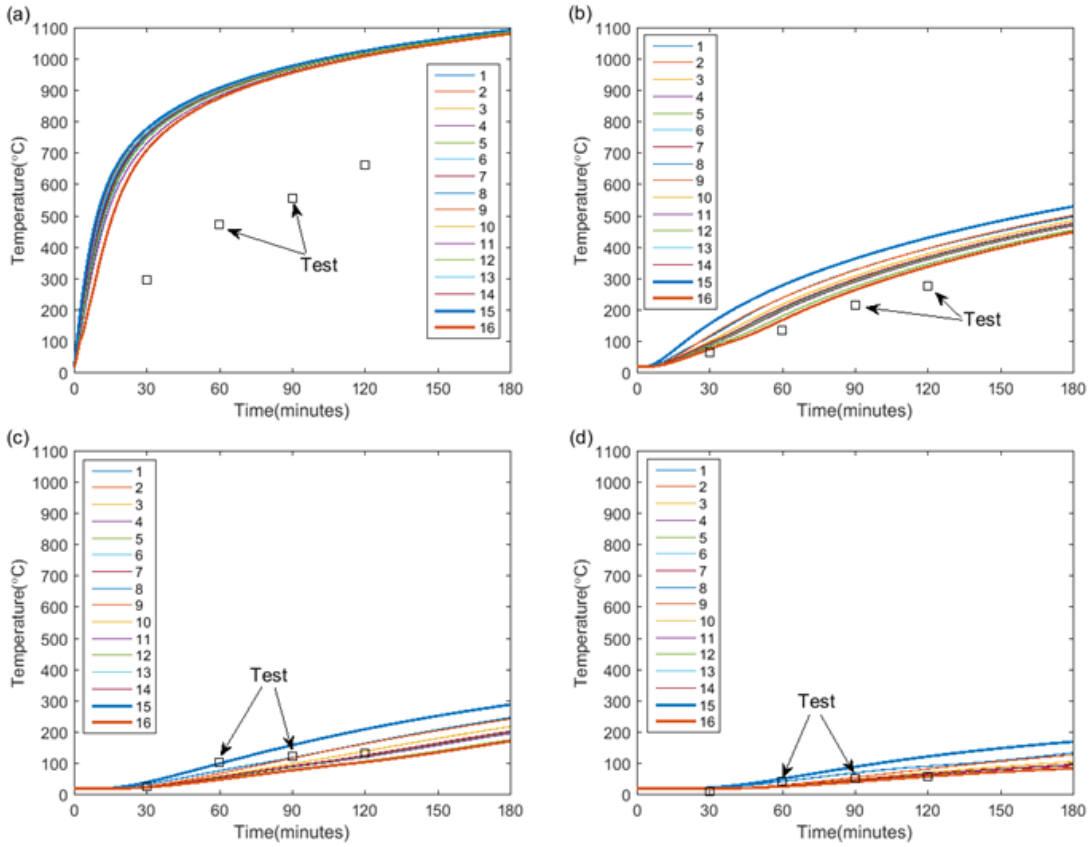

Figure 3.15: Temperature predictions with different thermal properties at (a) exposed surface, (b) 50 mm, (c) 100 mm, and (d) 150 mm from exposed surface

As discussed in the earlier section of the chapter, predicted temperatures at the exposed surface differ significantly from the measured temperatures. At other locations, the differences are not that significant. Prediction from case *No. 16* (Table 3.4) seems to match quite well with the measured temperatures at 50 mm, 100 mm, and 150 mm from the surface of exposure.

Individual comparison for the predicted temperature histories with varying thermal input parameters against 'base case' (see Table 3.4) is presented and discussed in the following section.

3.6.3.1 Thermal conductivity (*k*) value

Eurocode 2 (CEN, 2004) specifies two curves for the temperature-dependent concrete thermal conductivity values, the lower limit and upper limit in which both are non-linear with temperature. In this section, the sensitivity of these two limits is investigated.

Figure 3.16(a) below shows the comparison of temperature-time histories for the slab modelled with the lower and upper limit of concrete thermal conductivity values. The comparison is made at the exposed surface, 50 mm, 100 mm, and 150 mm from the exposed surface. Figure 3.16(b) shows the temperature profiles in the slab depth of the similar model.

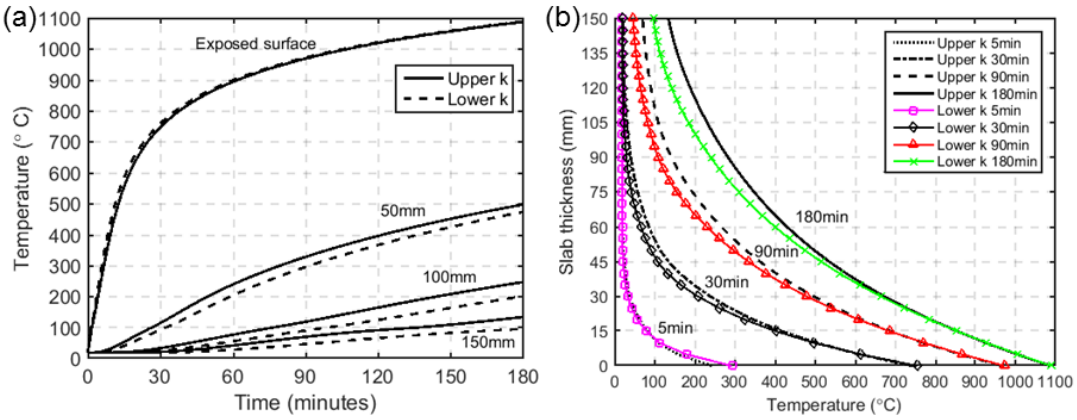

Figure 3.16: Comparison of the predicted temperatures using lower and upper limit of thermal conductivity values (a) temperature-time histories (b) temperature profile at 5 mins, 30 mins, 90 mins, and 180 mins of exposure

No significant difference on the temperature prediction was observed when either the lower or upper limit of the thermal conductivity value was used in the heat transfer analysis. At the exposed surface, a higher temperature was predicted for the slab modelled with lower thermal conductivity value during the first 60 minutes of exposure. With a lower thermal conductivity value defined, a longer time was required for the heat to absorb into the slab's thickness which might explain why the temperature at the exposed surface was higher when the lower limit thermal conductivity value was used in the model.

Comparison at 50 mm, 100 mm, and 150 mm from the exposed surface obviously showed higher temperature predictions with an upper limit thermal conductivity value. Throughout 180 minutes of exposure to fire, the difference between the temperature prediction using the lower and upper limit thermal conductivity was found to be less than 50 °C (specifically in this study, the maximum value found is 47 °C).

Mid-span deflection

As mentioned in the previous thermal analysis section, using either lower limit of thermal conductivity or upper limit produces a difference in temperature results of less than 50 °C. In this section, the sensitivity of these two limits of concrete thermal conductivity to the predicted mid-span deflection is presented.

Obviously, more deflection is found for slabs heated with temperatures predicted using the upper limit of the thermal conductivity value. However, this difference is not significant and can be concluded that using either limit will not significantly influence the deformation behaviour of the slab. Figure 3.17 shows this comparison together with test results. If the mid-span deflection is set as the slab's performance indicator, varying concrete thermal conductivity values will have extremely minimal effects to the fire resistance rating for the current slab.

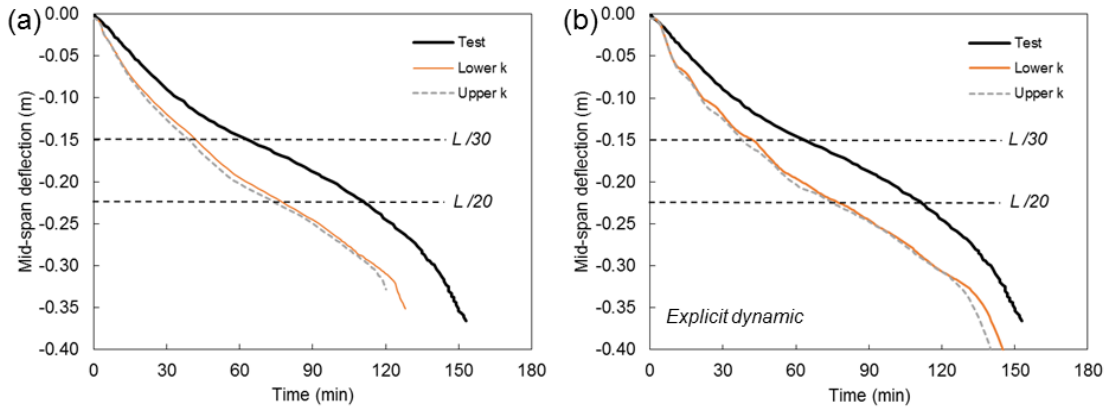

Figure 3.17: Prediction of mid-span deflection using the temperature load predicted with the upper and lower limit of concrete thermal conductivity, *k* (a) implicit static analysis and (b) explicit dynamic analysis

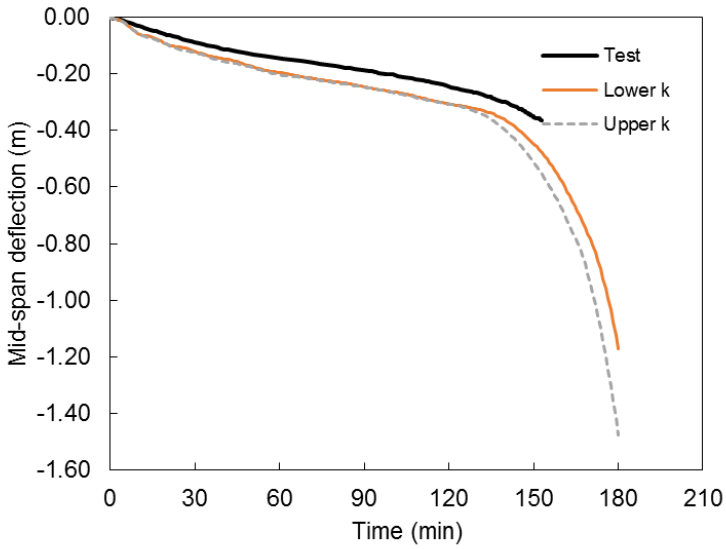

Figure 3.18: Overall prediction of mid-span deflection using the temperature load predicted with the upper and lower limit of concrete thermal conductivity, *k* from explicit dynamic analysis

3.6.3.2 Moisture content

Existence of moisture in concrete makes heat transfer analysis for concrete elements more challenging. Mass transfer or moisture migration must be addressed in heat transfer analysis for concrete elements to obtain accurate results.

Eurocode 2 (CEN, 2004) provides a simplified way to mimic and capture this moisture migration influence in a heat transfer analysis by modifying specific heat properties of the concrete. Temperature dependent specific heat in Eurocode 2 (CEN, 2004) suggests a sudden spike of specific heat when temperature in the concrete is at 100 °C. Between 100 °C to 115 °C, the high value is constant and thereafter reduces linearly from 115 °C to 200 °C. The magnitude of the sudden increase depends on the moisture content in the concrete.

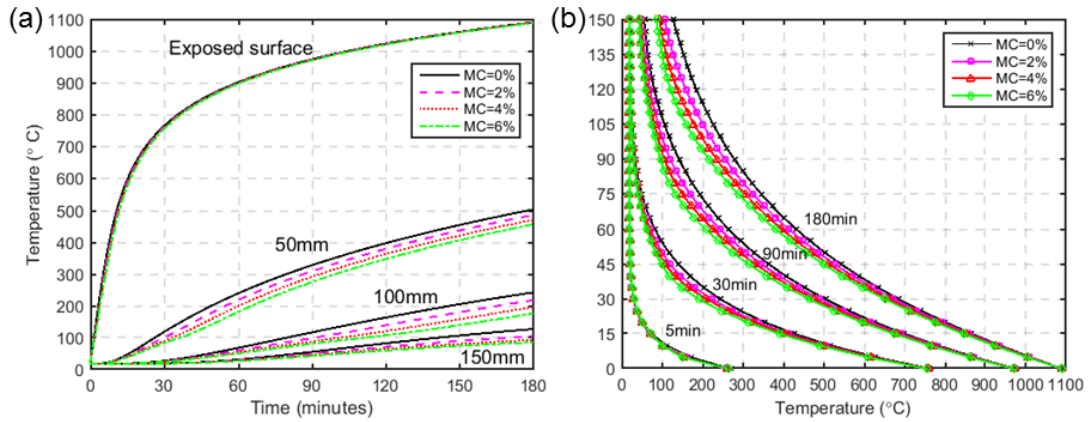

Figure 3.19: Comparison of predicted temperatures with varying moisture content values (a) temperature-time histories (b) temperature profile at 5 mins, 30 mins, 90 mins, and 180 mins of exposure

Figure 3.19(a) shows the comparison of predicted temperature-time histories while Figure 3.19(b) shows the predicted temperature profile during 5 mins, 30 mins, 90 mins, and 180 mins of exposure for concrete with different moisture content. Moisture content of concrete does not seem to affect the heat transfer process during the first 5 minutes of exposure. In Figure 3.19(b), the temperature increase trend was moving away from the location of 0 mm (exposed surface) towards 150 mm (unexposed surface) as the heating time progressed. This seems to agree that, during the fire test, the water in the concrete pores tend to move away from the heating source. Consequently, manipulating the specific heat properties of concrete as suggested in the Eurocode 2 (CEN, 2004) which would enable moisture migration in the concrete to be determined rather accurately.

The temperature prediction difference between the heat transfer modelled using 0% (dry concrete) and 6% moisture was found to be less than 67 °C throughout the 180 minutes of exposure. Maximum difference in temperature was found at the depth of 120 mm from the fire-exposed surface, occurring during the 180 minutes of exposure to fire and the value was 67°C. For every 0%, 2%, 4%, and 6% of moisture in the concrete, the temperature prediction difference was approximately less than 30 °C.

Mid-span deflection

In the previous thermal analysis section, sensitivity of different concrete moisture content to the predicted temperature histories and temperature profile of the slab were presented. Moisture content in the range of 0% to 6% was selected. Concrete with 0% moisture (dry concrete) showed a higher temperature prediction than the rest i.e. 2%, 4%, and 6%.

The effect of higher temperature for the case of 0% moisture was reflected in the mid-span deflection prediction shown in Figure 3.20 below. Consequently, runaway deflection occurred much earlier for the case of 0% moisture content as compared to the model with 6% moisture. Runaway deflection occurred during the 113 minutes of exposure for the case of 0% moisture while for the case of 6% moisture, runaway started at 130 minutes of exposure to fire. Similar to the analysis presented for the base case analysis (presented later in Section 3.7.1), the analysis in this section was also terminated pre-maturely due to numerical instability. This issue will be discussed in detail in Section 3.7.1.5.

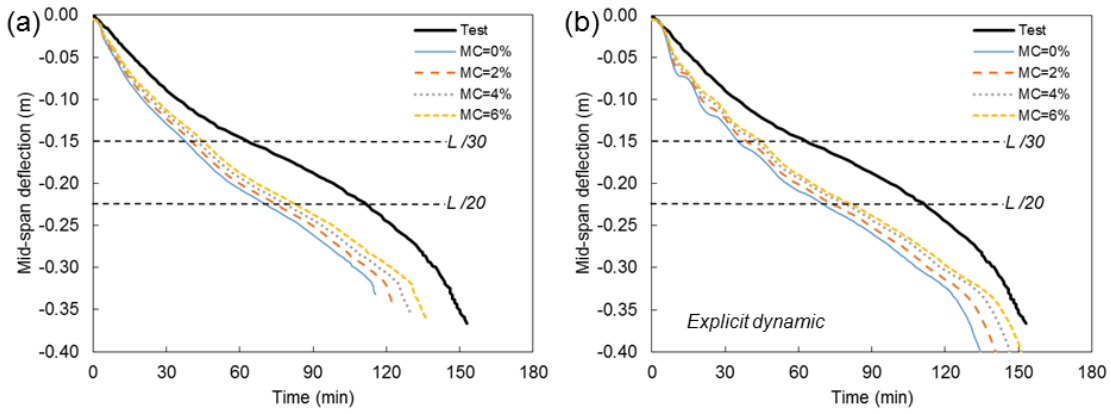

Figure 3.20: Prediction of mid-span deflection using temperature load predicted with different moisture content (a) implicit static analysis and (b) explicit dynamic analysis

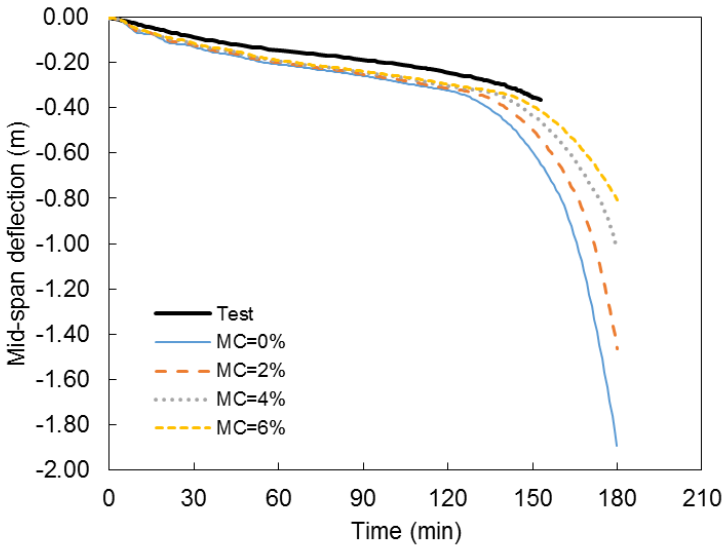

Figure 3.21: Overall prediction of mid-span deflection using temperature load predicted with different moisture content from explicit dynamic analysis

As opposed to the thermal conductivity value, moisture content has a more profound influence on the prediction performance of the finite element model. However, as explained earlier in the thermal analysis section, capturing moisture migration behaviour during heat transfer analysis is still far from easy. If this is to be translated into the structural response of the slab under consideration, it explains why during the very early stage of heating i.e. first 5 minutes, mid-span deflection for all the analysis cases (moisture content 0%, 2%, 4%, and 6%) were almost identical (refer Figure 3.20). Within the internal depth, in all cases, the temperature was not high enough (less than 100 °C) to cause the moisture movement in the slab depth. Referring to Figure 3.19(b), note that the temperature profiles in the slab during the 5 minutes of exposure for all the cases were almost identical.

If for the current slab under consideration, failure was to be defined based on runaway deflection criteria, slab modelled with 6% moisture would have failed 17 minutes later than the slab modelled with 0% moisture contents. It is worth mentioning that this slab was designed to have 90 minutes of fire resistance (Cooke, 2001) based on UK Regulatory Guidance (Morris et al., 1988).

3.6.3.3 Coefficients of convection

For the case of structural elements exposed to standard ISO 834 (ISO, 1999) fire, Eurocode 1 (CEN, 2002a) recommends a coefficient of convection of 25 W/m^{2}K at the surface exposed to fire. For more severe fire curve, for instance Hydrocarbon (CEN, 2002a) fire, the recommended convective coefficient is 50 W/m^{2}K. For both fire curve, the convective coefficient for the unexposed surface is 4 W/m^{2}K whenever heat transfer by radiation is assumed not to occur at the particular location. Whenever the effect of radiation is taken into consideration, the coefficient should be 9 W/m^{2}K (CEN, 2002a).

In this section, the influence of differing values of convective coefficient at the exposed surface to the heat transfer process is investigated. At the unexposed surface, the coefficient was fixed at 9 W/m^{2}K. The intention was to provide some simple information to non-experts in the field on heat transfer analysis as to whether varying these convective coefficient values would have any significant impact on the predicted temperatures.

Figure 3.22 shows the temperature-time histories predicted at the exposed surface for the slab modelled with 10, 20, 30, 40, and 50 W/m^{2}K convective coefficients. A similar plot, but only a close-up during the first 60 minutes of exposure is shown in Figure 3.23. In general, varying the convective coefficients does not have significant effect on the predicted temperatures throughout the fire duration. Slight difference can only be seen during the first 30 minutes of exposure as shown in Figure 3.23.

As a rough estimation, the temperature difference for the model developed using convective coefficients of, h = 50 W/m^{2}K and h = 10 W/m^{2}K were found to be less than 100 °C. In addition, varying the convective coefficients only affected the prediction during the first 30 minutes of exposure. In contrast, varying concrete emissivity value, which will be discussed in the following section, affected the temperature prediction up to 60 minutes of exposure to fires. This seems to agree with the general understanding in the field of heat transfer knowledge that the influence of radiation is more dominant at a later stage in the heat transfer process whereas the

influence of convection would not affect the heat transfer process after a certain period of fire exposure.

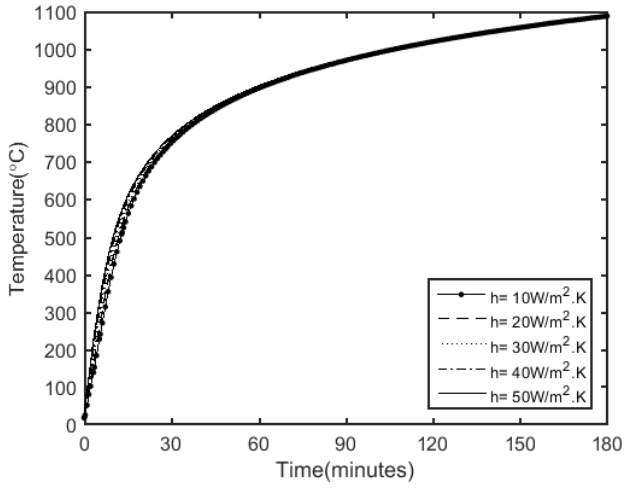

Figure 3.22: Predicted temperatures at the exposed surface using different values of convective coefficients, *h*

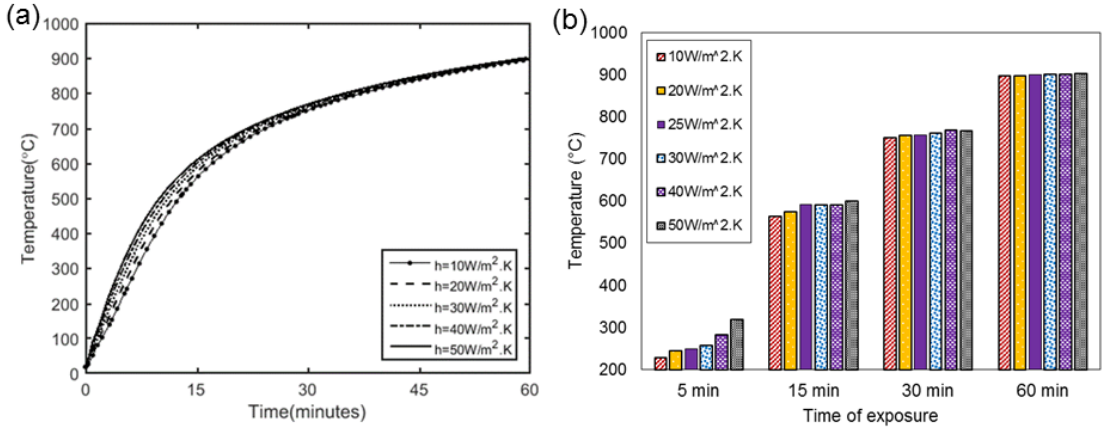

Figure 3.23: (a) Close-up plot of temperatures at the exposed surface and (b) bar chart showing temperature differences at the exposed surface for slab modelled with varying coefficients of convection during the first 60 minutes of exposure

3.6.3.4 Concrete emissivity

In estimating heat flux resulting from radiation, emissivity of fire exposed surface, $\mathcal{E}_m$ and emissivity of fire, $\mathcal{E}_f$ have to be taken into consideration. Eurocode 1 (CEN, 2002a) suggests value for $\mathcal{E}_m$ and $\mathcal{E}_f$ to be taken as 0.8 and 1.0 respectively. In this section, the effect of varying the value $\mathcal{E}_m$ to the temperature prediction at the exposed surface of the slab is investigated. Throughout the analysis, emissivity of fire was fixed at 1.0. Value of $\mathcal{E}_m$ in the range of 0.6 to 1.0 was selected. Figure 3.24 shows the predicted temperature-time histories at the exposed surface throughout the fire duration while Figure 3.25 shows a close-up of similar plot for the first 60 minutes of fire exposure.

$\mathcal{E}_m$ of 1.0 and $\mathcal{E}_m$ = 0.6 gave a temperature difference of less than 100°C. The difference is more profound between the 10 minutes to 20 minutes of exposure to fire. As opposed to convective coefficient, varying values of emissivity affected the temperature prediction up to 120 minutes of fire exposure even though it was not so significant beyond 60 minutes of fire exposure.

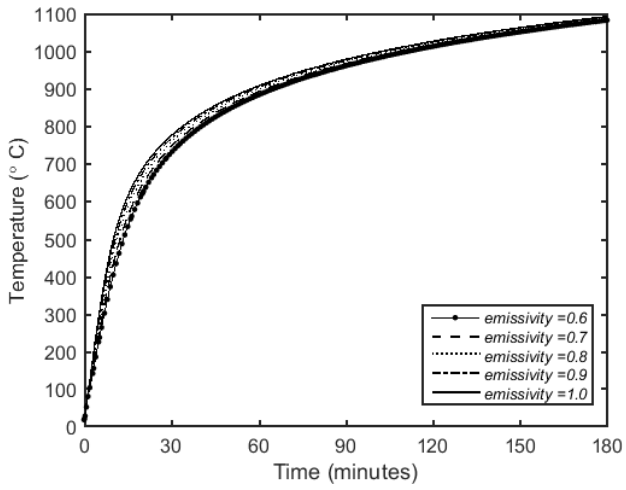

Figure 3.24: Predicted temperatures at the exposed surface using different concrete emissivity values, $\mathcal{E}$

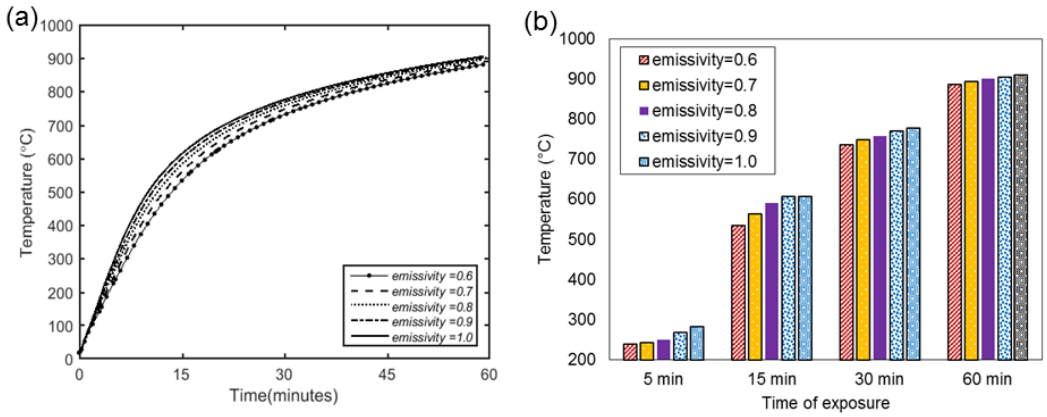

Figure 3.25: Close-up plot of temperatures at the exposed surface and (b) bar chart showing temperature differences at the exposed surface for slab modelled with varying concrete emissivity values during the first 60 minutes of exposure

3.6.3.5 Hottest and coolest thermal properties

Referring to Table 3.4, the predicted temperatures resulting from thermal properties as in case *No. 15* (noted as 'hottest' in the table) and *No. 16* (noted as 'coolest' in the table) are presented in this section and shown in Figure 3.26(a). The maximum difference in the predicted temperature histories was found to be 189 °C, occurring at 8.5 minutes of exposure at the exposed surface. Second highest was at 25 mm from the surface of exposure occurring at 22 minutes of exposure.

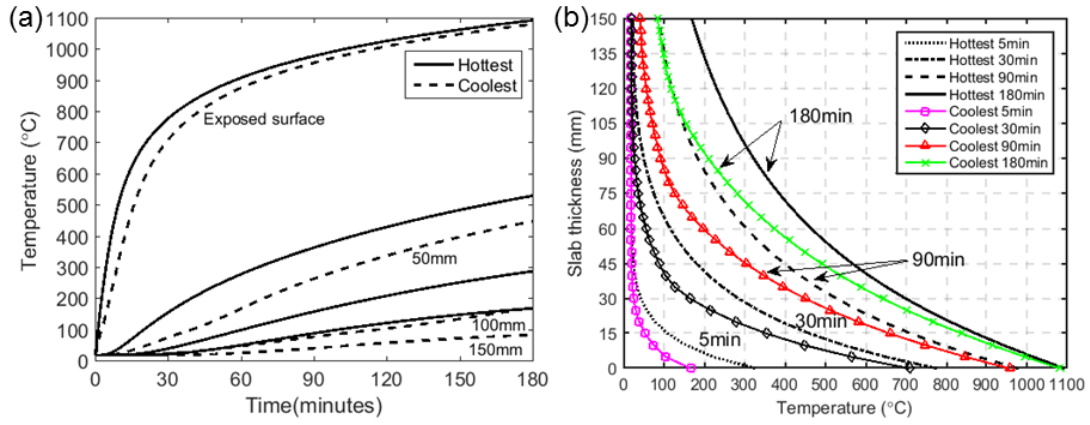

Figure 3.26: Comparison of predicted temperatures using 'hottest' and 'coolest' thermal properties (a) temperature-time histories (b) temperature profile at 5 mins, 30 mins, 90 mins, and 180 mins of exposure

Mid-span deflection

The corresponding mid-span deflections for the slab loaded with temperatures resulting from 'hottest' and 'coolest' thermal input properties are presented in Figure 3.27 below. Figure 3.27 demonstrates that the mid-span deflection predicted for the slab loaded with temperature from the 'coolest' thermal properties gave the closest prediction to match the test results.

It is plausible that, given the fact that the comparison of temperature prediction (from the 'coolest' thermal properties) against the test results (refer Figure 3.15) did not compare well at the exposed surface, but here the mid-span deflection compared quite well with the test result. In addition, the comparison of temperature prediction at other locations i.e. 50 mm, 100 mm, and 150 mm showed differences between the reported temperatures (Cooke, 2001) and the predicted temperatures were within reasonable range. This again, led us to think that for some reason, the measurement and recording of temperatures at the exposed surface during the experimental test was not done properly. Slab modelled with the 'hottest' thermal properties and 'coolest' thermal properties failed $L/20$ (BSI, 1987) deflection limiting criteria at 65 mins and 87.5 minutes of exposure respectively. Note that the slab was designed to have 90 minutes of fire resistance in accordance to the UK Regulatory Guidance (Morris et al., 1988).

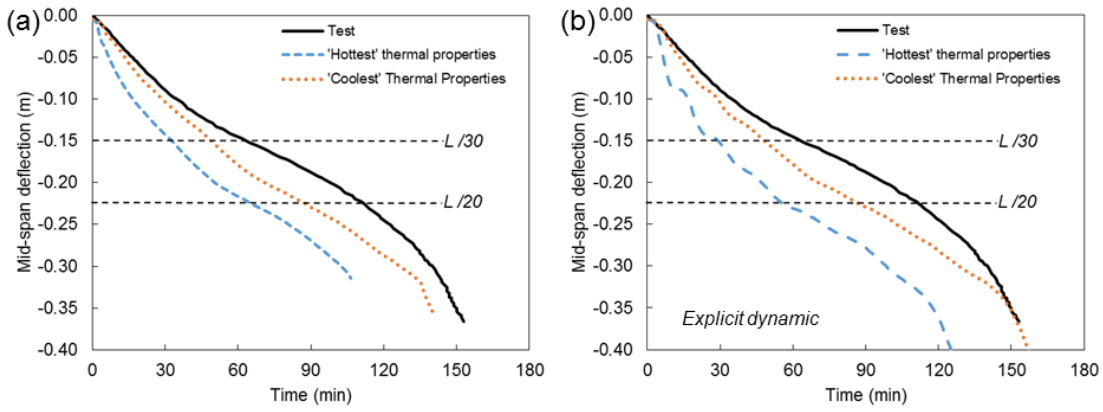

Figure 3.27: Prediction of mid-span deflection using temperature load predicted with 'Hottest' and 'Coolest' thermal properties (a) implicit static analysis and (b) explicit dynamic analysis

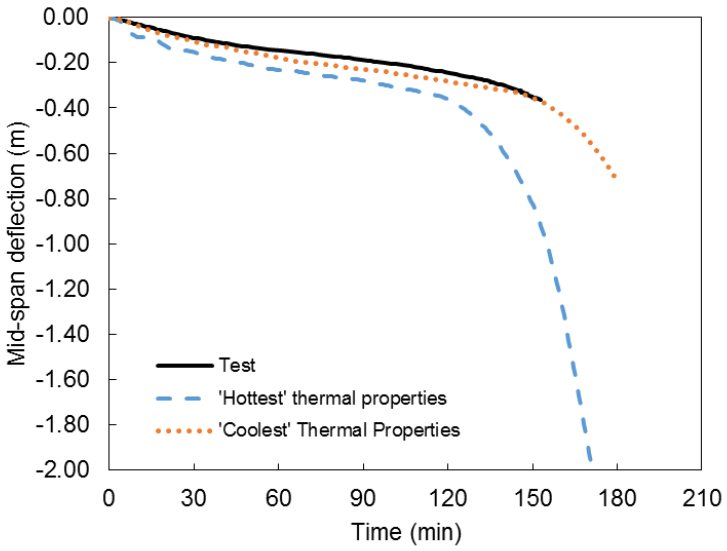

Figure 3.28: Overall prediction of mid-span deflection using temperature load predicted with 'Hottest' and 'Coolest' thermal properties from explicit dynamic analysis

3.6.4 Summary

Modelling heat transfer analysis for concrete slabs exposed to fire in a furnace environment remains a challenging task. Specifically, capturing the behaviour at the surface interacting with fire and/or ambient temperature is difficult. From an experimental perspective, proper and accurate measuring and recording of temperature histories are extremely important. From the investigation, it was found that the significant variation of reported temperatures at the exposed surface were recorded by different experimentalists for the case of the slab exposed to ISO 834 (ISO, 1999) fire curves. In an ideal case, this should not be the case given that all the slabs were exposed to similar fires i.e. ISO 834 (ISO, 1999). This challenges the credibility of standard fire tests in accordance to ISO 834 (ISO, 1999) if this is to be used as a tool to characterise fire performance of concrete slabs. Nevertheless, it is acknowledged that there were many uncertainties involved during experiments, which could influence the thermal behaviour during the furnace fire tests.

In regards to the heat transfer analysis, conduction of heat within a slab's depth is not really a concern. Prediction of temperatures generally compares reasonably well with

the test temperatures. Unfortunately, this is not the case at the boundary surface. Defining a correct boundary condition is a challenging task given the complexities of the fire environment in furnace.

With the exception of moisture-dependent thermal properties in the concrete, several range of material thermal properties and heat transfer parameters recommended in Eurocode 2 (CEN, 2004) and Eurocode 1 (CEN, 2002a) respectively, will not significantly affect the performance of heat transfer models in predicting the temperature distribution in the slab's thickness.

As opposed to the model developed for slab by Cooke (2001), better prediction during the heat transfer analysis that matched quite well with experimental results was found for the slab tested by Rickard et al. (2015). For that reason, it can be assumed that the temperatures experienced by the slabs both in finite element model and test sample were the same. However, the tested slab experienced some degree of spalling, which was not accounted for in the finite element model.

3.7 Mechanical analysis

In this section, finite element models were developed to predict the structural response of concrete slabs heated with temperature load calculated previously in Section 3.6.1 and Section 3.6.2 for Slab 1 and Slab 2 respectively. Geometrical non-linearity was included in all the models. Different finite element packages were also utilised to model structural behaviour of the slabs. The intention was to interrogate the capability of different finite element packages in predicting structural response of the slabs heated to similar temperature load.

Mathematical model (stress-strain behaviour) for both concrete and reinforcing steels were formulated based on the recommendations from Eurocode 2 (CEN, 2004) in all the finite element software packages used. For concrete, the stress-strain relationship in compression was defined in accordance to Clause 3.2.2.1(2) as well as Table 3.1, Eurocode 2 (CEN, 2004) where the parameter required was compressive strength (F_c). In LS-Dyna and SAFIR, the stress-strain curve was devised automatically once compressive strength (F_c) value was inputted whereas in ABAQUS this must be done

manually. In tension, simple linear ascending and descending branch were implemented. Biaxial stress behaviour of concrete in ABAQUS was based on the yield surface proposed by Lubliner et al. (1989) (see Section 2.11.4 in Chapter 2 for more details). Unfortunately, no information available to the author on how yielding behaviour was treated in both LS-Dyna and SAFIR. The temperature load input was at 5 mm interval in all the finite element models. Rational of this decision (i.e. 5 mm temperature interval input) will be further discussed in the following paragraphs.

In ABAQUS, a 4-node doubly curved thin shell; reduced integration formulation with finite membrane strains was selected to model the slab. The shell had single in-plane integration point and 19 through thickness integration points were defined for the current model. Simpson's integration rules were implemented. ABAQUS (2012) offers two (2) integration rules for shell finite element, *Simpson's* integration and *Gauss* Integration. *Simpson's* integration is recommended by the manual (ABAQUS, 2012) as is more efficient and stable. Detailed explanation of the theories for both *Simpson's* and *Gauss* integration can be found in the user's manual (ABAQUS, 2012).

In ABAQUS, there is a limitation on the maximum number of temperature points in the slab's thickness, if sequent thermo-mechanical analysis is to be done interactively. Interactive means temperatures calculated from heat transfer analysis can be automatically imported into structural models. It only allows a maximum of 19 temperature points through the slab's thickness. It is still possible to define more than 19 temperature points in the slab's thickness but the convenience of modelling heat transfer and structural analysis interactively cannot be exploited. In other words, it must be done manually. For the slabs under consideration, if only 19 through thickness temperature points are defined, this gives an interval of 8.33 mm and 13.9 mm through the slab's thickness for Slab 1 and Slab 2 respectively.

High resolution of slab's temperature interval is required to capture the non-linear distribution of temperature in the slab's depth. It has been stated by Gillie et al. (2004) and discussed by Deeny (2010) on the importance of capturing this non-linear and steep thermal gradient of temperatures in the slab's depth for proper modelling of the structural response. For consistency in the analysis for both slabs, it was decided that

the temperatures were inputted manually at 5 mm thickness interval (note that the thickness for Slab 1 and Slab 2 is 150 mm and 250 mm respectively).

In ABAQUS, this was defined using '*Predefined field*' command. The setback for this method is, each 'increment' of temperature load into the mechanical model had to be done as an individual 'step' analysis. For example, modelling slab tested by Rickard et al. (2015), heated to 62 minutes of fire exposure requires 64 steps of static analysis to model the structural response. In the first step, gravity load was ramped-up and in the second step, this load was kept constant to simulate static gravity loading on the slab. Temperature loads were then introduced from Step-3 until Step-64 (the last of 62 temperature load steps). The last 62 steps simulating 62 minutes of exposure to fire, which also means temperature increase was defined at 1-minute intervals.

In LS-Dyna, *Belytshcko-Tsay* shell element (Livermoore Software Technology Corporation, 2012) was selected to model the slab. Similar to ABAQUS, this shell has single in-plane integration points. This formulation of element is very efficient since it requires less computational resources as opposed to shell with four (4) numbers of in-plane integration points. The disadvantage of this element is that it is prone to poor mesh distortion. This behaviour is called hourglass. Hourglass is a term used for a 'zero energy deformation modes' typically occurs in explicit dynamic modelling. In LS-Dyna, *Gauss* scheme was implemented for the depth integration rules.

In SAFIR, the selection of single in-plane integration point for shell element is not available. Instead, the general shell element with 2 × 2 (4 points) in-plane integration was available and implemented in the current study. *Gauss* scheme was implemented for the depth integration rules. Details on the formulation of shell element and material model implementation in the code have been explained in detail by Gernay (2012), Lim (2003), and Wang (2006) thus they will not be repeated here.

3.7.1 Slab 1

3.7.1.1 Base case analysis

A quantitative assessment and comparison between the predicted structural response and test results cannot be established since the thermal analysis from the previous section shows that the predicted temperatures and the reported temperatures by Cooke (2001) differed quite significantly. Figure 3.29 shows the comparison between deflections predicted from the model against the test results.

It is worth noting that the overall trend of deflection from the model compares reasonably well with the test results. The first 40 minutes of exposures demonstrated a high rate of vertical deflection due to thermal bowing. Non-linear distribution of temperature profile i.e. very hot at the bottom and cold at the top caused this bowing behaviour.

At approximately 128 minutes of exposure to fire, the analysis was terminated due to failure of analysis to find a converge solution. Careful examination of the problem indicated that this was due to sudden loss of strength in reinforcing steels in an element at slab mid-span. This suggests that the rupture of reinforcement could potentially happen at this location. However, it is worth noting that this premature termination of analysis can possibly be avoided if a higher fracture energy was adopted in the finite element analysis (refer both Section 3.5.3 – Modelling tensile behaviour of concrete and Section 3.7.1.5 – Sensitivity studies). This behaviour of potential rupture of reinforcement will be further presented and discussed in Section 3.7.1.4 where the model was re-developed using solid elements. Slightly more detailed results regarding the state of stress, strain, and temperature in steel reinforcement is further explained in the section.

Fracture energy value, G_f adopted in the current base case analysis was based on recommendation by CEB-FIP (2010). Realistically, there is no definite answer on what is the 'correct' value to adopt to get a reasonable response prediction. Some researchers adopted high value of fracture energy i.e. 1085 N/m (Law, 2010) to ensure stability of the numerical simulation. This value is considered as 'artificial' as none of the

available codes or manuals recommend a value this high. Ellobody and Bailey (2009) adopted fracture energy equivalent to 217 N/m and successfully obtained a stable and reasonable prediction. In this study, the fracture energy adopted was 135 N/m and this is based on recommendation by CEB-FIP (2010). ABAQUS user's manual (ABAQUS, 2012) recommends value of fracture energy in the range of 40 N/m to 120 N/m. 40 N/m is suggested based on the concrete compressive strength of 20 MPa while 120 N/m is based on 40 MPa concrete compressive strength. Sensitivity of different values of fracture energy to the predicted mid-span deflection for the current slab is presented in Section 3.7.1.5.

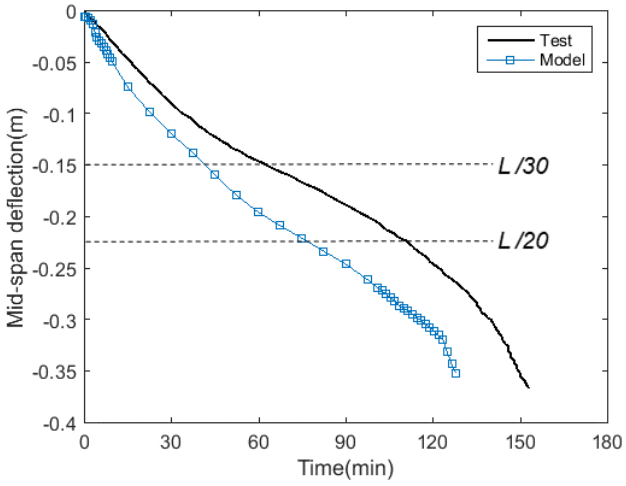

Figure 3.29: Comparison of mid-span deflection between model and test

Figure 3.30 shows the (a) through thickness stress, (b) temperature profile, (c) mechanical strain, and (d) thermal strain of the slab. Note that the state of stress, temperature, mechanical strain, and thermal strain of steel reinforcement were excluded in all the plots.

From Figure 3.30(a), concrete lost its tensile strength at the middle of the concrete depth as early as 10 minutes of exposure to fires. After that period, the concrete section near the exposed and unexposed surface was in compression. This complex behaviour is a result of thermal bowing due to the non-linear distribution of temperature through the slab's depth. Hot section at the bottom of the slab tried to expand due to the direct exposure to fire while the uppermost section of the slab (unexposed surface) was still

cold and restrained the expansion. The low thermal conductivity of concrete means it would take some time before sufficient heat is transferred to the section close to the unexposed surface of the slab. This behaviour continued up to 60 minutes of exposure as demonstrated in Figure 3.30 below. Note that in Figure 3.30 (d), no more thermal expansion occurred at the section close to the exposed surface at 60 minutes and 120 minutes of exposures. This is due to the maximum thermal strain/elongation being 0.014.

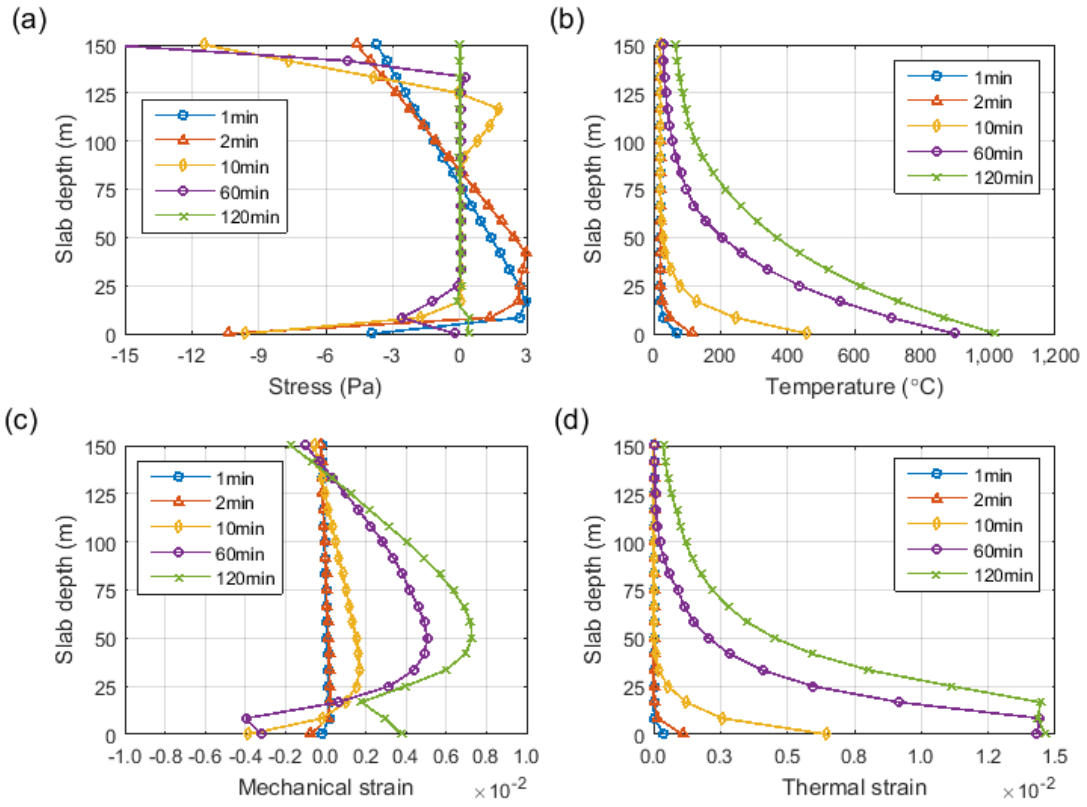

Figure 3.30: Through thickness (a) Stress (b) temperature (c) mechanical strain and (d) thermal strain in the concrete at 1 min, 2 mins, 10 mins, 60 mins, and 120 mins of exposure

3.7.1.2 Heated with measured temperature (Cooke, 2001)

The performance of numerical models in predicting the structural response of fire-exposed concrete elements relies heavily on the input temperature loaded into the model. Thus, it is extremely important that the temperatures were inputted carefully and accurately into the model to obtain a good prediction. In the previous thermal

analysis section, prediction of temperature histories using 1-D finite element approach did not yield comparable results against the reported temperatures from the test. Therefore, a quantitative assessment is not possible since both slabs (from model and test sample) did not experience similar temperature load.

Against the background mentioned above, in this section, finite element model was re-developed and in the model, reported temperatures (Cooke, 2001) were carefully inputted into the model. Due to the limitations on the availability of data, some numerical manipulation had to be done to approximate the data, whenever they are not available. Cubic polynomial fitting was done and Figure 3.31 shows the comparison of the cubic polynomial lines against the reported temperature data. Note that the curve fitting analysis was done up to 120 minutes of exposure only. This is because no physically realistic curve can be fitted to the available data beyond 120 minutes of exposure. It is also worth mentioning that Cooke (2001) did not report any data beyond 120 minutes of exposure.

Figure 3.32 shows the comparison of predicted mid-span deflection for the slab loaded with the reported temperatures from the test (Cooke, 2001) plotted against the mid-span deflection result from the test. Obviously, less deflection was predicted from the model in comparison to the results from the test.

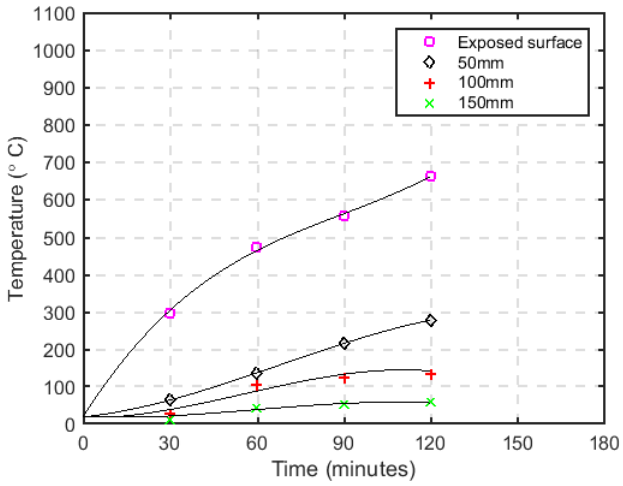

Figure 3.31: Reported temperature histories fitted with cubic polynomial

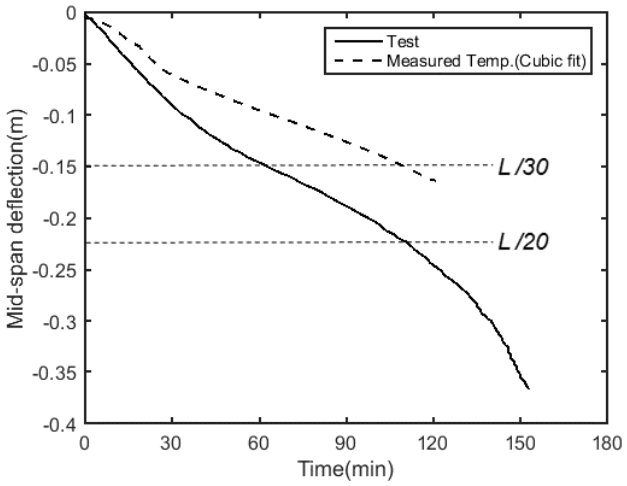

Figure 3.32: Comparison of predicted mid-span deflection for slab loaded with reported temperatures (Cooke, 2001) **against measured mid-span deflection**

With the mid-span deflection result presented above, it raises more questions regarding the accuracy of finite element model prediction and/or measured and reported mid-span deflection from the test. With less deflection predicted in the finite element model, one can simply conclude that the possible reason this is happening is the temperature load inputted into the model was less severe than what has been actually experienced by the slab during the testing in furnace. In other words, the slab in the finite element model was not heated enough to produce deflection comparable to the one from the test. It is worth mentioning that it is well covered in literature (e.g. (Gillie et al., 2004)) and the structural fire engineering community are generally in agreement that mechanical load (self-weight + imposed load) has little influence on the mid-span deflection of a fire exposed concrete slab especially during the early stage of heating.

Therefore, it is believed that the temperature load is the main reason and it heavily influences the performance prediction of finite element models. It is of the author's opinion that, the temperature histories inputted into the structural finite element model are not actually representative to those experienced by the tested slab.

3.7.1.3 Comparison of ABAQUS – LS-Dyna – SAFIR

Figure 3.33 below shows a plot of vertical mid-span deflections of the slab modelled with ABAQUS, LS-Dyna, and SAFIR. In ABAQUS and SAFIR, the analysis was terminated at 128 minutes and 136 minutes of exposure respectively.

For the case of static analysis in ABAQUS and SAFIR, the termination was due to the analysis failing to converge. Convergence problem occurred potentially due to the rupture of steel reinforcement at mid-span of the slab. As seen in the plot, just before the reinforcing steel ruptured, a runaway type of displacement occurred for the three models developed. For the case of the model developed in LS-Dyna, there was no issue of convergence since explicit dynamic approach was implemented. However, severely and poorly distorted element during the runaway displacement gave a sign that the solution was diverging.

It is worth noting that all the three models developed a trend and magnitude of deflection almost identical to each other during the first 40 minutes of exposure. From 40 minutes of exposure onwards, the trend of deflection from ABAQUS followed a different path from the other two program analyses (LS-Dyna and SAFIR). The deflection trend for the slab modelled with LS-Dyna started to differ from SAFIR at approximately 80 minutes of exposure.

If limiting the deflection of $L/20$ (BSI, 1987) was set as the performance indicator for the slab, all model prediction from ABAQUS, LS-Dyna, and SAFIR would demonstrated that the slab satisfies 90 minutes of fire resistance as what it had been designed for and mentioned in Cooke (2001). The 90-minute fire resistance criterion was specified in accordance to the UK Regulatory Guidance (Morris et al., 1988). It is however worth mentioning that the comparison between the temperature predicted from the heat transfer analysis (and consequently inputted into the model) against the measured temperatures (Cooke, 2001) do not compare well.

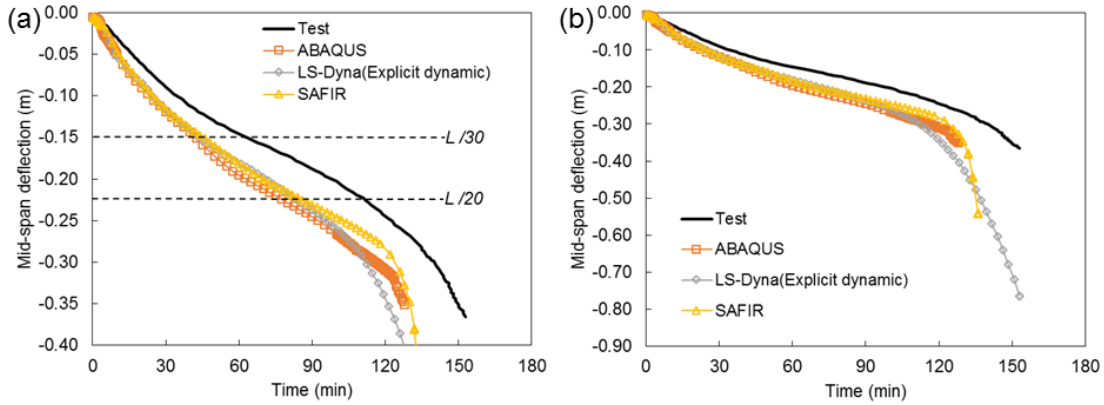

Figure 3.33: Mid-span deflection predicted using different finite element software packages (a) close-up (b) overall results

Figure 3.34 shows axial displacement of the slab modelled using ABAQUS, LS-Dyna, and SAFIR. The axial displacement was calculated at the mid-depth and at the slab's edges near support. Negative values represent the displacement going away from the centre/mid-span of the slab while positive values represent the displacement going towards centre/mid-span of the slab.

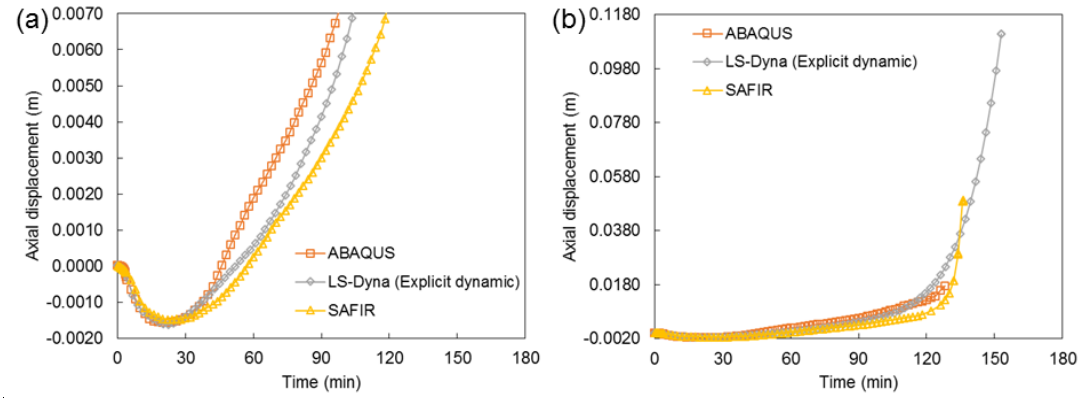

Figure 3.34: Axial displacement at the support predicted using different finite element software packages (a) close-up (b) overall results

First 22 minutes of exposure demonstrated the slab displacing axially away from its mid-span and thereafter displaced towards mid-span. All three finite element packages, ABAQUS, LS-Dyna, and SAFIR captured this behaviour and agreed with each other very well.

3.7.1.4 Thermo-mechanical analysis using solid elements

In this section, similar finite element models presented in Section 3.7.1.1 is re-developed using solid elements. Full 3-D analysis for the thermomechanical analysis was developed and presented in this section.

For thermal analysis, 8-node linear heat transfer brick, DC3D8 (ABAQUS, 2012) was selected while 2-node heat transfer link was selected to model heat transfer in steel reinforcement. Interaction between steel reinforcement and the surrounding concrete was modelled using *Constraint-Tie* (ABAQUS, 2012) command where reinforcing steel's nodes were tied to their nearest concrete nodes.

Heat was transferred at the bottom of the slab via convection and radiation. Within slab depth, heat is transferred via conduction and heat released at the unexposed surface through convection and radiation mechanism. Except for the bottom and top surfaces, other surfaces of the slab were assumed perfectly insulated. All heat transfer parameters and material thermal properties followed the recommendations from Eurocode 2 (CEN, 2004).

For structural modelling, an 8-node linear brick, reduced integration formulation denoted as C3D8R (ABAQUS, 2012) was selected to model concrete. 2-node linear 3-D truss, T3D2 was selected to model steel reinforcement. In contrast to heat transfer analysis, *Constraint-Embedded Region* (ABAQUS, 2012) was selected to model the interaction between reinforcing steels and their surrounding concrete. This constraint formulation required less computational effort. It assumed perfect bond between reinforcing steels and concrete. Reinforcing steels, acted as an embedded region perfectly tied to its host region i.e. concrete. Unfortunately, this constraint formulation cannot be used for thermal analysis (heat transfer), which explains why different constraint formulation was defined during thermal analysis.

Figure 3.35 below shows the graphical representation of a typical mesh defined to model concrete, symmetrical condition, line of vertical support, and steel reinforcement. Note that reinforcing steels is shown for graphical illustration only

because in actual modelling, the steel reinforcement is embedded into concrete and not outside the concrete as shown.

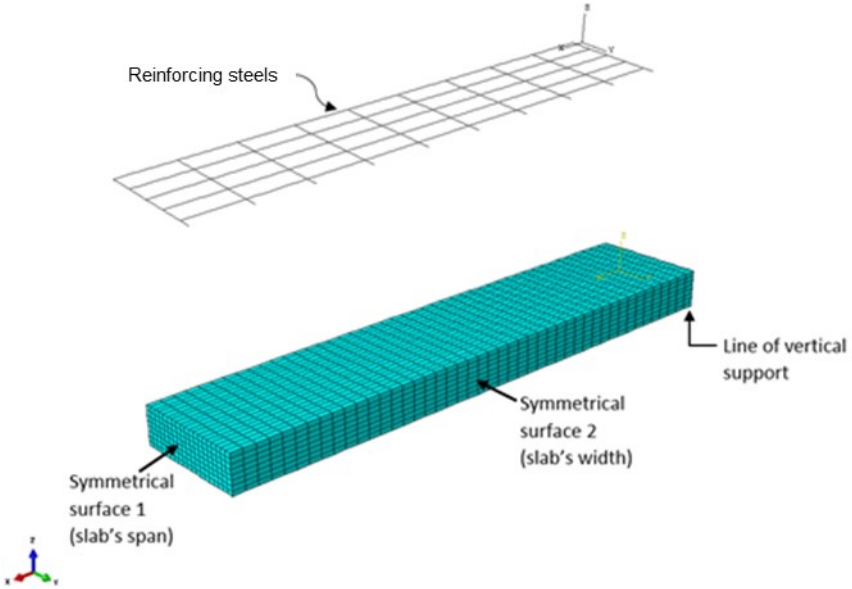

Figure 3.35: Mesh of a quarter of the slab

Formulation of heat transfer model for both plane and solid element is different. For the case of plane element, 2-dimensional process was implemented whereas for the case of solid element, the process was 3-dimensional. In addition, for plane heat transfer, steel reinforcement was not considered during the heat transfer analysis. In solid element, steel reinforcement was modelled explicitly. In other words, longitudinal heat transfer was not considered for the case of 2-dimensional process whereas for the case of 3-dimensional process, longitudinal heat transfer was considered, potentially resulting small discrepancy in the temperature prediction. Although it is unlikely that the temperature prediction from both element formulation would significantly differ, thorough check is necessary to ensure that the temperature load inputted later into the structural model will be essentially identical. This is an important aspect to ensure that beneficial comparison can be obtained when comparing structural response prediction from both model developed and presented later in the current chapter. Conceptual idealisation on 2-dimensional and 3-dimensional finite heat transfer elements is shown in Figure 3.36.

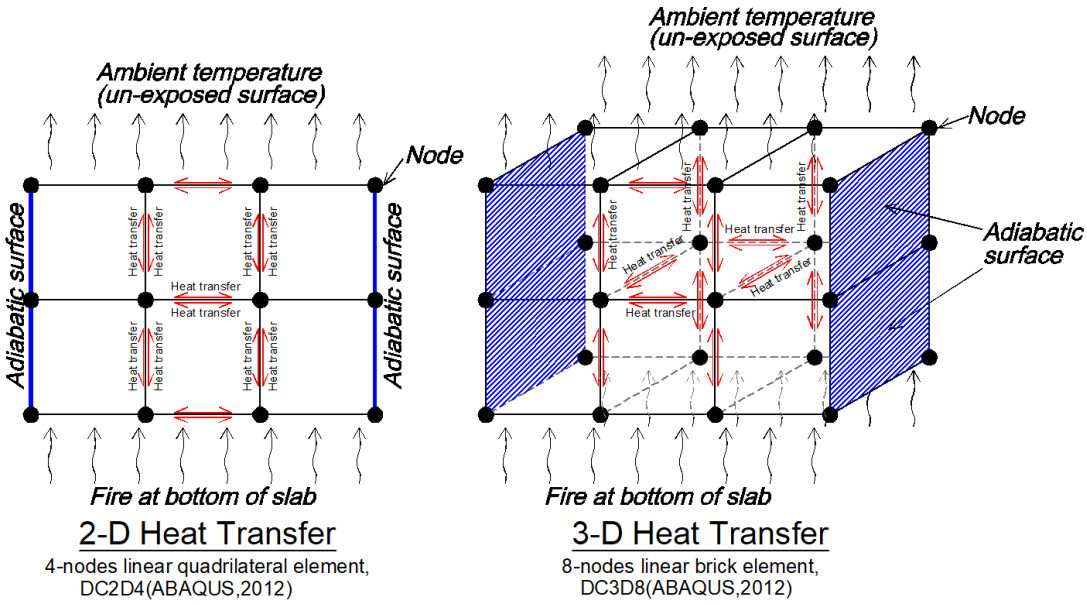

Figure 3.36: Conceptual illustration for 2-D and 3-D finite element heat transfer

Figure 3.37 below shows the comparison of temperature prediction using plane elements heat transfer model against temperature prediction using solid elements. Comparisons were made at the exposed surface, in the reinforcing steels, 75 mm from the exposure surface, and at the unexposed surface (150 mm). Note that for the case of plane element, temperature in reinforcing steel was approximated using linear interpolation from temperatures in the concrete during structural analysis (reinforcement was not modelled during heat transfer analysis). Excellent agreement was found in all the locations. Therefore, it can be assumed that the structural model developed using solid element can be compared with the structural model developed using shell elements. Note that, in a structural model developed using shell element, temperature load was calculated from plane finite element heat transfer.

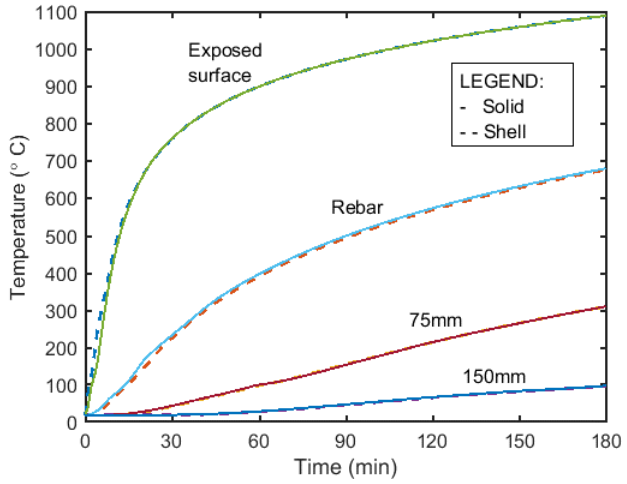

Figure 3.37: Comparison of temperature prediction and inputted into shell finite elements and solid finite elements

Mid-span deflection modelled with either shell or solid element produced result that was identical for the first 60 minutes of fire exposures (see Figure 3.38). Thereafter, higher deflection in terms of rate and magnitude was predicted with the shell element. It is believed that this is due to the way the interaction between reinforcing steels and their surrounding concrete was modelled for both shell elements and solid elements (this has been explained previously thus it will not be repeated here).

In solid element, each reinforcing steel was physically modelled whereas in shell element, existence of steel reinforcement was modelled as smeared within the concrete material.

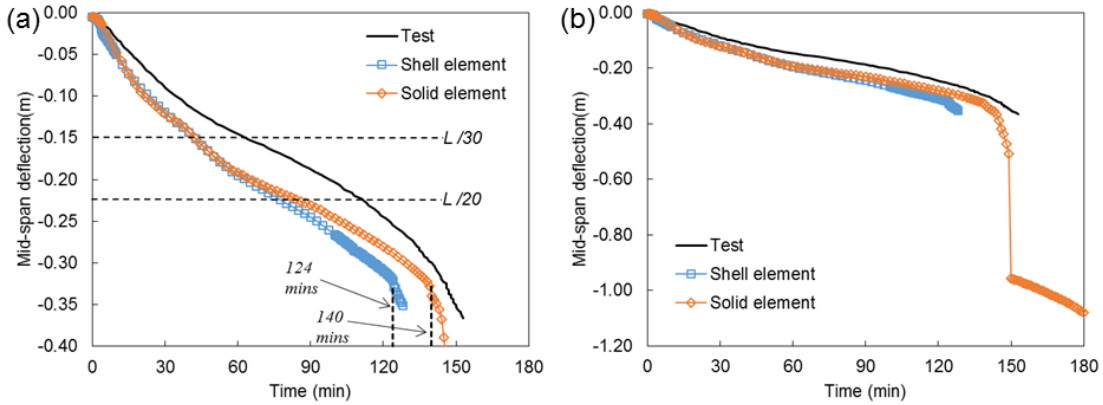

Figure 3.38: Comparison of predicted mid-span deflection modelled using shell element and solid element (a) close-up (b) overall results

The state of stress in concrete during selected duration of exposure is presented. The selected durations were at ambient temperature, with 1 minute, 4 minutes, 8 minutes, 10 minutes, 14 minutes, 30 minutes, and 120 minutes of exposure. Beyond this duration, the strength of concrete material was severely degraded due to high temperature and therefore not presented and shown here. Note that the stress in reinforcing steels is not included in the figures. Magnitude of stress in reinforcing steels was very high and if included, will over-shadow the stress in concrete. Therefore, the reinforcing steel's stress for graphical clarity was excluded. Sign conventions follow those shown in Figure 3.35.

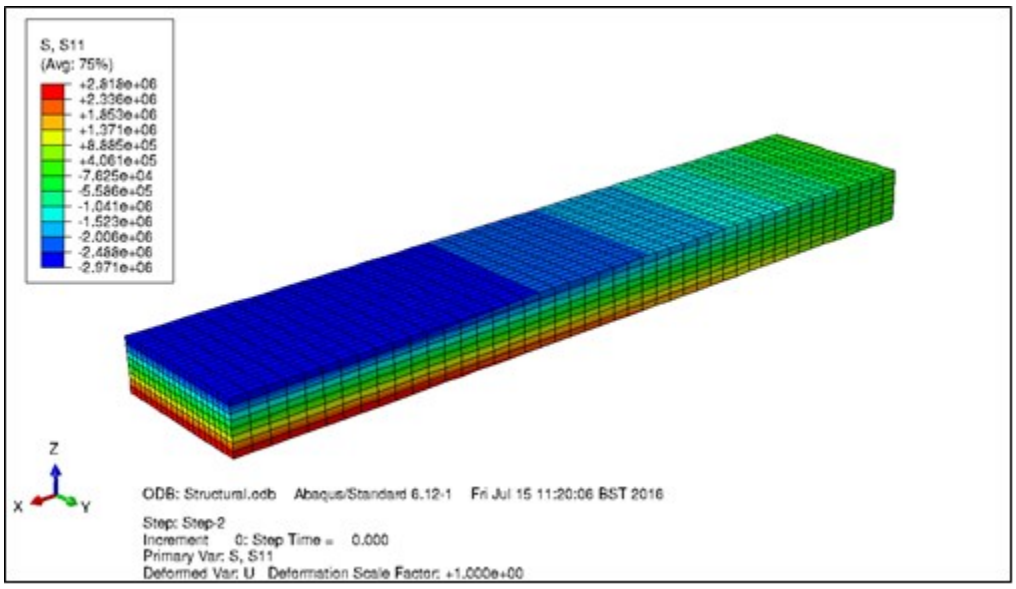

Figure 3.39: Stresses in concrete at ambient temperature

At ambient temperature, with only gravity load, the bottom of the slab experienced tension while the top of the slab experienced compression. This agrees well with the common flexural theory (at ambient temperature) and therefore proved that the model is working correctly. Maximum tensile stress at the bottom of the slab was found to be 2.82 MPa while maximum compressive stress at the top of the slab was 2.97 MPa.

As the slab was heated, tension in the bottom concrete gradually transitioned towards compression. Referring to Figure 3.40, tension at the bottom of concrete reduced to 2.47 MPa where it was initially at 2.82 MPa. Figure 3.40 shows the state of stress in concrete during 1 minute of exposure to fires. In addition, compressive stress in concrete at top of the slab increased from 2.97 MPa to 3.08 MPa.

As the heating progressed, sections at the top and bottom of the slab were in compression while at the mid-depth, the concrete was in tension. From this behaviour, tensile cracking was then initiated at the slab's mid-depth. This was illustrated from Figure 3.41 to Figure 3.45. Compression state at the bottom of the slab was due to the restrained thermal expansion whereas compression at the top of the slab was due to combination of bending and thermal bowing. Bottom of the slab experienced very high temperatures and tried to expand but the colder concrete section at top restrained the

expansion. It is suspected that this restrained expansion caused the compressive stress at bottom of the concrete.

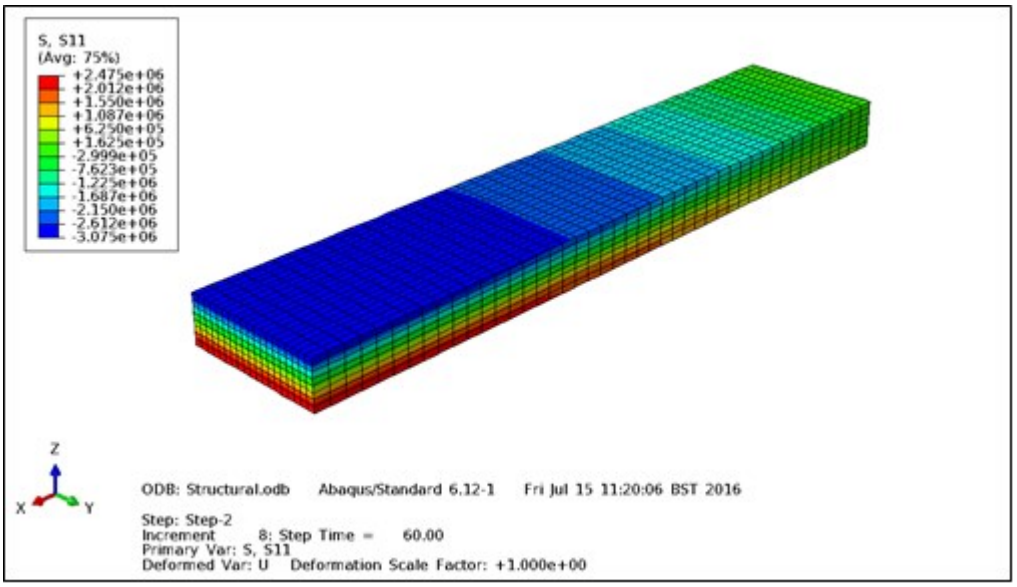

Figure 3.40: Stresses in concrete at 1 minute exposure

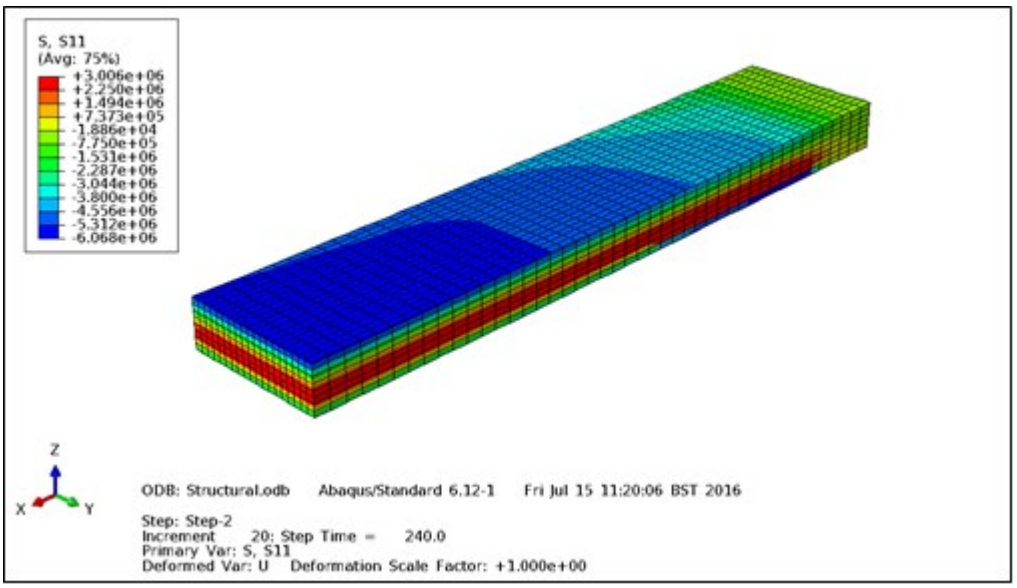

Figure 3.41: Stresses in concrete at 4 minutes exposure

Up to 8.3 minutes for the case of solid element, and 10 minutes for the case of shell element, upper half (75 mm to 150 mm from exposed surface) of the slab's section were still at an ambient temperature. Far top of the slab's section was in compression due to combination of flexural and thermal bowing as discussed above.

Figure 3.46 shows the state of concrete stress during 120 minutes of exposure, only a few minutes before runaway deflection occurred. Distribution of compressive and tensile stresses were scattered in the slab. Compressive stress however dominated throughout the slab's section. This suggests that severe cracking took place and load carrying capacity of the slab was handled by reinforcing steels and compressive strength in the concrete. Due to the assumption of smeared cracking behaviour, no realistic conclusion can be drawn from this behaviour.

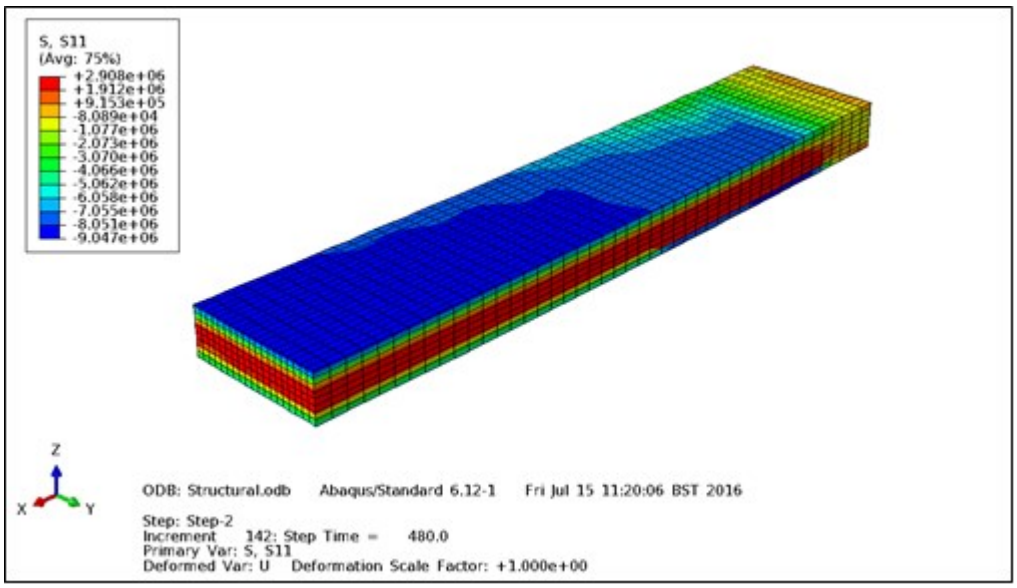

Figure 3.42: Stresses in concrete at 8 minutes exposure

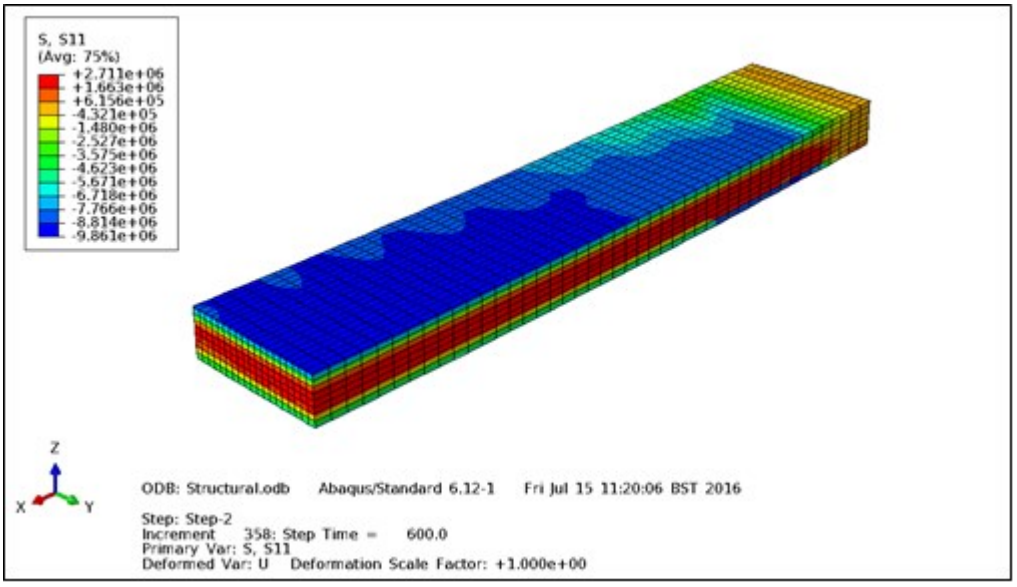

Figure 3.43: Stresses in concrete at 10 minutes exposure

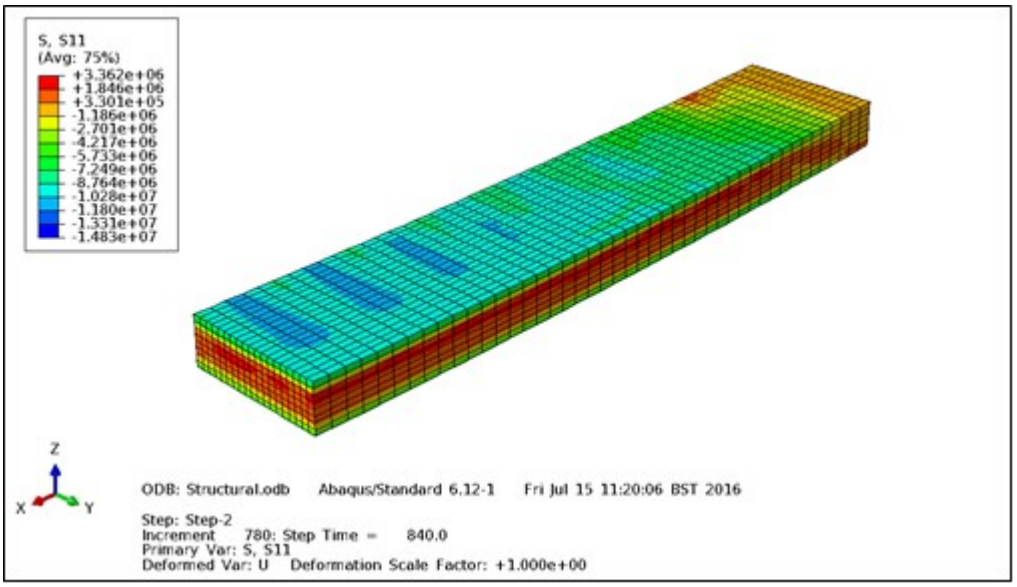

Figure 3.44: Stresses in concrete at 14 minutes exposure

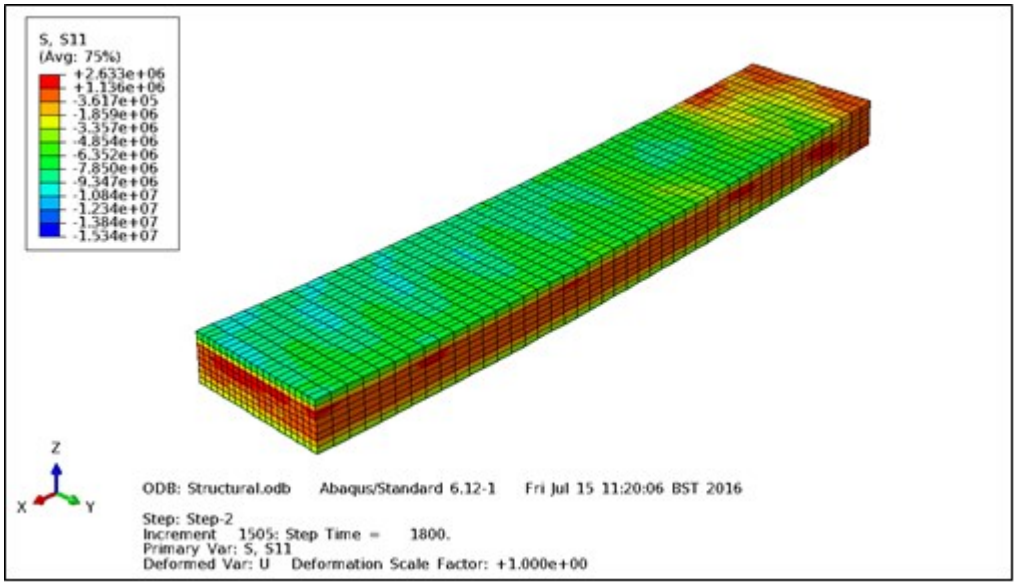

Figure 3.45: Stresses in concrete at 30 minutes exposure

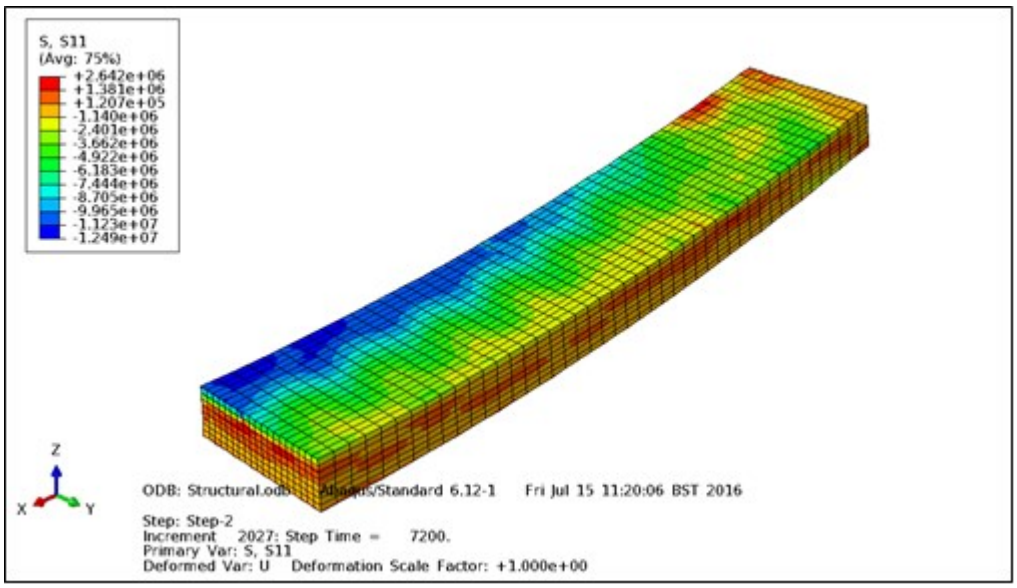

Figure 3.46: Stresses in concrete at 120 minutes exposure

The state of stress, strain, and temperature in reinforcing steels at the location near the centre of the slab in both longitudinal and transverse dimension are presented. Figure 3.47 below shows the approximate location where the stress, strain, and temperature were extracted and presented. Along the longitudinal dimension, the locations of reinforcement are labelled as 1, 2, 3, 4, 5, 6, 7, 8, 9 while along the transverse dimension, the locations are labelled as a, b, c, and d.

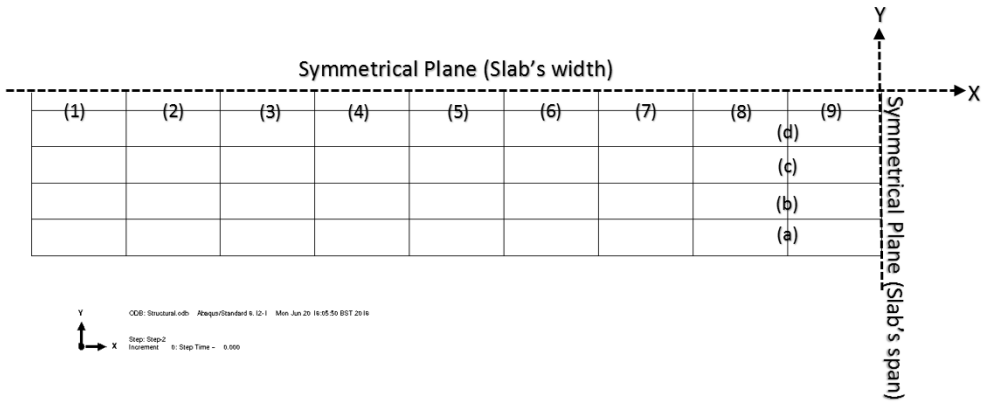

Figure 3.47: Plan of steel reinforcement

Normalised stresses for all the reinforcement locations are presented in Figure 3.48 below. Along the longitudinal dimension, all reinforcing steels were stressed more than their 50% strength at their corresponding temperature after 15 minutes of exposure. During 150 minutes of exposure, results from the finite element model suggests that at the location reinforcement (9), rupture was triggered. It must be emphasized that no attempt was made to conclude that actual failure would happen at this time of exposure given the assumption made in the finite element model. Among others, reinforcement was assumed to have a perfect bond with concrete while in reality, this is not the case.

Along the transverse dimension, reinforcing steel closest to centre of the slab experienced more stress (in tension). Referring to reinforcing steel at location (c), and (d), it is suggested that the closer the reinforcing steel to the centre of the slab, the greater the stress experienced by the reinforcing steel. This means even for one-way slab, the slab typically bows in two directions and this was also highlighted by Wang (2006). This result also suggests that transverse reinforcement at centre of the slab also provided some structural capacity for a fire exposed reinforced concrete slabs. In contrast, in a structural design of similar slab geometry at ambient temperature, transverse reinforcement usually provided to only control cracking and shrinkage.

At the duration of 150 minutes of exposure, reinforcing steel stresses in transverse direction (a, b, c, and d) dropped to zero. Even though the analysis continued until the

end of simulation time i.e. 180 minutes, no clear conclusion can be drawn from this behaviour. Sudden drop of stresses in the reinforcing steels is also translated in the elastic strain plotted in Figure 3.49. However, the plot of plastic strain in Figure 3.51 does not show any similar (sudden increase/drop in strain) behaviour. Therefore, it is not clear whether reinforcing steels at these locations (a, b, c, and d) have failed or not.

The state of elastic and plastic strains for all the locations discussed above are shown in Figure 3.49, Figure 3.50, and Figure 3.51 below. Note that, mathematical formulation of reinforcing steel material behaviour in the model was defined with maximum mechanical strain of 15% (elastic + plastic), where from this point onwards, linear descending branch up to 20% of total mechanical strain was defined to model the rupture of the steel reinforcement. This behaviour applicable to steel at any temperatures, was defined in the model.

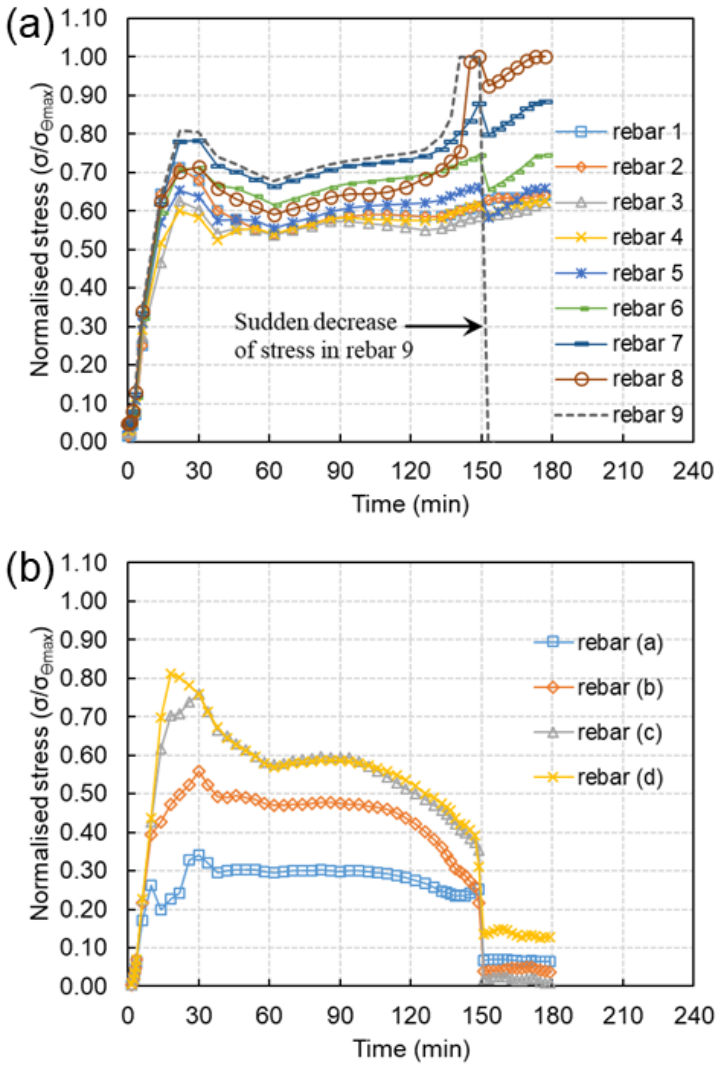

Figure 3.48: Normalised stress in (a) longitudinal reinforcing steels at location '1', '2', '3', '4', '5', '6', '7', '8', and '9' (b) transverse reinforcing steels at location 'a', 'b', 'c', and 'd'

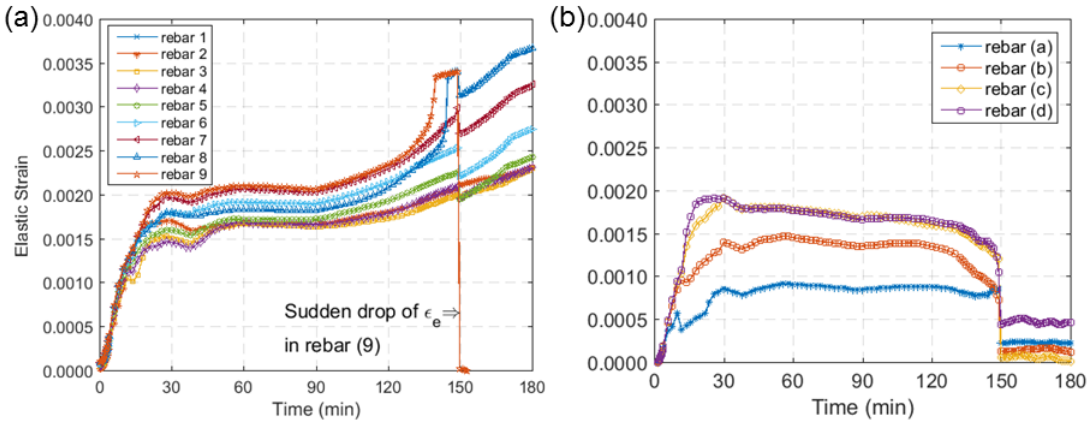

Figure 3.49: Elastic strain in (a) longitudinal reinforcing steels at location '1', '2', '3', '4', '5', '6', '7', '8', and '9' (b) transverse reinforcing steels at location 'a', 'b', 'c', and 'd'

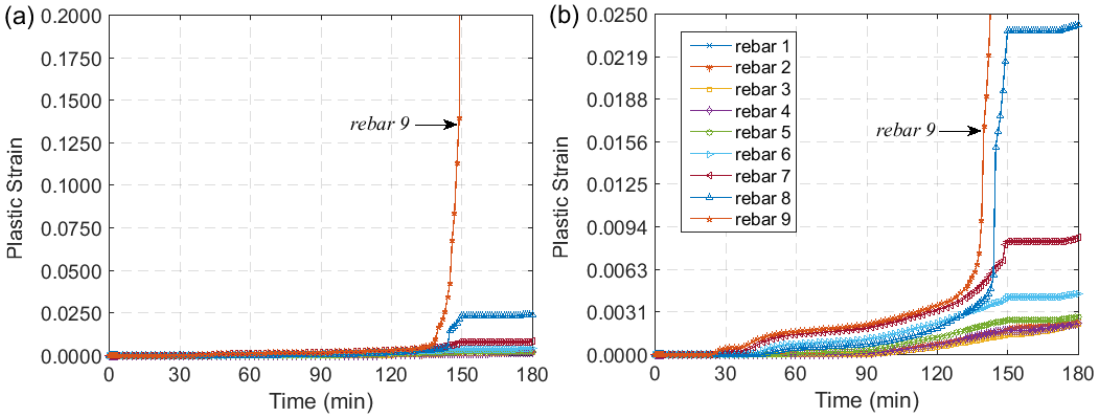

Figure 3.50: (a) Plastic strain in longitudinal reinforcing steels at location '1', '2', '3', '4', '5', '6', '7', '8', and '9' and (b) close up of similar plot

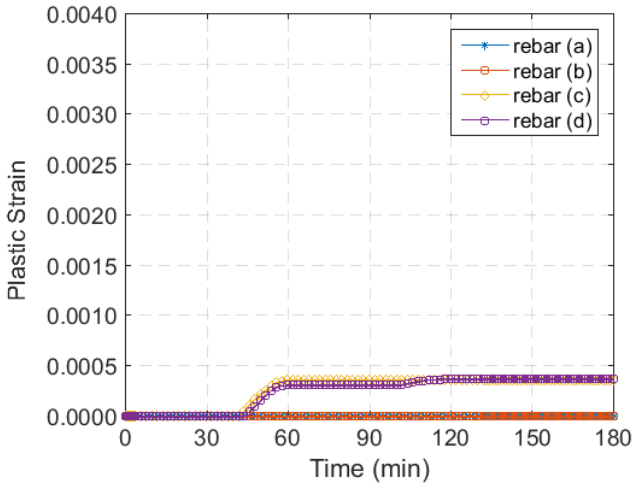

Figure 3.51: Plastic strain in transverse reinforcing steels at location 'a', 'b', 'c', and 'd'

Comparison of results between models developed using shell element and solid element is presented in Figure 3.52 below for the state of (a) elastic strain, (b) normalised stress, (c) plastic strain, and (d) temperature. For the case of solid element, the result above is extracted at the location '9' (refer Figure 3.47) while for the case of shell element, reinforcing steels stress and strain within an element near the centre of the slab was extracted. Interestingly, all the results in Figure 3.52 compares well with each other.

If reinforcement at this location is to be assessed in order to establish the structural fire resistance for the slab, it seems that the integrity of the reinforcing steels and its stiffness deteriorated at the duration of 124 mins and 140 mins of exposure for shell element and solid element modelling respectively These are when the runaway type of deflection triggered for both models (see Figure 3.38). At this period, reinforcing steels temperatures from shell element and solid element modelling were calculated as 578 °C and 614 °C respectively. Recommendation by ASTM (2015) on the critical steel reinforcement temperature of 593 °C seems to agree reasonably well with the findings from finite element modelling results. Plastic strain in the reinforcing steel were predicted as 0.51% (at 124 mins) and 1.97% (at 140 mins) calculated from shell element and solid element modelling respectively.

On the other hand, it must be stated that the location of the reinforcement discussed above is not exactly at the mid-span of the slab. It is approximately 125 mm from mid-span of the slab. This was done so that the location where results were produced was identical both of the shell and solid elements. For the shell element, stress is typically calculated at the integration point, whereas in this case, it was located at the centre of the element mesh. However, it is worth noting that, thorough checking on the results from solid element modelling indicated that the predicted plastic strain at exactly central of the slab is less than the one calculated at location '9' (see Figure 3.47).

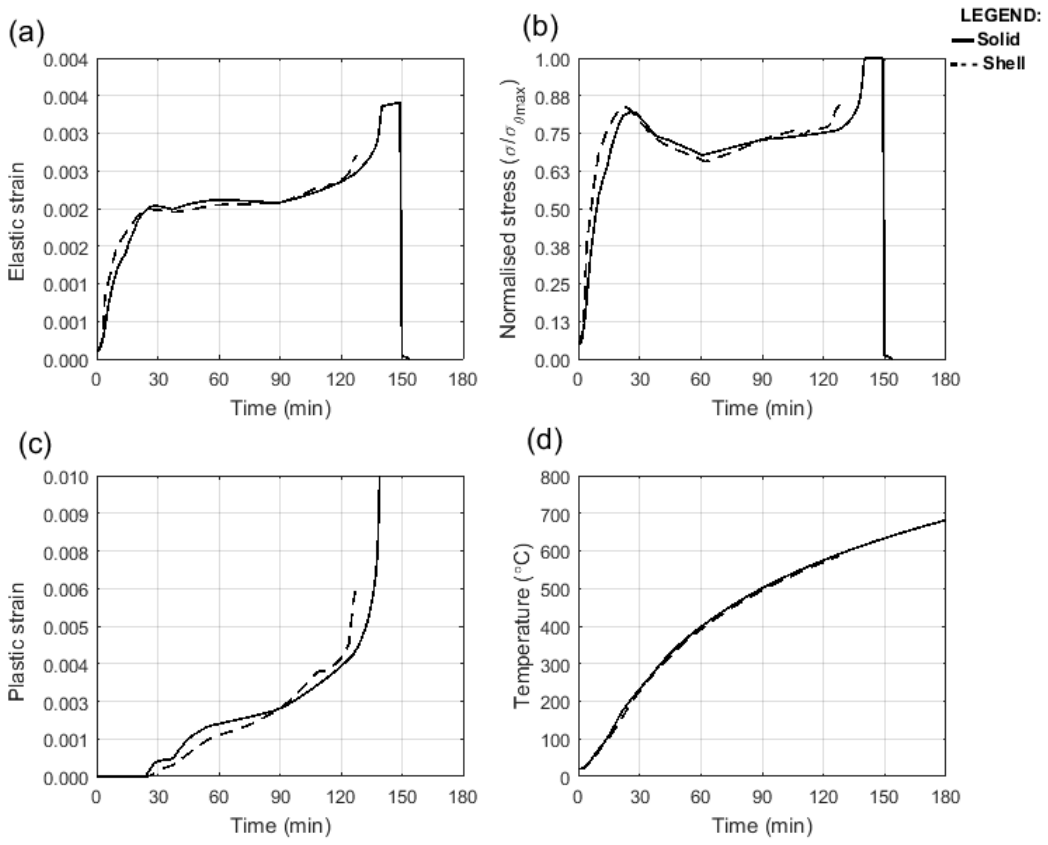

Figure 3.52: Plot of (a) elastic strain (b) normalised stress (c) plastic strain, and (d) temperature in longitudinal reinforcing steels near centre of the slab for both case model developed using shell element and solid element

3.7.1.5 Sensitivity studies

It has been demonstrated earlier in the thermal analysis section that the level of uncertainty in validating finite element models against furnace testing concrete slabs specifically in heat transfer analysis is still high. Many factors contribute to this, of which are; (1) sample locations, (2) furnace wall lining, and (3) thermocouples placing amongst others.

In this section, the sensitivity of available mechanical input parameters recommended in Eurocode 2 (CEN, 2004) to the predictive performance of finite element models was evaluated. Within practical perspective, this is important as to provide information to the practising structural fire engineers when assessing fire behaviour of concrete structures/elements.

Concrete tensile strength

Concrete tensile strength, F_t is typically defined in the range of 2% to 12% of the characteristic of concrete compressive strength, F_c. In this section, sensitivity of the defined concrete tensile strength, F_t to the predicted mid-span deflection is presented. For the base case analysis, F_t was defined as 2.9 MPa based on $0.3(F_c)^{2/3}$ relationship as recommended by CEB-FIP (2010). This value accounts for 9.7% of concrete compressive strength, F_c.

The selected range of F_t for this investigation was in the range of 0.1% to 9.7%. Therefore, F_t were defined as 0.1%, 1%, 5%, and 9.7% of the characteristic of concrete compressive strength. These gave the values of F_t to be equal to 0.03 MPa, 0.3 MPa, 1.5 MPa, and 2.9 MPa respectively. For the current study, zero concrete tensile strength was not possible because it would cause numerical instabilities. 0.03 MPa was intended to simulate concrete slab with very small concrete tensile strength.

Within the range of 1% to 9.7%, the predicted deflections seemed to agree with each other reasonably well. No significant difference in the magnitude of deflection was found throughout the simulation time. Also within this range, except for 9.7%, more numerical stability and convergence were obtained for the analysis. Note that the

fracture energy was fixed in all the analyses. With the fracture energy fixed, lower concrete tensile strength translates to a greater stress-free crack displacement width. With the current assumption in the model, the area under stress-displacement curve after cracking must be equal. With a lower peak value (or concrete tensile strength, F_t) the stress-free crack displacement (or failure cracking) will be projected further away. This issue will be discussed further in the following section.

From the results in this section, as shown in Figure 3.53, it is suggested that concrete tensile strength, F_t of less than 0.3MPa (1%) would not yield a credible deflection prediction. Lim et al. (2004) in their study suggested that zero concrete tensile strength would overpredict the deflection. They suggested that zero concrete tensile strength can be used as a conservative estimate for the slab behaviour. With different formulation of concrete yielding criteria, results from their study are not comparable to the current study. Lim et al. (2004) modelled a biaxial behaviour of concrete using Von Mises plane stress associated plasticity model with Rankine cut off in tension while for the current study, yield criteria of concrete proposed by Lubliner et al. (1989) with some modifications from Lee and Fenves (1998) was implemented to account for the different evolution of strength under tension and compression.

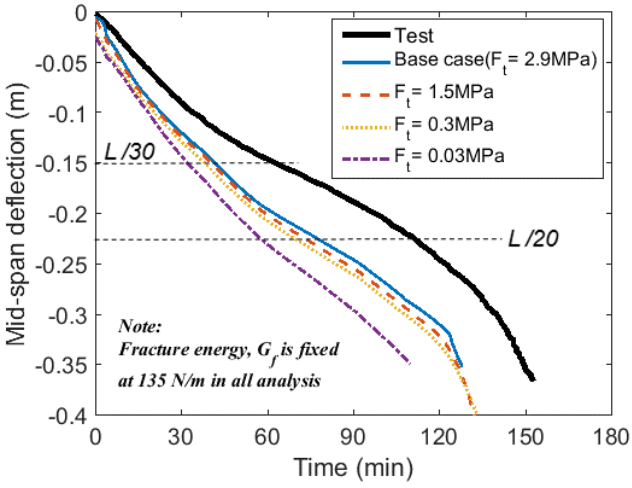

Figure 3.53: Mid-span deflection predicted with different concrete tensile strength, F_t for Slab 1

Fracture energy

Concrete material behaviour at elevated temperature is non-linear. As compared to steel material, constitutive material formulation for concrete is more complex. One of the obvious reasons is the compressive strength of concrete is far higher than its tensile strength whereas this is not the case for steel.

In the current study, post-cracking behaviour of concrete was modelled using stress-displacement relationship. The crack displacement of concrete beyond yield stress was modelled using fracture energy theory and based on the work of Hillerborg et al. (1976), as discussed in the earlier section of the chapter. In this section, the influence of varying value of fracture energy to the deformation behaviour i.e. deflection of the slab under consideration was investigated.

Prediction of deflections was found to be converging for the slab modelled using fracture energy of 75 N/m, 150 N/m, and 250 N/m. In other cases, where fracture energies were greater, lower deflections were predicted. In addition, structural response prediction was excessively ductile, in particular for the case of 1000 N/m and 1250 N/m fracture energy. Figure 3.54 illustrates this behaviour.

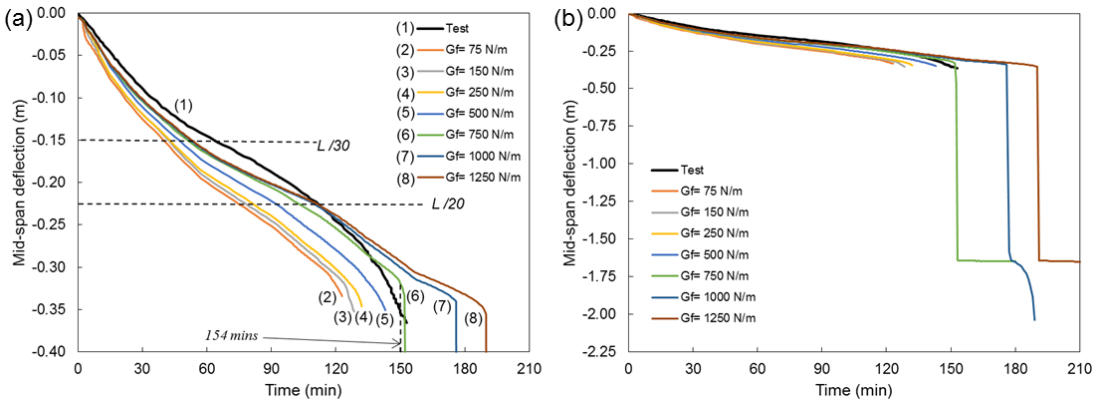

Figure 3.54: Influence of fracture energy, G_f to mid-span deflection prediction for Slab 1 (a) close-up (b) overall results

More stable analyses were found when fracture energy was defined as equal to and greater than 750 N/m. However, it is not clear whether using fracture energy of this high is a good practice for the current slab. Increasing fracture energy means more

energy is required to open a crack, resulting in a concrete that is more ductile as if the concrete became more difficult to fail under tensile cracking.

If fracture energy is taken as 500 N/m, when heated to 500 °C, the resulting stress-free crack displacement (fully open crack) is estimated as 1.7 mm. Similarly, if fracture energy is taken as 1250 N/m, this translates to a stress-free crack displacement of 4.3 mm when heated at 500°C. Table 3.5 below shows some of the crack displacement values with different fracture energy to further illustrate this.

Table 3.5: Crack displacement values at ambient temperature and 500 °C with different fracture energy, G_f calculated from Hillerborg et al. (1976) **and F_c= 30 MPa**

Fracture energy, G_f (N/m)	Stress free crack displacement at 20 °C (mm)	Stress free crack displacement at 500 °C (mm)
75	0.052	0.259
150	0.103	0.517
250	0.172	0.862
500	0.345	1.724
750	0.517	2.586
1000	0.690	3.448
1250	0.862	4.310

Fracture energy theory is a discipline of knowledge by itself. Therefore, it is not fair to conclude (in this study) on what is the correct value of fracture energy to be inputted into the model and thereafter what is the exact stress-free crack displacement for a concrete under consideration. Nevertheless, for the current slab in this study, it is suggested that fracture energy of 250 N/m or less would yield appropriate prediction and response. Fracture energy of 750 N/m and above would produce a very ductile concrete behaviour, resulting in huge amounts of energy required to fully open a crack in the concrete.

Although premature termination of analysis was found when fracture energy of 250 N/m and less was defined, it is suspected that this behaviour occurred due to sudden and drastic change of deflection in the slab. The splitting of tension reinforcement at the centre of the slab caused this sudden and drastic drop of deflection. However, it must be emphasized that in the current study, no attempt was made to predict failure

of the slab. Even though it is suggested that the premature termination of analysis was due to splitting of tension reinforcement at slab's mid-span, it is acknowledged that the smeared cracking approach was implemented in dealing with the concrete cracking behaviour. As the name implies, cracks were smeared uniformly within the slab whereas in actual testing condition, cracks might be localised in nature.

In ensuring a stable analysis, it is acceptable to use high fracture energy as long it is justified and the modeller clearly understands the consequences of using different fracture energies and the response of the concrete elements under exposure to fire. For the current slab under consideration, defining fracture energy of 750 N/m and above would result to a very ductile behaviour, underpredict the deflection, and finally overestimate the structural fire resistance of the slab.

For the case of slab modelled with fracture energy, G_f= 750 N/m, a runaway deflection would be triggered at 154 minutes of fire exposure (see Figure 3.54). At this point of time, plastic strain in reinforcing steel at slab mid-span was calculated as 1.99% (in tension). For the case of the model developed with G_f= 1000 N/m and G_f= 1250 N/m, a runaway deflection occurred at 177 minutes and 190 minutes respectively. Plastic strains were calculated as 1.99% and 2.01% for both model with fracture energy, G_f= 1000 N/m and G_f= 1250 N/m respectively. Interestingly, higher fracture energy delayed the time for runaway deflection but the time at which it triggered was when the plastic strain in reinforcing steels was at 1.99%, and was independent of temperature.

Coefficients of thermal expansion (CTE)

Recommendations on values for coefficients of thermal expansion (CTE) to be used in structural fire modelling are widely covered in literature. Thermal expansion behaviour of concrete at elevated temperature can be categorised as linear and non-linear. For linear thermal expansion behaviour, values of CTE would typically be in the range of 9×10^{-6} C^{-1} to 13.2×10^{-6} C^{-1}. Building Research Board (1951) reported a value of 13.2×10^{-6} $°C^{-1}$ while 10.5×10^{-6} $°C^{-1}$ was reported by Buch and Jahangirnejad (2008) and 9.4×10^{-6} $°C^{-1}$ by Ndon and Bergeson (1995). Non-linear and temperature-dependent coefficient of thermal expansion are such as recommended by Eurocode 2

(CEN, 2004) and Structural Fire Protection: Manual of Practice by American Society of Civil Engineers (ASCE, 1992).

Several coefficients of thermal expansion (CTE) that are non-varying with temperature (linear thermal expansion/elongation) and temperature-dependent coefficients of thermal expansion (non-linear thermal expansion/elongation) were selected for assessment on their influence on structural response. The influence of these different values of coefficients of thermal expansion to the predicted mid-span deflection is presented and shown in Figure 3.55 below. For the case of linear thermal expansion behaviour, values of constant coefficients of thermal expansion (CTE) selected for numerical assessment were 7×10^{-6} °C^{-1}, 9×10^{-6} °C^{-1}, 11×10^{-6} °C^{-1}, and 13×10^{-6} °C^{-1}. For the case of non-linear thermal expansion behaviour, temperature-dependent coefficients of thermal expansion (CTE) based on the recommendations from Eurocode 2 (CEN, 2004) and Structural Fire Protection: Manual of Practice by American Society of Civil Engineers (ASCE, 1992) were selected.

Figure 3.55 shows mid-span deflection predicted using different values of coefficients of thermal expansion (CTE). Interestingly, with the exception of model using Eurocode 2 (CEN, 2004), all predicted deflections were in good agreement. Higher deflection was predicted with Eurocode 2 (CEN, 2004) thermal expansion properties. Interestingly, even though the temperature prediction from heat transfer analysis and subsequently entering into the model do not match the reported test temperatures (Cooke, 2001), predicted deflections shown here are in good agreement with the test result at least during the first 100 minutes of exposure for all CTE cases with the exception of model developed using CTE recommended from Eurocode 2 (CEN, 2004).

This behaviour makes one wonder whether the reported temperatures were correct or not, and whether the recommended thermal expansion properties by Eurocode 2 (CEN, 2004) is defensible or not. However, no clear conclusion can be made from the results of this analysis only. In the next section, similar strategy of analysis is implemented for the case of slab tested by Rickard et al. (2015) and the outcome of this analysis will be compared and general conclusion will be drawn at the end of this chapter.

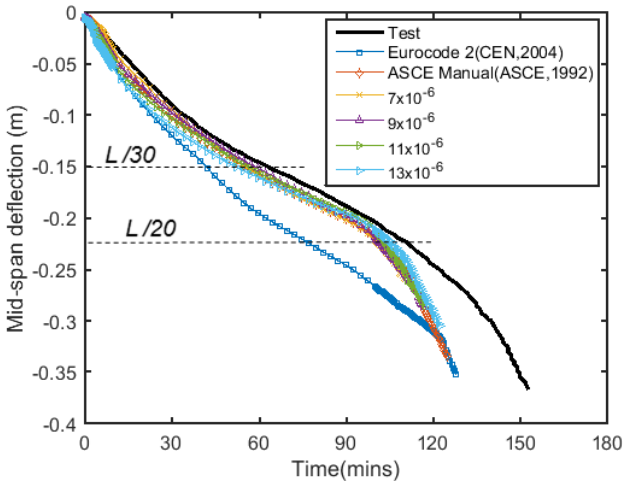

Figure 3.55: Mid-span deflection predicted with different coefficients of thermal expansion (CTE) for Slab 1

3.7.1.6 Summary

Thermal bowing and deflection trend of concrete slabs are heavily influenced by the input temperature in slab's depth. Reasonable temperature interval must be defined to capture the thermal bowing behaviour of reinforced concrete slabs. This is important since the distribution of temperature in the slab's thickness is non-linear due to the poor thermal conductance of concrete materials.

Modelling cracking behaviour of concrete is an important aspect in predicting the structural fire response of concrete slabs. Specifically, proper modelling of post-cracking behaviour is very crucial to produce a credible prediction of structural behaviour. Defining large crack displacement or large cracking strain produces stable analysis but will produce excessively ductile behaviour, leading to under predicting the deflection. It is acceptable to define high crack displacement or crack strain to study the global behaviour of reinforced concrete slabs provided the modeller fully understands the sensitivity of this input parameter.

Strain in reinforcing steels can be used as an indicator on structural fire performance for one-way slabs exposed to severe heating from below, based on the investigation in the current chapter. With the runaway type of deflection demonstrated in both model and test results, it is suggested that the slab was also losing its load carrying capacity

when the runaway deflection was triggered. In this regard, reinforcing steel's plastic strain is critical at 2% for both shell element and solid element modelling respectively. Based on these findings, reinforcing steels plastic strain of 2% was proposed and can be used as an indicator in assessing the performance of one-way reinforced concrete slabs under the exposure to severe heating from below.

Summary of fire resistance rating for the slab investigated in the current section is shown in Table 3.6. Fire resistance rating specified in accordance to Eurocode 2 (CEN, 2004) and International Building Code (International Code Council, 2009) shown in the table is based on the minimum concrete cover and minimum thickness of the slab. Provision of fire resistance rating from Eurocode 2 (CEN, 2004) is conservative, where the slab is only specified with 60 minutes of fire resistance. On the other hand, specifying limiting tensile plastic strain in reinforcing steels at 2% provides slab with 140 minutes of fire resistance rating, well in excess of both criteria from Eurocode 2 (CEN, 2004) and International Building Code (International Code Council, 2009).

Table 3.6: Summary of structural fire resistance rating for slab tested by Cooke (2001)

Fire resistance criterion	*L/20* (BSI, 1987)	Tensile plastic strain in reinforcing steels: 2%	Eurocode 2 (CEN, 2004)	International Building Code (International Code Council, 2009)
Test	112 mins	-	60 mins	120 mins
Temperature: *Heat transfer*	85* mins	140* mins		
Temperature: *Measured temperature*	>120 mins	>120 mins		

** Based on model developed using solid element*

3.7.2 Slab 2

3.7.2.1 Base case analysis

Temperature histories predicted in the previous heat transfer analysis were used as input temperature load for structural analysis in this section. Temperatures were inputted at 5 mm interval. This means 51 temperature points through the slab thickness

was required. Consequently, the convenience of interactively modelling sequent-couple thermo-mechanical analysis cannot be utilized to model the slab.

For structural modelling, 33 points through thickness integration points were defined. This gives an interval of approximately 7.8 mm between each depth integration points. Simpson's integration rules were implemented similarly in modelling Cooke (2001) slab. Many integration points i.e. 33 points were required to capture the flexural behaviour of the slab during exposure to fires. From the sensitivity studies were performed, defining less than 33 points produced non-smooth deflections. It is suspected that this is because the flexural response was not properly modelled and captured. This is due to the non-linear material behaviour of concrete during crushing and cracking within the slab's thickness.

Since the test was not intended for structural testing, heating was only done up to 62 minutes of exposure. As such slab modelled in the current section was also heated up to 62 minutes of exposure only i.e. not until 'failure'. In addition, preliminary investigation also indicated that the predicted mid-span deflection did not match well with the test results although the temperature prediction from heat transfer analysis and measured temperature from test (Rickard et al., 2015) compared well. Therefore, investigation in the current section will only interrogate on the capability of finite element model in predicting the behaviour and no detailed discussion on structural failure will be made. Throughout the 62 minutes of exposure, both predicted mid-span deflection and measured deflection (Rickard et al., 2015) did not reach limiting deflection criteria of $L/20$ and $L/30$ (BSI, 1987), which explains why the lines for deflection limit were not included in the plots presented in the current section.

Figure 3.56 shows a plot of mid-span deflection comparison between finite element model prediction and the test results. Results from the model overpredicted the mid-span deflection significantly. As mentioned previously in Section 3.4.2, the tested concrete slab experienced some spalling. Whether this spalling had an effect on the measured mid-span deflection during the test was not clear to the author. In addition, no clear explanation can be given on whether this spalling would have increased or

reduced the mid-span deflection of the tested slab during the test. However, it must be emphasized that the spalling was very minimal.

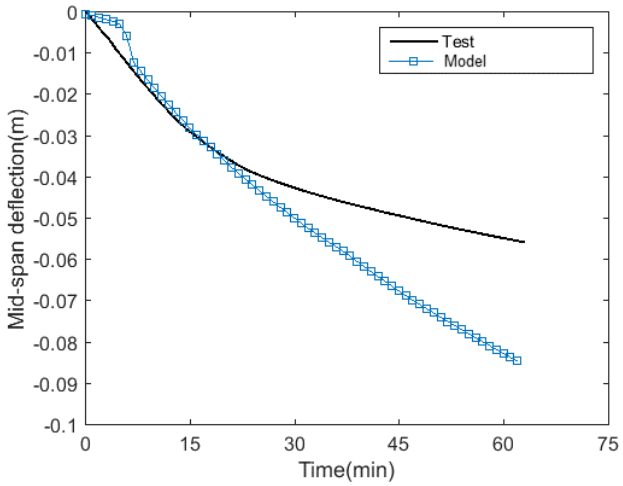

Figure 3.56: Comparison of predicted mid-span deflection against test

Note that the early trend of deflection also differed between the model and the test results. High vertical downward deformation behaviour demonstrated in the tested slab was not happening in the finite element model. It is well covered in literature that the high rate of vertical downward deformation (or simply rate of vertical deflection) is a result thermal bowing. Non-linear temperature distribution in the slab's thickness caused the slab to displace vertically in a quick manner. However, for the case of the current finite element model, the inability of the model to capture this trend was suspected due to the insufficient cracking occurring at mid-depth of the slab. This will be further discussed in Section 3.7.2.4 where the influence of concrete tensile strength and its effect on the predicted mid-span deflection is presented.

3.7.2.2 Comparison of ABAQUS – LS-Dyna – SAFIR

Similar strategy for modelling Slab 1 i.e. Cooke (2001), finite element model of slab tested by Rickard et al. (2015) was re-developed using different finite element software packages, LS-Dyna and SAFIR. Material model for both concrete and steel reinforcement defined and implemented in all the software packages are those recommended in the Eurocode 2 (CEN, 2004).

In the analysis for Slab 1, the model developed using ABAQUS predicted mid-span deflection greater than LS-Dyna and SAFIR. Similar to the analysis in the current section, mid-span deflection predicted with ABAQUS produced higher values than the rest. It is suspected that this was due to the selected number of depth integration points in the slab model amongst others.

33 numbers of integration points through the slab's thickness was defined for slab modelled in ABAQUS and LS-Dyna. In comparison, only 10 points were defined for the model in SAFIR. The flexibility of defining integration points of more than 10 was not possible as the code was programmed to accept only a maximum of 10 integration points through the slab's thickness. It is believed that few integration points i.e. 10 in this case were not sufficient to capture high non-linearity of concrete behaviour within the slab's depth. More integration points were required to capture the alternate compressive-tensile-compressive state of stress in the slab's depth. Figure 3.57 presents the mid-span deflection predicted using different FE software packages.

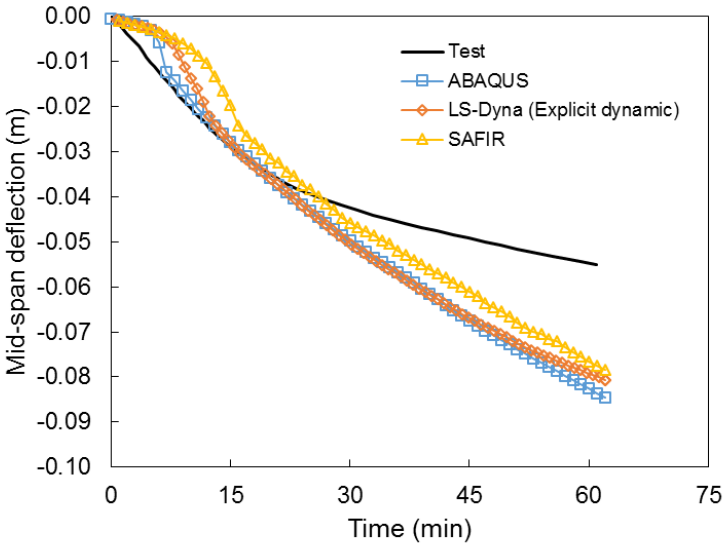

Figure 3.57: Mid-span deflection predicted using different software packages

3.7.2.3 Thermo-mechanical analysis using solid elements

Reasonably matching predictions were observed between heat transfer analysis using both plane element and solid element except in reinforcing steels. Note that heat transfer analysis (1-D) using plane stress/strain element did not consider the existence of steel reinforcement. The temperatures for reinforcing steels plotted in the Figure 3.58 below are the representation of temperature load experienced by the steel reinforcement during structural analysis by means of linear interpolation between two nearest temperature points from the concrete. Whereas in solid element, reinforcing steels were explicitly modelled both during the heat transfer analysis and structural analysis.

Maximum temperatures experienced in reinforcing steels with shell element (note that shell element is mentioned instead of plane element) formulation was 402 °C while solid element formulation was 378 °C. Both occurred at 62 minutes of exposure time. The difference is thus 24 °C. The difference is small, therefore a comparison on the structural analysis results between both models developed using shell element and solid element is possible.

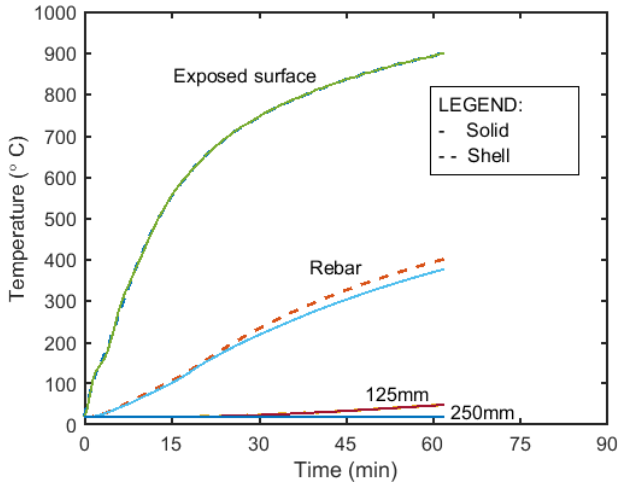

Figure 3.58: Comparison of predicted temperature for heat transfer model developed using shell elements and solid elements

Both models from solid element and shell element could not capture the rate of deflection during the first 5 minutes of exposure (with F_t defined as 4.07MPa). Overall, the trend for both models was similar throughout 62 minutes of exposure.

The common rule when selecting either solid element or shell element depends on the ratio of the body/subject span to its thickness. Generally, the span must be at least 20 times the body thickness whenever the use of shell element is desirable. However, this is not a definite rule and only serves as a guide when selecting either solid or shell element in developing a finite element model. For the current slab under consideration, span is 4080 mm while thickness of the slab is 250 mm and this gives a ratio of 16.32, indicating that the use of shell element might not be suitable. However, with careful examination on the output results from both shell and solid element, it is believed that the outcome did not affect the results and the selection of shell element for the current study is appropriate. Figure 3.59 shows the comparison between mid-span deflection predicted from shell element and solid element modelling.

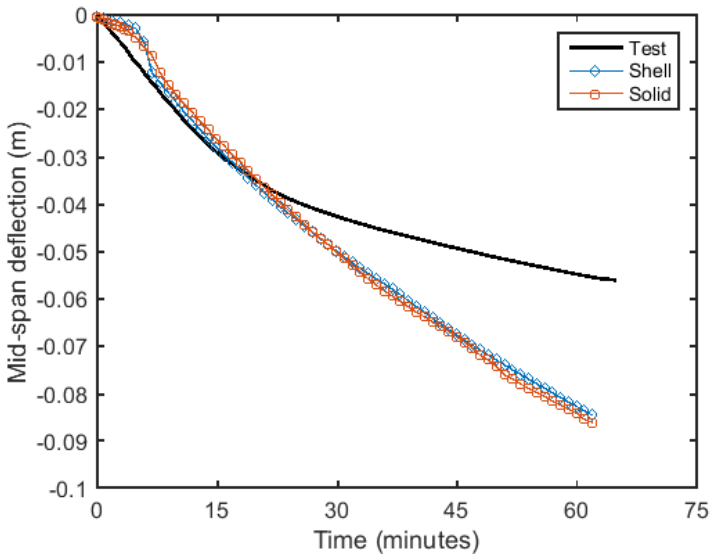

Figure 3.59: Comparison of mid-span deflection predicted using shell element and solid element together with test result

Stress state in concrete throughout exposure to fires is examined and presented in this section. Reinforcing steel's stress was omitted for clarity purposes, as the magnitude of stress in reinforcing steels was far higher than the stress in concrete. Concrete stress

at ambient temperature, during 5 minute exposure, 10 minutes, and 62 minutes are presented in Figure 3.60, Figure 3.61, Figure 3.62, and Figure 3.63 respectively.

Relatively similar behaviour results as presented in Section 3.7.1.4 for Slab 1 Cooke (2001) were found for the current slab. Note that tensile stress state in concrete at 10 minutes exposure to fire occurring at approximately 70% of the slab's thickness. Only a small portion of the slab's thickness experienced compressive stresses. As opposed to Slab 1 (Cooke, 2001), this slab had relatively lower span-to-depth ratio. Due to that, it is believed that correctly modelling tensile behaviour of concrete is relatively more important for modelling thick slabs rather than thin slabs. As most of the slab's depth is in tension, definition of tensile behaviour of concrete seems to have a profound influence on the predictive performance of thick concrete slab.

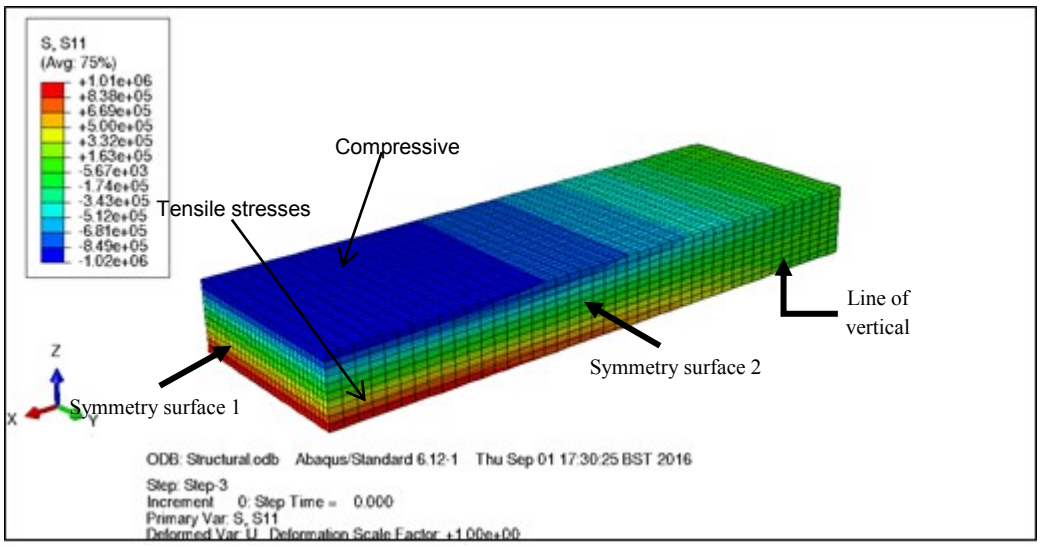

Figure 3.60: Stress distribution in concrete at ambient temperature

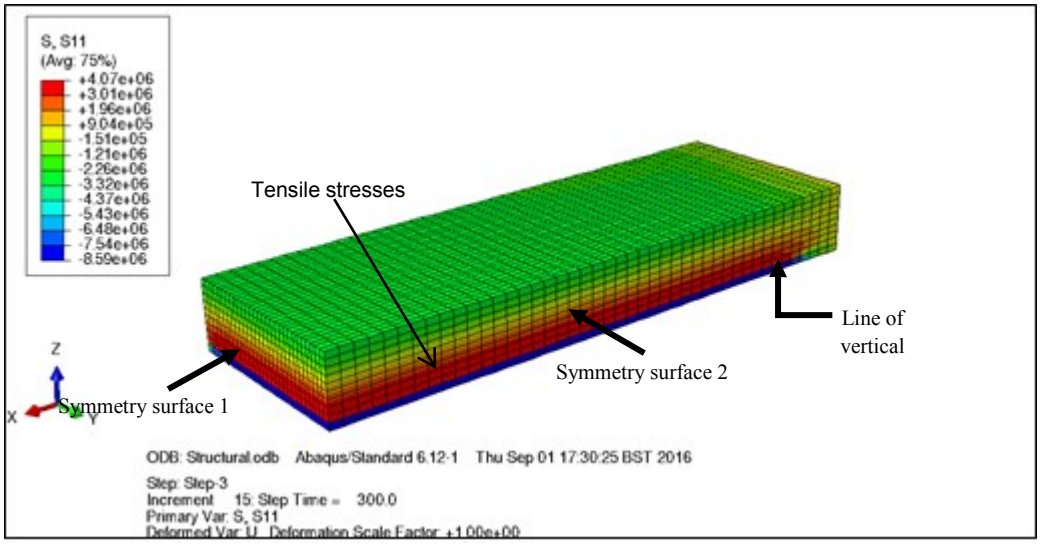

Figure 3.61: Stress distribution in concrete at 5 minutes exposure

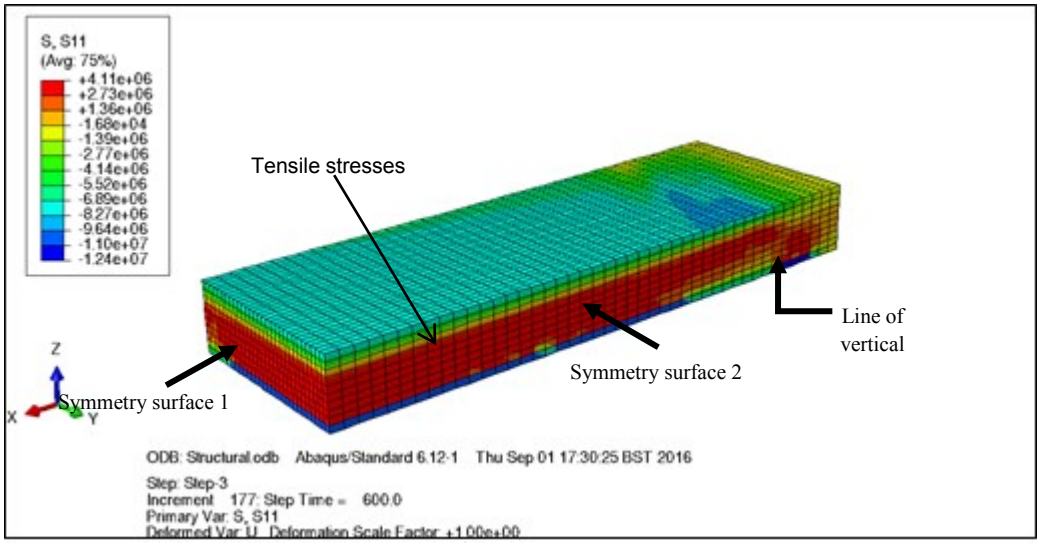

Figure 3.62: Stress distribution in concrete at 10 minutes of exposure

During 62 minutes of exposure to fire, almost all concrete sections that were initially in tension and compression had now all turned into compression. This is suspected to be due to the tensile failures having occurred within the slab's depth. Note that even until 62 minutes of exposure, the unexposed face of the slab was still at an ambient temperature (predicted at 21 °C).

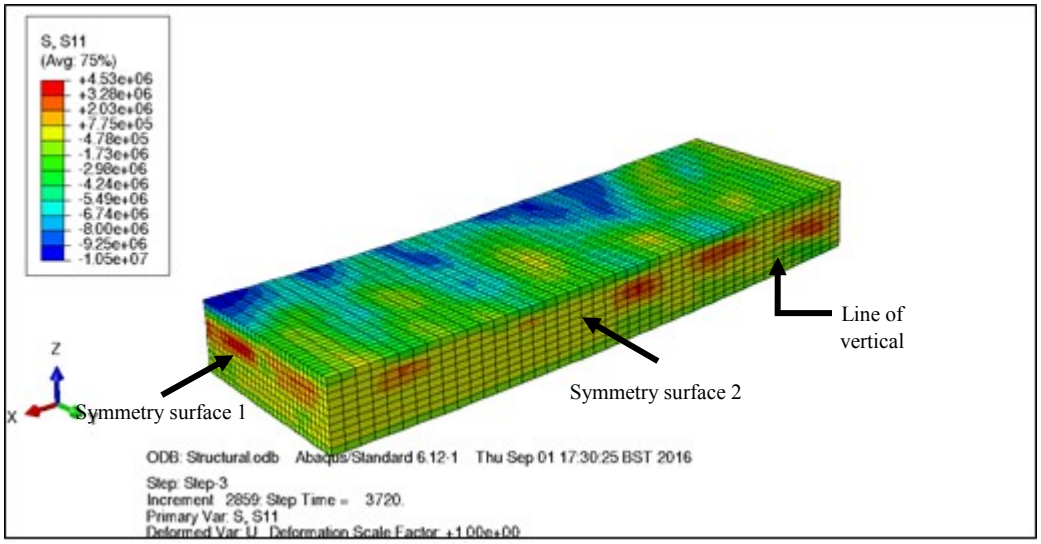

Figure 3.63: Stress distribution in concrete at 62 minutes exposure

3.7.2.4 Sensitivity studies

Concrete tensile strength

This section presents the results on the influence of concrete tensile strength, F_t to the predicted mid-span deflection for Slab 2. As hypothesised earlier in the chapter, F_t affects the trend of mid-span deflection during early stage of heating. Figure 3.64 below presents results of mid-span deflection of the slab modelled with F_t = 4.07 MPa (CEB-FIP, 2010), 2.5 MPa, 1.0 MPa, and 0.05 MPa. 2.5 MPa represents case of concrete tensile strength of 5% of the characteristic concrete compressive strength while 1 MPa represents the case of concrete tensile strength of 2% of the characteristic concrete compressive strength. 0.05 MPa concrete tensile strength was defined to simulate a slab with very low tensile strength i.e. 0.1% of concrete compressive strength.

Throughout the 62 minutes of exposure, all cases of F_t except 0.05 MPa produced mid-span deflection of almost similar in trend and values except during the first 5 minutes of exposure. For this analysis, definition of F_t seems to have a pronounced influence on the deflection rate during the first 5 minutes of exposure. It is believed that for the case of higher F_t, the model was unable to provide sufficient crack opening at the slab's mid-depth for the slab to deflect downwards in a high rate. Sensitivity of mesh size

with respect to concrete tensile strength definition was not the case for this analysis since extensive mesh sensitivity analysis has been performed beforehand in order to get a solution that is mesh convergence.

Slab model with F_t = 0.05 MPa overpredicted the deflection throughout the entire simulation time. This led us to believe that defining very low concrete tensile strength would excessively overpredict the mid-span deflection. Defining this value in the model would probably result in a safe design but might not be an economical one.

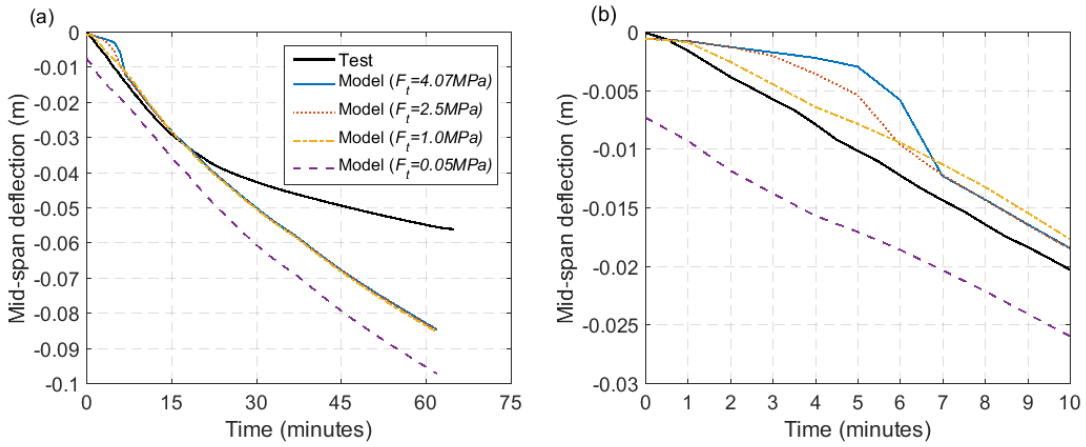

Figure 3.64: (a) Influence of concrete tensile strength to predicted mid-span deflection (b) close-up similar plot for the first 10 minutes for Slab 2

Fracture energy

Similar strategy during the analysis for Cooke (2001) slab, influence of fracture energy to the predicted mid-span deflection is presented again for the case of Rickard et al. (2015) slab. Since concrete tensile strength of 1 MPa seems to produce better prediction as highlighted in the previous section, sensitivity study was also performed for the case of model developed with 1 MPa tensile strength. Figure 3.65 presents the study for the case of 4.07 MPa while Figure 3.66 presents the result for the case of 1 MPa concrete tensile strength.

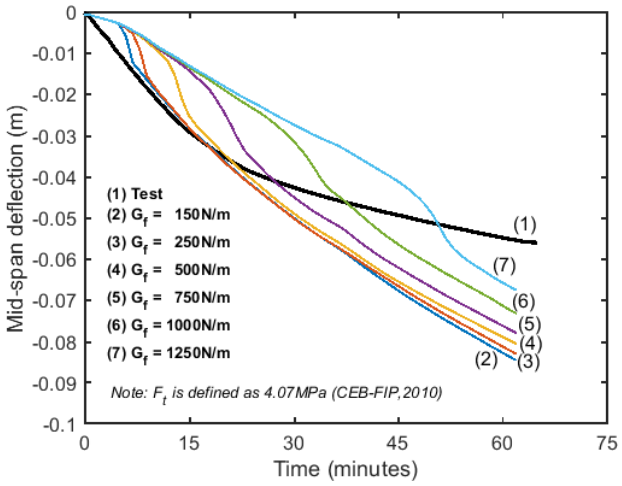

Figure 3.65: Mid-span deflection predicted with different fracture energy, G_f

Defining concrete tensile strength equals to 4.07 MPa did not produce good prediction of deflection, a finding which has been demonstrated in the previous Section 3.7.2.1 for base case model. In this section, it is also found that defining higher fracture energy with tensile strength fixed at 4.07 MPa produced an even worse prediction. It is believed that sufficient cracking was not captured in the model. On the other hand, Figure 3.66 demonstrates slightly better prediction of mid-span deflection with concrete tensile strength defined as 1 MPa.

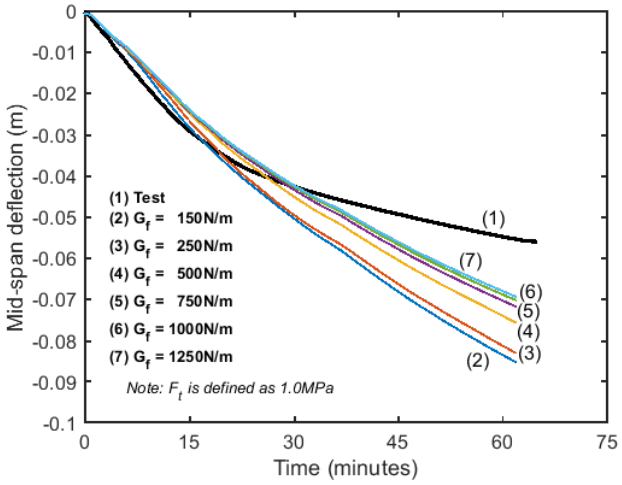

Figure 3.66: Mid-span deflection predicted with different fracture energy, G_f (F_t assumed as 1 MPa)

Coefficients of thermal expansion (CTE)

Similarly in the analysis for Cooke (2001) slab, four (4) temperature independent coefficients of thermal expansion i.e. 7×10^{-6} °C^{-1}, 9×10^{-6} °C^{-1}, 11×10^{-6} °C^{-1} °C^{-1}, 13×10^{-6} °C^{-1} together with thermal expansion properties in accordance with recommendations from Eurocode 2 (CEN, 2004) and Structural Fire Safety: Manual of Practice by American Society of Civil Engineers (ASCE, 1992) were selected for the numerical assessment. The only difference is the above thermal expansion properties were selected to model the slab with concrete tensile strength defined at 4.07 MPa and 1.0 MPa. Figure 3.67 and Figure 3.68 shows the mid-span deflection of the slab with different CTE for F_t equals to 4.07 MPa and 1.0 MPa respectively. For both plots (Figure 3.67 and Figure 3.68), different CTE influenced the deflection trend in a same manner irrespective of the value of F_t defined. One thing to note, similarly to the analysis in the previous section, definition of concrete tensile strength, F_t affected the rate of deflection in the early stage of heating.

From the plots, constant CTE of 9×10^{-6} °C^{-1} and 11×10^{-6} °C^{-1} produced mid-span deflection prediction closest to the test results in terms of overall trend and values. Eurocode 2 (CEN, 2004) thermal expansion properties seemed to produce a good prediction for the first 20 minutes of exposure. Thereafter, the predicted mid-span deflection is far higher than the measured deflection from the test. This seems to be in agreement with the studies by Ellobody and Bailey (2009). Ellobody and Bailey (2009) suggested that concrete thermal expansion properties recommended by Eurocode 2 (CEN, 2004) tend to overpredict mid-span deflection of the modelled pre-stress slab in their studies as heating progressed.

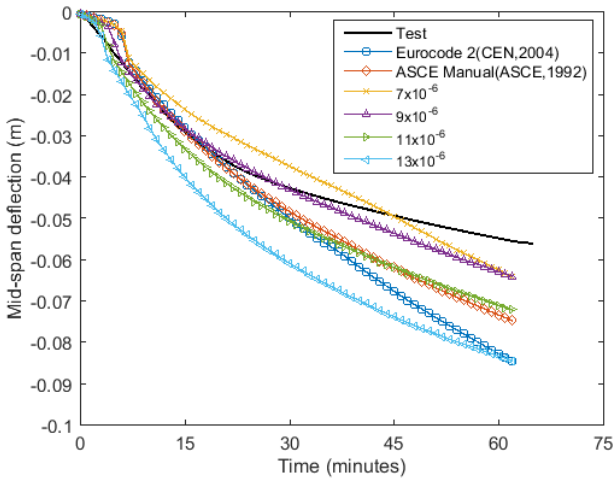

Figure 3.67: Mid-span deflection predicted with different coefficients of thermal expansion (CTE)

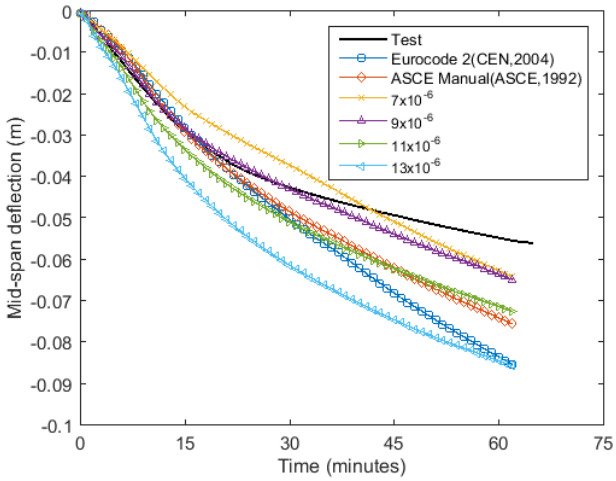

Figure 3.68: Mid-span deflection predicted with different coefficients of thermal expansion (CTE) – with F_t assumed as 1 MPa

3.7.2.5 Summary

Defining value for concrete tensile strength, F_t is very crucial as it affects the predictive performance of finite element models. Studies by Lim et al. (2004) also suggested this but the authors however demonstrated that the overall trend of deflection is approximately similar and the only difference is the magnitude of deflection. In this study, it is suggested that the defined concrete tensile strength also influences the trend

of deflection during the early stage of heating. Higher concrete tensile strength will not produce sufficient crack opening at mid-depth of a slab, leading to low rate of deflection during the early stage of heating.

With regard to the sensitivity of the response to the defined coefficient of thermal expansion (CTE), thermal expansion behaviour recommended by Eurocode 2 (CEN, 2004) seems to over-predict deflection during later stage of heating but provides a reasonably good prediction during early stage of heating. Studies by Ellobody and Bailey (2009) also demonstrated this behaviour. Temperature-independent CTE in the range of 7×10^{-6} °C^{-1} to 11×10^{-6} °C^{-1} was found to produce deflection closest to the deflection measured in the test.

Table 3.7 presents a summary of fire resistance rating for the current slab. Note that no detailed discussion on the fire resistance rating can be provided since no results beyond 62 minutes of fire exposure were available.

Table 3.7: Summary of fire resistance rating for slab tested by Rickard et al. (2015)

Fire resistance criterion	*L/20* (BSI, 1987)	Tensile plastic strain in reinforcing steels: 2%	Eurocode 2 (CEN, 2004)	International Building Code (International Code Council, 2009)
Test	> 62* mins	-	90 mins	120 mins
Model	> 62* mins	> 62 mins		

** Both test results and model predictions only available up to 62 minutes of exposure*

3.8 Overall summary and conclusion

In this chapter, it has been demonstrated that the finite element model can be used to predict performance of one-way reinforced concrete slabs under exposure to fire. However, accuracy of the prediction depends on several parameters that need to be better understood. Instead of simply presenting results of validated models, sensitivity of input parameters to the predictive performance of the model should be carefully examined and presented.

3.8.1 Thermal analysis

To produce a beneficial comparison between experiment results and model prediction, careful measuring and recording of temperatures during experimental tests are very crucial. Whenever there are unexpected errors during test, they must be acknowledged and reported in the paper. Furthermore, measured gas temperatures during the test should also be reported and not just temperatures in the slab's thickness.

Complexity of performing heat transfer analysis lies in defining the boundary condition at the surfaces interacting with the ambient temperature and fires. Characterising this is also not straightforward given the uncertainties occurring within the furnace environment. Dynamics of fire is beyond the scope of this study. However, structural engineers must work together with fire engineers to bring the field closer for the progress of the field.

Within a concrete slab's depth, existence of moisture has influence on the temperature prediction. With 0% moisture (dry) and 6% moisture, the maximum prediction of temperature difference was 67 °C throughout the 180 minutes of simulation. The provision of lower and upper limit of thermal conductivity values in Eurocode 2 (CEN, 2004) gave a maximum difference in temperature prediction equalling to 47 °C throughout 180 minutes of simulation for the case of Cooke (2001) slab analysis.

3.8.2 Mechanical analysis

Predictive performance of finite element model is sensitive to the defined concrete tensile strength and coefficient of thermal expansion. For a thick slab (span-to-depth ratio= 18.8 in this case), concrete tensile strength of approximately 10% of characteristic concrete compressive strength would produce low rate of vertical deflection during early stage of heating. Thermal expansion properties recommended in Eurocode 2 (CEN, 2004) tend to overpredict deflection in both cases of slab analysis (Cooke (2001); Rickard et al. (2015)). Linear and temperature-independent coefficients of thermal expansion (CTE) in the range of 9 to 11×10^{-6} C^{-1} predicted deflection which compared reasonably well with the test results for the case of Rickard et al. (2015). Whereas, for the case of Cooke (2001), with the exception of thermal expansion properties recommended by Eurocode 2 (CEN, 2004), all defined CTE produced relatively close predictions.

In this study, it is found that varying moisture content in the slab does have an effect on the deformation behaviour of the slab. Slab loaded with temperature modelled assuming 0% moisture (dry concrete) failed (runaway) 17 minutes earlier than similar slab loaded with temperatures predicted using 6% moisture in the concrete. Varying thermal conductivity values of either upper or lower limit as recommended in Eurocode 2 (CEN, 2004) does not have a noticeable difference in the deflection behaviour of the slab.

Investigation in this chapter also demonstrated that plastic strain of 2% can be used as an indicator of the slab structural performance under exposure to severe heating from below. With a higher fracture energy, G_f defined, the time at which runaway deflection occurred also delayed as a result of more ductile behaviour of concrete. However, the time at which runaway deflection occurred was when the plastic strain in reinforcing steels equals to 2%. Therefore, it is suggested that the tensile plastic strain of 2% can be used as an indicator for one-way reinforced concrete slab's structural performance under exposure to severe heating from below. It is however acknowledged that more validation is required.

Chapter 4:

Parametric studies on one-way reinforced concrete slabs exposed to severe heating from below

4.1 Introduction

The previous chapter has demonstrated aspects of validating finite element model of one-way reinforced concrete slabs exposed to fires. Factors influencing the differences between reported experimental results and predicted responses from finite element models have been discussed, including the sensitivity of input thermal and mechanical properties.

In this chapter, one-way reinforced concrete slab tested by Cooke (2001) is selected for parametric studies. The slab, as has been described by the author, represents a typical one-way precast concrete slab simply supported at both ends. Some modification to the slab configuration i.e. reinforcement is proposed in a certain section in this chapter to ensure consistency and for beneficial comparison with regard to different parameters investigated will be explained in the respective section.

The general objective of this chapter is to gain better understanding on structural fire response of one-way reinforced concrete slabs under exposure to fires and to provide some insight and guidance in selecting a design configuration (dimension and reinforcement) for the case of one-way reinforced concrete slabs exposed to fires. The design will be in accordance to recommendation in Eurocode 2: Design of concrete structures – Part 1-1: General rules and rules for buildings (CEN, 2014) and Part 1-2: General rules- Structural fire design (CEN, 2004).

Structural design of reinforced concrete elements typically involves selecting an optimum dimensions and amount of reinforcement that provide the required strength for the slab to sustain the anticipated design load. With these elements forming a building frame, process of selecting the optimum dimension (size) and reinforcement is not always straightforward. Within the context of design at ambient temperature, the availability of computer aided design (CAD) tools however, aids the process where different design schemes can be assessed in a quick manner. In the context of design for fire, the state of current knowledge is not mature enough to enable the CAD tools for the designing of reinforced concrete structures under fire load. Finite element model (FEM) is typically used. Therefore, assessment of various design scheme is not

something that is convenient within the design offices. In addition, this type of analysis is in general, time consuming.

The design for fire is slightly more complicated in a sense that concrete loses both compressive and tensile strength with the increase in temperature and this behaviour is not linear. In addition, development of computational capability (FEM software) involves only small community of people and more often than not, these software packages require certain specialist skills to use them. The need for academic research to help make further progress in the field is therefore very crucial for the benefits of structural fire engineering community in general.

4.2 Description of slab for parametric studies

The details of slabs in all sections in this chapter are presented in such a way that, unless described otherwise, the configuration of slab (steel reinforcement) will all be the same as what will be explained here. Some modification to the original configuration of the slab tested by Cooke (2001) is proposed in the current study. This is to ensure consistency in comparing the responses predicted from all parameters investigated. Top reinforcement, with similar bar size and numbers as bottom reinforcement i.e. ten (10) numbers of 8 mm diameter are proposed. Details of these are shown in Figure 4.1 below. Note that this configuration will serve as the base case slab where, later in the chapter, some changes in reinforcement configuration are implemented, for instance, the bar curtailment.

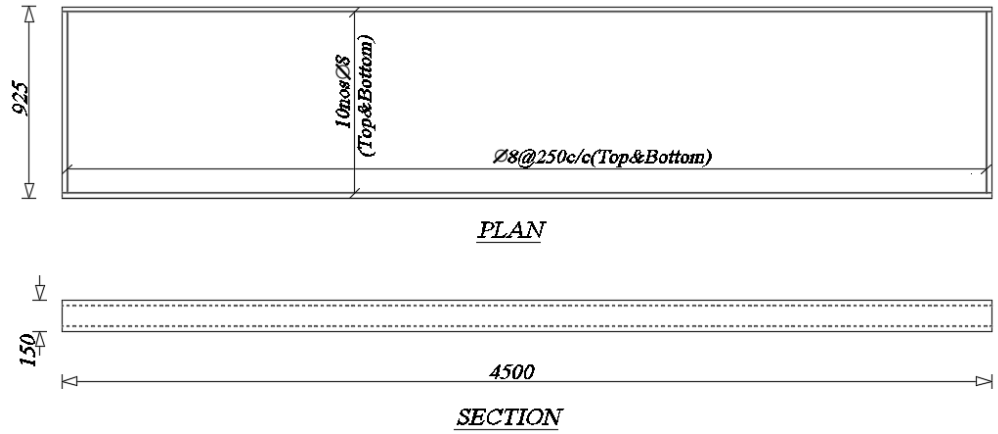

Figure 4.1: Configuration of slabs for parametric studies

The slab was exposed to ISO 834 (ISO, 1999) fires from below for a full span i.e. 4500 mm for simplicity and 1-D heat transfer analysis was carried out to predict the temperatures within slab's depth.

Parameters that will be investigated in the current chapter are fire scenario, restraint condition at support, curtailment of top reinforcing steels, as well as span-to-depth ratio. The influence of varying these parameters to the predicted mid-span deflection and plastic strain in reinforcing steels are presented.

4.3 Finite element model

A quarter of the slab was modelled taking advantage of symmetrical configuration of the tested slab. A 4-node doubly curved thin shell; reduced integration formulation with finite membrane strains (ABAQUS, 2012) was selected to model the slab.

4.4 Criteria for assessing slab's performance

In this chapter, performance of the slab models under exposure to ISO 834 (ISO, 1999) fire from below will be made against two (2) criteria; (1) limiting deflection criteria of $L/20$ as recommended by BS 476-20:1987 (BSI, 1987) and (2) critical plastic strain of 2% in reinforcing steels. The critical plastic strain value of 2% is proposed based on findings presented previously in Chapter 3, where it was found that one-way slabs loses their load carrying capacity under exposure to ISO 834 (ISO, 1999) fire from below when plastic strain in reinforcing steels reached 2%.

4.5 Fire scenario

Standard fire i.e. ISO 834 (ISO, 1999) is in general a representative fire for evaluating fire resistance of an element exposed to cellulosic fires. The idea is to produce extreme fires that an element might be exposed to during its lifetime. However, in reality, fire has a dynamic behaviour. The burning rate involves several factors such as ventilation and fuel load. In the attempt to account for different fire fuels and environment, several fire curves are recommended and available within Eurocode 1 (CEN, 2002a).

In more extreme fires, for example fires in tunnel involving petrochemical as fuel load, Hydrocarbon (CEN, 2002a) fire curve is proposed. A slow fire development is represented by Slow Heating curve or also called Smouldering Fire (CEN, 2002a). To account for realistic compartment fire, Eurocode 1 (CEN, 2002a) suggests Parametric Fire curve. This fire curve is slightly more realistic in a sense that it takes into consideration a few factors contributing to the burning rate and the length of fire duration occurring within compartments.

In this section, structural response of one-way reinforced concrete slabs exposed to the range of selected fire scenario is investigated and presented. All of the fire scenarios mentioned above are chosen to define a reasonable range of fire scenario that the slab might experience during its design life, ranging from Slow Heating (CEN, 2002a) fire up to severe Hydrocarbon (CEN, 2002a) fire. The predicted mid-span deflection with regards to all of these fire scenarios will be discussed and presented.

In deriving Parametric Fire curve (CEN, 2002a) for the current study, fire compartment size was assumed as 4.16 × 3.16 × 3 m (H). This configuration was defined to demonstrate fire in a typical size of offices or bedroom of a residential type of occupancy classes. Fire load density related to floor area was assumed as 948 MJ/m^2 with medium fire growth rate. Two (2) Parametric Fire curves (CEN, 2002a) were defined. First case, denoted as Parametric 1, was defined to simulate faster and hotter fires while second case, denoted as Parametric 2, defined to simulate longer and colder fires. Total area of vertical openings is 5.25 m^2 and 2.25 m^2 for Parametric 1 and Parametric 2 respectively. The selected fire curves for assessment of structural fire response in this section are shown in Figure 4.2 below.

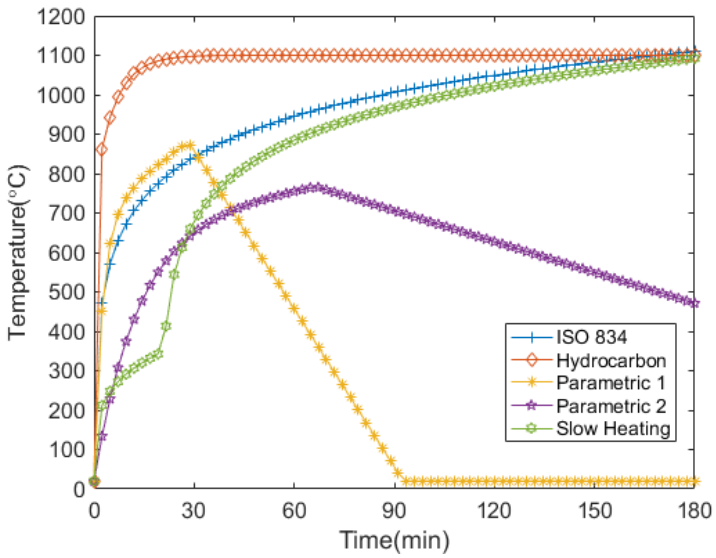

Figure 4.2: Selected design fire curve

The predicted temperature histories in slab's depth are shown in Figure 4.3 at the (a) exposed surface, (b) 50 mm, (c) 100 mm, and (d) 150 mm from surface of exposure respectively. Note that in Figure 4.3(d), the predicted temperatures for all fire cases show none of them exceeds limiting temperature criteria specified in ASTM (2015), which is 139 ℃ after 180 minutes of exposure to fires. This emphasizes that fire testing of this slab under all the fire curves mentioned previously would produce results that satisfy the limiting temperature at the un-exposed surface as specified in the standard (ASTM, 2015). Similar plot, but with larger scale is shown in Figure 4.4 below for clarity purposes.

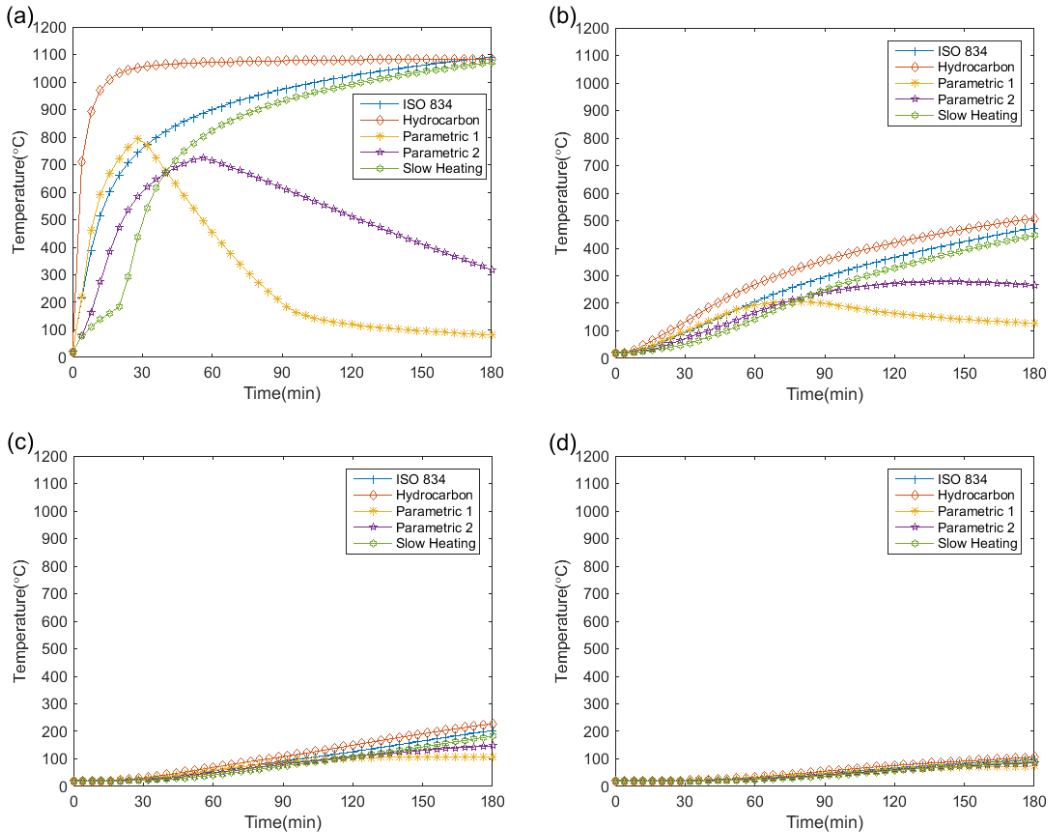

Figure 4.3: Predicted temperatures at (a) exposed surface (b) 50 mm from exposed surface (c) 100 mm from exposed surface and (d) unexposed surface (150 mm) for slab heated with different fire scenario

In Figure 4.4, temperature predicted at the unexposed surface for the case of Parametric 2 fire is still in the ascending branch. Note that Parametric 2 fire represents longer and colder fires. While the defined fire curve for Parametric 2 demonstrates the cooling trend started during 67 minutes onwards, low thermal conductivity in the concrete makes the temperature at 100 and 150 mm away from the heat sources to still be in the ascending branch.

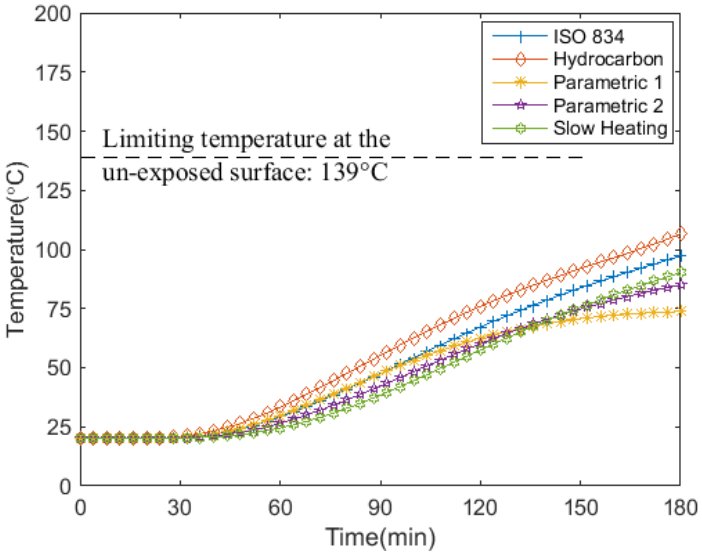

Figure 4.4: Predicted temperatures at the unexposed surface for slab heated with different fire curves

Predicted mid-span deflection for the slab heated with different fire curves mentioned above is shown in Figure 4.5 below. Note that for the case of parametric fire (Parametric 1 and Parametric 2), the selected fire exposure period involves cooling stage. However, it must be emphasized that the constitutive formulation of material model implemented in the model does not take into consideration reduction of concrete strength during cooling (residual strength) while performing the analysis during the cooling stage. Instead, full strength recovery is considered in the model during the cooling stage. Residual strength of concrete after exposure to fires is a topic of considerable uncertainties and research on this is actively ongoing. Therefore, it is not fair to discuss the predicted response for these two fires (Parametric 1 and Parametric 2) in detail here even though it is still worthy to present the results.

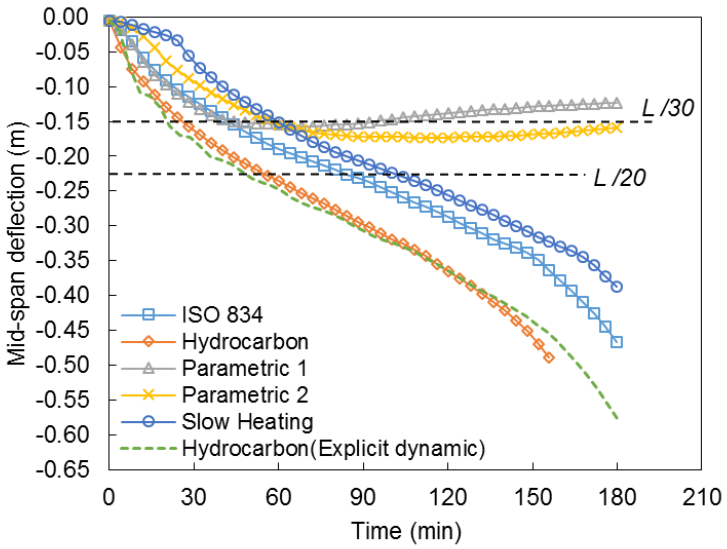

Figure 4.5: Predicted mid-span deflection with different design fire curve

Considering the deflection failure criteria as specified in BS 476 (BSI, 1987) i.e. $L/20$, the modelled slab would not survive 60 minutes (1 hour) of exposure to Hydrocarbon (CEN, 2002a) fire. This indicates that the selected design configuration i.e. thicknesses, and reinforcement are not adequate for the slab to have fire resistance of more than 1 hour. In other words, if the slab is designed as forming a space in car park buildings, alternative design configuration would be required.

In contrast, exposure to ISO 834 (ISO, 1999) gives a fire resistance rating of slightly less than 90 minutes while exposure to Slow Heating (CEN, 1999), Parametric 1, and Parametric 2 (CEN, 2002a) produce fire resistance rating of well above 90 minutes of fire exposure. As described by Cooke (2001), the slab was designed to have 90 minutes fire resistance, designed in accordance to UK Regulatory Guidance (Morris et al., 1988). It is worth mentioning that during the experimental fire test of this slab, the specimen satisfied 90 minutes of exposure to ISO 834 (ISO, 1999) based on the criteria specified in BS 476 (BSI, 1987); this has been presented in Chapter 3, which is contradictory to the predicted response from finite element model presented here. This is anticipated as the input temperatures in the model differs significantly from the measured temperatures reported by Cooke (2001), all of which have been described in

the previous chapter of this thesis (Chapter 3). Also, the slab modelled here has a top reinforcement while in the test, only bottom reinforcement was provided.

Temperature histories experienced by bottom reinforcing steel while performing mechanical analysis (note that thermal analysis was done separately and in the analysis, the existence of reinforcing steel was neglected) are plotted for different fire scenario and shown in Figure 4.6. In other words, the plotted temperature in Figure 4.6 are simply temperature load interpolated from the closest temperature points within concrete's depth in the slab for the purpose of mechanical analysis. In the plot (Figure 4.6), critical reinforcing steel temperature specified in ASTM (2015) is also plotted to give some indication on the anticipated time of failure for all the slabs if critical reinforcing steel temperature is to be used as the failure criteria.

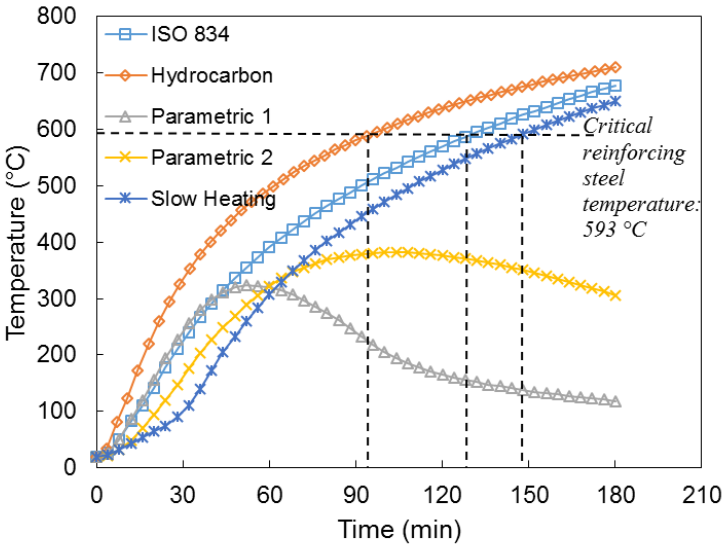

Figure 4.6: Predicted temperatures in bottom reinforcement for slab heated with different design fire curves

Bottom reinforcing steel temperature for the slab heated with Parametric 1 and Parametric 2 fire never exceeded critical reinforcing steel temperature throughout 180 minutes of fire exposure. Maximum temperature in reinforcing steel for both cases are 323 °C and 382 °C, occurring at 38 minutes and 70 minutes for Parametric 1 and Parametric 2 respectively.

Summary of fire resistance rating based on the limiting deflection criteria i.e. $L/20$ (BSI, 1987) as well as critical reinforcing steel plastic strain (2%) is shown in Table 4.1. As discussed previously, slab heated to Hydrocarbon (CEN, 2002a) failed limiting deflection criteria earlier than the rest. Limiting plastic strain at 2% in the current section is conservative, considering mid-span deflection predicted for the case slab heated to ISO 834 (ISO, 1999) fire and Slow Heating (CEN, 2002a) fire (see Table 4.1). All slabs presented here were simply supported.

Although limiting tensile plastic strain in reinforcing steels seems slightly on the 'unsafe' side with regard to specifying fire resistance rating for the case slab heated to Hydrocarbon (CEN, 2002a) fire, it is of the author's opinion that the limiting plastic strain criteria is more rational and realistic. Even though the slab has reached the limiting deflection criteria at 54 minutes of exposure in this case, there was no sign that the slab was losing its load-bearing capacity (see Figure 4.5). On the other hand, rate of deflection was found as increased at 120 minutes of exposure onwards, which signed that the slab started to lose its load carrying capacity. Tensile plastic strain of 2% was predicted at 177 minutes of exposure in this case.

Table 4.1: Summary of structural fire resistance rating for slabs exposed to different fire scenarios

Fire resistance criterion	*L /20* (BSI, 1987)	Tensile plastic strain in reinforcing steels: 2%	Eurocode 2 (CEN, 2004)	International Building Code (International Code Council, 2009)
ISO 834	83 mins	>180 mins	90 mins	120 mins
Hydrocarbon	54 mins	177 mins	90 mins	120 mins
Parametric 1	>180 mins	>180 mins	90 mins	120 mins
Parametric 2	>180 mins	>180 mins	90 mins	120 mins
Slow heating	101 mins	>180 mins	90 mins	120 mins

4.6 Restraint condition at support

While generally precast concrete slabs are simply supported at both ends, cast in-situ concrete slabs are typically continuous at their supports. This continuity introduces some degree of restraint. Structural fire engineering community are in general consensus that degree of restraint, either translational or rotational enhances the structural fire resistance of concrete elements.

Realistic studies looking at the effect of continuity or full frame behaviour of reinforced concrete structures requires huge amount of resources especially experimental type of studies. Even numerical studies also require huge amount of computational resources to perform such big scale simulation. Full frame reinforced concrete structures have been studied numerically by Huang (2010) and Law (2010) however much work still need to be carried out to fill the gap in knowledge in order to make progress in the field. Huang (2010) centred his studies on the frame behaviour by looking at the effects of spalling on the performance of the reinforced concrete building. While both studies are very promising, they involve certain simplification and generalization to minimize the computational effort required to obtain reasonable results and these involve the way cracking behaviour of concrete is modelled and selected mesh sizes among others to ensure the analysis was feasible to perform.

In this chapter, continuity at supports was modelled with a series of translational and rotational spring stiffness with the intention to simulate behaviour of continuous elements in reinforced concrete buildings. Lim (2003) and Lim et al. (2004) in their studies on the membrane behaviour of fire exposed one-way concrete slabs have extensively investigated how different restraint condition at slab's support affects fire performance of one-way concrete slabs under exposure to ISO 834 (ISO, 1999) fires where 2D beam element was used in the studies. Relatively similar parameters, implemented using shell elements were conducted here and the study at hand distinguished from the studies by both Lim (2003) and Lim et al. (2004) with the following:

a) Looking at the effects of different degrees of rotational stiffness, acting independently and together with translational restraint stiffness to the structural response of one-way reinforced concrete slabs;
b) 3D shell element was implemented, giving different insights into the problems

4.6.1 Translational spring stiffness

For 0.925 m width of slab, the estimated elastic axial spring stiffness, k_t is 1.68×10^8 N/m. This is estimated based on AE/L where A is cross sectional area (transform section) of the slab, E is the elastic stiffness and L is the slab's span. The calculated stiffness value assumes as if there is another slab next to the current slab. Graphical representation of the modelled slab is shown in Figure 4.7 below. The axial spring and vertical support are defined to act at the slab's mid-depth.

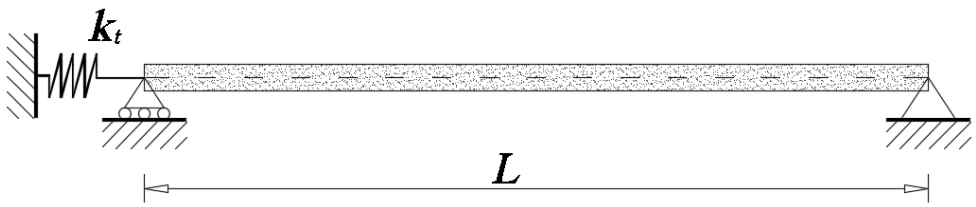

Figure 4.7: Slab's with axial spring stiffness

Axial spring stiffness of the slab is defined in the range of 1% to 100% of the calculated elastic axial stiffness. This is shown as a multiplier in Figure 4.8, where the predicted mid-span deflection is presented. $0.01k_t$ denotes 1% of k_t while 100% represents $1.0k_t$ case.

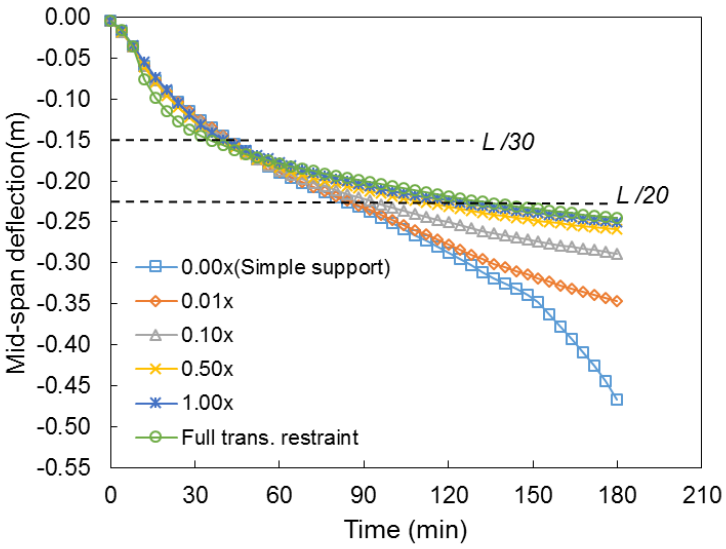

Figure 4.8: Effect of degree of axial restraint to mid-span deflection

In general, the existence of axial restraint reduces mid-span deflection of the slabs. Without axial restraint, as demonstrated from simply supported slab in Figure 4.8, runaway displacement was triggered at approximately 150 minutes of exposure to fire. In contrast, as the degree of axial restraint increased, the runaway displacement behaviour starts to diminish as presented in the figure. The deflection behaviour is converging for the slab restrained with 50% of elastic axial stiffness and above (approaching fully restraint). More interesting behaviour is witnessed when the location of axial restraint (or axial thrust at support) changes at different slab's height as studied by Lim (2003). Since Lim (2003) has extensively looked at this aspect, it will not be repeated here. Area not covered by the author i.e. slab with different degrees of rotational stiffness, will be presented in the section that follows.

Axial displacement for the slab with different degrees of axial restraint is plotted in Figure 4.9 to demonstrate how the slab displaced axially with time. In the plot, negative values represent displacement away from slab's support while positive values represent displacement towards slab (or towards slab mid-span). It can be seen in the plot, during the early stage of heating, expansion of slab caused the nodes at slab's support to move away from slab's mid-span.

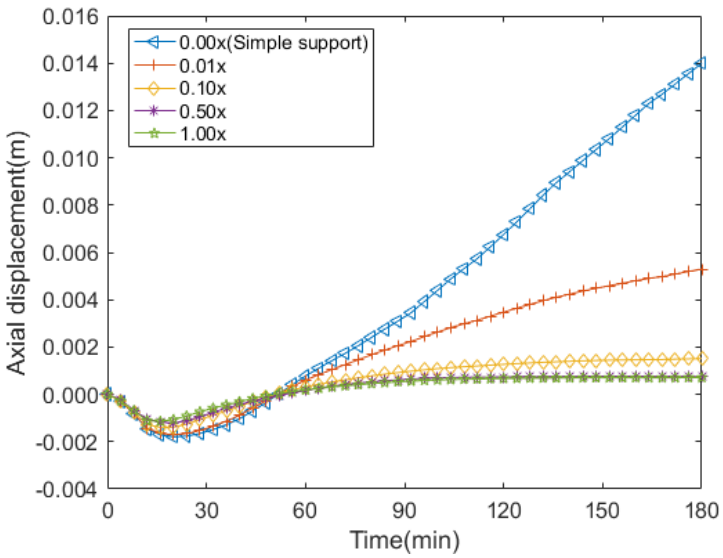

Figure 4.9: Effects of degree of axial restraint to axial displacement at support

This negative displacement at support however occurs at a very small magnitude i.e. approximately 2 mm. Positive movement (towards slab's mid-span) however, occurs at a much higher magnitude. For the case of simply supported slab, this value reached 14 mm during 180 minutes of fire exposure. Note that for the boundary condition defined in this finite element model, the slab will never lose its vertical support while in reality, this might not be the case. Simply supported precast concrete slab typically rests on a bearing column or primary beam, which has a certain 'seating' length. From the results of the current finite element model, provision of 'seating' length of more than 16 mm would seem adequate to ensure the slab does not fall from the support.

4.6.2 Rotational spring stiffness

Cast in-situ slab construction is typically designed as continuous elements rather than isolated elements. Due to this, some degree of restraint exists at the slab's support. The restraint typically exists in the form of both translational and rotational. For the case of continuous slab, exposure to fire results in redistribution of moment. This behaviour is explained by Buchanan and Abu (2017). After a certain period of fire exposure, there is a possibility for the sagging moment at mid-span to completely shift to hogging moment. Before this happens, reaction moment at support increases in response to the

shift. It is therefore important to look into the behaviour of one-way reinforced concrete slabs with certain degree of rotational restraint stiffness.

Realistic degree of rotational stiffness (and also translational stiffness) of a fire exposed concrete element is not easily approximated. This is because during the fire events, slab's supports are also heated due to the heat transfer along the slab plane, in addition to along the slab's depth. This heating will introduce thermal expansion and degradation of material properties thus reducing the stiffness of the joint (slabs' supports). Unfortunately, some simplification is required in the current study since shell element is implemented and heat transfer along the plane is not possible for this type of element formulation.

Elastic rotational spring stiffness is modelled and the behaviour of the spring is independent of temperature, meaning degradation of strength at elevated temperature is not taken into consideration. The rotational spring stiffness adopted is 2.26×10^5 Nm/rad. This is estimated based on EI/L relationship. The value is a bending stiffness for estimating an angular deflection of an elastic beam section where E is the elastic modulus, I is the second moment of area, and L is the span of the slab. Second moment of area, I was approximated in the current analysis with an assumption of cracked elastic section. Graphical configuration of the modelled slab is shown in Figure 4.10 below.

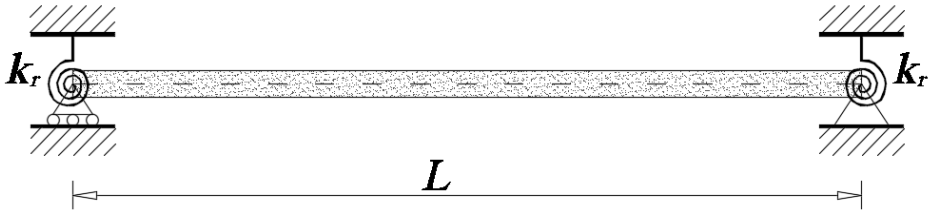

Figure 4.10: Slab with rotational spring stiffness

Similar to the previous Section 4.6.1, the degree of rotational stiffness is defined as a percentage of the approximated elastic rotational stiffness. 1%, 10%, 50%, and 100% of 2.26×10^5 Nm/rad are defined and denoted as 0.01×, 0.10×, 0.50×, and 1.00×

respectively. The predicted mid-span deflections for slab based on these values of rotational restraint stiffness are shown in Figure 4.11 below.

As compared to the slab with translational spring stiffness, rotational spring stiffness has a more pronounced effect to the predicted mid-span deflection behaviour of the slabs. Less magnitude of deflection is predicted when rotational spring stiffness is introduced at the slab's support. With 50% and 100% of the elastic bending stiffness defined, the mid-span deflection values reduced significantly (see Figure 4.11).

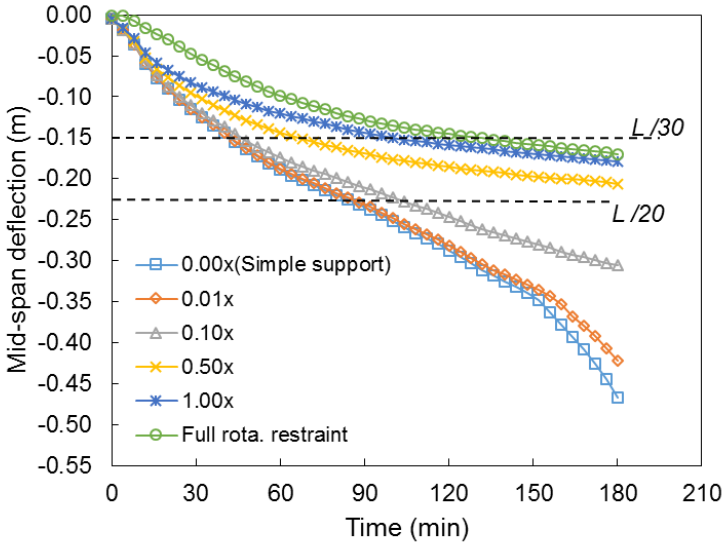

Figure 4.11: Effects of degree of rotational spring stiffness to mid-span deflection

Findings from this section support arguments within the structural fire engineering community that testing a single element (isolated), simply supported at both ends, gives misleading information on the structural performance of one-way reinforced concrete slabs under exposure to fires. It is justified that testing simply supported member is enough to present the worst possible case as is presented in the Figure 4.11, where deflection is greatest for the case of simply supported slab and also runaway type of deflection was triggered. It also justifies that the degree of restraint (both translational and rotational) somehow improves structural fire resistance of the slab. But the effect that this behaviour produced is neglected for instance, the redistribution of moment causes moment at support increases. Either the support is designed to cater

for this moment to increase is something that needs more studies. In addition, top reinforcement in a realistic construction typically curtailed for economic reason. All of these issues will be presented and discussed in the later sections of this chapter. Having said that, it is also acknowledged that from an experimental perspective, realising rotational restraint in the setup is not a simple task, which is one potential reason why this kind of test is not very popular.

4.6.3 Combination of translational and rotational spring stiffness

Previous Sections 4.6.1 and Section 4.6.2 have presented the behaviour of one-way reinforced concrete slabs with certain degree of translational and rotational restraint acting individually at slab's support. In most cases, these restraints exist in combination rather than individual. But it is acknowledged that in some cases, for instance, precast slab construction, translational restraint acts individually. In this section, behaviour of the slab under the action of combined restraints are investigated and presented. Similar to the previous section, the degree of restraint is defined as a percentage of elastic spring stiffness (both translational and rotational), these being 1%, 10%, 50%, and 100%. The setup of the model is graphically shown in Figure 4.12 and the predicted mid-span deflection from the model is presented in Figure 4.13.

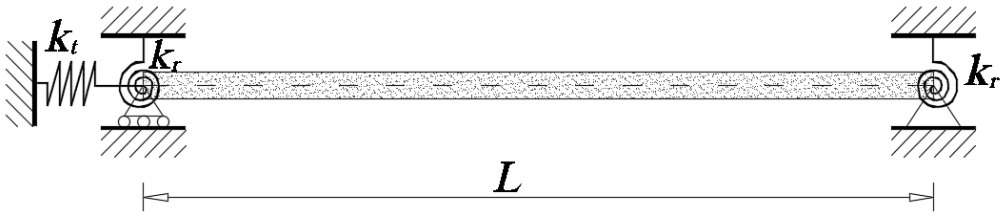

Figure 4.12: Slab with combination of translational and rotational spring stiffness

Lesser deflection is found when the degree of both translational and rotational stiffness increases and the trend continuous up to the defined stiffness of 50% (0.50× elastic spring stiffness) with no sign of integrity failures or runaway type of displacement. But this behaviour does not converge as the degree of spring stiffness increases. Instead, with 100% (1.00× elastic spring stiffness), the sign of integrity failure is

witnessed with the sdeflection trend changing from approximately 89 minutes of fire exposure onwards.

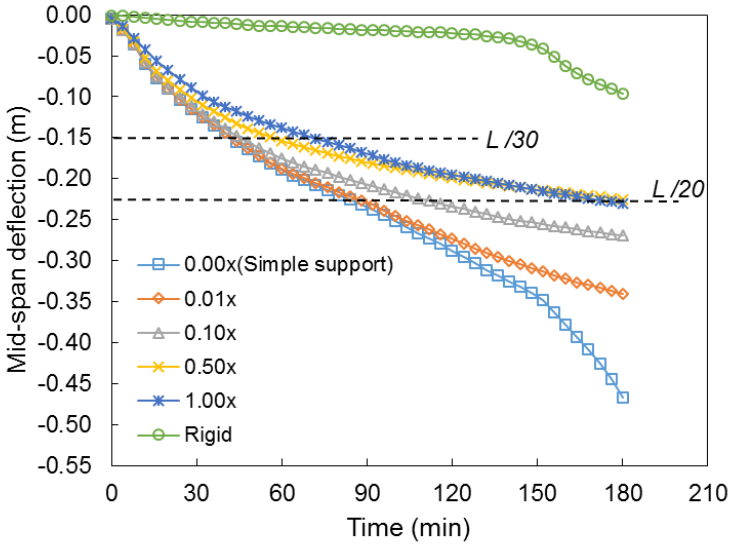

Figure 4.13: Effects of different degrees of translational and rotational spring stiffness to mid-span deflection

In order to get better understanding on the deflection behaviour of the slab (shown in Figure 4.13), vertical displacements along the slab's span at selected duration of fire exposures are plotted and shown in Figure 4.14 below. The plot of bending moment diagrams (BMD) are also plotted and shown in Figure 4.15.

Greater rotational restraint stiffness producing higher results to a reaction moment at support and this behaviour is shown in Figure 4.15(d). It was found that the change of trend in mid-span deflection as shown in Figure 4.13 is due to the plastic hinge formation near slab's support. Early sign of plastic hinge is also witnessed for the case of slab with 50% of elastic spring stiffness (both translational and rotational) but the reaction moment was not high enough to cause the change in trend of vertical mid-span deflection.

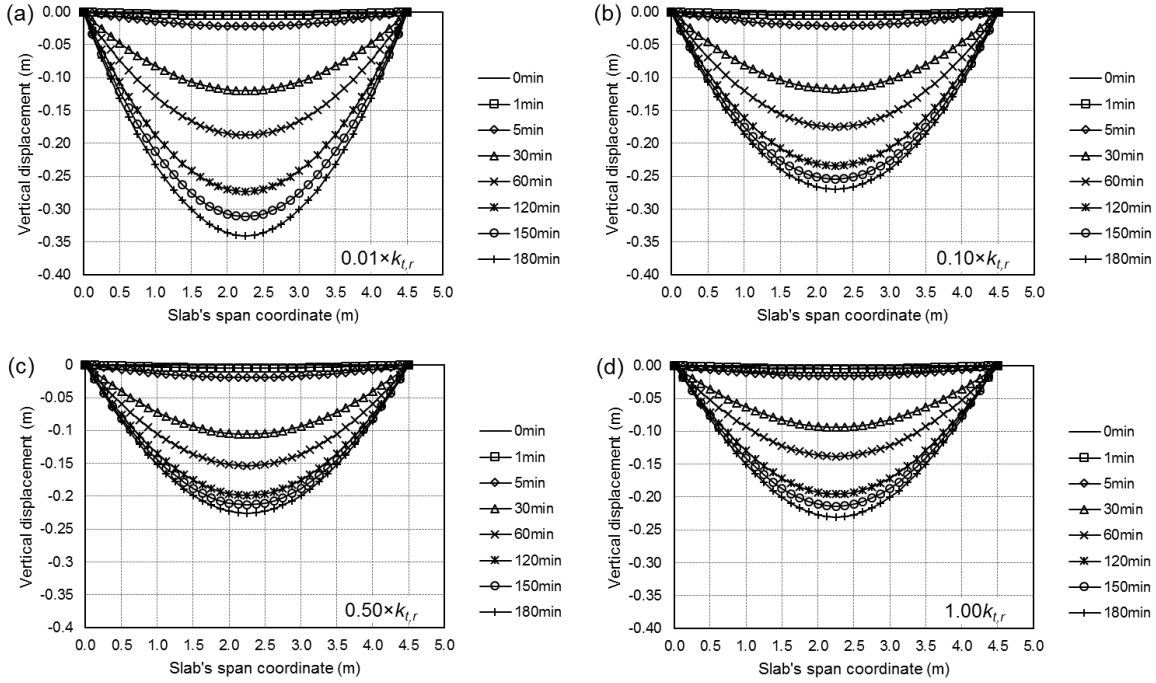

Figure 4.14: Mid-span deflection along slab's span at selected duration of fire exposure with spring stiffness at (a) 0.01×$k_{t,r}$ (b) 0.10×$k_{t,r}$ (c) 0.50×$k_{t,r}$ (d) 1.00×$k_{t,r}$

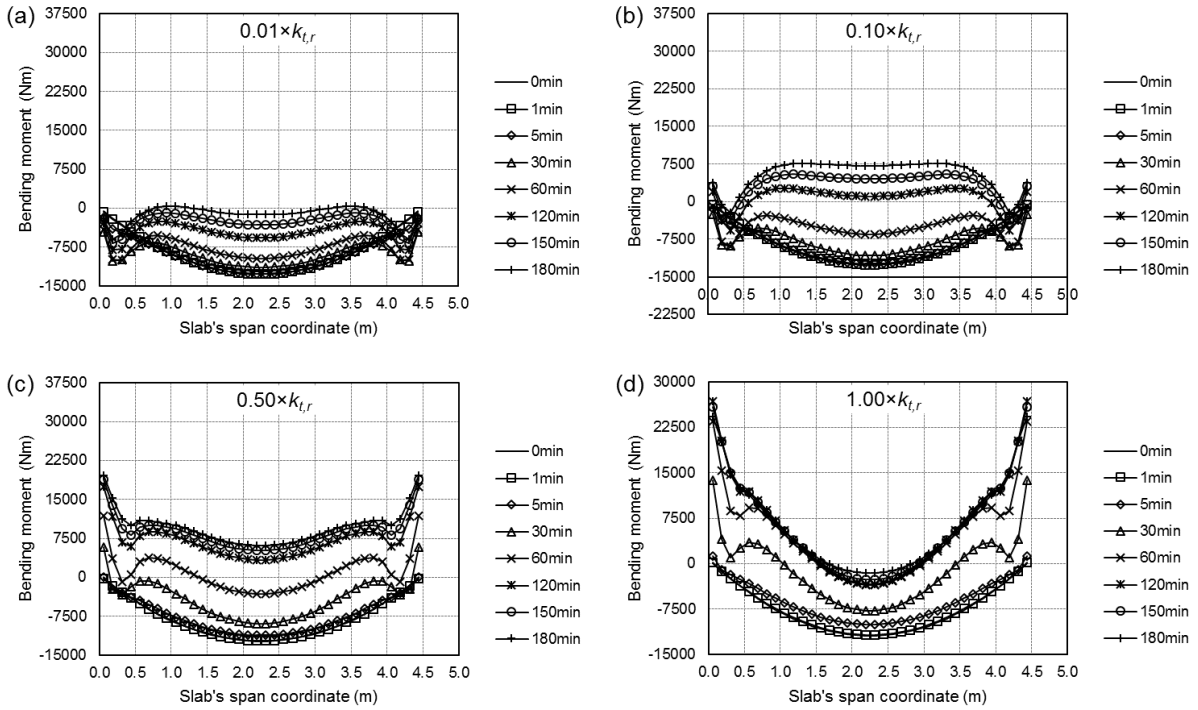

Figure 4.15: Bending moment diagram (BMD) at selected duration of fire exposure with spring stiffness at (a) 0.01×$k_{t,r}$ (b) 0.10×$k_{t,r}$ (c) 0.50×$k_{t,r}$ (d) 1.00×$k_{t,r}$

4.6.4 Summary

Studies presented in the current section discussed the structural response of one-way reinforced concrete slabs under exposure to ISO 834 (ISO, 1999) fires from below for 3 hours with varying degrees of support's stiffness. Table 4.2 below summarises the outcome from the studies in the current section.

Assessing structural fire resistance of the slabs with limiting mid-span deflection criteria and limiting temperatures in reinforcing steels i.e. 593 °C (ASTM, 2015) do not give a comprehensive insight into the performance of the slabs under severe heating from below. Other aspect, which is limiting plastic strain must be included as one of the performance indicators when assessing the structural performance of the slabs. Indeed this is true especially when plastic hinges formed in the slabs with high rotational restraint condition at supports (for instance $1.00k_r$ and $1.00k_{t,r}$ in this case). High rotational restraint at support reduces mid-span deflection but at the same time increases strain in both concrete and top reinforcing steels at the section close to supports. With rotational restraint defined at $1.00k_r$, the slab satisfied limiting deflection criteria of $L/20$ (BSI, 1987) throughout 180 minutes of exposure. However, limiting plastic strain to 2% provides the slab with only 96 minutes of fire resistance rating. Note that validation of finite element models presented in the previous Chapter 3 suggests tensile plastic strain of 2% is critical for one-way slabs, simply supported at each end.

Table 4.2: Summary of structural fire resistance rating for slab with varying restraint condition

#	Fire resistance criterion	*L /20* (BSI, 1987)	Tensile plastic strain in reinforcing steels: 2%	Eurocode 2 (CEN, 2004)	International Building Code (International Code Council, 2009)
1	Simple support	83 mins	>180 mins	60 mins	120 mins
2	Trans restraint: *0.01*×	85 mins	>180 mins		
3	Trans. restraint: *0.10*×	93 mins	>180 mins		
4	Trans. restraint: *0.50*×	110 mins	>180 mins		
5	Trans. restraint: *1.00*×	122 mins	>180 mins		
6	Full translational restraint	131 mins	>180 mins		
7	Rot. restraint: *0.01*×	85 mins	>180 mins		
8	Rot. restraint: *0.10*×	101 mins	>180 mins		
9	Rot. restraint: *0.50*×	>180 mins	>180 mins		
10	Rot. restraint: *1.00*×	>180 mins	96 mins		
11	Full rotational restraint	>180 mins	22 mins		
12	Combined restraint: *0.01x*	86 mins	>180 mins		
13	Combined restraint: *0.10x*	109 mins	>180 mins		
14	Combined restraint: *0.50x*	178 mins	>180 mins		
15	Combined restraint: *1.00x*	170 mins	111 mins		
16	Rigid	>180 mins	>180 mins		

4.6.5 Recommendation for best practice guidance

In general, the presence of restraint (both translational and rotational) improved fire resistance rating of the slabs if limiting deflection criteria specified in BS 476-20:1987 (BSI, 1987) is used. However, it does not provide the modeller with a comprehensive understanding on the behaviour of one-way slabs under exposure to severe heating from below.

Examining reinforcing steels plastic strain provide better performance indicator when assessing the structural fire performance of one-way slabs exposed to fires from below. Indeed, this is true especially when a plastic hinge has formed at any location along the slab's span, and trend of mid-span deflection did not signal the formation of this plastic hinge. Formation of plastic hinges will result high plastic strain in reinforcing steels. Therefore, it is suggested that both criteria i.e. limiting deflection and limiting tensile plastic strain must be used as the structural performance criteria when modelling the response of one-way reinforced concrete slabs exposed to severe heating from below.

4.7 Curtailment of top reinforcement

For economical reason, top and also bottom reinforcement of continuous reinforced concrete slabs is normally curtailed to a certain length. The total length of the reinforcement is typically provided to cater to the flexural capacity as well as shear. The design of reinforced concrete elements in accordance to Eurocode 2 (CEN, 2014) specifies that top reinforcement must be provided beyond the length where it is no longer required for flexural reinforcement to a certain length.

This extra length is provided to ensure reinforcing steel has enough bonding strength to ensure smooth load transfer and also for provision of shear reinforcement in some cases. In general, the total length of top reinforcement for continuous elements in accordance to Eurocode 2: Design of concrete structures (CEN, 2014) is equivalent to; 'length required for resisting bending + l_{bd} + 1.0d'. Length required for resisting bending is equals to 0.2113×span, typically found in classical structural mechanics book. l_{bd} is the bond length which depends on several factors such as quality of concrete and reinforcing steel among others and 1.0d is the length dependent on the effective depth of the concrete.

The approach described above is currently applicable for the design at both ambient temperature and fire design although it is not mentioned explicitly that this method is also applicable for fire design. It is mentioned in such a way as there are no studies conducted so far on this topic to provide guidance if special treatment is required for fire design. This section will attempt to address this aspect for the design of one-way reinforced concrete slabs exposed to ISO 834 (ISO, 1999) fires. For simplicity, only top reinforcement will be curtailed and bottom reinforcement is assumed to extend into supports.

Selected total length of top reinforcement are 0.125L, 0.25L, and 0.375L where L is the span of the slab. These values are randomly selected to define the length within the range of extreme minimum and maximum length possible for the current slab under consideration. If estimation of this length follows the recommendations from Eurocode 2 (CEN, 2014), the total length would be equivalent to 1392 mm or simply 0.31L. This is approximated based on assumption poor quality of concrete casting, giving l_{bd} =

40Ø, where Ø is the reinforcing steel diameter. l_{bd} typically range from 36Ø to 40Ø depending on several factors (CEN, 2014).

The analysis on the influence of curtailment length is divided into four (4) groups. These four groups are categorised based on different types of slab supports. The first case (refer Section 4.7.1) will assume the slab is fully restraint against both translational and rotational displacements (rigid), second case (see Section 4.7.2) will present slabs with translational spring stiffness, third case (see Section4.7.3) will present the slab with rotational spring stiffness while the final case (see Section 4.7.4) will discuss response of slabs with both translational and rotational spring stiffness. For each of the four groups, length of top reinforcement is defined as 0.125*L*, 0.25*L*, and 0.375*L*.

Buchanan and Abu (2017) quoted the length of reinforcing bars for resisting negative moment (hogging) should be extended 15% to 20% more to cater for moment redistribution in a continuous element. However, the authors did not mention the source or base for this recommendation. However, the redistribution of moment clearly increases the length of reinforcement required for resisting hogging moment as the moment shifts from positive (sagging) to negative (hogging) and the absence of reinforcement for resisting tensile stresses could pose serious problems to the fire resistance of the elements, which will be further discussed in the sections that follow.

4.7.1 Slab fully restrained against translational and rotational displacement

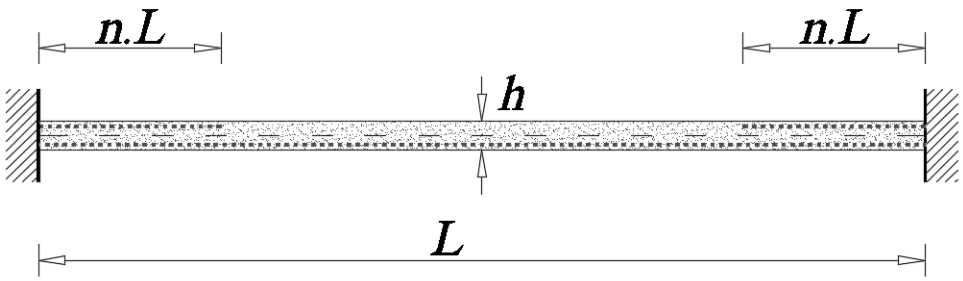

Figure 4.16: Slab fully restraint against rotational and translational displacement with varying reinforcement curtailment lengths

With the support condition assumed as fully fixed against translational and rotational (see Figure 4.16) displacement, there is no significant effect to the predicted mid-span deflection as shown in Figure 4.17 for slabs with varying lengths of top reinforcement. However, in the absence of the top reinforcement (no reinforcement at all), a snap trough occurred, and this is shown in Figure 4.17 (see curve labelled as 0.00*L*). Snap trough is a phenomenon in which slabs transition from compressive membrane action to tensile membrane action, occurring in an abrupt manner. For the case of one-way slabs, snap trough would lead to catenary mode with axial tensile forces generated in the slab (Lim, 2003). Slabs will fail (collapse) if supports cannot sustain these axial forces. In contrast, tensile net at the central section of slabs is supported by the surrounding compressive ring for the case of two-way slabs. It must also be noted that the condition of fully fixed (rigid) at the support rarely exists in a realistic reinforced concrete building frame. For this reason, the influence of curtailment to slabs with a certain degree of restraint at support will be presented in the following sections.

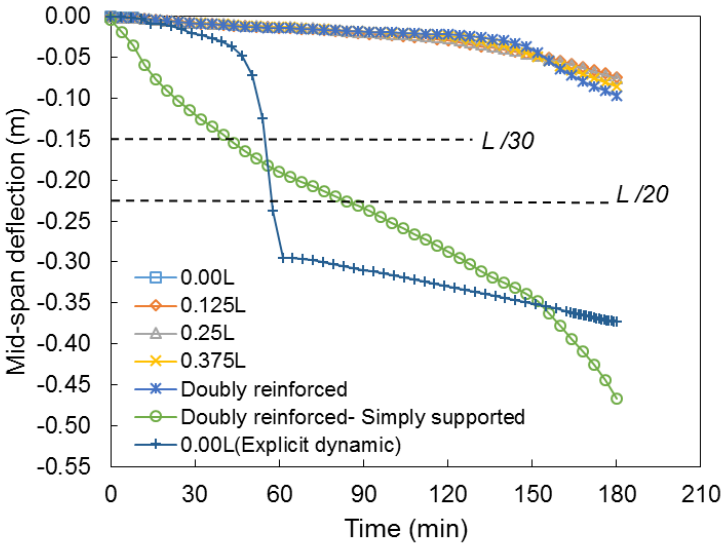

Figure 4.17: Effect of curtailment length to mid-span deflection

4.7.2 Slab with translational spring stiffness

As anticipated, with only axial restrain stiffness defined, there is no noticeable effect on the predicted mid-span deflection for slabs with different length of curtailment. While axial restraint limits axial expansion of the slab, the introduction of additional moment due to high vertical displacement (the magnitude of vertical displacement exceeds slab's line of thrust) is very minimal and not enough to cause any detrimental effects both at slab's mid-span and support. Graphical configuration of the model setup is shown in Figure 4.18. The predicted mid-span deflection with different curtailment length is shown in Figure 4.19: (a) spring stiffness at $0.01k_t$, (b) spring stiffness at $0.10k_t$, (c) spring stiffness at $0.50k_t$, and (d) spring stiffness at $1.00k_t$

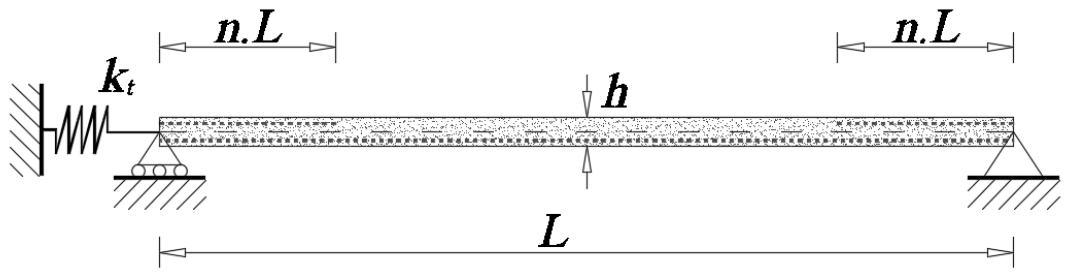

Figure 4.18: Slab with elastic translational spring stiffness and varying reinforcement curtailment lengths

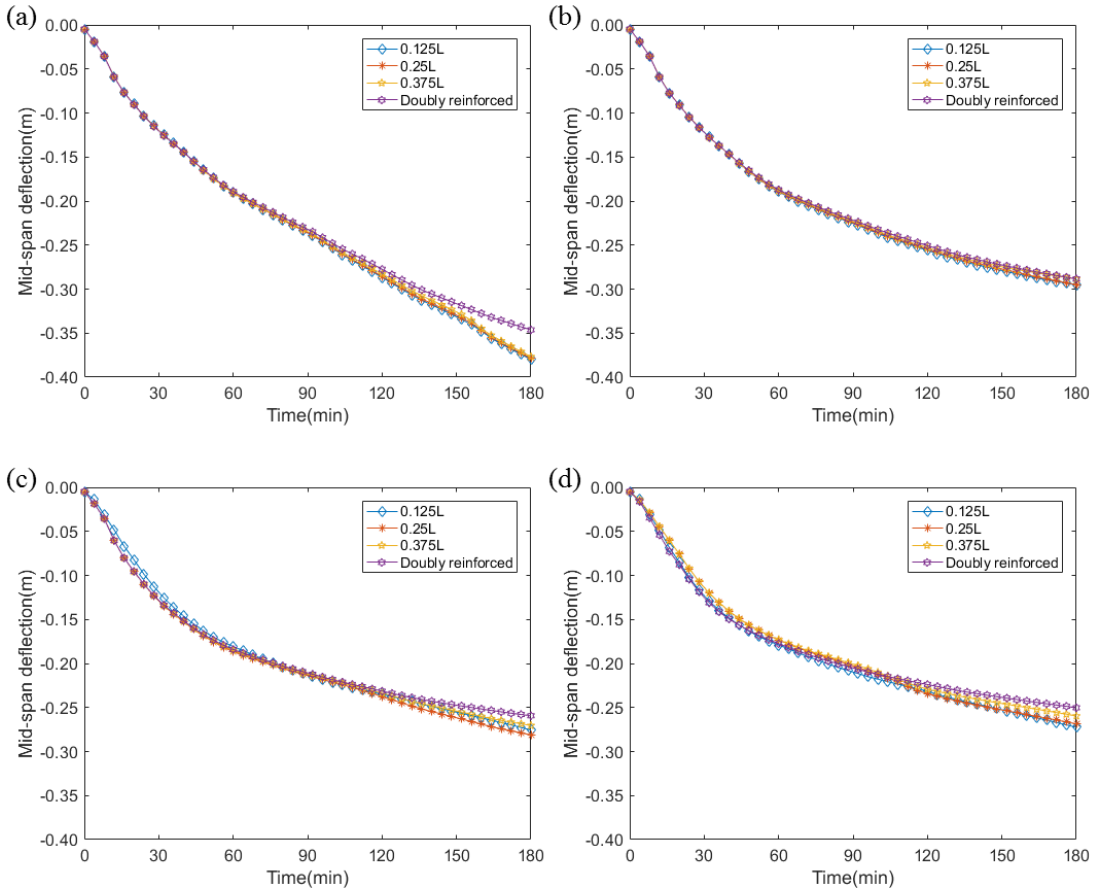

Figure 4.19: Mid-span deflection for slabs with varying length of curtailment of top reinforcement and different translational spring stiffness (a) 0.01k_t (b) 0.1 k_t (c) *0.5* k_t (d) 1.0 k_t

4.7.3 Slab with rotational spring stiffness

Configuration of the model setup is shown in Figure 4.20 while the predicted mid-span deflection is shown in Figure 4.21. With different stiffness of rotational spring defined, the provision of different lengths of top reinforcement have a significant effect on the predicted mid-span deflection. In Figure 4.21(a), the predicted mid-span deflection for the slab with varying lengths of top reinforcement and spring stiffness defined at $0.01k_r$ is shown. Slabs with spring stiffness defined at $0.10k_r$, $0.50k_r$, and $1.00k_r$ are shown in Figure 4.21(b), Figure 4.21(c), and Figure 4.21(d) respectively.

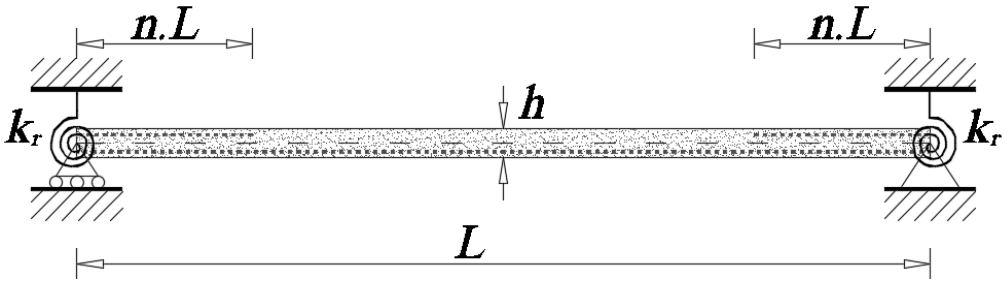

Figure 4.20: Slab with elastic rotational spring stiffness and varying reinforcement curtailment lengths

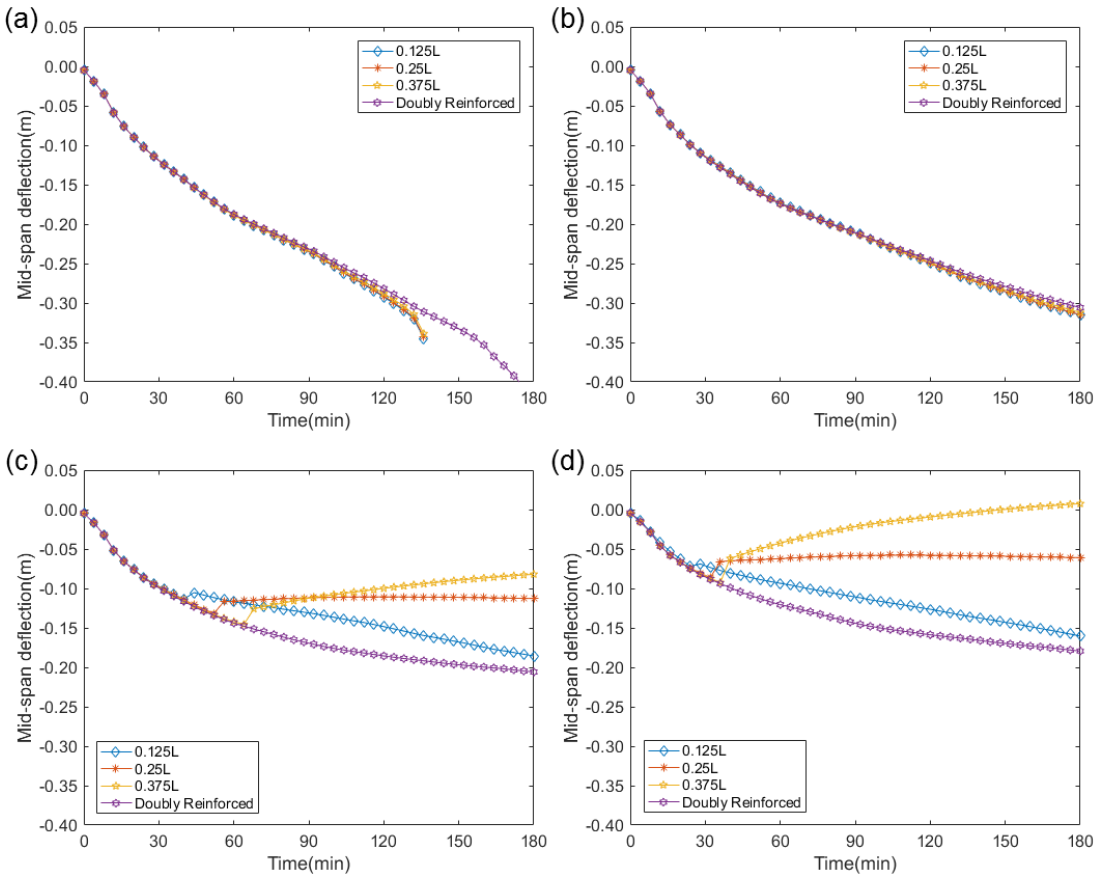

Figure 4.21: Mid-span deflection for slabs with varying length of curtailment of top reinforcement and different rotational spring stiffness (a) 0.01k_r (b) 0.1 k_r (c) *0.5* k_r (d) 1.0 k_r

With a relatively higher value of spring stiffness (50% of elastic bending stiffness and above), high reaction moment at support results in response to thermal bowing and deflection of the slab. This high reaction moment resulted in plastic hinge formation at the location where top reinforcement is curtailed. With the absence of tension reinforcement, this 'cut-off' point has become a weak point where the slab is trying to resist rotation due to negative moment (hogging). This is demonstrated with a sudden upward deflection at mid-span with rotational spring stiffness defined at 50% and 100% of the elastic bending stiffness (refer Figure 4.21 (c) and (d)).

In order to get better insight into the behaviour of the slab with different curtailment lengths, vertical displacement along the slab's span at selected duration of fire exposure for the slab with rotational spring stiffness defined at 1.0k_r is shown in Figure

4.22. Only spring stiffness of $1.0k_r$ is presented for discussion here as representative case to the behaviour. Length of top reinforcement specified at $0.125L$, $0.25L$, and $0.375L$, and $1.0L$ (doubly reinforced) is shown in Figure 4.22(a), Figure 4.22(b), Figure 4.22(c), and Figure 4.22(d) respectively. Similar plot for bending moment diagram (BMD) is shown in Figure 4.23(a), Figure 4.23(b), Figure 4.23(c), and Figure 4.23(d) respectively.

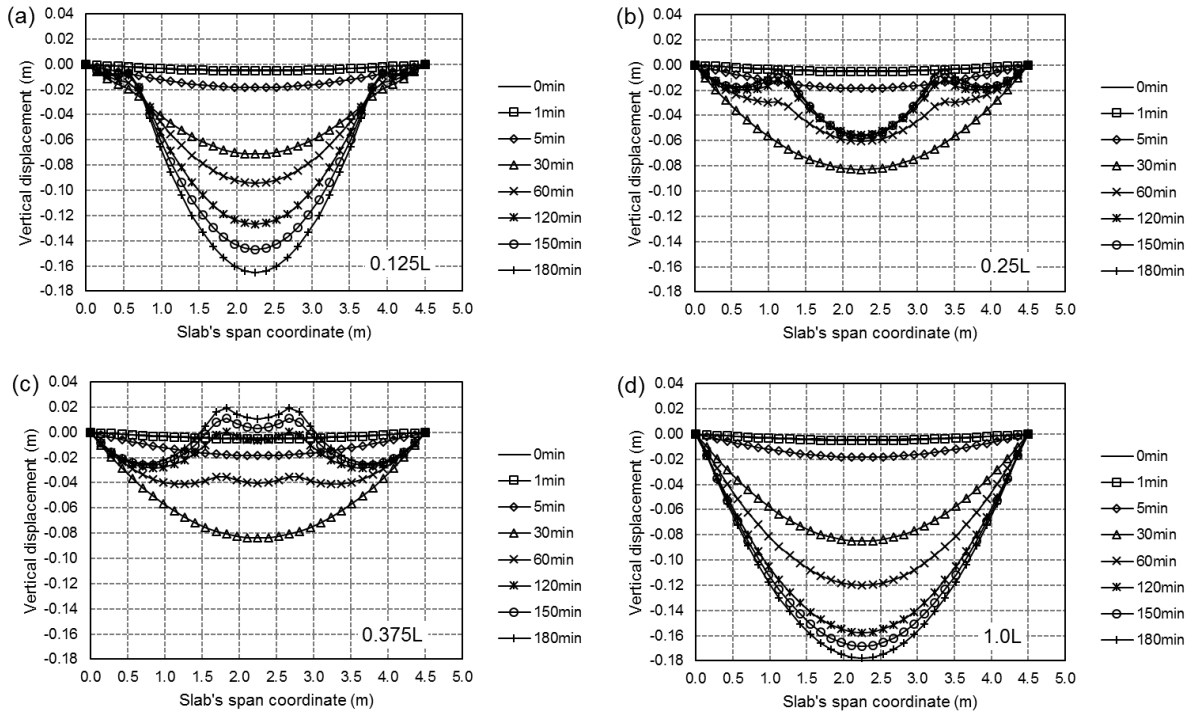

Figure 4.22: Vertical displacement along slab's span at selected time of fire exposure for slab with different curtailments lengths of top reinforcement and rotational spring stiffness at $1.0k_r$

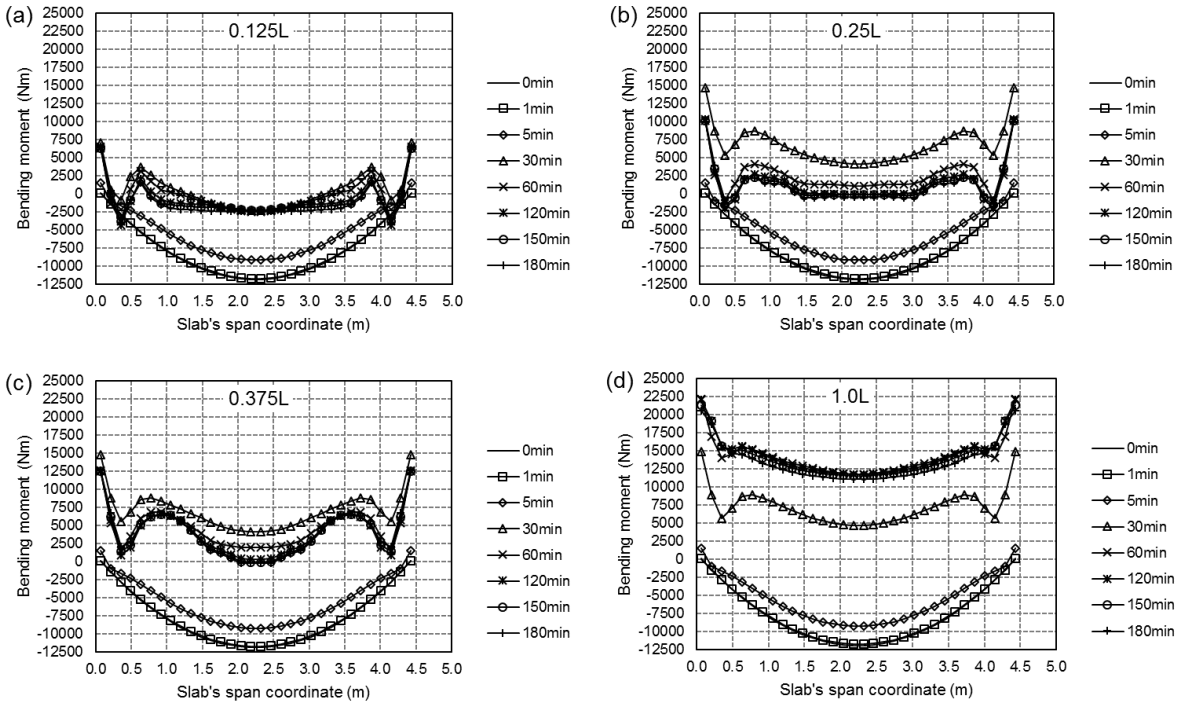

Figure 4.23: Bending moment diagram (BMD) at selected time of fire exposure for slab with different curtailment lengths of top reinforcement and rotational spring stiffness at $1.0k_r$

With the plastic hinges formed (see Figure 4.22(a), Figure 4.22(b), and Figure 4.22(c)), integrity of the slabs is in doubt with regard to the load-carrying capacity. In contrast, provision of full length of top reinforcement (doubly reinforced) produces slab with good fire resistance rating and resisting high hogging moment (approximately 22.5kNm) as demonstrated in Figure 4.22(d).

In Figure 4.22 (c), with top reinforcement provided as 0.375*L* (1687.5 mm), section at the slab mid-span where there is no provision of top reinforcement displaced upwards after plastic hinge has formed. Interestingly, this upward trend of deflection is not high enough for the case of slab with top reinforcement curtailed at relatively shorter length i.e. 0.125*L*, and 0.275*L* although it must be emphasized here that plastic hinges still formed. It was not high enough to cause the mid-span to be in positive displacement vertically. This is because, with a shorter length of top reinforcement, the span between plastic hinges is greater thus higher downwards gravity load (self-weight +

superimposed load) imposed on the slabs, therefore requiring greater reaction moment at support to push the slab upwards.

Note that the elastic rotational spring stiffness at support was defined as independent of temperature, meaning it is not affected by the temperature increase. As temperature increases, stiffness in the slab section also decreases but the stiffness in the spring maintains at the same stiffness, which might also explain this behaviour. In that respect, this might not be realistic with regards to actual continuous reinforced concrete elements.

If this behaviour is to be translated to the actual reinforced concrete slabs in a building, it shows how important it is to provide reinforcement to full length extent of the slab's span. Within the context of assumption in the current model, it can be concluded that the provision of extra 15-20% of top reinforcement length is not sufficient to prevent formation of plastic hinge that deteriorates the integrity of the slab.

4.7.4 Slab with combined translational and rotational spring stiffness

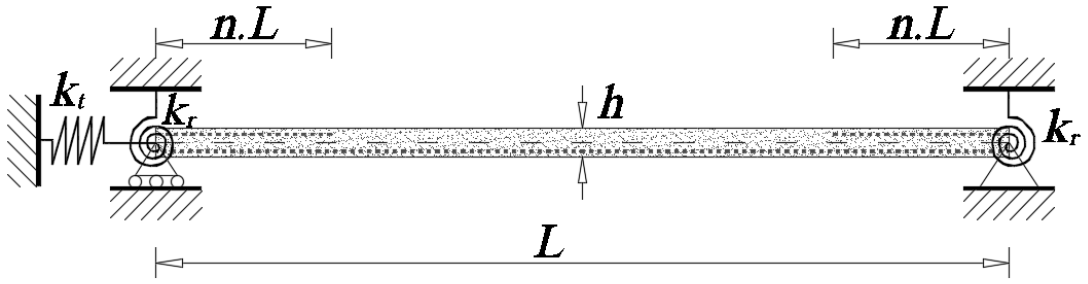

Figure 4.24: Slab with elastic rotational and translational spring stiffness and varying reinforcement curtailment length

Similar points highlighted in Section 4.6.3, typical cast in-situ continuous reinforced concrete slabs would usually have restraint in both translational and rotational. Previous two (2) sections have presented and discussed the aspect of slab with reinforcement curtailed at certain length have had either translational or rotational spring stiffness acting individually on the slabs. In this section, response of slab with curtailed top reinforcement and has combination of translational and rotational spring

stiffness at support will be presented and discussed. Similar multiplier (percentage of elastic spring stiffness) will be applied to both translational and rotational spring for each model with specified top reinforcement length.

No doubt that the existence of both translational and rotational spring stiffness has improved the structural behaviour in all cases of curtailment of the slab with the exception of slab with $0.125L$ of top reinforcement. Note that $0.125L$ provides length that is in the extreme low limit of curtailment length for the slab, not only for fire design but also for ambient temperature design. In other words, this has never been the case even for the design of similar slab at ambient temperatures. This is shown with the predicted mid-span deflections shown in Figure 4.25.

Referring to the findings presented in Section 4.6.3, where structural response of slabs with combination of translational and rotational restraint at supports was investigated, formation of plastic hinges is still possible even though the full length of top reinforcement was provided. The plastic hinges formed for slab with restraint stiffness of $1.0k_{tr}$. The hinge formed at location close to supports. However, a greater reaction moment at supports is required in order for the hinges to form for the case of slabs with top reinforcement run for full length of the slabs.

Here in this section, although the plot of bending moment diagrams is not presented, it is worth to imply that the formation of plastic hinges is still possible. However, throughout 180 minutes of exposure, the predicted reaction moment at supports is not enough to cause vertical upward displacement at slab's mid-span. This can be seen in the plot for mid-span deflection presented in Figure 4.25.

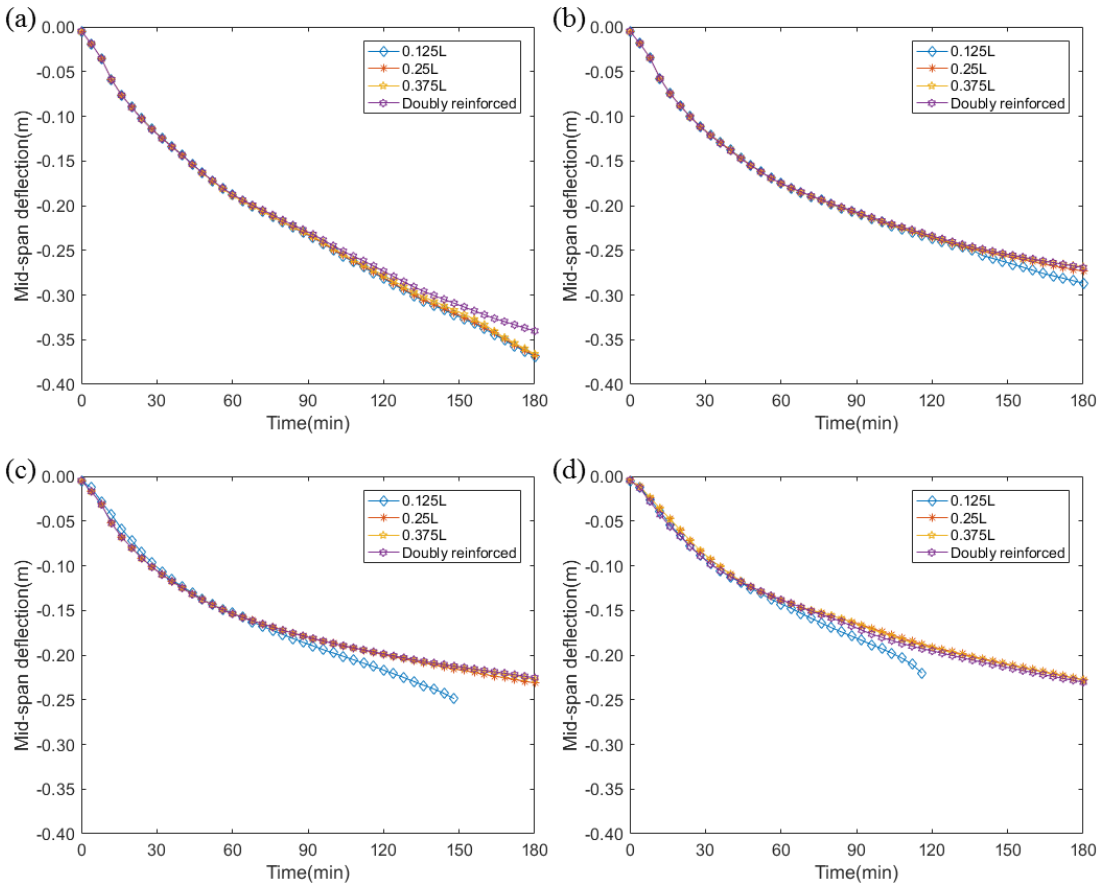

Figure 4.25: Mid-span deflection with varying length of curtailment of top reinforcement with different translational and rotational spring stiffness (a) 0.01 k_{tr} (b) 0.1 k_{tr} (c) *0.5* k_{tr} (d) 1.0 k_{tr}

4.7.5 Summary

The influence of top reinforcing steels curtailment length to the predicted structural response of one-way slabs exposed to ISO 834 (ISO, 1999) fire is presented in the current section. Summary of the fire resistance rating for all the cases investigated with regard to limiting the deflection criteria and limiting tensile plastic strain is shown in Table 4.3 and Table 4.4 respectively.

Table 4.3: Summary of structural fire resistance rating for slab with varying curtailment lengths: BS 476-20:1987 (BSI, 1997)

#	Fire resistance criterion	*L /20* (BSI, 1987)			
	Curtailment's length	*0.125L*	*0.250L*	*0.375L*	*1.000L*
1	Trans restraint: *0.01*×	82 mins	82 mins	83 mins	85 mins
2	Trans. restraint: *0.10*×	90 mins	90 mins	91 mins	93 mins
3	Trans. restraint: *0.50*×	105 mins	105 mins	108 mins	110 mins
4	Trans. restraint: *1.00*×	110 mins	111 mins	115 mins	122 mins
5	Rot. restraint: *0.01*×	83 mins	83 mins	84 mins	85 mins
6	Rot. restraint: *0.10*×	100 mins	100 mins	100 mins	101 mins
7	Rot. restraint: *0.50*×	>180 mins	>180 mins	>180 mins	>180 mins
8	Rot. restraint: *1.00*×	>180 mins	>180 mins	>180 mins	>180 mins
9	Combined restraint: *0.01x*	84 mins	84 mins	85 mins	86 mins
10	Combined restraint: *0.10x*	107 mins	107 mins	108 mins	109 mins
11	Combined restraint: *0.50x*	128 mins	166 mins	175 mins	178 mins
12	Combined restraint: *1.00x*	117 mins	175 mins	174 mins	169 mins
13	Rigid	>180 mins	>180 mins	>180 mins	>180 mins

The higher the value of rotational stiffness at support, the higher the reaction moment would result as the slabs exposed to severe heating from below. Higher reaction moment increases the possibility of plastic hinge formation and the location at which this is likely to occur is typically at the section where the top reinforcement is curtailed. It is also suggested that limiting the deflection criteria cannot be used as the sole criteria in assessing fire resistance rating for slabs with varying top reinforcement curtailment's length as it potentially hinders an important aspect that need to be better assessed for instance plastic hinges.

With a higher combined translational and rotational restraint at supports, lower mid-span deflections were predicted. On the other hand, higher restraint stiffness increases tensile plastic strain in reinforcing steels (see Table 4.4) thus reducing fire resistance rating for the slabs if limiting tensile plastic strain is set as the performance indicator.

Table 4.4: Summary of structural fire resistance rating for slab with varying curtailment lengths: 2% tensile plastic strain

#	Fire resistance criterion	Tensile strain in reinforcing steels: 2% (Wang et al., 2013)			
	Curtailment's length	*0.125L*	*0.250L*	*0.375L*	*1.000L*
1	Trans restraint: *0.01*×	>180 mins	>180 mins	>180 mins	>180 mins
2	Trans. restraint: *0.10*×	>180 mins	>180 mins	>180 mins	>180 mins
3	Trans. restraint: *0.50*×	>180 mins	>180 mins	>180 mins	>180 mins
4	Trans. restraint: *1.00*×	>180 mins	>180 mins	>180 mins	>180 mins
5	Rot. restraint: *0.01*×	>120 mins**	>120 mins**	>120 mins**	>180 mins
6	Rot. restraint: *0.10*×	>180 mins	>180 mins	>180 mins	>180 mins
7	Rot. restraint: *0.50*×	42 mins*	56 mins*	67 mins*	>180 mins
8	Rot. restraint: *1.00*×	25 mins*	34 mins*	38 mins*	86 mins
9	Combined restraint: *0.01x*	>180 mins	>180 mins	>180 mins	>180 mins
10	Combined restraint: *0.10x*	>180 mins	>180 mins	>180 mins	>180 mins
11	Combined restraint: *0.50x*	>180 mins	>180 mins	>180 mins	>180 mins
12	Combined restraint: *1.00x*	>180 mins	126 mins	118 mins	111 mins
13	Rigid	>180 mins	>180 mins	>180 mins	>180 mins

**Plastic hinges formed and caused vertical upward displacement at mid-span*
***Analysis did not finish the 180 minutes simulation (premature termination)*

4.7.6 Recommendation for best practice guidance

Limiting mid-span deflection criteria and limiting tensile plastic strain criteria shall be used as complimentary to each other. Using either limiting mid-span deflection or limiting tensile plastic strain as a sole performance indicator could hinder an important aspect in assessing the structural performance of one-way slabs under exposure to severe heating from below.

It is also recommended to provide full length of top reinforcement if the possibility of plastic hinges formation is to be reduced as low as possible. On the other hand, it also needs to be emphasized that the higher the support restraint stiffness, the higher the reaction moment as the heating progress. With a higher reaction moment, the possibility of plastic hinges formation is also increased.

4.8 Span-to-depth ratio

Preparing design scheme for reinforced concrete structures typically involve determining the optimum dimension of members as well as the optimum amount of area of reinforcement (tension and compression). The selected dimension and

reinforcement area are chosen to provide flexural, shear (either flexural shear and/or punching shear), and axial strength capacity for the element under consideration.

With regard to designing one-way reinforced concrete slabs, flexural shear is not always a concern as typically a concrete material itself can provide enough shear capacity. In addition, design load sustained by concrete slabs in general is not as high as sustained by beams. But in some cases, shear reinforcement has to be provided to provide shear strength to the designed elements.

In contrast to structural fire design of steel structures, designing concrete structures/elements is unique in a sense that concrete is always thought as having good fire performance. This is due to the low thermal conductance of concrete materials as opposed to steel materials. As a result, approximating a suitable geometrical dimension of a concrete elements is not really an interesting topic to explore, as the only design strategy is to ensure reinforcing steel (in concrete elements) temperatures does not exceed the critical temperatures, this being the design criteria. This is achieved by providing sufficient concrete cover. With this being the design objective for designing reinforced concrete structures/elements for fire resistance, fundamental understanding of the structural mechanics of the elements is thought to be not so important, thus hindering the crucial progress in designing full frame behaviour of reinforced concrete structures.

Two-way reinforced concrete slabs are also claimed to have good structural performance under exposure to fires from below by utilising membrane action while sustaining large vertical deflection. This behaviour is now being adopted in designing steel-concrete composite construction where concrete slab provides structural protection to the unprotected steel beams in the events of fires. Tensile membrane action occurs under high vertical deflection and typically limiting deflection criteria is potentially not relevant when assessing the structural fire performance of this kind of slab. On the other hand, if limiting deflection is the criteria for fire resistance of this kind of structures, it is worth to look at the aspect of selecting a range of possible thickness of a concrete slab so as to investigate whether a thicker slab would further

enhance structural performance of the slabs; an aspect applicable to both one-way and two-way slabs.

With the above points as the motivation, this section will present studies looking at the aspect of span-to-depth ratio to fire resistance rating of one-way reinforced concrete slabs. Specifically, an attempt will be made in looking at whether increasing or even decreasing the slab thickness will improve structural fire resistance rating of a one-way reinforced concrete slab or otherwise.

In doing so, four (4) span-to-depth ratios, 46.9, 37.2, 30.8, and 26.3 were selected to represent the slab thickness of 125 mm, 150 mm, 175 mm, and 200 mm respectively. Span is fixed at 4500 mm in all cases. Both simply supported case (Section 4.8.1) and continuous (Section 4.8.2) are investigated and presented. Detailed explanation is given in the section that follows separately for each case.

Thermal analysis (heat transfer) is done beforehand to predict the temperature distribution within the slab's depth for each of the cases. Predicted temperature histories at the exposed surface, in reinforcing steel, and at the unexposed surface for different slab's thicknesses are shown in Figure 4.26 above. Note that the presented reinforcing steel's temperature is simply the interpolated temperature outputted from structural (mechanical) model to illustrate the temperature in the reinforcing of steel while performing mechanical analysis. Of course, there are some variations in the predicted temperatures at other locations within the slab's depth for slabs with different thicknesses, but they are not shown in the figure for clarity purposes. Note that in the figure, temperatures at the unexposed surface show differences where the thinness slab i.e. 125 mm predicted the highest temperature while thickest slab i.e. 200 mm predicted the lowest temperature. Given the temperature at the surface unexposed from fires is one of the criteria for assessing fire performance of reinforced concrete slab in (ASTM, 2015), studies presented in the following section will demonstrate the extent at which this is correlated with the predicted structural response of the slab. Slab with span-to-depth ratio of 46.9 (125 mm thick) attained temperature of 139 °C (being limiting temperature according to (ASTM, 2015)) at 174 minutes of exposure to ISO

834 (ISO, 1999) while for other cases, predicted temperatures at the un-exposed surface never exceeds 139 °C throughout 180 minutes of exposure.

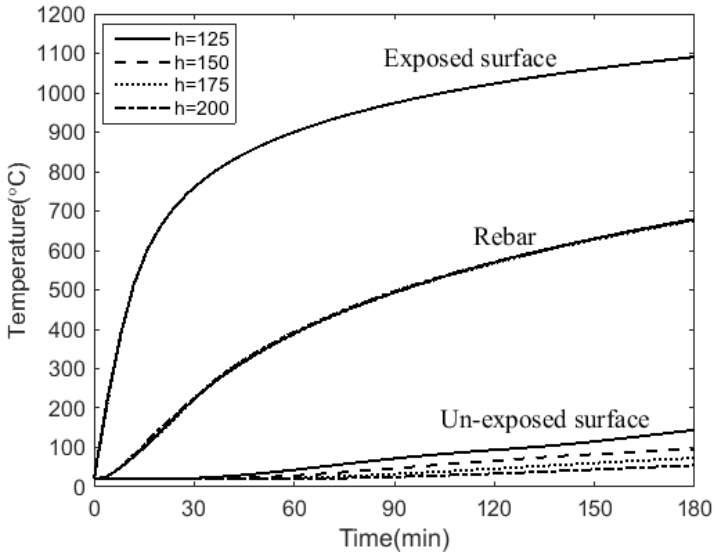

Figure 4.26: Predicted temperature histories at the exposed surface, in reinforcing steels, and unexposed surface for slab with different thicknesses (span-to-depth ratio)

4.8.1 Simply supported case

Slabs are designed based on recommendations from Eurocode 2: Design of concrete structures-Part 1-1(CEN, 2014) and Part 1-2 (CEN, 2004). Design input data are shown in Table 4.5. Live load is fixed at 2 kPa in all cases. The general idea of the studies is to investigate the influence of selected slab's thickness to the structural response, given similar design input requirements. Assuming a structural fire engineer is designing one-way reinforced concrete slabs for fire, an assessment will be made here as to whether choosing a different range of reasonable slab's thickness would improve the structural fire resistance of the simply supported slab's case, exposed to ISO 834 (ISO, 1999) fire. Figure 4.27 shows graphically the selected span-to-depth ratio for investigation in the current section.

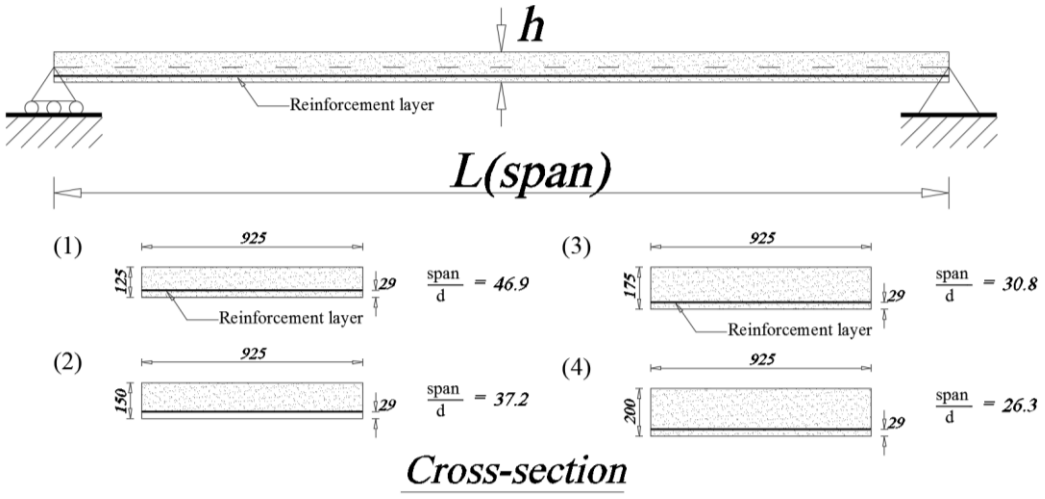

Figure 4.27: Slab' elevation and four (4) different cross sections

To ensure the consistency in all the analysis, the provided area of steel reinforcement (A_s provided) will be simply defined equivalent to the area of steel required (A_s required), with the diameter of reinforcing steel fixed at 8 mm. This is not realistic within the practical aspect as this will end up with selecting an odd reinforcing steel spacing e.g. 108 mm instead of rounding it to 100 mm as typically a design engineer would do. This is done (and it is very important) for consistency and note that the study is purely academic. Table 4.6 presents the resulting design moment and the provided area of reinforcement (A_s provided = A_s required).

Table 4.5: Design input data for simply supported slab

Case	Span, L (mm)	Thickness, h (mm)	Axis distance (mm)	Eff. depth, d (mm)	Span / d	Dead Load (N/m^2)	Live Load (N/m^2)	Design Load$_{ult}$ ($1.35G_k+1.5Q_k$) (N/m^2)	Design Load$_{fire}$ ($1.0G_k+0.5Q_k$) (N/m^2)
1	4500	125	29	96	46.9	2943	2000	6973	3943
2	4500	150	29	121	37.2	3532	2000	7768	4532
3	4500	175	29	146	30.8	4120	2000	8562	5120
4	4500	200	29	171	26.3	4709	2000	9357	5709

Table 4.6: Design moment and selected area of reinforcement (A_s) for simply supported slab

Case	Span, L (mm)	Thickness, h (mm)	Ø reinforcing steel (mm)	Design moment_{ult} (kNm)	z (mm)	A_s required (mm^2)	A_s (%)
1	4500	125	8	16.3	90.3	452	0.51
2	4500	150	8	18.2	115	395	0.35
3	4500	175	8	20.1	139	361	0.27
4	4500	200	8	21.9	162.5	337	0.21

Mid-span deflections for slabs with different span-to-depth ratio are shown in Figure 4.28. In the plot, limiting deflection criteria as specified in BS 476-20:1987 (BSI, 1987) is also included for assessment on the structural fire resistance. Limiting deflection criteria simply gives lower fire resistance rating for slab with higher span-to-depth ratio and greater rating for thicker slab i.e. lower span-to-depth ratio. However, it is interesting to see that neither of the slab showed sign of collapse or integrity failure, and providing fire resistance rating of well above 90 minutes of fire exposure, if a collapse was set as the performance criteria. This finding highlights the level of complexities in providing design guidance for the design of concrete elements for fire resistance. However, certain criteria have to be specified, which might explain why limiting the criteria of $L/20$ (BSI, 1987) is there within the code but whether the collapse is anticipated when slabs exceed this criteria is a totally different subject requiring more assessment.

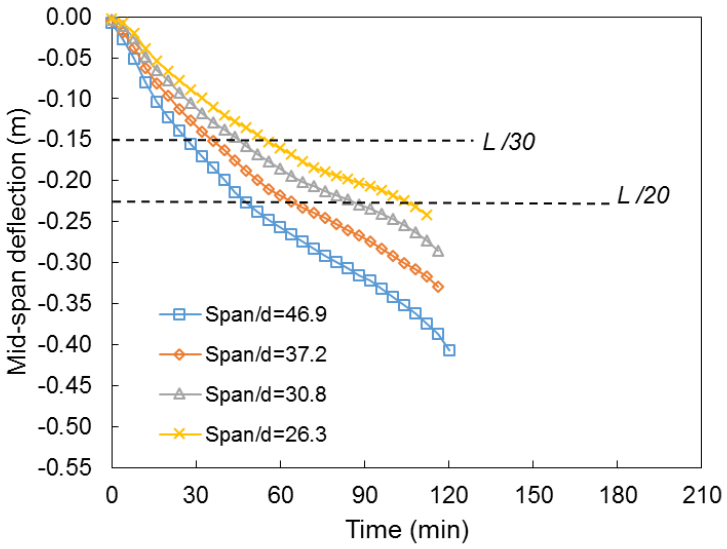

Figure 4.28: Mid-span deflection for slab with different span-to-depth ratio

Results from studies in this section suggest that for the case of simply supported slabs, varying span-to-depth ratio (within the range presented above) does not affect the integrity of the slabs, meaning the anticipated time of collapse for all the span-to-depth ratio cases is the same. From a different perspective, the slabs would have failed at 47 minutes, 64 minutes, 85 minutes, and 104 minutes for the case of slab with span-to-depth ratio of 46.9, 37.2, 30.8, and 26.3 respectively, if limiting the deflection criteria specified in BS 476-20: 1987 (BSI, 1987) is adopted. The comparison between the estimated fire resistance rating from limiting deflection criteria (as discussed here) and limiting tensile plastic strain in reinforcing steels will be made and discussed later in the summary section.

4.8.2 Continuous

Analysis and design of one-way reinforced slabs in this section are grouped into two (2) main categories. The first category will look into the response of the slab with supports fully restraint against translational and rotational displacement (Section 4.8.2.1) while second group will repeat the same analysis but with modification on the degree of restrain stiffness at the support (see Section 4.8.2.2). In the first group (Section 4.8.2.1) there will be sub-topics dealing with the manner in which bottom reinforcement near supports is defined and modelled. The reinforcement is either

extended into support or cut to a certain length where it is no longer required for the slab to resist the design bending moment. This is graphically presented in Figure 4.29. It is acknowledged that from a practical perspective, this will never be the case in design as bottom reinforcing steel will always be extended into support. However, this study is purely academic and designing this slab to resist bending does not require provision of flexural reinforcement since negative moment (hogging) at support resulting concrete section at bottom will be in compression rather than tension.

Provision of length of top reinforcement for resisting negative (hogging) moment is designed following the recommendations from Eurocode 2 (CEN, 2014). Note that this provision is also dependent on the effective depth, *d* of the slab, which in turn is also dependent on the defined span-to-depth ratio. The total length of top reinforcement is equal to $0.2113L + 40\emptyset + 1.0d$ where *L* is the span of the slab, Ø is the reinforcing steel diameter, and *d* is the effective depth. This was also described in the earlier section of this chapter and graphically presented in Figure 4.29 below.

4.8.2.1 Rigid supports

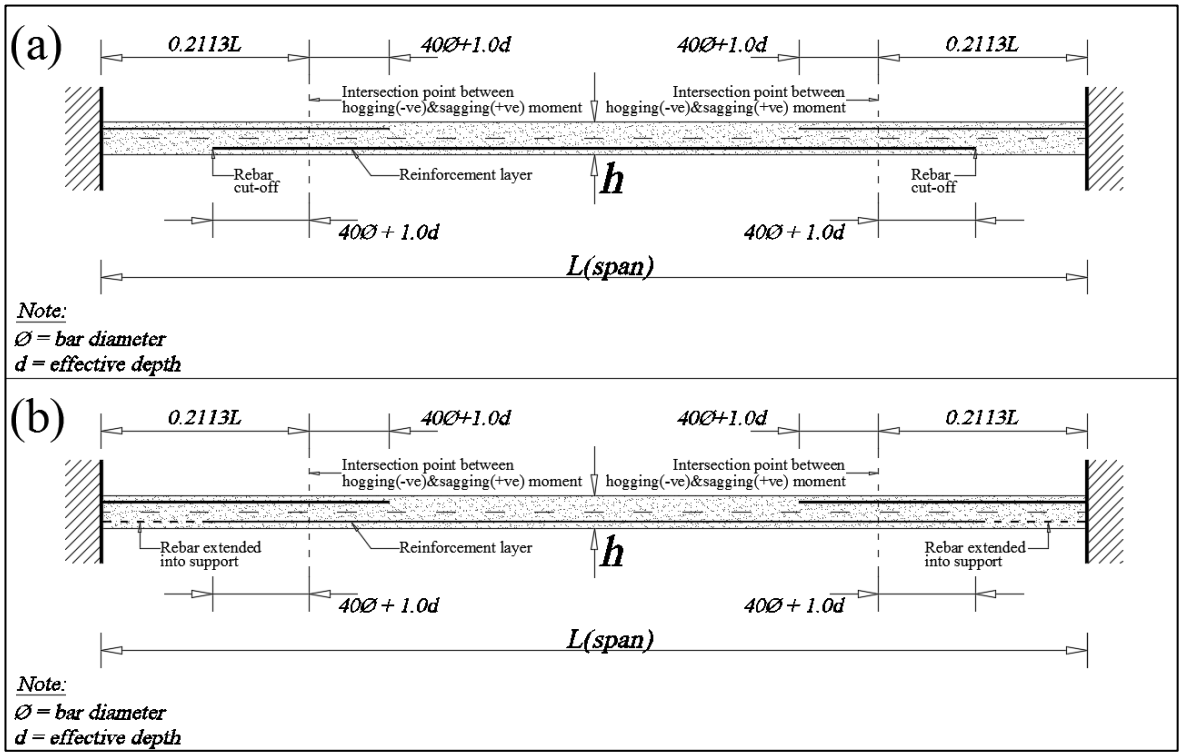

Figure 4.29: Slab's drawing showing arrangement of reinforcements

Selected inputs for performing analysis and design of the continuous slabs are tabulated in Table 4.7. In contrast to the analysis and design for simply supported case, live load is fixed at 3 kPa and reinforcing steel diameter, Ø is fixed at 6 mm. Note that the selected reinforcing steel diameter is smaller than the one adopted in the previous section i.e. 8 mm. This is to ensure that the spacing between each of the provided reinforcing steel is not too large, making the condition is unrealistic. The lowest percentage area of reinforcement is approximated as 0.08% for the case of slab with 200 mm thick. Note that the recommendation in Eurocode 2 (CEN, 2014) is that the area of reinforcement provided has to be within 0.13% to 4% of the area of concrete cross section. Unfortunately, this is something not feasible within the context of the current study as the area of steel reinforcement required ($A_{s\ required}$) = area of steel provided ($A_{s\ provided}$). The rationale of this decision has been described in the previous section thus it will not be repeated here.

Table 4.7: Design input data for continuous slab

Case	Span, L (mm)	Thickness, h (mm)	Axis distance (mm)	Eff. depth, d (mm)	Span/d	Dead Load (N/m^2)	Live load (N/m^2)	Design Load$_{ult}$ ($1.35G_k+1.5Q_k$) (N/m^2)	Design Load$_{fire}$ ($1.0G_k+0.5Q_k$) (N/m^2)
1	4500	125	29	96	46.9	2943	3000	8473	4443
2	4500	150	29	121	37.2	3532	3000	9268	5032
3	4500	175	29	146	30.8	4120	3000	10062	5620
4	4500	200	29	171	26.3	4709	3000	10857	6209

The design moment, provided area of reinforcement, and curtailment's length are tabulated in Table 4.7, Table 4.8, and respectively. With regard to the total length of top reinforcement, similar strategy applied in selecting area of reinforcement, the specified length of top reinforcement is exactly as what required. No rounding of the value to a 'practical' value, for instance,s 1300 mm instead of 1288 mm, where this is common practice in the design office for ease of measurement and fabrication at site.

Table 4.8: Design moment for continuous slabs

Case	Span, L (mm)	Thickness, h (mm)	Ø reinforcing steel (mm)	Design hogging moment_{ult} (kNm)	Design sagging moment_{ult} (kNm)	z: hogging (mm)	z: sagging (mm)
1	4500	125	6	13.23	6.61	92.15	92.15
2	4500	150	6	14.47	7.23	115.90	115.90
3	4500	175	6	15.71	7.9	140.00	140.00
4	4500	200	6	16.95	8.47	163.40	163.40

Table 4.9: Selected area of reinforcement (A_s) and curtailment length for continuous slab

Case	A_s required (top) (mm^2)	A_s (%)	A_s required (bottom) (mm^2)	A_s (%)	Curtailment's length: (40Ø+1.0d), (m)	Length of top reinforcement: (0.2113L+40Ø+1.0d), (m)
1	359	0.4	179	0.20	337	1288
2	312	0.28	156	0.14	362	1313
3	281	0.21	141	0.10	387	1338
4	260	0.16	130	0.08	412	1363

The mid-span deflection predicted with the bottom reinforcing steel curtailed is shown in Figure 4.30 while prediction of mid-span for the case of slab with bottom reinforcement fully extended into slab's support is shown in Figure 4.31. Figure 4.31 (b) shows the close-up plot of deflection shown in Figure 4.31 (a).

The mid-span deflection predicted with the bottom reinforcing steel curtailed is shown in Figure 4.30 while prediction of mid-span for the case of slab with bottom reinforcement fully extended into slab's support is shown in Figure 4.31. Figure 4.31(b) shows the close-up plot of deflection shown in Figure 4.31(a).

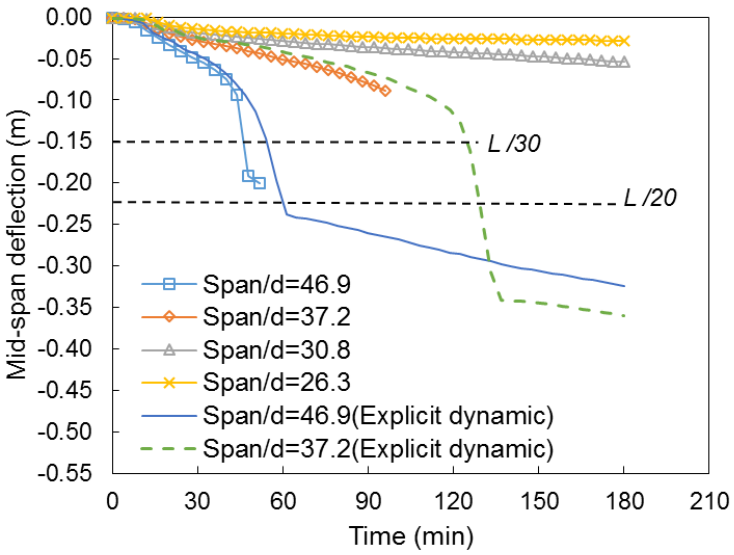

Figure 4.30: Mid-span deflection for slabs with different span-to-depth ratios and curtailed bottom reinforcement for the case of slabs with rigid supports

As compared to simply supported slab, rigidly supported slab in this section in general produces much less deflection. With span-to-depth ratio of 30.8 and smaller, the response shows slabs have better structural fire performance than their other two configurations i.e. span-to-depth ratio of 37.2 and 46.9. One of the interesting findings here is that with a slab perfectly restraint against translational and rotational displacement, in general it will have a good structural performance with regard to the deflection criteria (very small deflection) but whenever its integrity starts to deteriorate or triggers failures, the manner in which it happens will be sudden and drastic. If this is to be translated in a real reinforced concrete building frame, this kind of failure is something that has to be avoided as some ductility is always preferred so as to give ample time for the safe evacuation of people from the building.

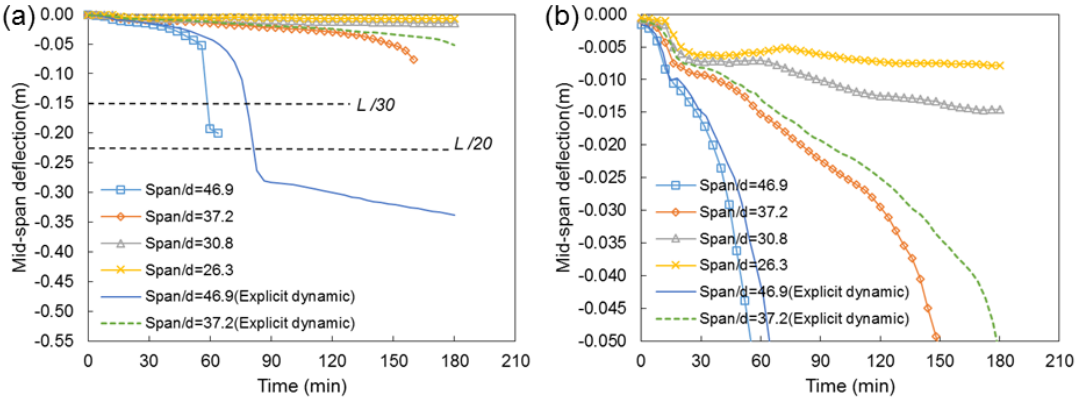

Figure 4.31: (a) Mid-span deflection for slab with different span-to-depth ratios and bottom bars extended into support and (b) close-up similar plot for the case of slabs with rigid supports

Without bottom reinforcement curtailed, the trend of deflection is always downwards as shown previously in Figure 4.30. In contrast, with the full bars extending into supports, a slight change of trend (upwards) in deflection occurs for the case of slab with span-to-depth ratio of 30.8 and 26.3. A similar trend, but occurring at a very short period of time also occurring for the case of span-to-depth ratio of 37.2. This behaviour is suspected to occur due to the formation of plastic hinges, as has been discussed and presented in the earlier section of the chapter.

To confirm this behaviour, the plot of displacement along the slab span and bending moment diagram for the case of span-to-depth ratio equalling to 26.3 (slab thickness of 200 mm) are plotted and shown in Figure 4.32. Figure 4.32(a) shows the vertical displacement along the slab's span while Figure 4.32 (b) shows the bending moment diagram (BMD) at the selected duration of fire exposure.

Overall results of the vertical mid-span displacement and bending moment diagram (BMD) comparison for different span-depth-ratios are shown in Figure 4.33 to Figure 4.36. Figure 4.33. Figure 4.34 presents the results for the selected duration of fire exposure for the case of bottom reinforcement curtailed while Figure 4.35 and Figure 4.36 show the plot for the case of bottom reinforcement fully extended into slab's support.

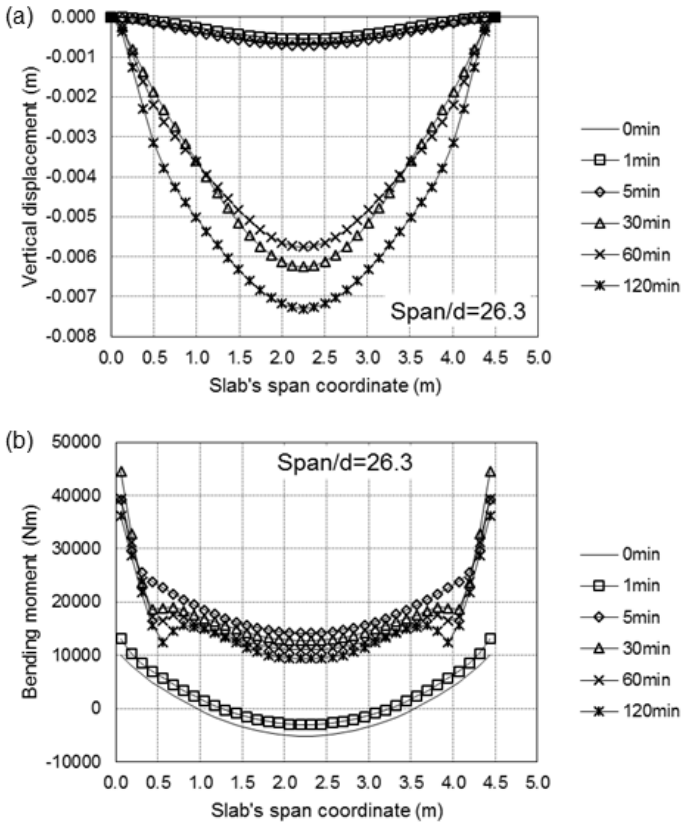

Figure 4.32: (a) Vertical displacement along slab's span at selected duration of fire exposure for span-to-depth ratio of 26.3 and (b) Bending moment diagram (BMD)

Upward trend of deflection can be seen in the above Figure 4.32(a) between the curve for 30 minutes and 60 minutes of fire exposure. At mid-span, upward deflection is found where the magnitude of deflection is smaller at 60 minutes of exposure than 30 minutes of exposure. Referring to these two (2) curves, it is also noted that the point where this behaviour occurs is at the point where reinforcing steel is curtailed (1353 mm from support). These two (2) curves crossed each other at the location where top reinforcing steel terminates. Note that the plotted points in the figure are simply nodal displacement thus some lack of accuracy is anticipated as the plotted displacement interval is equal to the mesh size. Interval smaller than the mesh size is not possible.

Whenever the bottom reinforcement is curtailed i.e. not extending into supports, no such trend is found (upward deflection). During heating, bottom and top section of the slab experience compressive stresses. This is a result of thermal bowing behaviour

where mid-section of the slab typically experiences tension. Even though both top and bottom of the slab experienced compressive stresses, degradation of concrete materials occurred much earlier at the bottom of the slab due to severe heating. In addition, examination on the bending moment diagram also demonstrates how the state of bending moment at mid-span shifted from positive (sagging) to negative (hogging) as heating progressed. With the bottom reinforcement present near the slab's support, additional strength is available for the case of thicker slab where the reaction moment is higher compared to thinner slab, (this being negative (hogging) moment: refer both Figure 4.34(d) and Figure 4.36(d)). The incompatibility of moment capacity at this section and section at mid-span have resulted in a slightly upward trend of deflection at slab's mid-span. However, note that this displacement occurs at a very small magnitude i.e. approximately 2.5 mm.

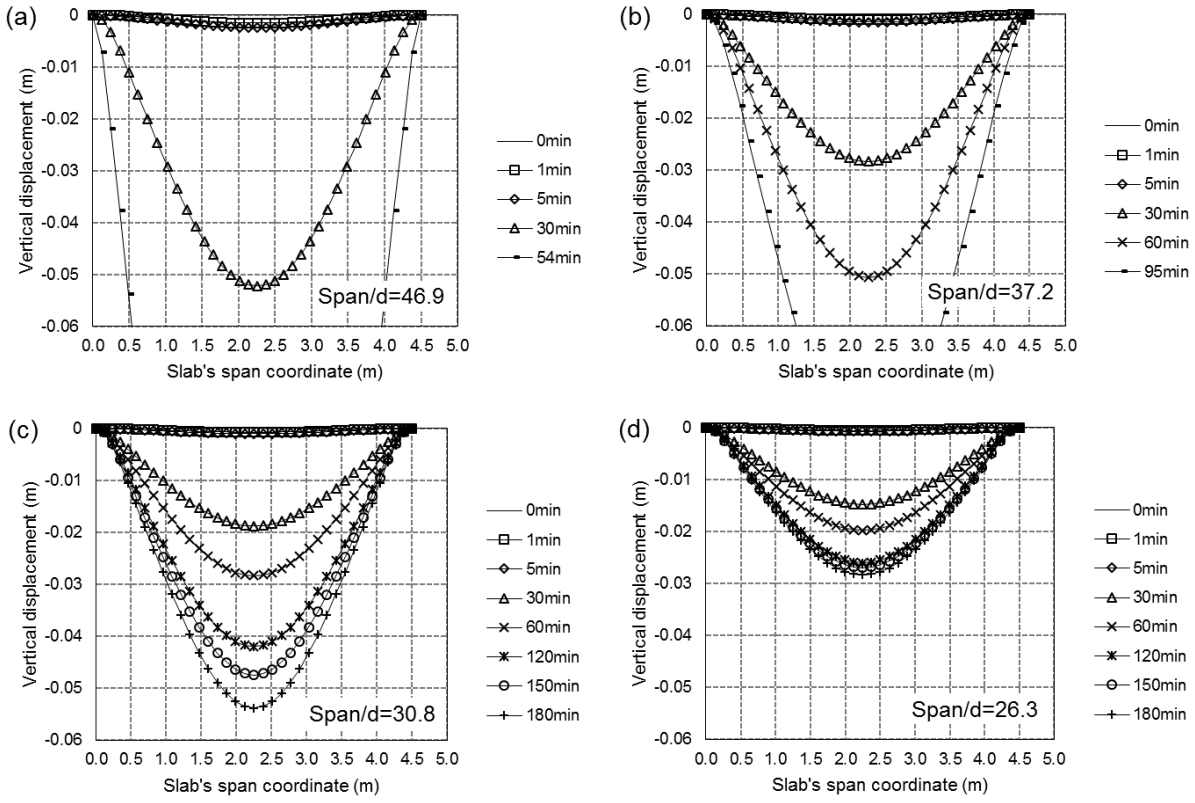

Figure 4.33: Vertical displacement along slab's span at selected time of fire exposure for slab with different span-to-depth ratios and curtailed bottom reinforcement

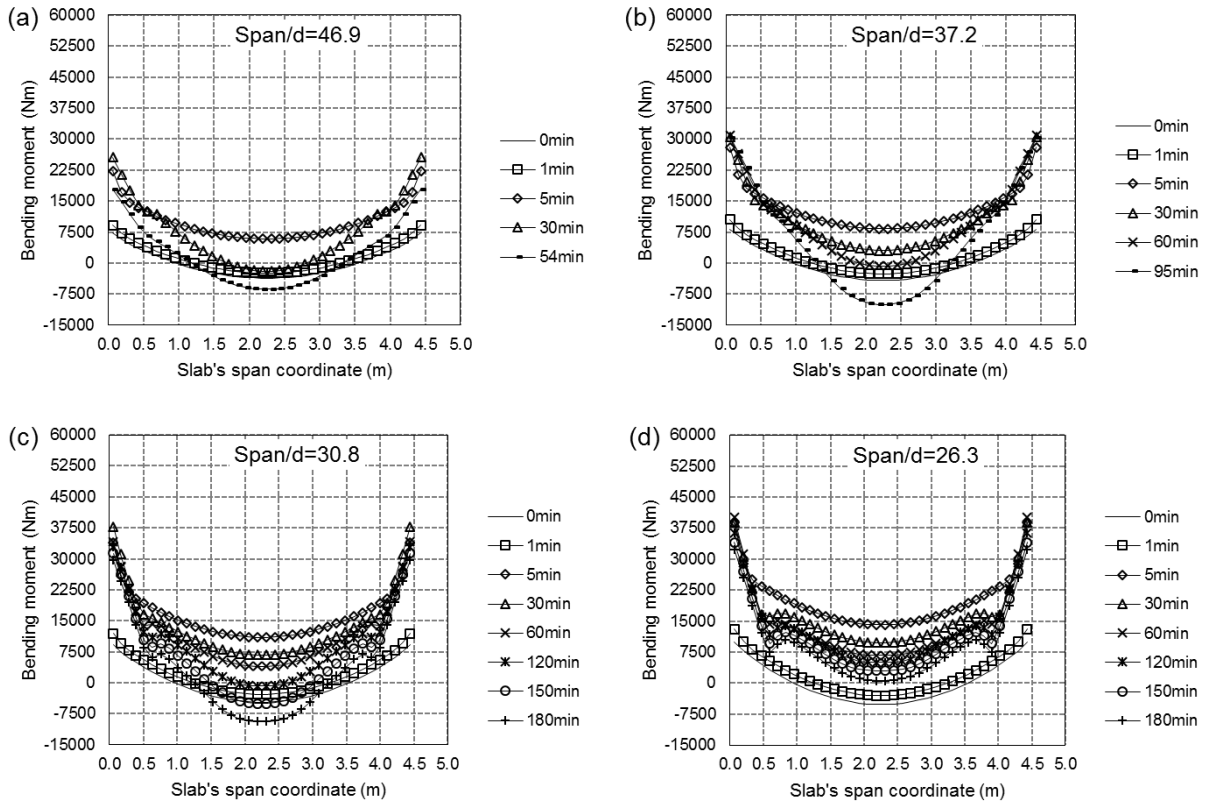

Figure 4.34: Bending moment diagram (BMD) at selected time of fire exposure for slab with different span-to-depth ratios and curtailed bottom reinforcement

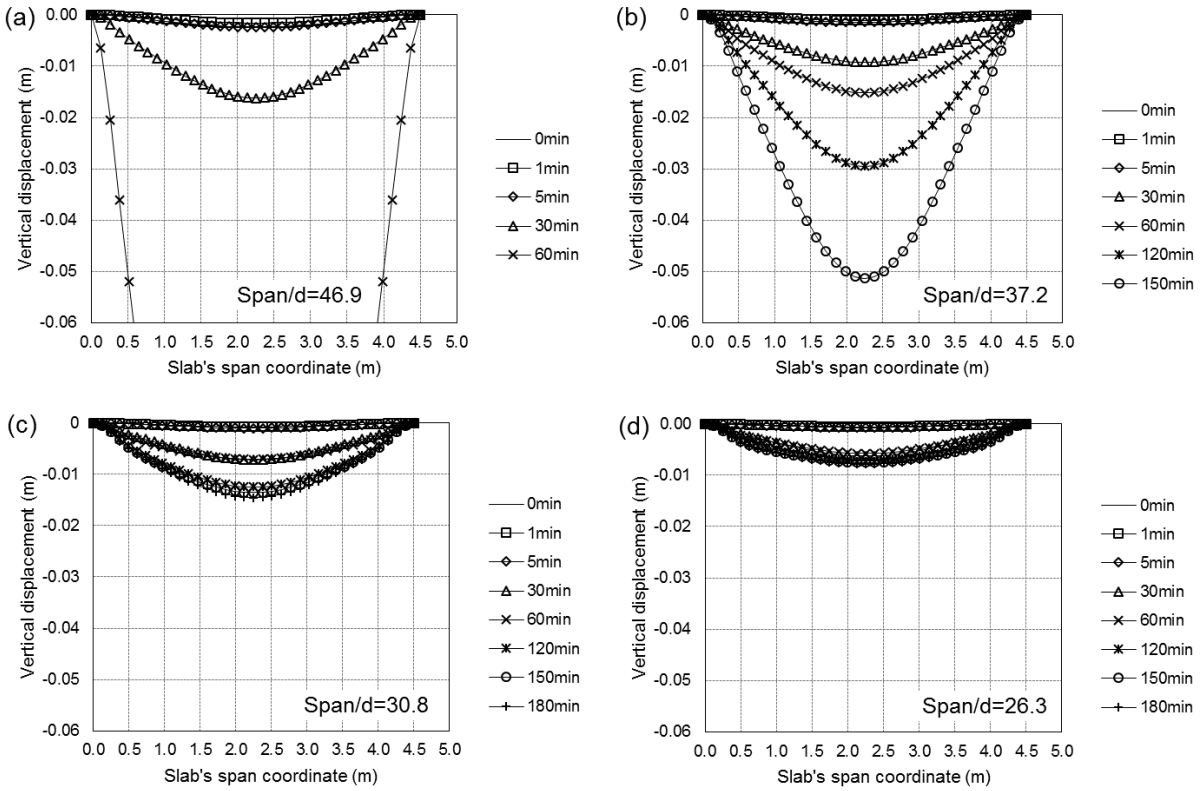

Figure 4.35: Vertical displacement along slab's span at selected time of fire exposure for slab with different span-to-depth ratios and bottom reinforcement extended into support

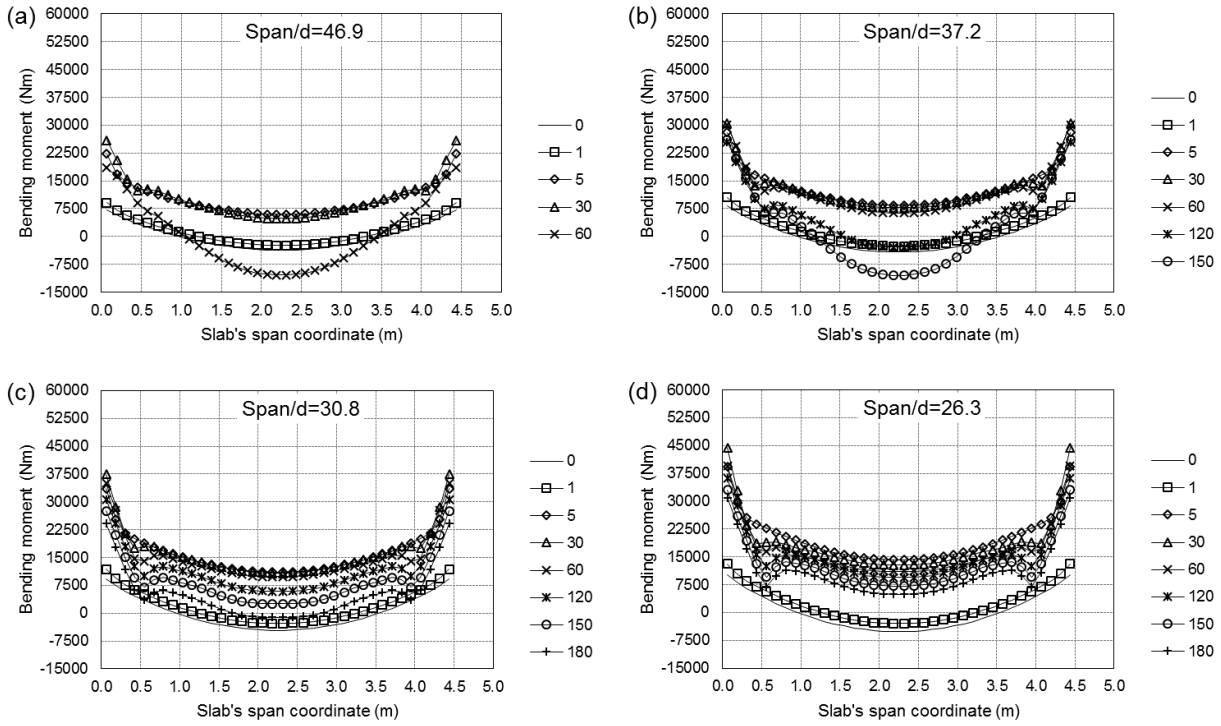

Figure 4.36: Bending moment diagram (BMD) at selected time of fire exposure for slab with different span-to-depth ratios and bottom reinforcement extended into support

4.8.2.2 Intermediate support stiffness

This section presents study relatively similar to the previous section but there is no curtailment of bottom reinforcement included in the study, meaning bottom reinforcement extends fully into supports. In addition, support restraint stiffness is also modified in the attempt to simulate more realistic support condition. The restrain stiffness values are evaluated as the elastic stiffness of the concrete section near support (under hogging moment). It is acknowledged that approximating this value is not simple as there is a section along the span where reinforcing steel is curtailed thus some of the assumption will no longer be valid. However, it is not the intention to exactly replicate the restrain stiffness that the slab will have in an actual construction but instead it is merely to get a reasonable value for support stiffness.

Support translational and rotational stiffness were modelled using elastic spring stiffness. Elastic spring stiffness for both translational and rotational displacement are calculated based on 'un-cracked' section.

To maintain the consistency in the study on the structural behaviour of continuous reinforced concrete slabs with different span-to-depth ratios, similar area of steel reinforcement in Section 4.8.2.1 is adopted here in this section. The selected area of steel reinforcement, and the estimated elastic spring stiffness are tabulated in Table 4.10, and Table 4.11 respectively.

Table 4.10: Selected span-to-depth ratio with their corresponding steel area and effective depth

Slab thick. (mm)	Span/depth	$A_{s(top)}$ (mm^2)	$A_{s(bottom)}$, (mm^2)	d (mm)	d' (mm)
125	46.9	359	179	96	29
150	37.2	312	156	121	29
175	30.8	281	141	146	29
200	26.3	260	130	171	29

Table 4.11: Estimated translational and rotational spring stiffness

N.A (m)	$I_{un\text{-}cracked}$ (m^4)	EI/L (Nm/rad)	AE/L (N/m)
0.06300	1.5739E-04	6.2605E+05	9.4186E+07
0.07600	2.7139E-04	1.0795E+06	1.0058E+08
0.02890	4.2951E-04	1.7085E+06	1.0632E+08
0.03038	6.3900E-04	2.5418E+06	1.1180E+08

Figure 4.37 presents the predicted mid-span deflection for slabs with different span-to-depth ratios and finite spring stiffness at supports. In the plot, some analysis did not finish until 180 minutes of simulation and pre-mature termination of analysis occurred. This pre-mature termination of analysis is suspected due to the sudden and drastic increase of vertical mid-span deflection. This abrupt change in deformation has made the analysis not being able to find a converge solution while solving the stiffness matrix. Predictions from the explicit dynamic analysis are included for the case where

models experienced premature termination of analysis to give an insight into overall behaviour of the slabs. In an explicit dynamic analysis, no stability condition is imposed while solving the equation for dynamic equilibrium (note that quasi-static analysis was implemented in the current study), meaning no issues of premature termination of analysis occurred. However, accuracy checking is less rigorous than common static analysis in ABAQUS and it is therefore good practice to compare static solutions and explicit solutions to ensure the explicit solution is on track (Deeny, 2010).

If limiting the deflection criteria as specified in BS 476 (BSI, 1987) set the slab's performance criteria, thinner slabs in general will fail earlier than thicker slabs. However, this is not necessarily the case if limiting tensile plastic strain is defined as the indicator for the slab's performance. Referring to Table 4.15, which will be shown in the next section i.e. Section 4.8.3 (Summary section), limiting tensile plastic strain to 2% gives relatively similar fire resistance rating for the slabs with varying span-to-depth ratios, based on an investigation in the current section. 27 mins, 30 mins, and 32 mins of fire resistance rating are given if limiting tensile plastic strain in reinforcing steels is set as the criteria for the case of slabs with span-to-depth ratios of 46.9, 37.2, and 30.8 respectively.

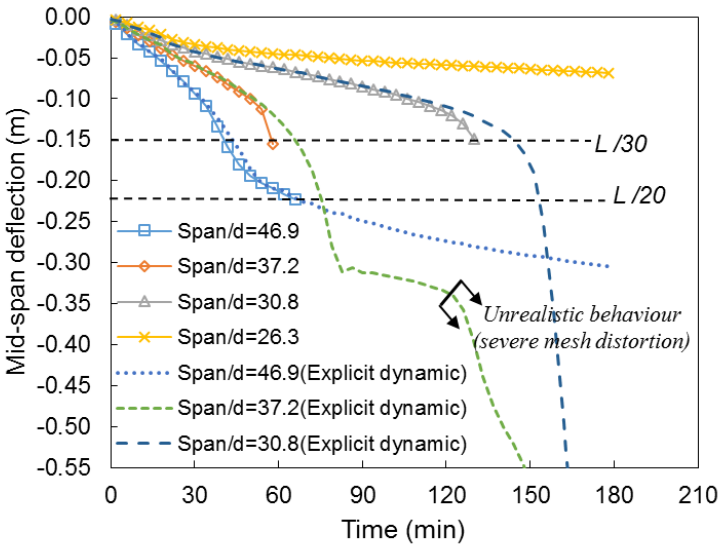

Figure 4.37: Mid-span deflection for slab with different span-to-depth ratios and combination of elastic translational and rotational spring stiffness

4.8.3 Summary

Summary on fire resistance rating for the case of slabs with varying span-to-depth ratios is shown in Table 4.12, Table 4.13, Table 4.14, and Table 4.15 for simply supported slabs, slabs with rigid support and curtailed bottom reinforcement, slabs with rigid support and bottom reinforcement fully extended into support, and slabs with intermediate spring stiffness at support (bottom reinforcement fully extended into support) respectively.

For the case of simply supported slabs, higher span-to-depth ratio provides slab with lower fire resistance rating if limiting deflection based on recommendation from BS 476-20:1987 (BSI, 1987) is adopted. A similar trend is observed for the slabs with rigid as well as intermediate spring stiffness at supports.

Table 4.12: Summary of structural fire resistance rating for slab with varying span-to-depth ratios: simply supported case

Fire resistance criterion	*L/20* (BSI, 1987)	Tensile plastic strain in reinforcing steels: 2%	Eurocode 2 (CEN, 2004)	International Building Code (International Code Council, 2009)
46.9	47 mins	>120 mins	60 mins	120 mins
37.2	64 mins	>118 mins		
30.8	85 mins	>117 mins		
26.3	104 mins	>115 mins		

Table 4.13: Summary of structural fire resistance rating for slab with varying span-to-depth ratios: rigid support and bottom reinforcement curtailed

Fire resistance criterion	*L/20* (BSI, 1987)	Tensile plastic strain in reinforcing steels: 2%	Eurocode 2 (CEN, 2004)	International Building Code (International Code Council, 2009)
46.9	60 mins*	50 mins*	60 mins	120 mins
37.2	129 mins*	117 mins*		
30.8	>180 mins	>180 mins		
26.3	>180 mins	>180 mins		

**Results from explicit dynamic analysis*

Table 4.14: Summary of structural fire resistance rating for slab with varying span-to-depth ratios: rigid support and bottom reinforcement extended into supports

Fire resistance criterion	*L/20* (BSI, 1987)	Tensile plastic strain in reinforcing steels: 2%	Eurocode 2 (CEN, 2004)	International Building Code (International Code Council, 2009)
46.9	81 mins*	76 mins*	60 mins	120 mins
37.2	>180 mins*	>180 mins*		
30.8	>180 mins	>180 mins		
26.3	>180 mins	>180 mins		

**Results from explicit dynamic analysis*

Limiting plastic strain criteria gives lower fire resistance rating as compared to limiting the mid-span deflection criteria (BSI, 1987) based on the investigation on varying slab's span-to-depth ratios for slabs with intermediate spring stiffness at supports (see

Table 4.15). This finding is contradictory to the investigation on slabs with simple supports. It is therefore suggested that, both criteria should be used when assessing the performance of one-way slabs under the exposure to severe heating from below.

From the investigation in the current section, it can be concluded that increasing slab's thickness (lower span-to-depth ratio) increases fire resistance of one-way reinforced concrete slabs exposed to severe heating from below. However, for the case of simply supported slabs, the conventional approach in assessing slab's fire resistance rating based on limiting deflection criteria of $L/20$ (BSI, 1987) should not be used as the slab's performance indicator.

Table 4.15: Summary of structural fire resistance rating for slab with varying span-to-depth ratios: intermediate support stiffness

Fire resistance criterion	*L/20* (BSI, 1987)	Tensile plastic strain in reinforcing steels: 2%	Eurocode 2 (CEN, 2004)	International Building Code (International Code Council, 2009)
46.9	68 mins	27 mins*	60 mins	120 mins
37.2	75 mins	30 mins*		
30.8	153 mins	32 mins*		
26.3	>180 mins	>180 mins		

**Result from explicit analysis*

4.8.4 Recommendation for best practice guidance

Prediction of mid-span deflection for the case of simply supported slabs with varying span-to-depth ratios highlights the inconsistencies in specifying fire resistance rating for one-way reinforced concrete slabs when applying the limiting deflection criteria of $L/20$ (BSI, 1987). Although slabs with higher span-to-depth ratio (thinner slabs) failed the limiting deflection criteria earlier than its lower span-to-depth ratio counterparts, this does not signal that the slab is losing its load-bearing capacity. It is therefore suggested that limiting plastic strain in reinforcing steels of 2% should be used as it provides more realistic performance indicator.

With rigid supports and bottom reinforcing steels curtailed (meaning they were not extended into supports), snap trough tends to occur earlier for slabs with higher span-

to-depth ratio. When the bottom reinforcement is extended into supports (as is common in practice), depending on the stiffness of the supports (both translational and rotational), plastic hinges typically triggered at the location where top reinforcing steels is curtailed. Designers can anticipate this behaviour (plastic hinges) whenever there is a slight upward trend in vertical mid-span deflection predicted from the FE models. Snap trough should always be avoided as the potential failure from this behaviour might be violent in nature.

Therefore, it is suggested that increasing slab thickness (lower span-to-depth ratio) will improve fire resistance rating for one-way slabs exposed to severe heating from below. However, both criteria of limiting deflection as well as limiting tensile plastic strain must be used in assessing and selecting the best design configuration for the slabs to have the optimum performance under exposure to severe heating from below.

4.9 Overall summary and conclusion

This chapter presents parametric studies on structural behaviour of one-way reinforced concrete slabs exposed to fires. Using finite element models, structural behaviour of the slabs under different parameters such as fire scenario, restraint condition, and configuration of reinforcement as well as span-to-depth ratio are investigated. In general, the aspect of structural design of one-way slabs under exposure to fire is interrogated. Specific findings from the current study are listed below:

- The present of rigid as well as flexible translational and rotational stiffness at support improves the structural performance of one-way reinforced concrete slabs under exposure to fires from below. With rigid support, a relatively small value of deflection is predicted from the FE models
- Plastic hinges are likely to form at locations where the top reinforcement is curtailed. Whenever a full length of top reinforcement is provided, plastic hinges are likely to form at the location close to supports but requiring a relatively greater reaction moment in order to form
- Selection of different span-to-depth ratio for simply supported slabs would produce relatively similar structural fire performance if integrity and load-bearing capacity are set as the performance indicator. However, if limiting deflection is set as the criteria, obviously a slab with higher span-to-depth ratio (thinner slab) would have less fire resistance as the slab displaced vertically in a relatively greater magnitude compared to thicker slab
- For the design of cast in-situ one-way reinforced concrete slabs for fire, selecting slab with lower span-to-depth ratio generally results in better structural fire performance, provided that the proper consideration and thorough study are carried out to look at the possibilities of plastic hinges formation. As such, both limiting mid-span deflection as recommended by BS 476-20:1987 and limiting tensile plastic strain of 2% should be used
- Studies presented in this chapter demonstrated that provision of 15% to 20% extra top reinforcement length is potentially not sufficient, depending on the restraint stiffness at supports. Findings from the current study demonstrated the possibility of plastic hinges formation at the location where the top reinforcement is curtailed,

even though the length of the top reinforcing steels was provided as equivalent to 0.375*L* (0.375× slab's span). Careful examination on both mid-span deflection and reinforcing steel plastic strain are required and if necessary, full length of top reinforcement should be provided.

Chapter 5:

Finite element modelling of two-way reinforced concrete slabs exposed to severe heating from below

5.1 Introduction

Aspect of validating finite element model against experimental results along with sensitivity of model to input parameters for the case of one-way reinforced concrete slabs have been presented in Chapter 3. In this chapter, studies are extended for the case of two-way slabs with relatively similar motivation and methodology. Three (3) experimental test results reported by Lim and Wade (2002), Zhang et al. (2014), and Wang et al. (2016) on two way reinforced concrete slabs heated in furnace to ISO 834 (ISO, 1999) are selected for numerical model assessment.

In contrast to the studies presented in Chapter 3, in this chapter, sensitivity of only mechanical input parameters is investigated and presented. Sensitivity of thermal input parameters have been extensively presented in Chapter 3, therefore it will not be repeated here. In addition, it is expected that there will be no output variation from the investigation since only 1D heat transfer analysis would have been adopted.

Varying mechanical input parameters is expected to have a variation of influence on the behaviour. This in particular is due to double curvature bending in two-way slabs whereas for the case of one-way slabs, bending is dominant on one axis only. Bending behaviour of one way slabs typically behave in a uniaxial manner although it is acknowledged that after certain period of fire exposure, even one way slabs also bend in double curvature, based on investigation reported by Wang (2006).

With the above points in mind, this chapter will present studies looking at the aspect of finite element modelling of two-way reinforced concrete slabs exposed to severe heating from below. Issues associated with varying mechanical input parameters to the structural response prediction is presented and discussed.

5.2 Available furnace tests on two-way reinforced concrete slabs

Full scale, two-way reinforced concrete slabs tested in furnaces have been reported by Lim and Wade (2002); Lin et al. (1989); Wang et al. (2016); and Zhang et al. (2014). Continuous full scale concrete slab in a steel frame building is reported by Wang et al. (2013) while several steel-concrete composite slab tests are available within the

literature, for instance Banerjee (2012); British Steel (1998); Guo and Bailey (2011); and Lim and Wade (2002). Composite concrete slab refers to slab with combination of conventional steel rebar and metal decking for resisting bending in the slab. Conventional steel rebar is typically provided at the top to control cracking and hogging moment resistance while metal decking at the bottom serves to provide strength for resisting sagging moment.

5.2.1 Slab 1 - (Lim and Wade, 2002)

As part of a testing program, which involved one (1) reinforced concrete slab and two (2) proprietary composite steel-concrete composite slabs carried out at the University of Canterbury (Lim and Wade, 2002), a specimen of 4300 × 3300 × 100 mm reinforced concrete slab exposed to ISO 834 (ISO, 1999) was selected for the current study. The slab was exposed to ISO 834 (ISO, 1999) fires for 3 hours from below. 8.7 mm diameter cold drawn deformed mesh was used as reinforcing bars and arranged at 300 mm centres in both transverse and longitudinal direction. The specified yield stress of the reinforcing steels was 565 MPa. Characteristic concrete compressive strength was 37 MPa and the aggregate used was siliceous.

Twenty 200-litre water drums were placed on the slab to simulate a uniformly distributed load of 3 kPa (Lim and Wade, 2002). All the drums were lifted and placed on the slab at least an hour before the slab was fire tested (Lim and Wade, 2002). Figure 5.1 shows cross section of the furnace short span reproduced from Lim and Wade (2002) to illustrate the loading arrangement on the slab The slab was simply supported at four edges and was unrestrained against horizontal movement. However, the inward horizontal travel was limited to prevent any excessive movement and potentially causing catastrophic damage to the specimen and equipment (Lim and Wade, 2002). Figure 5.2 presents graphical configuration of the slab. Description of the tested concrete slabs are explained in detail in Lim and Wade (2002). Numerical model for the slab was also developed by one of the authors and reported in the paper by Lim et al. (2004). For simplicity and beneficial comparison of the results, a similar slab candidate was re-modelled for the current study in this section.

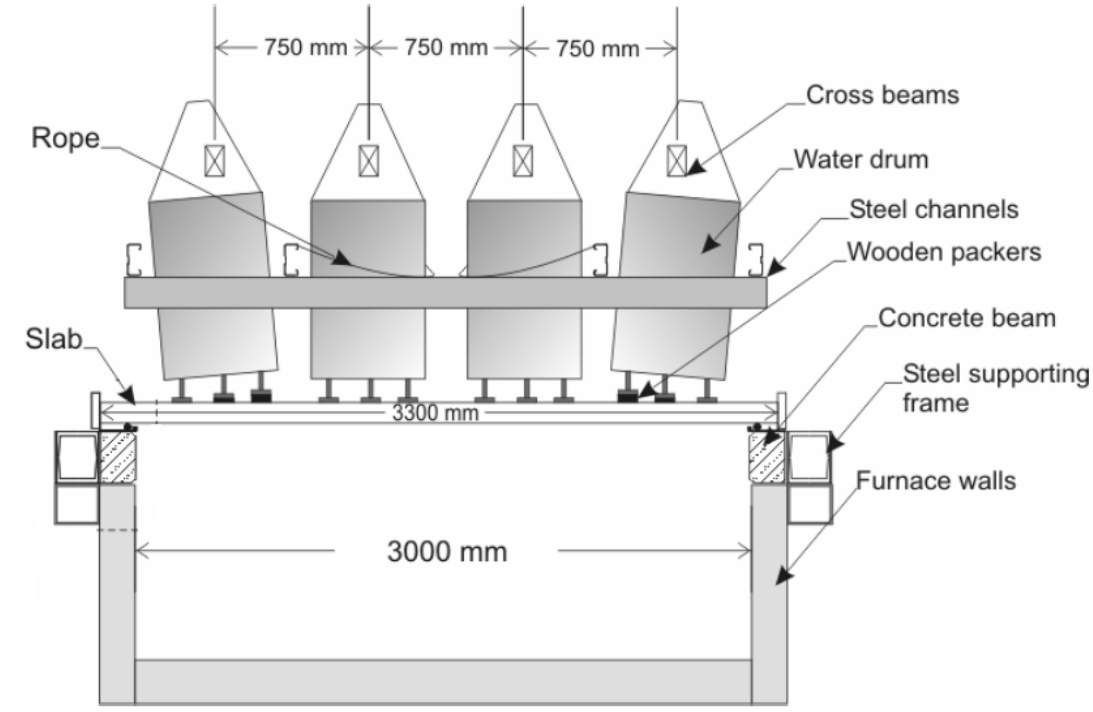

Figure 5.1: Cross section of the furnace short span reproduced from Lim and Wade (2002)

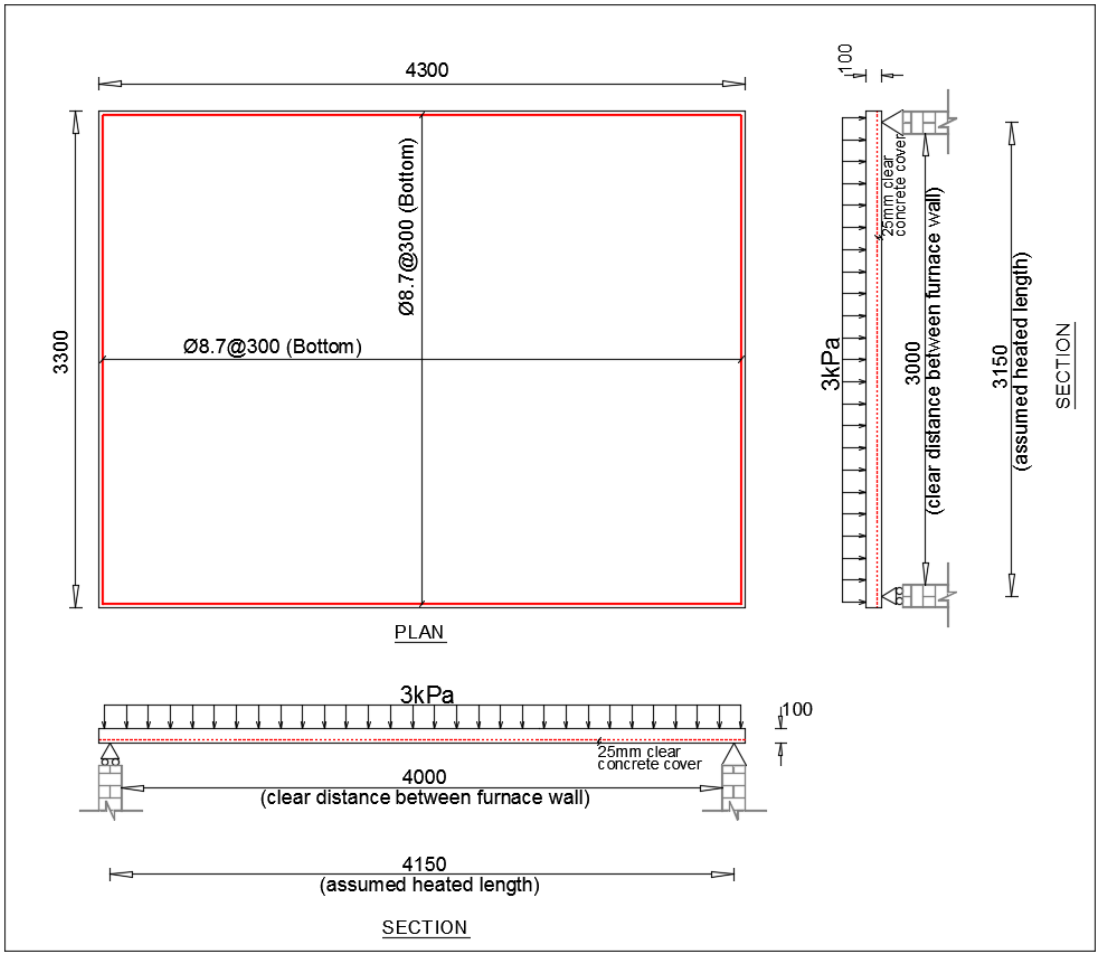

Figure 5.2: Configuration of slab tested by Lim and Wade (2002)

5.2.2 Slab 2 - (Zhang et al., 2014)

Full scale test of simply supported reinforced concrete slabs under exposure to standard ISO 834 (ISO, 1999) fires have been performed by Zhang et al. (2014) at Shandong Jianzhu University, Jinan, China. Zhang et al. (2014) believe there is a huge gap in the availability of experimental results for the purpose of understanding the behaviour of concrete slabs under exposure to fires, which was the main motivation behind the test.

6660 × 5000 × 120 mm thick slab with siliceous aggregate was casted. The reported actual concrete compressive strength is 31.5 MPa. 8 mm diameter steel reinforcement arranged at 200 mm centre in both directions at the top while 180 mm centre and 200

mm centre of 8 mm diameter reinforcing steels were arranged along shorter and longer span respectively for bottom reinforcement. Actual yield strength and ultimate strength of the reinforcing steels were reported as 435 MPa and 580 MPa, respectively. Slab S1 as denoted in Zhang et al. (2014) was selected for the current finite element modelling.

2 kPa uniformly distributed load was applied to simulate a live load on the slab. This was applied in five steps, at 0.4 kPa per step using dead weights (Zhang et al., 2014). The dead weights were placed on the slab before the fire test commenced and within the testing program (2 slabs were fire tested), load applications were completed at least 30 minutes before the test started. The slab was simply supported at four edges and was unrestrained against horizontal movement. Figure 5.3 shows graphical configuration of the slab specimen. More details about the test can be found in Zhang et al. (2014).

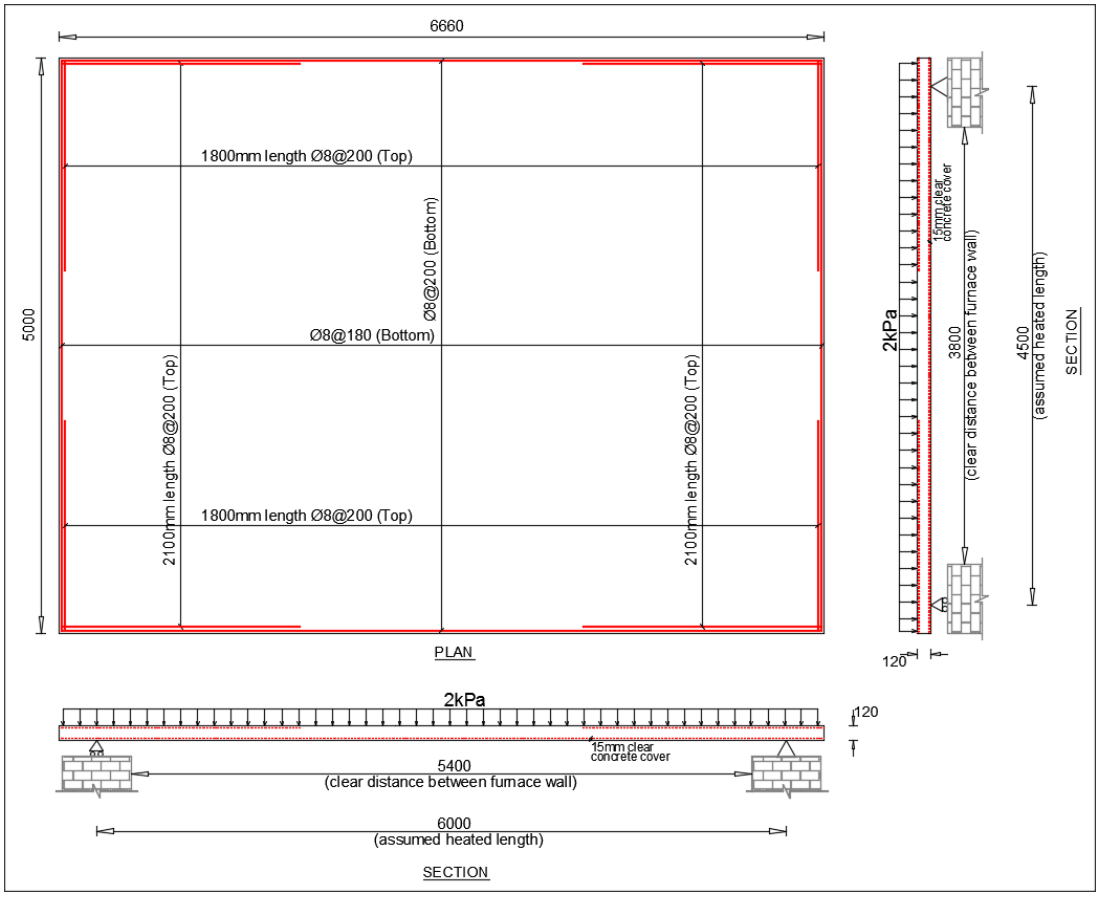

Figure 5.3: Configuration of slab tested by Zhang et al. (2014)

5.2.3 Slab 3 - (Wang et al., 2016)

More recently Wang et al. (2016) tested two-way reinforced concrete slabs also exposed to ISO 834 (ISO, 1999) fires to investigate the behaviour of the slabs under combined uniaxial in-plane and out of plane load. The slab selected for the current study, which has dimension of 3300 × 3300 × 100 mm, was reinforced with 8 mm diameter reinforcing steels arranged at 100 mm centre in both direction at bottom only. The reported concrete compressive strength is 28 MPa while the ultimate strength of the steel reinforcement is 475 MPa. Slab S4 (Wang et al., 2016) is selected for the current study. Siliceous type of aggregate was used for the concrete mix.

In addition to live load of 2 kPa, horizontal uniaxial in-plane load with a magnitude of 2 MPa was introduced at one edge of the slab. Sand bags, each weighing 50 kg were

placed on the slab to simulate uniformly distributed load of 2 kPa. Using an independent loading frame, horizontal uniaxial in-plane load was applied to the slab by high strength steel knife edges attached to the rams of three 500 kN hydraulic jacks along one edge of the slab (Wang et al., 2016). The loading frame rests on a separate furnace wall, meaning slab specimen was vertically supported on a different furnace wall. This was claimed as critical in ensuring the application of horizontal in-plane load was maintained throughout fire test as the loading frame could move up and down whenever the slab edge displaced (Wang et al., 2016). This is further illustrated in Figure 5.4. A restraining frame was installed at the edge opposite to the in-plane load edge. The other two edges were allowed to displace axially. Details about the test can be found in Wang et al. (2016). Graphical configuration of the tested slab is shown in Figure 5.5.

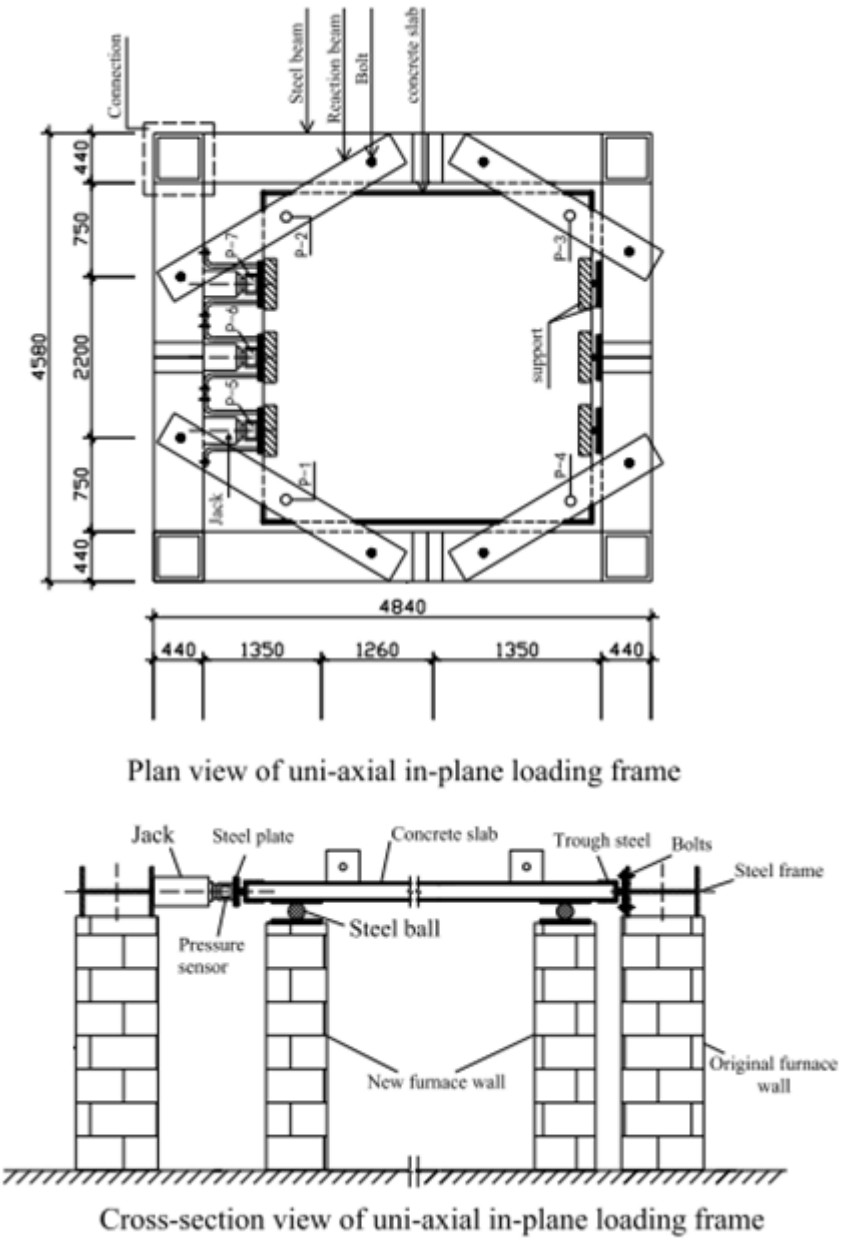

Figure 5.4: Plan view and cross-section view of in-plane loading frame reproduced from Wang et al. (2016)

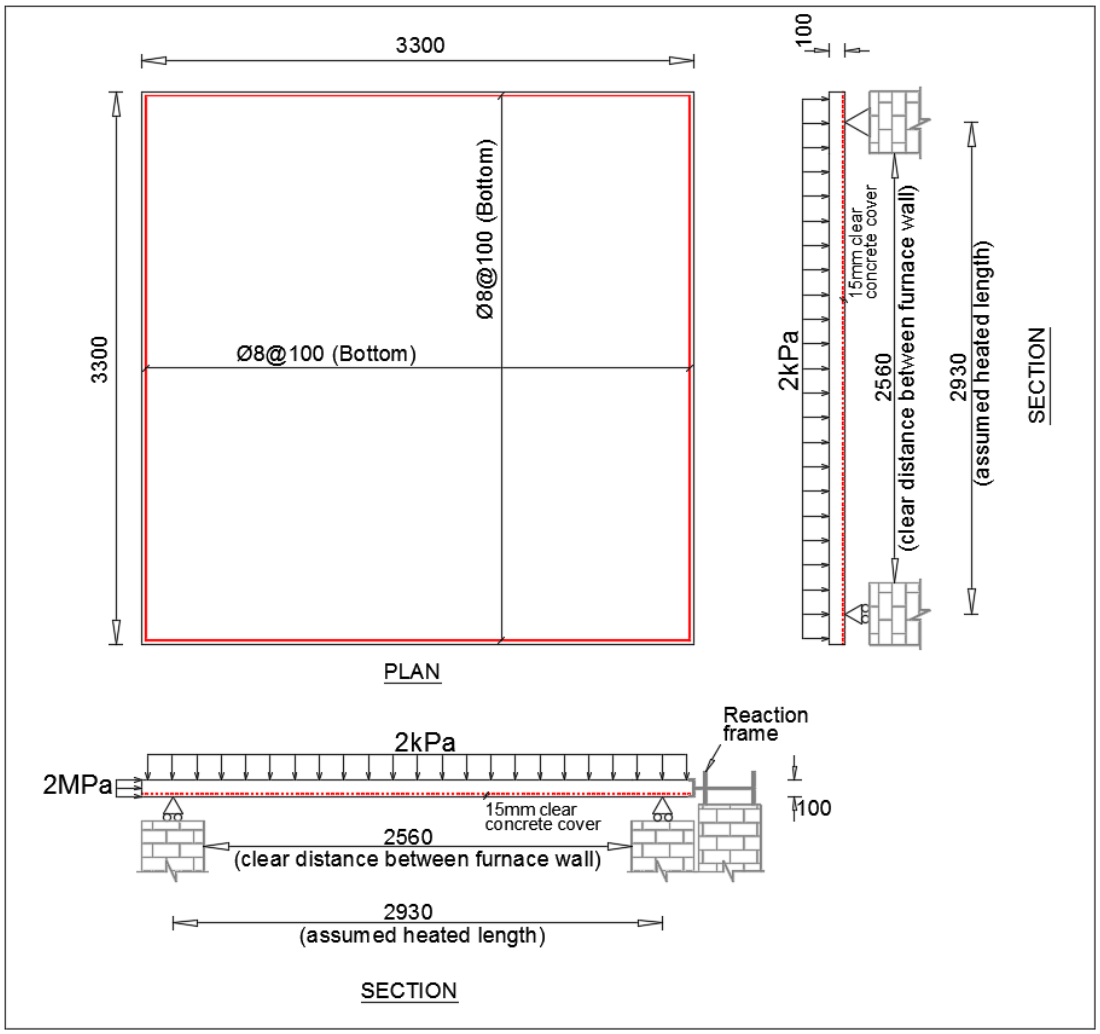

Figure 5.5: Configuration of slab tested by Wang et al. (2016)

5.3 Thermal analysis

1-D finite element (FE) heat transfer analysis was performed and concrete material thermal properties were defined based on recommendation from Eurocode 2 (CEN, 2004). Similar to thermal analysis presented in Chapter 3, a 4-node linear heat transfer quadrilateral (DC2D4) element available in ABAQUS (ABAQUS, 2012) was selected for the heat transfer analysis. It is a plane strain/stress element, of which is also available for thermal analysis. Existence of steel reinforcement was ignored during the heat transfer analysis.

Moisture migration was not explicitly considered during the heat transfer analysis. Instead, the influence of moisture condition in concrete was taken into consideration in the heat transfer analysis by modifying temperature dependent specific heat properties of the concrete. This is in accordance with the recommendation from Eurocode 2 (CEN, 2004). Temperature dependent thermal conductivity and specific heat were all in accordance to the recommendation in Eurocode 2 (CEN, 2004). The selection of either lower limit or upper limit of thermal conductivity values is summarised in Table 5.1 below. The assumed moisture contents, which will determine the specific heat properties of the slab are also shown in the table.

In performing heat transfer analysis for the case slab tested by Lim et al. (2004) and Zhang et al. (2014), gas temperatures were derived from standard ISO 834 (ISO, 1999) fire curve equation. Gas temperatures in the furnace were not reported by Zhang et al. (2014). For the case of furnace test by Lim and Wade (2002), the measured average gas temperatures followed closely the ISO 834 (ISO, 1999) curve with the exception of the first 30 minutes of fire test. In addition, previous finite element models presented by Lim et al. (2004) and Gernay (2012) also adopted gas temperature derived from ISO 834 (ISO, 1999) fire curve equation. As such, it is thought that the outcome from the current study will be more beneficial if similar strategy is adopted. For the case slab tested by Wang et al. (2016), measured and reported gas temperatures were entered and defined in the heat transfer model. Heat transfer parameters for all the three slabs modelled are identical. Coefficient of convection at exposed and unexposed surface were 25 W/m^2.K and 9 W/m^2.k, respectively. Concrete surface emissivity and fire emissivity were 0.8 and 1.0, respectively based on the recommendations of Eurocode 2 (CEN, 2004).

Table 5.1: Thermal input properties for 'base case' model

Parameters	Slab 1	Slab 2	Slab 3
Thermal conductivity, k	EC 2 (Lower limit)	EC 2 (Upper limit)	EC 2 (Lower limit)
Specific heat, C_p	EC 2	EC 2	EC 2
Density, ρ	EC 2	EC 2	EC 2
Moisture content	4.4%	4.8%	4% (assumed)

5.3.1 Slab 1

Moisture content was assumed as 4.4% based on the value reported by Lim and Wade (2002). Figure 5.6(a) shows the comparison between predicted temperatures against measured and reported temperatures from the test. Reasonably good agreement is found for the temperatures throughout the slab's thickness, although there are differences at all locations in the slab thickness and more obvious at the exposed surface and 55 mm from the exposed surface. The differences between the predicted values and the reported values are summarised in Table 5.2 and Table 5.3 for *Case 1 Temperature* and *Case 2 Temperature* analysis respectively.

Prediction of temperatures in another two slab models, which are presented in Section 5.3.2 and Section 5.3.3 later demonstrate the results from heat transfer analysis were not in such good agreement, especially at the exposed surface. As a result, two (2) temperature load cases, which would be later entered into structural models were defined and denoted as *Case 1 Temperature* and *Case 2 Temperature*. For the purpose of consistency in all the thermal and mechanical analyses presented in this thesis, similar strategy is implemented where two (2) load cases also denoted as *Case 1 Temperature* and *Case 2 Temperature* were defined here in this section. This definition of *Case 1 Temperature* and *Case 2 Temperature* will be adopted throughout the discussion in this chapter.

Table 5.2: Comparison of predicted temperatures from *Case 1 Temperature* analysis against test results (Lim and Wade, 2002) **at selected duration of fire exposures**

Duration	Distance from fire exposure surface	Temperatures		
		Test (°C)	Model (°C)	Difference (°C)
5 minutes	0 mm	138	259	121
	55 mm	53	20	-33
	100 mm	17	20	3
30 minutes	0 mm	606	761	155
	55 mm	116	79	-37
	100 mm	39	31	-8
60 minutes	0 mm	779	900	121
	55 mm	225	175	-50
	100 mm	72	74	2
90 minutes	0 mm	871	974	103
	55 mm	331	268	-63
	100 mm	114	104	-10
120 minutes	0 mm	944	1024	80
	55 mm	410	342	-68
	100 mm	173	148	-25
180 minutes	0 mm	1030	1092	62
	55 mm	532	456	-76
	100 mm	256	221	-35

Table 5.3: Comparison of predicted temperatures from *Case 2 Temperature* analysis against test results (Lim and Wade, 2002) **at selected duration of fire exposures**

Duration	Distance from fire exposure surface	Temperatures		
		Test (°C)	Model (°C)	Difference (°C)
5 minutes	0 mm	138	138	0
	55 mm	53	20	-33
	100 mm	17	20	3
30 minutes	0 mm	606	606	0
	55 mm	116	65	-51
	100 mm	39	28	-11
60 minutes	0 mm	779	779	0
	55 mm	225	145	-80
	100 mm	72	65	-7
90 minutes	0 mm	871	871	0
	55 mm	331	235	-96
	100 mm	114	96	-18
120 minutes	0 mm	944	944	0
	55 mm	410	306	-104
	100 mm	173	129	-44
180 minutes	0 mm	1030	1030	0
	55 mm	532	421	-111
	100 mm	256	207	-49

The only difference between heat transfer model in *Case 1 Temperature* and *Case 2 Temperature* is the definition of boundary interface at the fire exposed surface. For *Case 1 Temperature*, heat flux was evaluated from convection and radiation resulting from gas temperature whereas for *Case 2 Temperature*, measured and reported temperatures (Lim et al., 2004; Wang et al., 2016; Zhang et al., 2014) at the exposed surface were directly entered into the heat transfer model. Loss of heat at the un-exposed surface via convection and radiation is still however taken into consideration. Comparison between predicted temperatures (for *Case 2 Temperature*) and test results is shown in Figure 5.6(b).

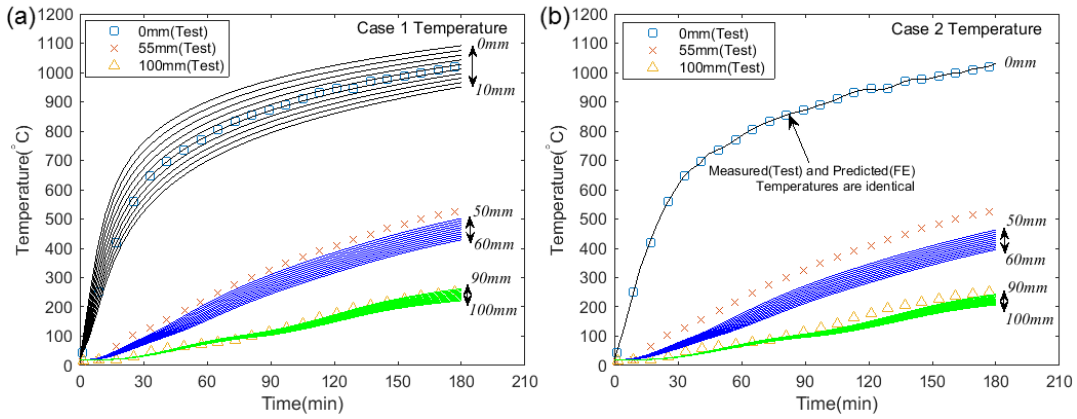

Figure 5.6: Comparison of predicted temperatures against measured temperatures (Lim and Wade, 2002)

5.3.2 Slab 2

For the purpose of heat transfer analysis, moisture content of concrete was defined as 4.8% based on the value reported by Zhang et al. (2014). Figure 5.7 shows comparison between the predicted temperatures against reported temperatures from the test. Comparison between both temperatures are found to be in poor agreement especially at the exposed surface with the difference being as high as 413 °C which occurred during 30 minutes of fire exposure.

Defining proper boundary conditions at the surface of elements that interact with fire environment is not always straightforward. In the context of experiments, placing thermocouples and measuring temperatures exactly at the exposed surface is difficult. As concrete has very low thermal conductivity value, a difference of only 4 mm will cause large differences in the measured (and consequently the reported) temperatures. It is also worth mentioning that, 4 mm distance is hardly visible with naked eyes and therefore there is a high possibility that the temperature measurement was slightly varied. As part of a testing program performed by University of Edinburgh PhD student, Ieuan Rickard, it was observed that the tested 250 mm thick concrete slab under exposure to ISO 834 (ISO, 1999) produced temperature difference of 81 °C between the location of 1 mm and 5 mm from the surface of exposure during 17 minutes of fire furnace test. Part of findings from the experimental test are reported in

Rickard et al. (2015). Table 5.4 and Table 5.5 summarised the differences between the predicted temperatures and measured temperatures (Zhang et al., 2014) for *Case 1 Temperature* and *Case 2 Temperature*, respectively.

Table 5.4: Comparison of predicted temperatures from *Case 1 Temperature* analysis against test results (Zhang et al., 2014) **at selected duration of fire exposures**

Duration	Distance from fire exposure surface	Temperatures		
		Test (°C)	Model (°C)	Difference (°C)
5 minutes	0 mm	80	186	106
	40 mm	20	21	1
	80 mm	20	20	0
	120 mm	20	20	0
30 minutes	0 mm	340	753	413
	40 mm	110	121	11
	80 mm	65	36	-29
	120 mm	27	23	-4
60 minutes	0 mm	519	895	376
	40 mm	164	263	99
	80 mm	106	82	-24
	120 mm	55	45	-10
90 minutes	0 mm	625	976	351
	40 mm	265	374	109
	80 mm	110	133	23
	120 mm	75	76	1
120 minutes	0 mm	672	1024	352
	40 mm	330	447	117
	80 mm	145	187	42
	120 mm	85	95	10
180 minutes	0 mm	785	1090	305
	40 mm	432	556	124
	80 mm	231	281	50
	120 mm	95	146	51
220 minutes	0 mm	829	1124	295
	40 mm	490	615	125
	80 mm	282	336	54
	120 mm	133	185	52

Table 5.5: Comparison of predicted temperatures from *Case 2 Temperature* analysis against test results (Zhang et al., 2014) **at selected duration of fire exposures**

Duration	Distance from fire exposure surface	Temperatures		
		Test (°C)	Model (°C)	Difference (°C)
5 minutes	0 mm	80	80	0
	40 mm	20	20	0
	80 mm	20	20	0
	120 mm	20	20	0
30 minutes	0 mm	340	340	0
	40 mm	110	67	-43
	80 mm	65	27	-38
	120 mm	27	21	-6
60 minutes	0 mm	519	519	0
	40 mm	164	138	-26
	80 mm	106	55	-51
	120 mm	55	33	-22
90 minutes	0 mm	625	625	0
	40 mm	265	230	-35
	80 mm	110	91	-19
	120 mm	75	56	-19
120 minutes	0 mm	672	672	0
	40 mm	330	294	-36
	80 mm	145	121	-24
	120 mm	85	75	-10
180 minutes	0 mm	785	785	0
	40 mm	432	395	-37
	80 mm	231	193	-38
	120 mm	95	102	7
220 minutes	0 mm	829	829	0
	40 mm	490	449	-41
	80 mm	282	239	-43
	120 mm	133	128	-5

Because of the known sensitivity of structural outputs to the in-depth thermal field within reinforced concrete elements (see Chapter 3), for a solid comparison to be made during structural analysis in the current chapter, heat transfer analysis was repeated, using a similar strategy as described previously in Section 5.3.1 where the defined boundary condition at the exposed surface was revised. Instead of calculating heat flux resulting from convection and radiation of the fire environment, temperatures reported by Zhang et al. (2014) at the exposed surface were directly entered into the heat transfer model; this was set as boundary condition in the heat transfer analysis. Predicted temperatures from this analysis are denoted as *Case 2 Temperature* in the later structural analysis section. Temperatures predicted from the former analysis will

be referred to as *Case 1 Temperature*. Figure 5.7(a) shows comparison of predicted temperatures (*Case 1 Temperature*) against reported test temperatures while Figure 5.7(b) shows comparison of predicted temperatures for *Case 2 Temperature* against reported temperatures.

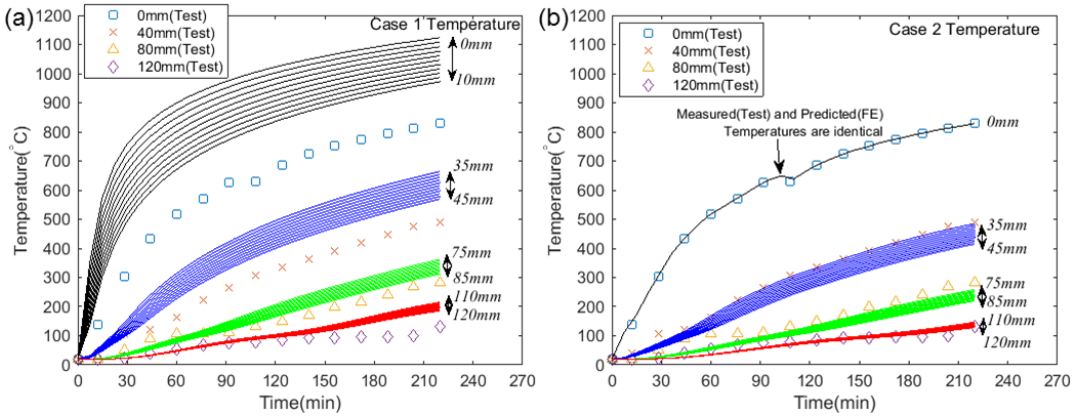

Figure 5.7: Comparison of predicted temperatures against measured temperatures (Zhang et al., 2014)

5.3.3 Slab 3

For the slab tested by Wang et al. (2016), moisture content was not reported in the paper. For the purpose of analysis, moisture content of 4 % was assumed. The selected value is solely based on the author's judgement as typically moisture content of concrete are reported to be within 3% to 5%. Moreover, sensitivity of thermal input properties presented in Chapter 3 of this thesis demonstrates that the selection value for moisture content would not significantly affect the predicted response, both thermally and mechanically.

Figure 5.8 shows the comparison between measured gas temperatures in the furnace and the standard ISO 834 (ISO, 1999) fire curve. Figure 5.9(a) shows a comparison of predicted temperatures against measured temperatures from the test (Wang et al., 2016). Contrary to the previous two (2) heat transfer analyses performed for the case slabs tested by Lim and Wade (2002) and Zhang et al. (2014), measured and reported gas temperatures by Wang et al. (2016) are used for the heat transfer analysis in this

section. The reported gas temperatures from the test deviated from standard ISO 834 (ISO, 1999) curve after approximately 7 minutes of fire test due to insufficient air ventilation into the furnace, which then caused incomplete combustion. This resulted in black smoke pouring out of the furnace (Wang et al., 2016).

Note that the predicted temperatures at 0 mm (exposed surface) are not smooth since measured gas temperatures (Wang et al., 2016) were used as boundary condition in the heat transfer analysis. It was found that the predicted temperatures are not in close agreement with the test temperatures at the exposed surface (0 mm) even though the measured gas temperatures from Wang et al. (2016) were used in the heat transfer analysis (refer Figure 5.9(a)). The difference was found to be as high as 159 °C. Overall, the comparison between predicted temperatures and measured temperatures (Wang et al., 2016) agree reasonably well, particularly at 20 mm, 60 mm, and 100 mm from the exposed surface (see summary in Table 5.6 and Table 5.7 for *Case 1 Temperature* and *Case 2 Temperature*, respectively).

Table 5.6: Comparison of predicted temperatures from *Case 1 Temperature* analysis against test results (Wang et al., 2016) **at selected duration of fire exposures**

Duration	Distance from fire exposure surface	Temperatures		
		Test (°C)	Model (°C)	Difference (°C)
5 minutes	0 mm	133	207	74
	20 mm	50	40	-10
	60 mm	18	20	2
	100 mm	19	20	1
30 minutes	0 mm	463	585	122
	20 mm	216	262	46
	60 mm	63	61	-2
	100 mm	19	29	10
60 minutes	0 mm	583	713	130
	20 mm	369	410	41
	60 mm	110	126	16
	100 mm	49	67	18
90 minutes	0 mm	623	764	141
	20 mm	464	500	36
	60 mm	153	198	45
	100 mm	75	95	20
120 minutes	0 mm	657	816	159
	20 mm	499	557	58
	60 mm	212	257	45
	100 mm	80	124	44
180 minutes	0 mm	722	813	91
	20 mm	578	621	43
	60 mm	307	348	41
	100 mm	163	192	29

Table 5.7: Comparison of predicted temperatures from *Case 2 Temperature* analysis against test results (Wang et al., 2016) **at selected duration of fire exposures**

Duration	Distance from fire exposure surface	Temperatures		
		Test (°C)	Model (°C)	Difference (°C)
5 minutes	0 mm	133	133	0
	20 mm	50	38	-12
	60 mm	18	20	2
	100 mm	19	20	1
30 minutes	0 mm	463	463	0
	20 mm	216	204	-12
	60 mm	63	53	-10
	100 mm	19	28	9
60 minutes	0 mm	583	583	0
	20 mm	369	341	-28
	60 mm	110	108	-2
	100 mm	49	60	11
90 minutes	0 mm	623	623	0
	20 mm	464	415	-49
	60 mm	153	166	13
	100 mm	75	88	13
120 minutes	0 mm	657	657	0
	20 mm	499	460	-39
	60 mm	212	218	6
	100 mm	80	108	28
180 minutes	0 mm	722	722	0
	20 mm	578	538	-40
	60 mm	307	297	-10
	100 mm	163	165	2

Similar to the strategy during the analysis in the previous section for modelling slab by Lim and Wade (2002), and Zhang et al. (2014), two temperature load cases were defined for structural modelling of Wang et al. (2016) slab. For *Case 2 Temperature*, temperature at the exposed surface reported by Wang et al. (2016) was defined as boundary condition in the heat transfer analysis. Figure 5.9 shows comparison of the results between predicted temperatures and measured and reported temperatures by Wang et al. (2016). Results of temperature-time histories shown in Figure 5.9(a) represents *Case 1 Temperature* for the structural analysis while results from Figure 5.9(b) will be entered as *Case 2 Temperature*.

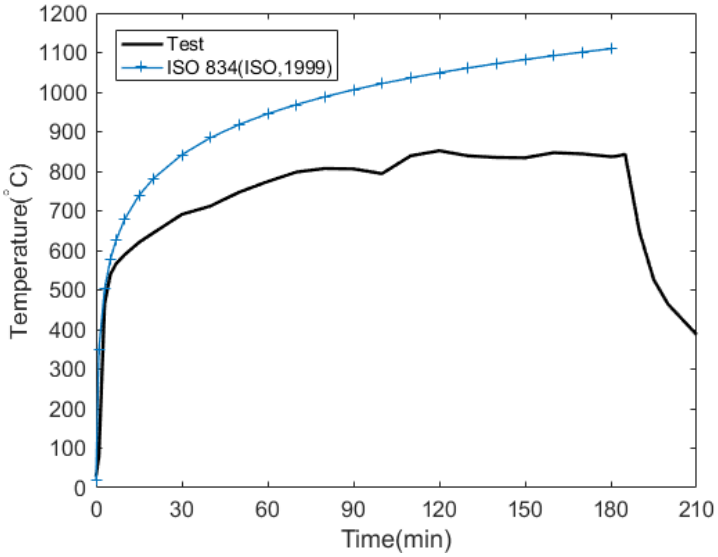

Figure 5.8: Comparison of measured gas temperature in the furnace and ISO 834 (ISO, 1999) **fire curve**

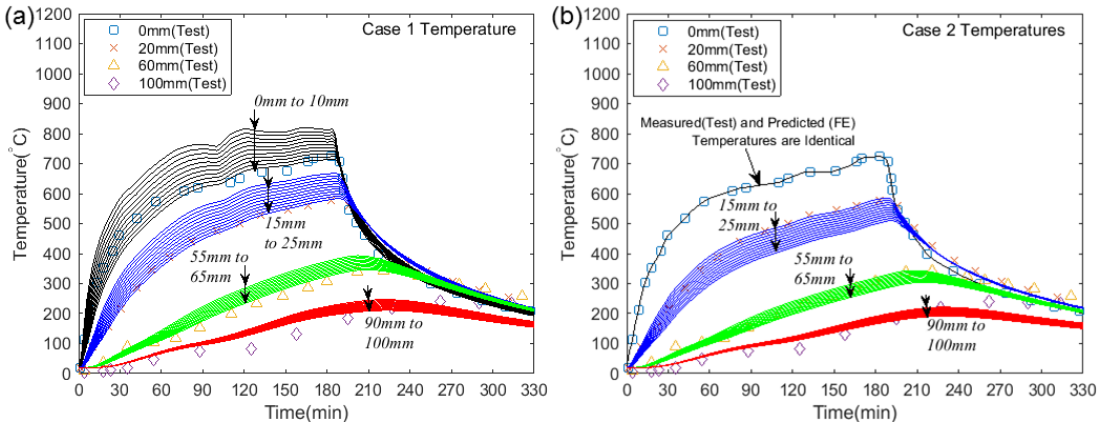

Figure 5.9: Comparison of predicted temperatures against measured temperatures (Wang et al., 2016)

Prediction of temperatures, presented as *Case 2 Temperature* in Figure 5.9(b) above show an excellent agreement with the measured temperatures from the test (Wang et al., 2016). This is then translated to a good prediction of mid-span deflection (ignoring response during cooling stage) shown in Figure 5.48(d), Figure 5.48(e), and Figure 5.48(f) shown later in Section 5.4.3.

5.4 Mechanical analysis

In performing mechanical analysis, either shell element with reduced integration (S4R) or without reduced integration (S4) can be used. S4 has 4 in-plane integration points while S4R has only single in-plane integration point (ABAQUS, 2012), which saves computational effort. Sensitivity analysis of these two options of element formulation was done beforehand and it was found that the predicted response is not influenced by the selection of these two types of element.

The sequential thermo-mechanical analysis was done using interactive module available within ABAQUS (ABAQUS, 2012) where temperature load was imported from thermal analysis results. For this method, S4R element (ABAQUS, 2012) was used for performing mechanical analysis while DS4 element (ABAQUS, 2012) was used for heat transfer (thermal) analysis. Note that the thermal element type adopted here for performing 'interactive' sequential thermo-mechanical analysis i.e. DS4 is not the same as used previously in Section 5.3 (Thermal analysis section). In the section, a 4-node linear heat transfer quadrilateral (DC2D4) element (ABAQUS, 2012) was used; similar to thermal analysis presented in Chapter 3 of the thesis. However, the temperature predictions from both element types are essentially identical, based on thorough checking on the output. Rationale of this decision was simply due to the very close temperature interval required to output the results i.e. 1 mm in the thermal analysis section i.e. Section 5.3. DS4 (ABAQUS, 2012) permits maximum number of 99 points through the element thickness while there were no limitations for DC2D4 (ABAQUS, 2012) element.

Note that, as discussed in the earlier chapter of the thesis (in Chapter 3), this interactive sequential thermo-mechanical analysis only allows maximum temperature points in the slab's thickness to be 19 for structural analysis step, even though thermal element DS4 permits a maximum of 99 through thickness points. This will give temperature interval in the slabs equal to 5.6 mm, 6.7 mm, and 5.6 mm for slab tested by Lim and Wade (2002), Zhang et al. (2014), and Wang et al. (2016) respectively. The selected spacing of temperature interval through the slab's thickness was found to be sufficient

to produce an identical mid-span deflection prediction compared to structural model developed with temperatures entered manually at 5 mm interval. Therefore, a decision was made to take advantage of the interactive capability available in ABAQUS to model the slab in the current study.

In mechanical analysis for modelling all the slabs, 'base case' models were defined with concrete tensile strength, F_t entered as $0.3(F_c)^{2/3}$ (CEB-FIP, 2010), thermal expansion properties follow those of Eurocode 2 (CEN, 2004) recommendation for the relevant aggregates, and fracture energy, G_f also follow recommendation from (CEB-FIP, 2010), where $G_f = 73.F_c^{0.18}$. F_c and F_t are the characteristic concrete compressive strength and tensile strength, respectively. Steel material mechanical properties follow recommendations from Eurocode 2 (CEN, 2004). All of these assumptions are applicable to all the three (3) slab models presented in this chapter. Table 5.8 shows a summary of the input mechanical properties for the models.

Table 5.8: Mechanical input properties for 'base case' model

Parameters	Slab 1	Slab 2	Slab 3
Concrete compressive strength, F_c	37 MPa	31.5 MPa	28 MPa
Concrete tensile strength, F_t	3.33 MPa	2.99 MPa	2.77 MPa
Thermal expansion (both concrete and steel)	EC 2	EC 2	EC 2
Fracture energy, G_f	140 N/m	136 N/m	133 N/m
Type of steel reinforcement	Cold drawn	Hot rolled	Hot rolled
Steel reinforcement ultimate strength, F_y (MPa)	565 MPa	580 MPa	475 MPa

5.4.1 Slab 1

5.4.1.1 Base case analysis

Central vertical mid-span deflection measured during the test was only done up to 186 mm, and this is shown in Figure 5.10. This is because central rotary potentiometer used to record the displacement had reached its maximum limit of travel (Lim and Wade, 2002). This occurred at approximately 144 minutes of exposure. However, at the end of test i.e. 180 minutes of fire exposure, physical measurement was done and the reading recorded was 271 mm (Lim and Wade, 2002). The measurement was done immediately when the test stopped after 3 hours exposure and before loads were

removed. A straight line is drawn (Lim and Wade, 2002) to connect these two points and are shown in Figure 5.10 and all other figures presented in the current section.

Comparison between prediction of mid-span deflection for base case analysis against test result (Lim and Wade, 2002) is shown in Figure 5.10 for both models heated to *Case 1 Temperature* and *Case 2 Temperature*. Due to severe numerical instability, both base case analyses representing *Case 1 Temperature* and *Case 2 Temperature* did not successfully finish the simulation. As an alternative, both models were re-developed using explicit dynamic approach. The predicted mid-span deflections were plotted together with identical model developed earlier using static analysis; this is also shown in Figure 5.10.

Termination of analysis for modelling reinforced concrete elements under exposure to fire is not unusual. Indeed, Buchanan (2008) in his work on '*The challenges of predicting structural performance in fires'* stated that it is common computational difficulties are found at one highly stressed or cracked element causing the program to terminate but this does not necessarily signal structural collapse in fires. Fractures of brittle materials in complex stress fields are a particular problem which code-writers are grappling with (Buchanan, 2008). In addition, Gillie et al. (2001) specifically stated the difficulties in obtaining a solution from the developed finite element models using ABAQUS had forced them to utilize another finite element code, FEAST (Finite Element Analysis of Shells at High Temperatures) that can interface with ABAQUS.

The cause for premature termination of analysis was further investigated. Contour plot for longitudinal (X-direction) plastic strain at exposed surface in reinforcing steels as well as concrete unexposed surface are plotted and shown in Figure 5.11 representing both *Case 1 Temperature* and *Case 2 Temperature*. Only plastic strain along X-direction is shown in the figure as the state of plastic strain along transverse (Y-direction) is far less than the strain along X-direction.

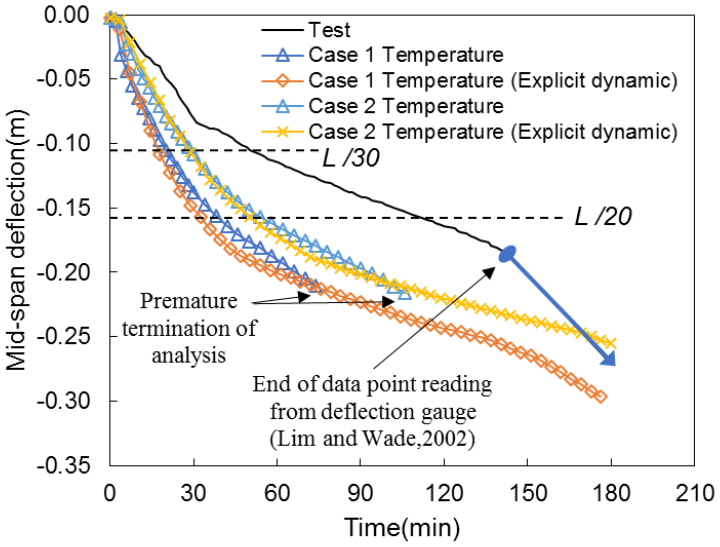

Figure 5.10: Comparison of mid-span deflection between model prediction and test results (Lim and Wade, 2002)

Analysis for *Case 1 Temperature* terminated at 74 minutes of exposure while analysis for *Case 2 Temperature* terminated at 107 minutes of exposure. It was found that for both cases, the termination occurred when tensile plastic strain in concrete at the unexposed surface reached approximately 1.7%. Specifically, *Case 1 Temperature* analysis terminated when tensile plastic strain in concrete reached 1.68% while *Case 2 Temperature* analysis terminated when 1.70% of plastic strain reached (see Figure 5.11). Temperatures predicted at the location were 90 °C and 112 °C from model heated to *Case 1 Temperature* and *Case 2 Temperature*, respectively. With the current assumption in the defined model, crack displacement width were calculated as 3.76 mm and 3.80 mm for *Case 1 Temperature* and *Case 2 Temperature*, respectively. Note that, with stress-displacement relationship for concrete in tension defined in the model rather than stress-strain relationship, a 'characteristic length' was specified (ABAQUS, 2012) in order to convert the plastic strain values to crack displacement (vice versa) width, where in this case it was defined as a diagonal length of plan view of a shell element; this has been explained previously in Chapter 3. Although it is slightly complicated, but this is important to ensure that the analysis is insensitive to the selection of mesh size.

However, the author is unaware as to the actual reason why the analysis stopped when crack displacement reached both 3.76 mm and 3.80 mm. While there is no detail explanation for this, it seems that ABAQUS solver could not obtain an equilibrium condition for the nonlinear equation formulated for the problem at hand. This is potentially due to cracking at the unexposed surface of the slab that propagated along the slab's shorter span at centre occurring in an abrupt manner, causing high jump in stress-free crack displacement width. This sudden and high jump in crack displacement width has caused the program to struggle to obtain an equilibrium condition for the nonlinear equation. Unfortunately there is no evidence to support this claim as the analysis stopped prematurely and no output can be obtained beyond that particular termination time.

In general, the mid-span deflection predicted from models with base case input parameters do not compare well with the test results. It is very obvious especially when limiting deflection criteria based on BS 476-20:1987 (BSI, 1987) is used as the slab's structural fire performance indicator. For instance, if $L/20$ (BSI, 1987) is to be set as the indicator, test result indicates that the slab would satisfy the criteria up to 112 minutes of exposure while model developed for *Case 1 Temperature* and *Case 2 Temperature* demonstrate that the slab would only satisfy the limiting deflection criteria up to 33 minutes and 51 minutes of ISO 834 (ISO, 1999) fire exposure, respectively. However, it is worth to mention that neither the model prediction nor the test result indicate that the slabs are losing the load carrying capacity at this point of time, judging from the magnitude as well as trend of mid-span deflection at 33 mins, 51 mins, and 112 mins. For *Case 1 Temperature* analysis, there was a sign of runaway deflection at approximately 135 minutes of fire exposure (see Figure 5.10) but similar trend was not happening for *Case 2 Temperature* analysis. This aspect of behaviour (runaway deflection) will be further discussed in Section 5.4.1.2, where selected model was used for more detail discussion on the slab's behaviour.

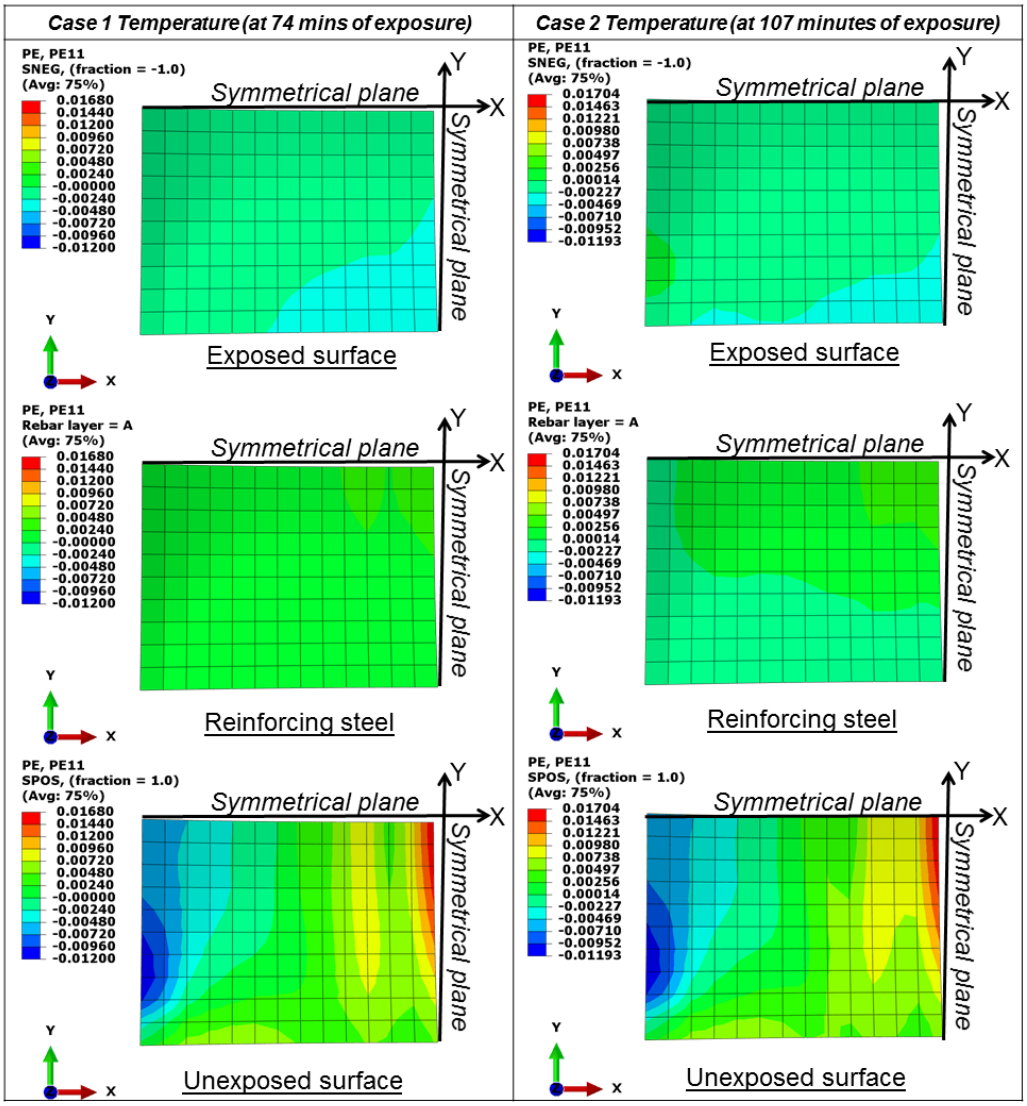

Figure 5.11: Plastic strain in X-direction at concrete exposed surface, reinforcing steels, and concrete unexposed surface for slab tested by Lim and Wade (2002)

5.4.1.2 Sensitivity analysis

Mid-span deflection predictions with various combinations of material input parameters are shown in Figure 5.12 to Figure 5.14 for *Case 1 Temperature* analysis and Figure 5.15 to Figure 5.17 for *Case 2 Temperature* analysis for the slab tested by Lim and Wade (2002). Severe numerical instabilities were found in most of the models. This was evident with premature termination of analysis in all the figures. As such, in the mid-span deflection plots shown in Figure 5.12 to Figure 5.17, results from explicit dynamic simulation are included to get a better insight into the response predictions.

Figure 5.12, Figure 5.13, Figure 5.14 show the effects of varying values of concrete tensile strength (F_t), fracture energy (G_f), and coefficient of thermal expansion (CTE) respectively, all of which represent *Case 1 Temperature* analysis. For *Case 2 Temperature* analysis, effect of varying concrete tensile strength values (F_t), fracture energy (G_f), and coefficient of thermal expansion (CTE) are shown in Figure 5.15, Figure 5.16, and Figure 5.17, respectively.

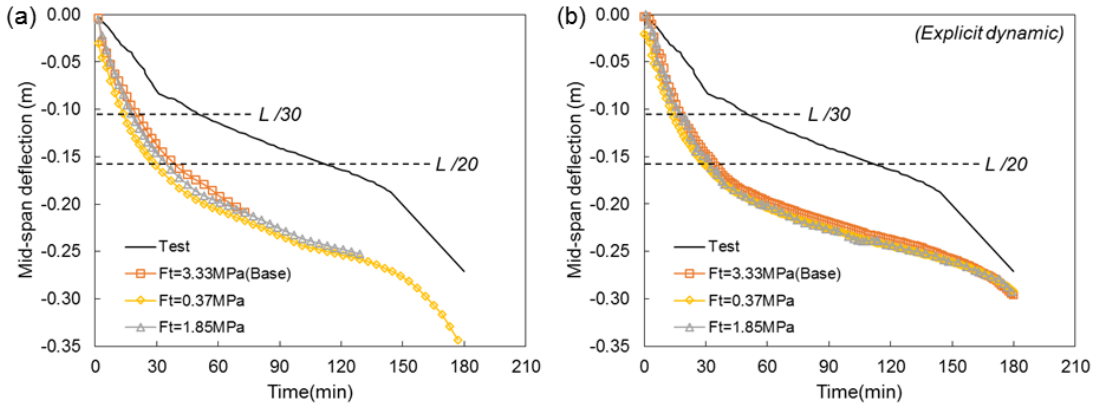

Figure 5.12: Mid-span deflection predicted with varying concrete tensile strength for '*Case 1 Temperature*' (a) implicit static simulation (b) explicit dynamic simulation for slab tested by Lim and Wade (2002)

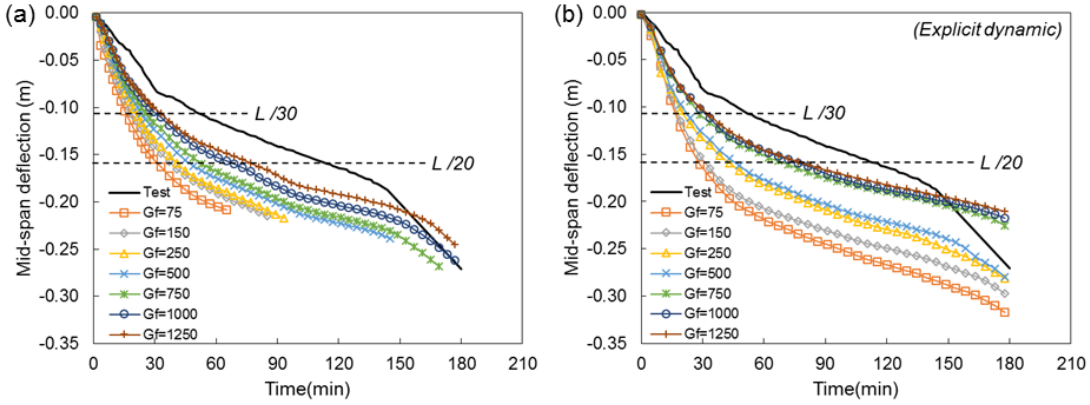

Figure 5.13: Mid-span deflection predicted with varying fracture energy values for '*Case 1 Temperature*' (a) implicit static simulation (b) explicit dynamic simulation for slab tested by Lim and Wade (2002)

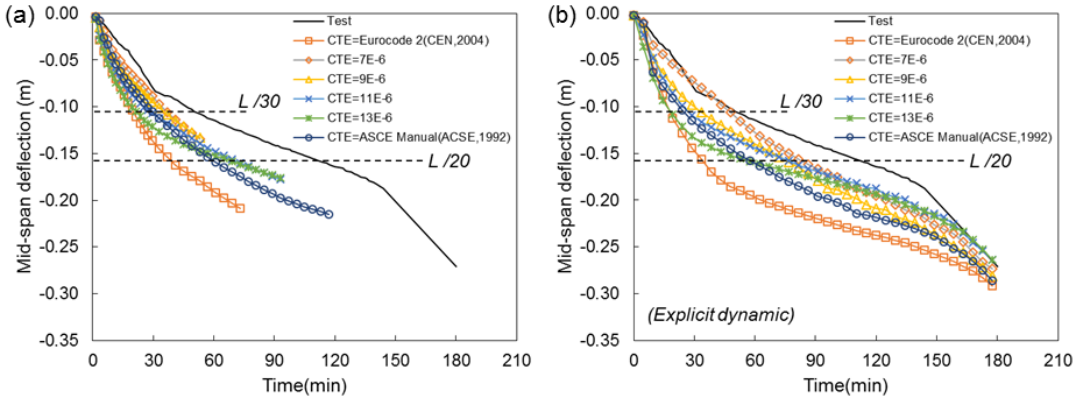

Figure 5.14: Mid-span deflection predicted with varying coefficient of thermal expansion (CTE) for '*Case 1 Temperature*' (a) implicit static simulation (b) explicit dynamic simulation for slab tested by Lim and Wade (2002)

Severe numerical instabilities were also reported by Gernay (2012) in modelling the same slab, which forced the author to resort to low concrete tensile strength i.e. 1 MPa and high 'tensile crack energy' (as defined in the work) equalling to 450 N.m/m. Although different terms (or perhaps parameters) are used i.e. 'fracture energy' in the current study and 'tensile crack energy' in the study by Gernay (2012), it is believed that they literally refer to the same ideology. It is the manner in which post-cracking behaviour is treated within finite element codes, within the context of smeared

cracking approach in modelling cracking behaviour of concrete. Higher 'fracture energy' and higher 'tensile crack energy' result in more ductile behaviour of concrete in tension.

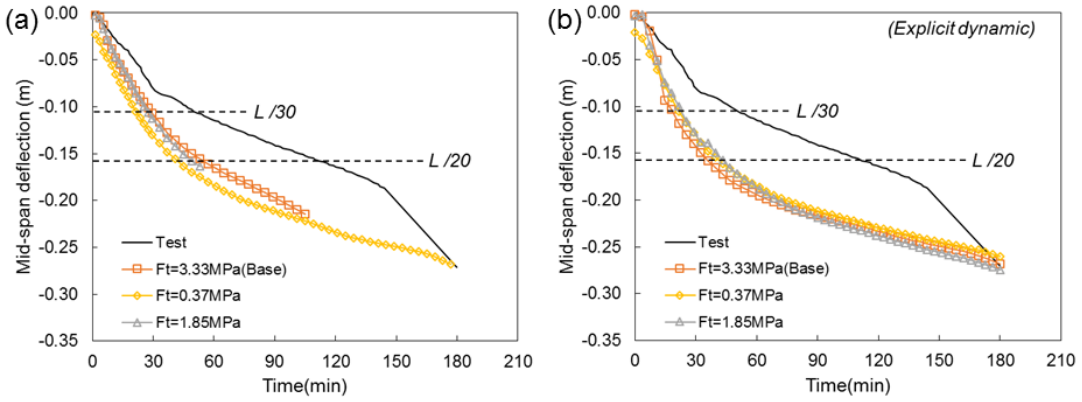

Figure 5.15: Mid-span deflection predicted with varying concrete tensile strength for '*Case 2 Temperature*' (a) implicit static simulation (b) explicit dynamic simulation for slab tested by Lim and Wade (2002)

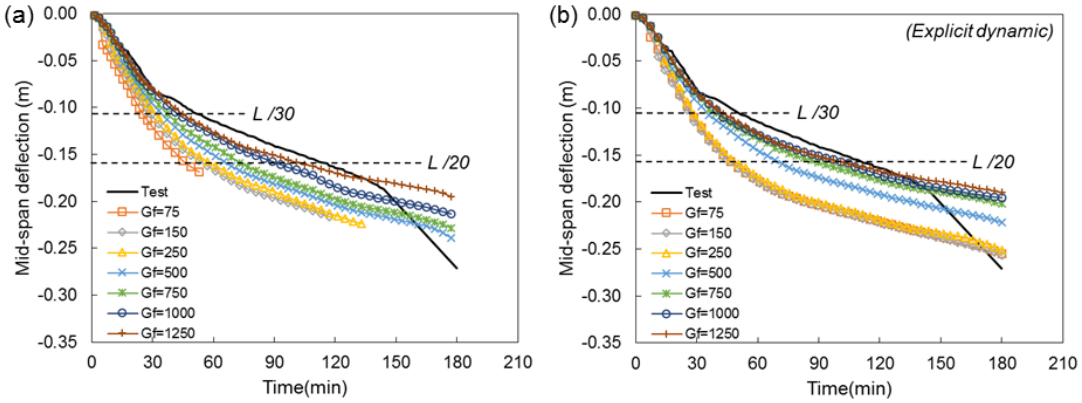

Figure 5.16: Mid-span deflection predicted with varying fracture energy values for '*Case 2 Temperature*' (a) implicit static simulation (b) explicit dynamic simulation for slab tested by Lim and Wade (2002)

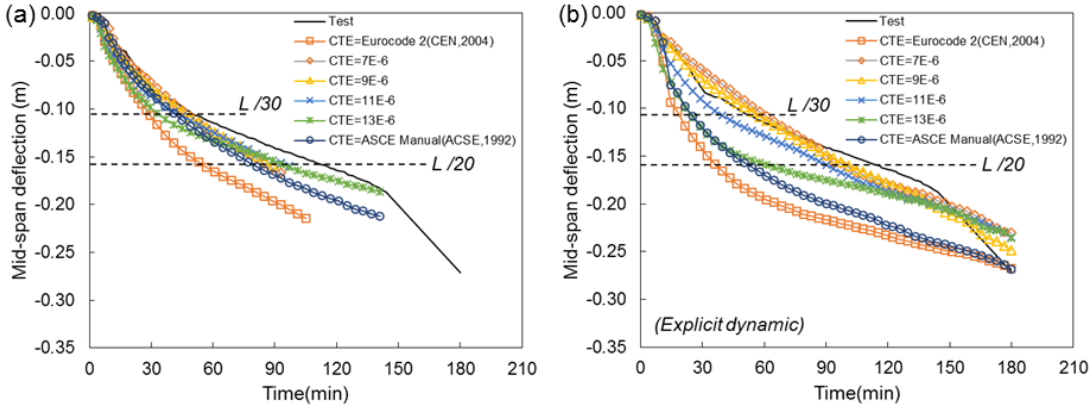

Figure 5.17: Mid-span deflection predicted with varying coefficient of thermal expansion (CTE) for '*Case 2 Temperature*' (a) implicit static simulation (b) explicit dynamic simulation for slab tested by Lim and Wade (2002)

Referring to Figure 5.12 and Figure 5.15, all model predictions, irrespective of values of the defined concrete tensile strength (F_t) demonstrate greater deflection compared to measured mid-span deflection reported by Lim and Wade (2002). In contrast, numerical modelling reported by Lim et al. (2004) and Gernay (2012) for the same slab showed that the mid-span deflection agree with the test results. However, predictions from Gernay (2012) are based on model defined with high value of 'tensile crack energy', which indicates that the results are comparable to the predictions with high fracture energy values presented in Figure 5.13 and Figure 5.16. In other words, in the current study, high fracture energy (in the range 750 – 1250N/m) would produce better predictions, which matched reasonably good with the test results for temperature load entered from *Case 1 Temperature*. Comparison of predicted mid-span deflection between model presented by Gernay (2012) and Lim et al. (2004) plotted together with prediction from Figure 5.13(a) with G_f= 1250 N/m is shown in Figure 5.18.

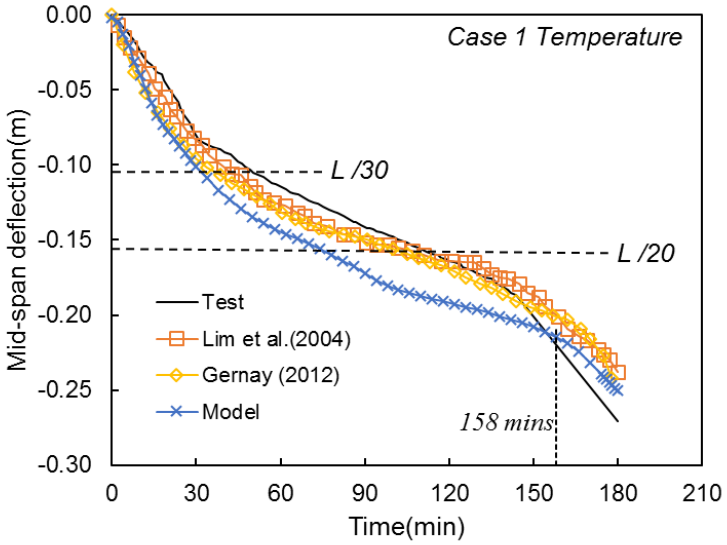

Figure 5.18: Comparison of predicted mid-span deflection against prediction reported by Lim et al. (2004) **and** Gernay (2012)

At 158 minutes of exposure, trend of mid-span deflection changed, indicating that runaway type of deflection was triggered (see prediction shown in Figure 5.18). Although occurring at different points of time during fire exposure, mid-span deflection prediction reported by Lim et al. (2004) and Gernay (2012) also demonstrated the same trend. Similar behaviour was also reported from the experiment (Lim and Wade, 2002). Therefore, it is fair to claim that the slab started losing its load carrying capacity, judging from the runaway type of deflection shown. The state of plastic strain in the reinforcing steels was further examined and discussed in the following section.

Concrete thermal expansion properties recommended in Eurocode (CEN, 2005, 2004) were found to predict relatively higher mid-span deflection based on studies by Ellobody and Bailey (2009). Similar findings were found in the current investigation and are shown in Figure 5.14 and Figure 5.17. Other thermal expansion properties i.e. constant coefficient of thermal expansion (CTE) and properties recommended by ASCE (1992) predict relatively less deflection. This indicates that free thermal strain behaviour recommended in Eurocode (CEN, 2005, 2004) are conservative, with regard to predicted deformation behaviour of concrete slabs.

In general, slightly better agreement for mid-span deflection predicted for *Case 2 Temperature* that closely matched the measured mid-span deflection during the test as compared to the prediction from models loaded with temperatures from *Case 1 Temperature*. This is applicable to all models with various mechanical input parameters. Similar numerical instability issues are found for models with *Case 2 Temperature* although relatively less severe. The reduced severity is obviously due to relatively lower temperature load entered into the model for *Case 2 Temperature* in comparison to *Case 1 Temperature*.

5.4.1.3 Plastic strain in concrete and reinforcement

Mid-span deflection predicted form most models demonstrate an increase in rate of deflection towards the end of fire exposure i.e. 180 minutes. To examine the issue further, the state of plastic strain in concrete at the bottom (exposed surface), as well as concrete at the top (unexposed surface) during 30 mins, 60 mins, 120 mins, and 180 minutes of exposure are shown in Figure 5.19 to Figure 5.22. Plastic strain along the longitudinal (X-axis) and transverse (Y-axis) direction at fire exposed concrete surface are shown in Figure 5.19 and Figure 5.20, respectively. Figure 5.21 and Figure 5.22 show similar results plot for concrete section at the surface unexposed to fire. Figure 5.23 shows photos taken during the test that reveal cracks on the surface exposed and unexposed to fires.

The model selected for showing the state of plastic strain here, as well as demonstrating tensile membrane action shown later in Section 5.4.1.4 was developed with F_t = 3.33 MPa (CEB-FIP, 2010), G_f = 1250 N/m, and coefficient of thermal expansion (CTE) following Eurocode 2 (CEN, 2004) recommendation for concrete with siliceous aggregates. The slab was heated with *Case 1 Temperature*. The selected model is essentially arbitrary, judging from the best matched mid-span deflection, both in terms of trend and magnitude.

Formation of plastic strain in concrete on longitudinal axis direction agree with the crack patterns witnessed in the test (see Figure 5.21 and Figure 5.23(a)). It indicates that cracks potentially occur along direction parallel to slab's shorter span, as has been

reported by extensive experimental investigation on small scale slabs by Bailey and Toh (2007). Higher plastic strains occur at the top of the slab rather than at the bottom. With another two cracks opening on each right and left of the central crack, it further indicates that potentially the concrete has failed under tensile cracking here, where tensile load carrying capacity was transferred to the other two locations (with two more lines of cracks). With plastic strain at 8.64% and temperature at the unexposed surface at 180 minutes of exposure being 203 °C, the calculated crack displacement width at this point of time was 19.3 mm. Although there is no definite value to claim what crack displacement value can be considered as high, it is of the author's opinion that crack displacement width of 19.3 mm can be considered as extremely high, given the brittle nature of concrete material. Note that all the points discussed above were confined to the assumption within the developed model, which is smeared cracking approach, meaning the cracks were uniformly distributed in an element in the model.

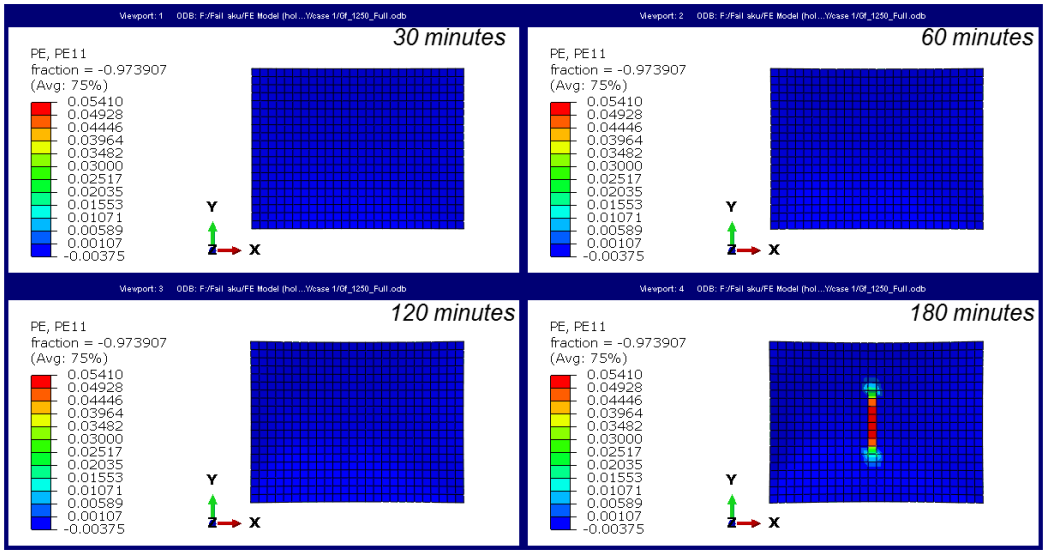

Figure 5.19: Plastic strain in X-direction at bottom section of concrete (fire exposed surface) at 30 minutes, 60 minutes, 120 minutes, and 180 minutes of exposure for slab tested by Lim and Wade (2002)

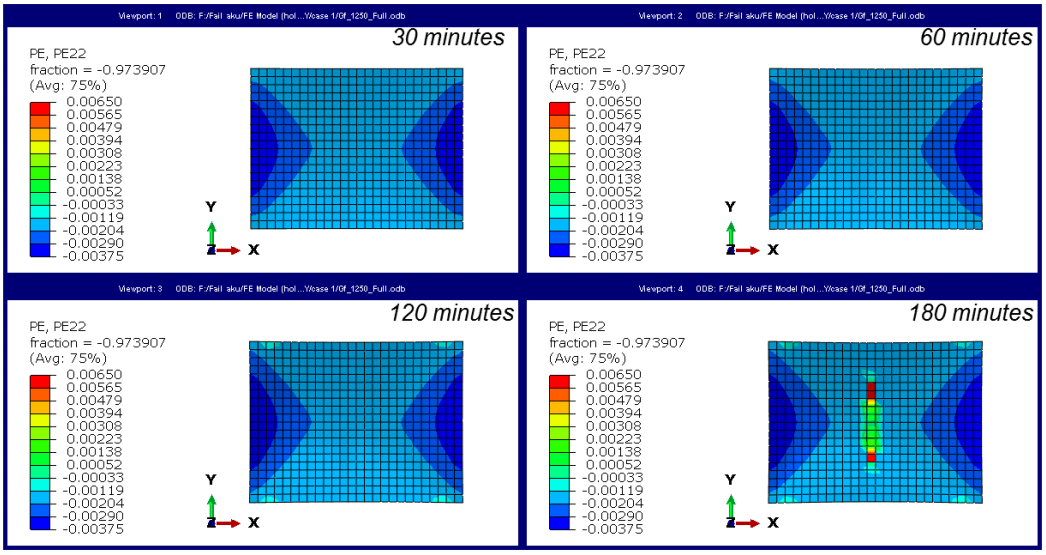

Figure 5.20: Plastic strain in Y-direction at bottom section of concrete (fire exposed surface) at 30 minutes, 60 minutes, 120 minutes, and 180 minutes of exposure for slab tested by Lim and Wade (2002)

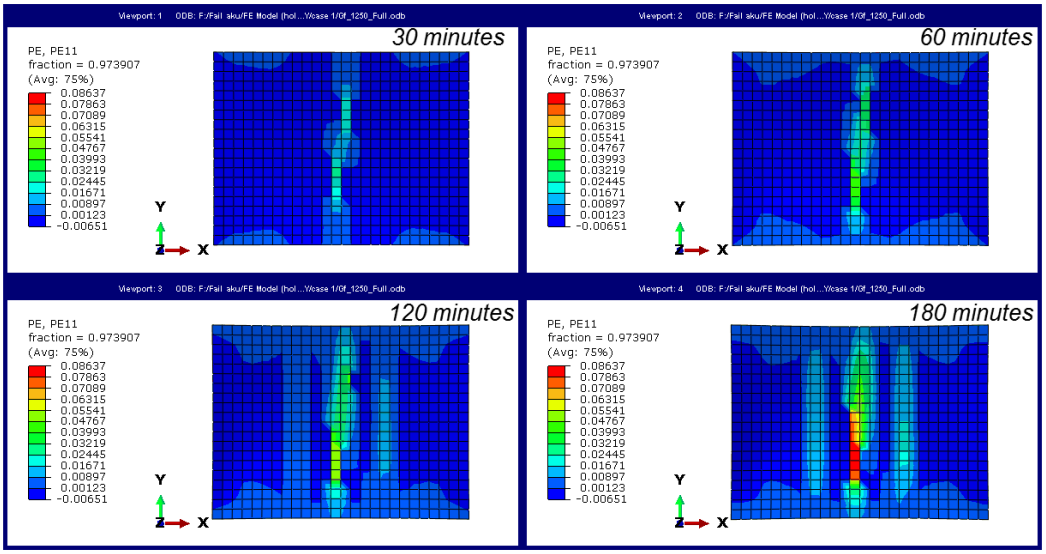

Figure 5.21: Plastic strain in X-direction at top section of concrete (surface unexposed to fire) at 30 minutes, 60 minutes, 120 minutes, and 180 minutes of exposure for slab tested by Lim and Wade (2002)

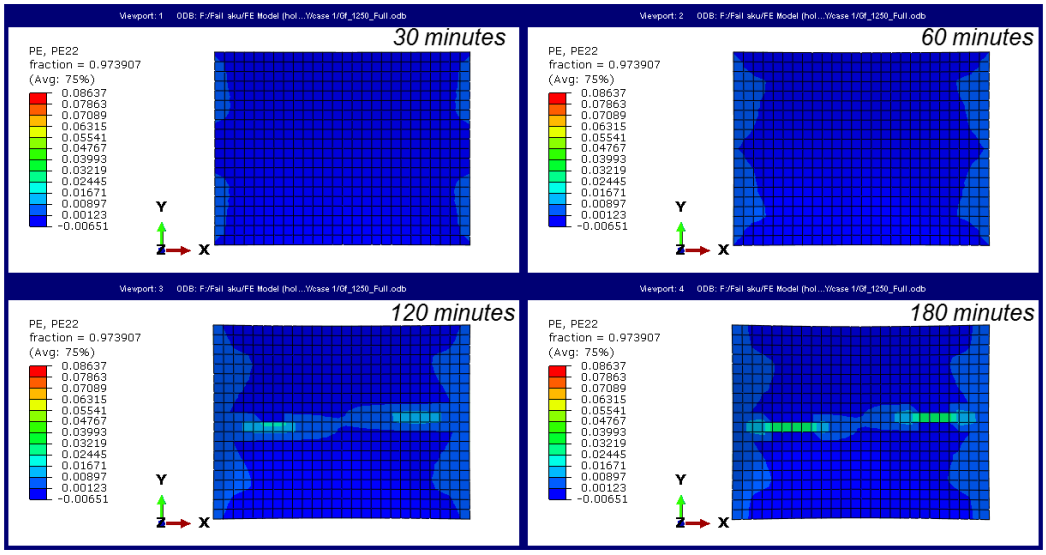

Figure 5.22: Plastic strain in Y-direction at top section of concrete (surface unexposed to fire) at 30 minutes, 60 minutes, 120 minutes, and 180 minutes of exposure for slab tested by Lim and Wade (2002)

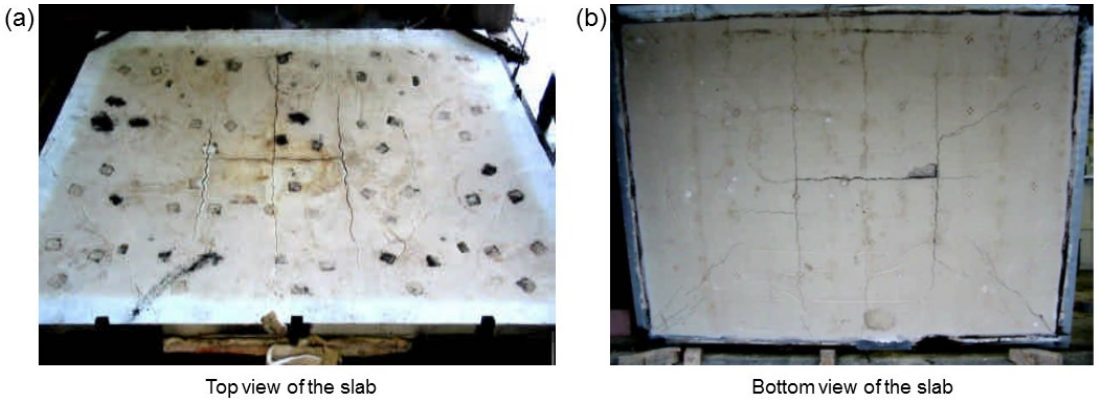

Figure 5.23: (a) Top view of slab and (b) bottom view of slab after the fire test reproduced from Lim and Wade (2002)

Evolution of plastic strain with time for reinforcing steels along the slab's centre line both along longitudinal (X-direction) and transverse (Y-direction) direction are shown in Figure 5.24 and Figure 5.25, respectively. The predicted plastic strain in the longitudinal reinforcement near central of the slab is 1.82% at 158 minutes of exposure

to ISO 834 (ISO, 1999). At this particular point of time, rate of deflection increased from model prediction, which indicates that runaway type of deflection was triggered.

Note that earlier in Section 5.4.1.1 it was discussed that the premature termination of analysis for base case models occurred when plastic strain reached 1.68% and 1.70% for slab heated to *Case 1 Temperature* and *Case 2 Temperature*, respectively. But the plastic strain values were predicted in concrete rather than in the reinforcing steels. In this section, fracture energy of concrete was increased, which means the crack displacement width (consequently concrete cracking strain) was also increased thus resulting in more ductile behaviour of concrete in tension. Although concrete cracking strain increased, it is interesting to note that the runaway type of deflection triggered when plastic strain in reinforcing steel reached 1.82%, a value that is close to 1.68% and 1.70% previously calculated for concrete. Study by Wang et al. (2013b) suggested that a value of tensile strain (mechanical strain) of 2% is critical, which is when runaway type of deflection is triggered for two-way reinforced concrete slabs exposed to fire from below. Note that this value i.e. 2% mechanical strain will be used as a performance indicator throughout this chapter.

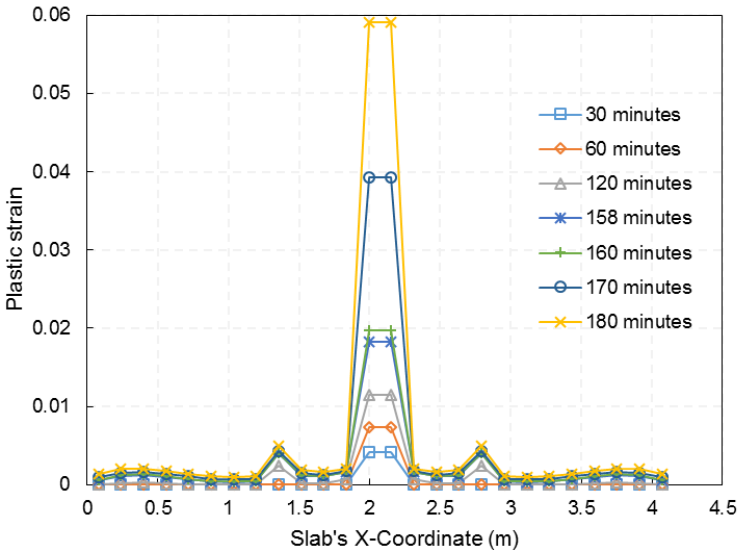

Figure 5.24: Evolution of plastic strain with time in bottom longitudinal (spanning along X-axis) reinforcing steel near centre of the slab predicted for slab tested by Lim and Wade (2002)

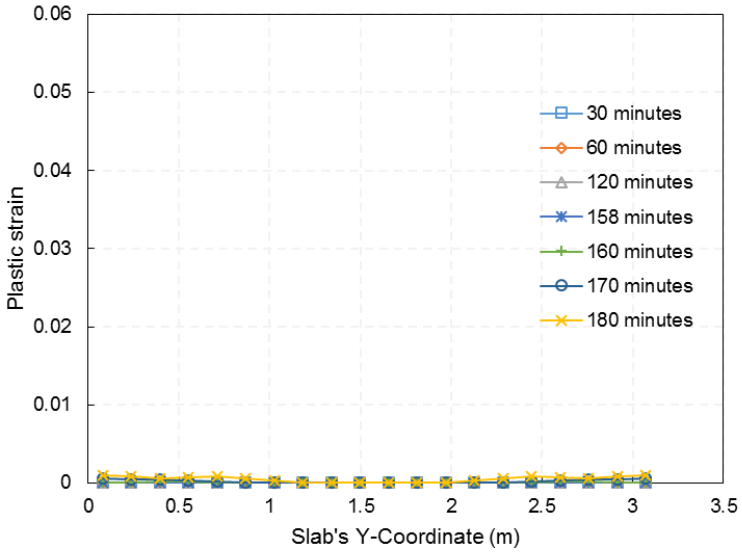

Figure 5.25: Evolution of plastic strain with time in bottom transverse (spanning along Y-axis) reinforcing steel near centre of the slab predicted for slab tested by Lim and Wade (2002)

5.4.1.4 Tensile membrane action

The state of membrane tractions at 15 mins, 120 mins, and 180 mins of fire exposure are shown in Figure 5.26, Figure 5.27, and Figure 5.28, respectively. Note that, similar slab model for showing the state of plastic strain in both concrete and steel reinforcement presented previously was selected here. The selected model for analysing membrane behaviour in this section is essentially arbitrary, but is based on the model with the best matched mid-span deflection to the measured mid-span deflection from the test (Lim and Wade, 2002). The plot for membrane forces shown in the figures demonstrate that the slab sustained high vertical deflection by utilising tensile membrane action, as is widely concurred within the structural fire engineering community.

Plots for principal membrane forces in Figure 5.27 and Figure 5.28 demonstrate where the section at central of the slab is critical, where slab was stretched along X-direction and therefore signalling a potential concrete cracking failure. At 120 minutes of exposure, the calculated temperature in the reinforcing steel was 572 °C, and stress in the reinforcing steel was calculated as 261 MPa. From mathematical formulation of steel material model, the peak strength of steel reinforcement at 572 °C is 269 MPa. Therefore, the normalised longitudinal (spanning along X-direction) reinforcing steel stress at 120 minutes of exposure in that location is 0.97. This means, at this point of time, 97% of the defined steel material strength has been utilised.

At 180 minutes of exposure (see Figure 5.28), at central of slab, inconsistent membrane forces were calculated. Compressive membrane traction was also demonstrated together with the tensile net. This occurred due to severe cracking (concrete crack failure). As smeared cracking approach was implemented in the current study, the scattered tensile-compressive membrane forces demonstrated in the figure was due to the analysis trying to find an equilibrium condition in that particular element.

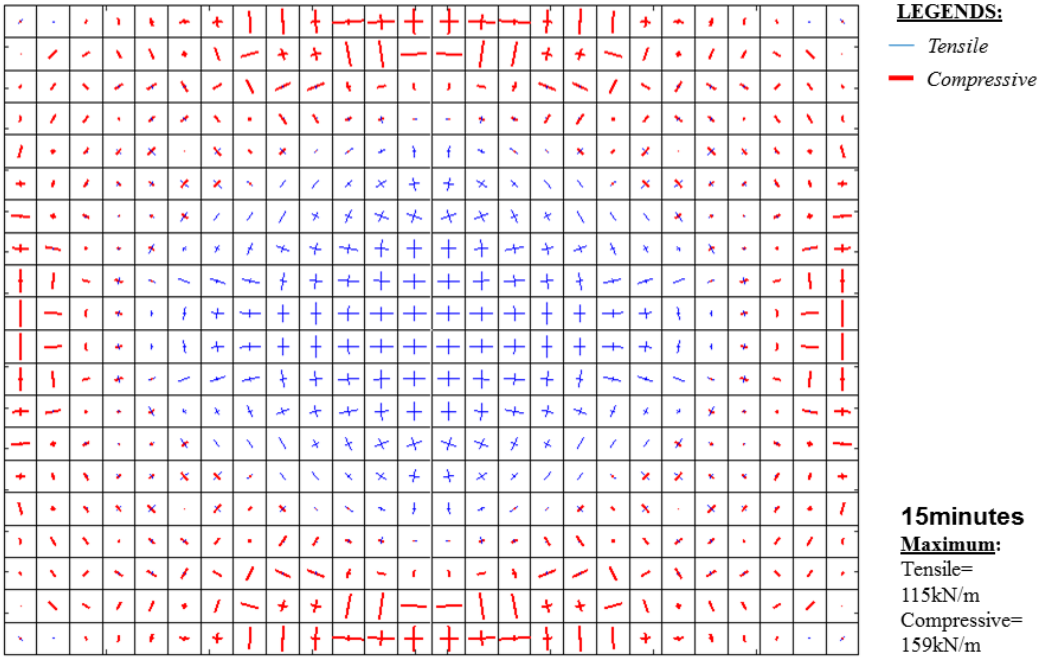

Figure 5.26: Principal membrane forces at 15 minutes of fire exposure for slab tested by Lim and Wade (2002)

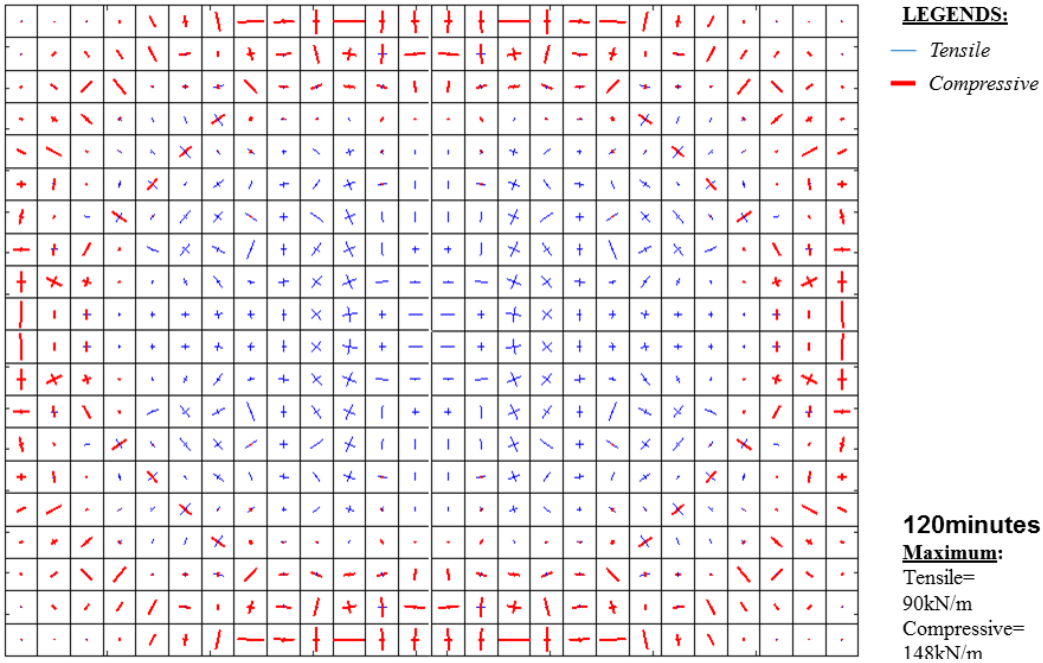

Figure 5.27: Principal membrane forces at 120 minutes of fire exposure for slab tested by Lim and Wade (2002)

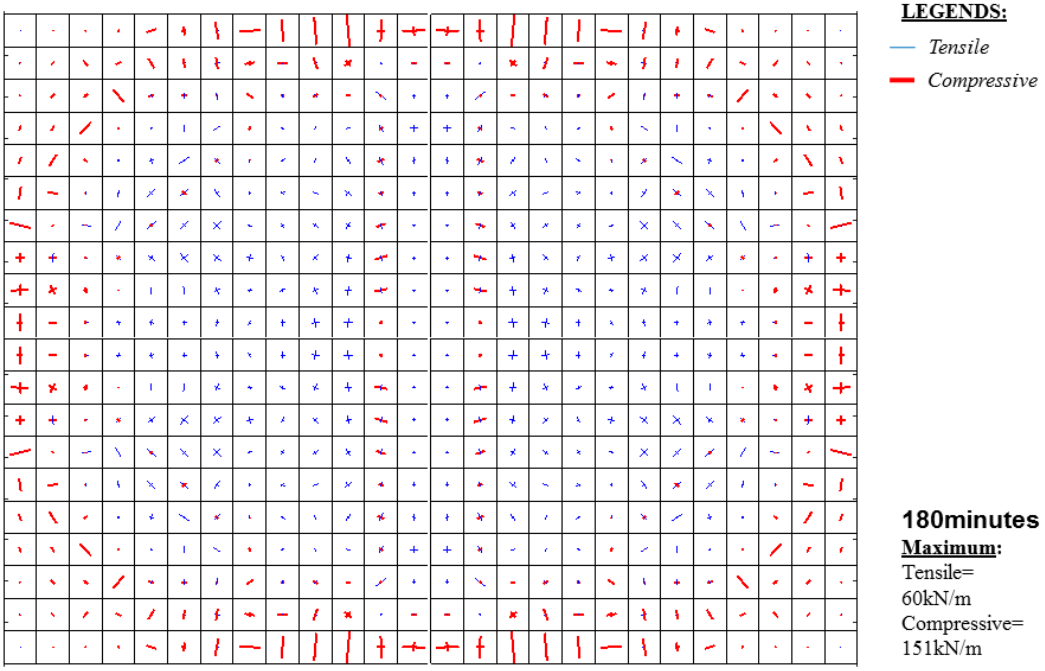

Figure 5.28: Principal membrane forces at 180 minutes of fire exposure for slab tested by (Lim and Wade, 2002)

5.4.1.5 Summary

Studies presented in the current section (Section 5.4.1) described aspect of modelling the behaviour of two-way reinforced concrete slabs exposed to fire, with fire furnace tested concrete slabs performed by Lim and Wade (2002) selected for validation. Table 5.9 presents summary of the predicted fire resistance rating for the slab.

Table 5.9: Summary of structural fire resistance rating for slab tested by Lim and Wade (2002)

Fire resistance criterion	*L/20* (BSI, 1987)	Tensile strain in reinforcing steels: 2% (Wang et al., 2013b)	Eurocode 2 (CEN, 2004)	International Building Code (International Code Council, 2009)
Test	112 mins	-	120 mins	60 mins
Case 1 Temperature	33 mins	154 mins		
Case 2 Temperature	50 mins	180 mins		

Note that, provision of fire resistance rating recommended in Table 5.8 of Eurocode 2 (CEN, 2004), shown in column 4 of Table 5.9 provide a more realistic performance indicator for the slabs. With runaway deflection reported at ± 144 minutes from test result and predicted at 158 minutes of exposure from the model, provision of minimum slab dimension and axis distance from Eurocode 2 (CEN, 2004) seem more realistic with regard to better economical design. In addition, limiting tensile strain in steel at 2% (Wang et al., 2013b) seems to align with this recommendation. Note that tensile strain of 2% was predicted at 154 minutes of exposure. In addition, both fire resistance ratings recommended in Eurocode 2 (CEN, 2004) and International Building Code (International Code Council, 2009) are based on selection of geometrical dimension of the slabs i.e. minimum thickness, as well as concrete cover etc.

5.4.2 Slab 2

5.4.2.1 Base case analysis

Similar to analysis presented previously in Section 5.4.1.1, premature termination of analysis was also found in modelling the current slab (Zhang et al., 2014). This occurred at 94 minutes of fire exposure. However, only slab heated to *Case 1 Temperature* suffered the problem. The model was re-developed using explicit dynamic approach to check if there was any indication of runaway type of deflection, or any similar behaviour that could potentially provide a sign that the slab was losing its load carrying capacity. For mid-span deflection predicted from explicit dynamic approach, no sign of runaway type of deflection was observed and this can be seen in Figure 5.29.

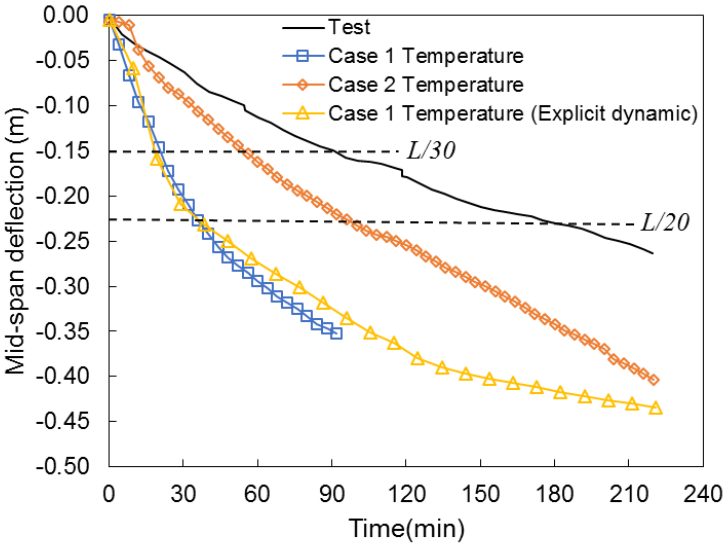

Figure 5.29: Comparison of mid-span deflection between model prediction and test results (Zhang et al., 2014)

Plastic strain in concrete at the surface exposed and unexposed to fires were examined to further understand the behaviour discussed previously. Consistent trend was found, as was the case for modelling Slab 1 in Section 5.4.1 previously where the termination of analysis occurred when plastic strain in concrete at the surface unexposed to fire reached a certain range of values. The plastic strain calculated for the current slab is 1.62% (see Figure 5.30 for *Case 1 Temperature*). Note that previous model presented in Section 5.4.1 demonstrated that the analysis stopped when plastic strain in concrete (also at the surface unexposed to fire) reached 1.68% and 1.70% for analysis *Case 1 Temperature* and *Case 2 Temperature*, respectively. Some discussion on the behaviour have been provided previously thus they will not be repeated here.

On the other hand, in modelling the slab heated to *Case 2 Temperature*, the predicted plastic strain in the unexposed surface at 220 minutes of exposure is 1.31%, which is less than the one predicted for analysis from *Case 1 Temperature*. This confirms that plastic strain in concrete between 1.62% - 1.70% seem to cause problems in modelling the structural behaviour of two-way slabs presented in the current chapter.

Limiting deflection criteria as recommended in BS 476 (BSI, 1987) as shown in Figure 5.29 with dotted lines drawn provide significant variation of the slab's structural fire performance for model heated to *Case 1 Temperature*, *Case 2 Temperature*, as well as measured deflection from the test (Zhang et al., 2014). Specifically, the slabs would have failed $L/20$ limiting deflection criteria at 37 mins, 137 mins, and 175 mins for slab heated to *Case 1 Temperature*, heated to *Case 2 Temperature*, and the tested specimen (Zhang et al., 2014), respectively.

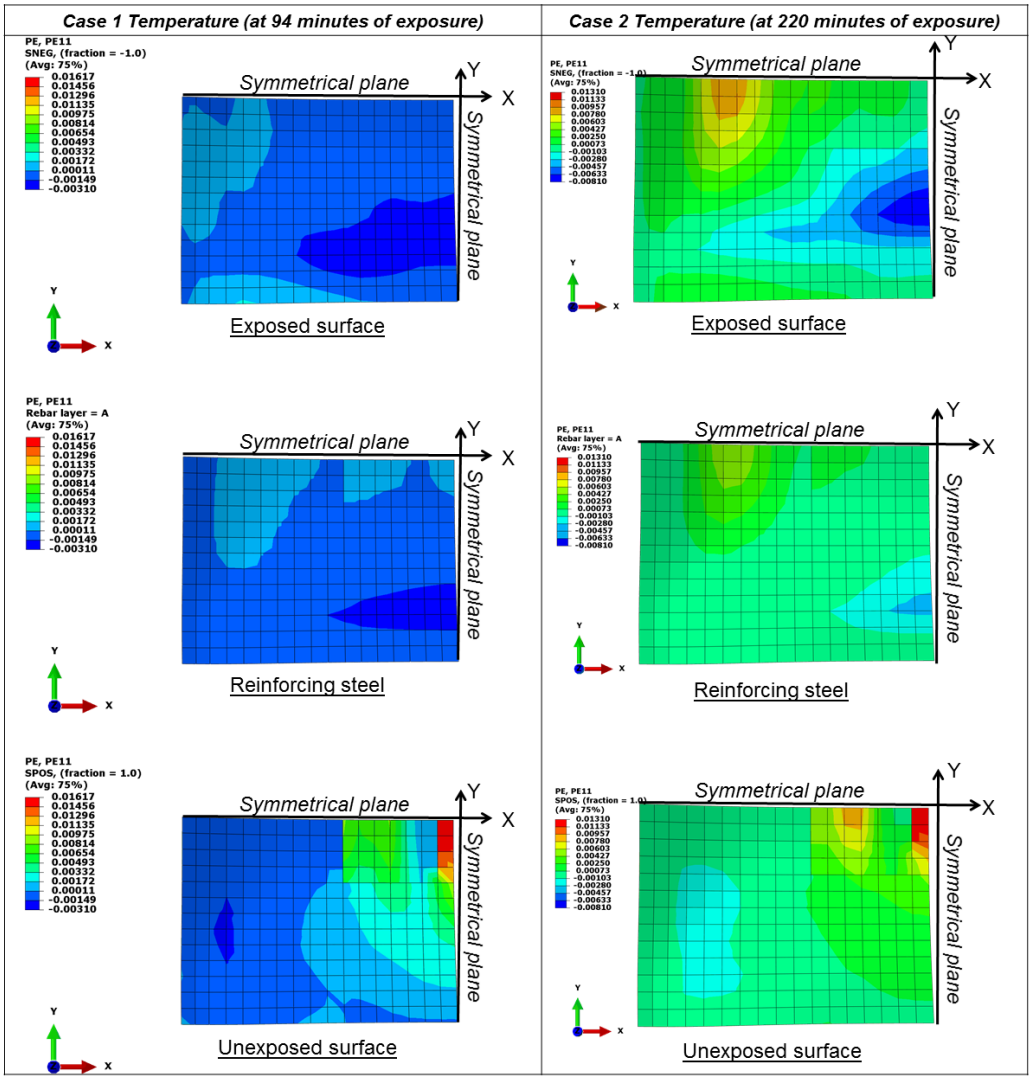

Figure 5.30: Plastic strain in X-direction for concrete exposed surface, reinforcing steels, and concrete unexposed surface for slab tested by Zhang et al. (2014)

5.4.2.2 Sensitivity analysis

Sensitivity of input mechanical properties to the predicted mid-span deflection is presented in this section. For *Case 1 Temperature* analysis, sensitivity of input concrete tensile strength, F_t, fracture energy, G_f, and coefficient of thermal expansion (CTE) are shown in Figure 5.31, Figure 5.32, and Figure 5.33, respectively. In each of the plots, mid-span deflection predicted from models developed using explicit dynamic approach are included. This is due to severe termination of analysis found for modelling most slabs heated to *Case 1 Temperature* and therefore predictions from model developed using explicit dynamic approach are included to give an overall insight into the response predictions.

In Figure 5.31, models developed with *Case 1 Temperature* predict mid-span deflection far higher than measured deflection during the test (Zhang et al., 2014). These predictions of mid-span deflections are not comparable at all to the measured deflection with regard to magnitude. Models with varying values of coefficient of thermal expansion (CTE) also demonstrate similar predictions with regard to magnitude; as shown in Figure 5.33.

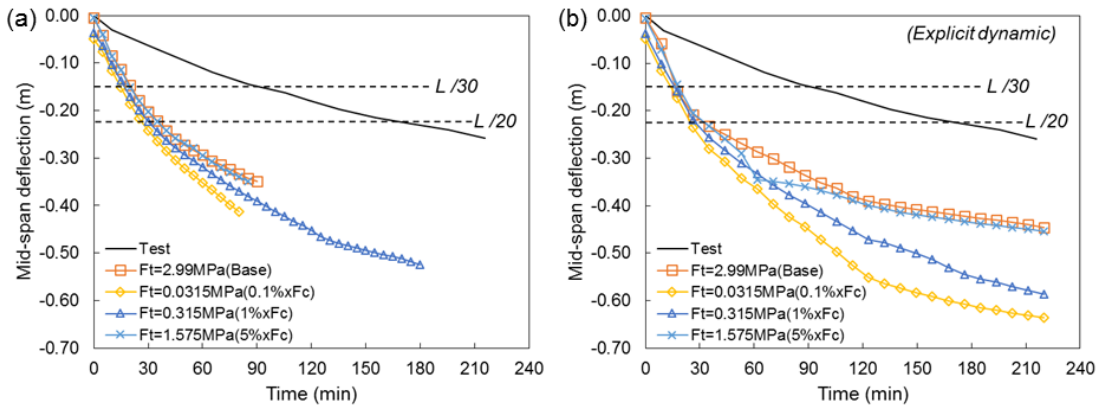

Figure 5.31: Mid-span deflection predicted with varying concrete tensile strength for '*Case 1 Temperature*' (a) implicit static simulation (b) explicit dynamic simulation for slab tested by Zhang et al. (2014)

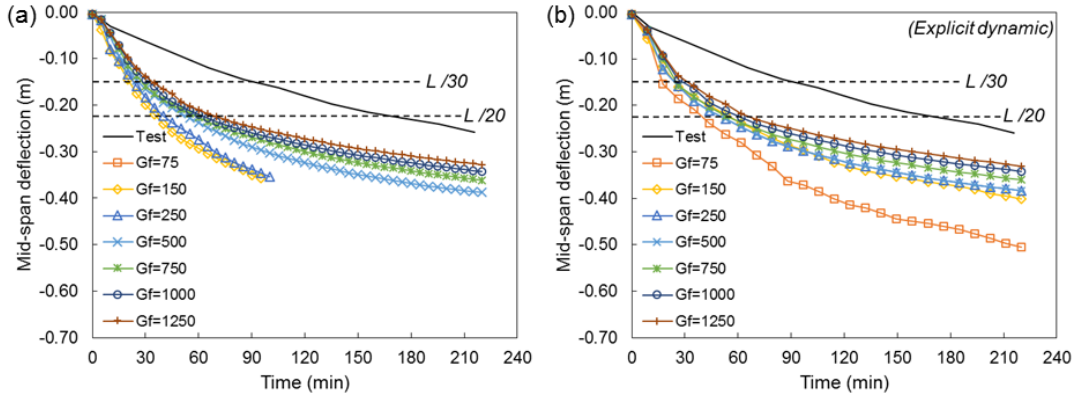

Figure 5.32: Mid-span deflection predicted with varying fracture energy values for '*Case 1 Temperature*' (a) implicit static simulation (b) explicit dynamic simulation for slab tested by Zhang et al. (2014)

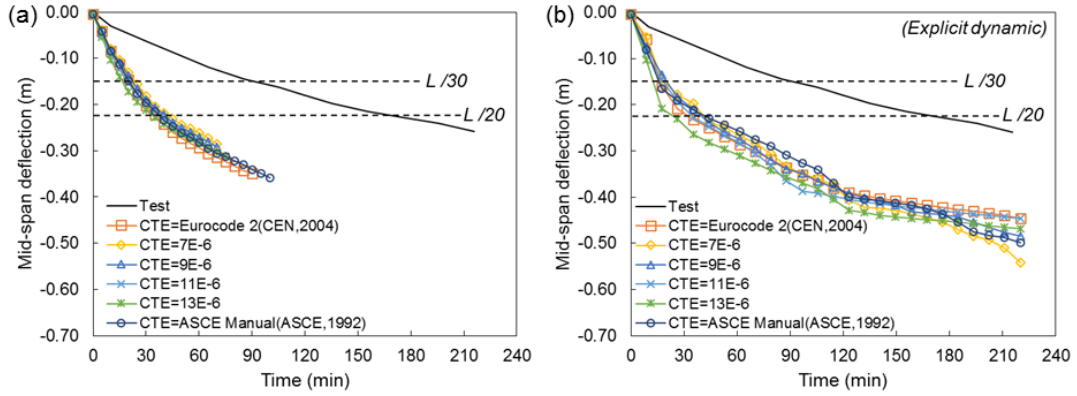

Figure 5.33: Mid-span deflection predicted with varying coefficient of thermal expansion (CTE) for '*Case 1 Temperature*' (a) implicit static simulation (b) explicit dynamic simulation for slab tested by Zhang et al. (2014)

It is suspected that the high deflection prediction for *Case 1 Temperature* is due to the large differences (see Table 5.4) between temperatures predicted from FE heat transfer analysis (consequently entered into structural model) and the actual temperatures measured during the test (and consequently actually experienced in the slab). This can be seen in Figure 5.7 shown earlier in this chapter. The difference is really significant especially at the surface exposed to fires. This issue has been discussed in detail in Chapter 3 thus it will not be repeated here. In summary, it is suggested that this is one of the disadvantages of testing concrete elements in furnaces, where different furnaces

typically produce different severity of heating. In other words, lack of consistency in the severity of heating was found although the prescribed gas temperature versus time curve for the tests are essentially identical i.e. ISO 834 (ISO, 1999).

In contrast to models heated with *Case 1 Temperature*, models defined with temperature load from *Case 2 Temperature* produce slightly better prediction in general. Figure 5.34, Figure 5.35, and Figure 5.36 show mid-span deflection predicted with varying concrete tensile strength, F_t, fracture energy, G_f, and coefficient of thermal expansion (CTE), respectively. The figures represent models developed for *Case 2 Temperature* analysis. Yet still, the maximum difference for magnitude of deflection was 140 mm occurring at the end of fire exposure i.e. 220 minutes between measured deflection (Zhang et al., 2014) and prediction from base case model (see Table 5.8 for input properties defined for the base case model). In addition, the deflection trend also differs especially during the early stages of heating.

Lower rate of vertical mid-span deflection was found from the model in comparison to the rate of deflection reported from the test. High rate of vertical deflection during early stage of heating is normally due to thermal bowing behaviour as a result of highly non-linear distribution of temperature through the slab's depth. This behaviour also interrelates with the formation of tensile crack at the slab's mid-depth at the element near mid-span of the slab. This was shown in the preliminary investigation by the author and reported in Baharudin et al. (2016).

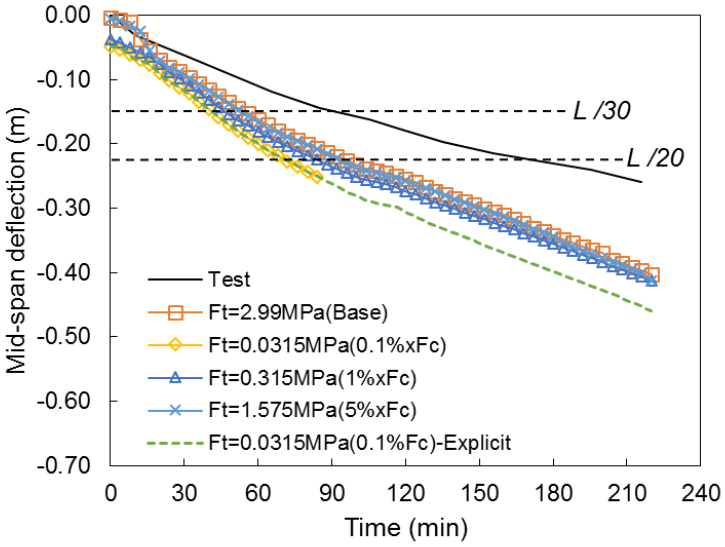

Figure 5.34: Mid-span deflection predicted with varying concrete tensile strength for slab tested by Zhang et al. (2014) **:** ***Case 2 Temperature***

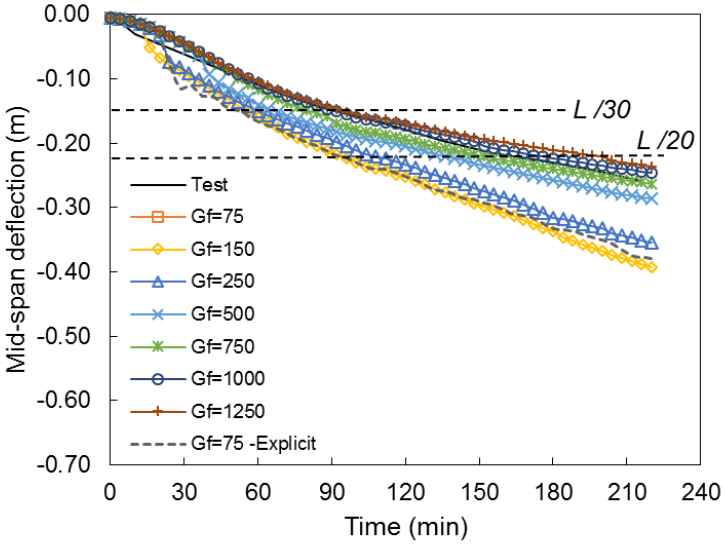

Figure 5.35: Mid-span deflection predicted with varying concrete fracture energy for slab tested by Zhang et al. (2014)**:** ***Case 2 Temperature***

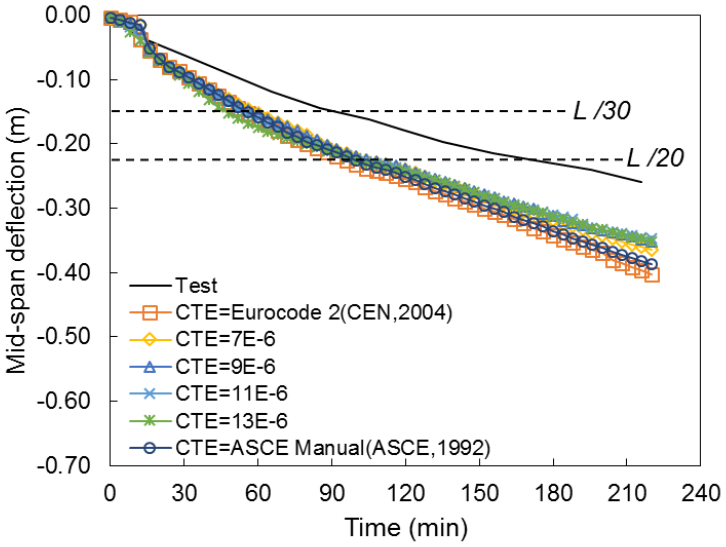

Figure 5.36: Mid-span deflection predicted with varying coefficient of thermal expansion (CTE) for slab tested by Zhang et al. (2014)**: *Case 2 Temperature***

With focus given to results for *Case 2 Temperature*, higher fracture energy (G_f) produce better prediction for mid-span deflections and these are shown in Figure 5.35. The difference between the predicted deflection and reported values (Zhang et al., 2014) is found to be less than 30 mm throughout fire exposure for model with G_f = 1250 N/m. Assuming the entered temperatures are similar to the one experienced in the slab during the test, it gives an impression that the models predicted mid span deflection with reasonably good accuracy with regard to magnitude. This further highlights the importance of accurately measuring and recording both temperature and deflection during fire tests. Moreover, comparing the reported temperatures (Zhang et al., 2014) at the exposed surface with other tests on concrete slabs for instance Bailey and Ellobody (2009); Lim and Wade (2002); Rickard et al. (2015); Wang et al. (2016), it is of the author's opinion that actual gas temperatures (which are unfortunately not reported in the paper (Zhang et al., 2014)) during the test significantly deviated from the standard ISO 834 (ISO, 1999) curve.

With similar findings from the previous Section 5.4.1 for modelling slab tested by Lim and Wade (2002), high fracture energy values are required for ensuring numerical stability and also better response prediction when compared against experimental

results. Both Slab 1 and Slab 2 have demonstrated that defining fracture energy value of 1250 N/m produce better mid-span deflection than the rest. In addition, thermal expansion properties recommended in Eurocode 2 (CEN, 2004) are always conservative with regard to prediction of mid-span deflection and consequently do not provide economical design if limiting deflection is used as the performance criteria.

5.4.2.3 Plastic strain in concrete and reinforcement

The states of plastic strain presented in the current section are based on model developed with F_t = 2.99 MPa (CEB-FIP, 2010), G_f = 1250 N/m, coefficient of thermal expansion (CTE) based on recommendation from Eurocode 2 (CEN, 2004), and heated with temperatures from *Case 2 Temperature.* The selected model is essentially arbitrary, based on the best matched mid-span deflection between model prediction and test results.

Contour plots for plastic strain in concrete section at the surface exposed to fire and unexposed to fire are shown in Figure 5.37, Figure 5.38, Figure 5.39, and Figure 5.40. Figure 5.37 and Figure 5.38 show contour plots for plastic strain at surface exposed to fire for longitudinal and transverse direction, respectively. Figure 5.39 and Figure 5.40 show the plot for section at the unexposed surface, also for plastic strain along longitudinal and transverse direction, respectively. The selected duration for showing the contour plots are 30 mins, 60 mins, 120 mins, and 220 mins of exposure.

By examining the state of plastic strain at the surface unexposed to fire, relatively similar finding from the previous modelled slab i.e. Lim and Wade (2002) was found here, except that the magnitude of plastic strain was relatively lower. The trend was however, similar for both models where slabs were stretched more along the longitudinal span rather than shorter span. In addition, surface unexposed to fire was critical where it was expected that the first crack will initiate here (see Figure 5.39) rather than bottom of the slab.

Maximum concrete plastic strain predicted was 3.81%, during 220 minutes of exposure while for the case slab tested by Lim and Wade (2002) was 8.6%, during 180

minutes of exposure. Note that, photo taken during test, both for slab tested by Zhang et al. (2014) and Lim and Wade (2002) presented similar behaviour, where cracks propagated along shorter span at the surface unexposed to fire. Interestingly, no cracks were visualised at the surface exposed to fire (soffit of the concrete) for slab tested by Zhang et al. (2014) (see Figure 5.41(b)).

Figure 5.41 shows photos taken at the surface exposed and unexposed to fires after the test finished (Zhang et al., 2014). No cracks can be visualised at the bottom of the slab. At the top surface, crack '2' and '3' run the full length of the slab along the shorter span. This again, confirms the behaviour mentioned earlier in Section 5.4.1, where first tensile cracking is more likely to be triggered at the slab's top surface rather than bottom.

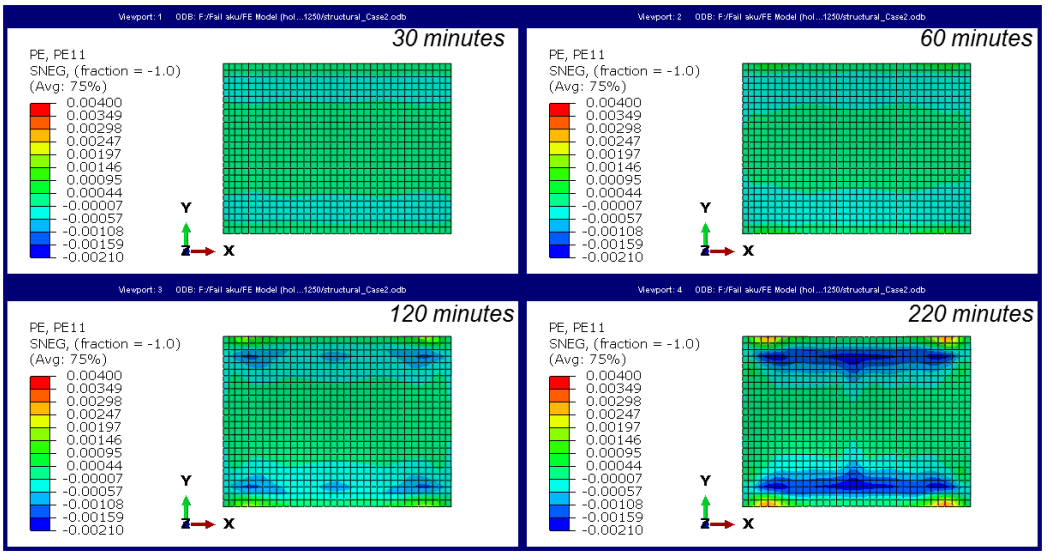

Figure 5.37: Plastic strain in X-direction at bottom section of concrete (fire exposed surface) at 30 minutes, 60 minutes, 120 minutes, and 220 minutes of exposure for slab tested by Zhang et al. (2014)

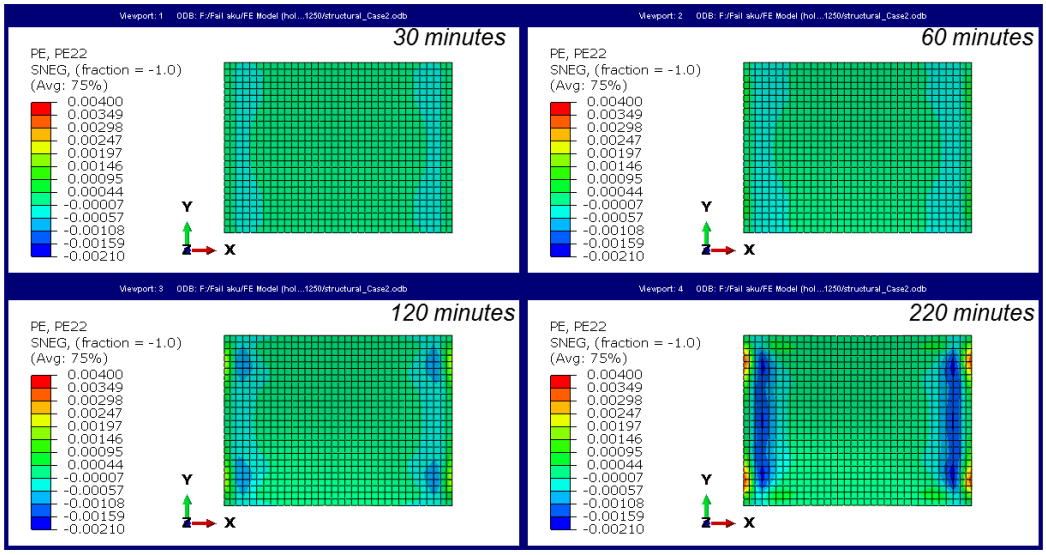

Figure 5.38: Plastic strain in Y-direction at bottom section of concrete (fire exposed surface) at 30 minutes, 60 minutes, 120 minutes, and 220 minutes of exposure for slab tested by Zhang et al. (2014)

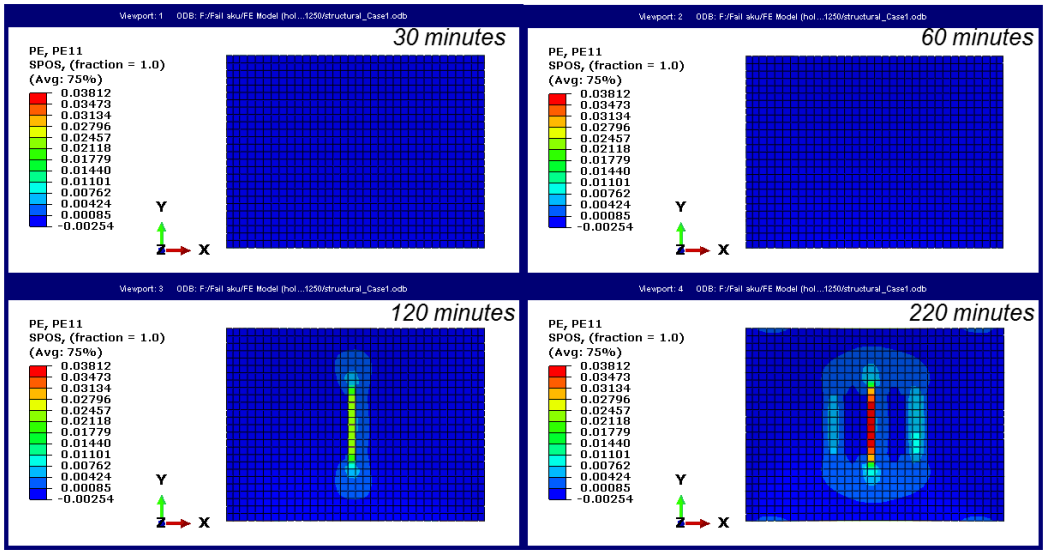

Figure 5.39: Plastic strain in X-direction at top section of concrete (surface unexposed to fire) at 30 minutes, 60 minutes, 120 minutes, and 220 minutes of exposure for slab tested by Zhang et al. (2014)

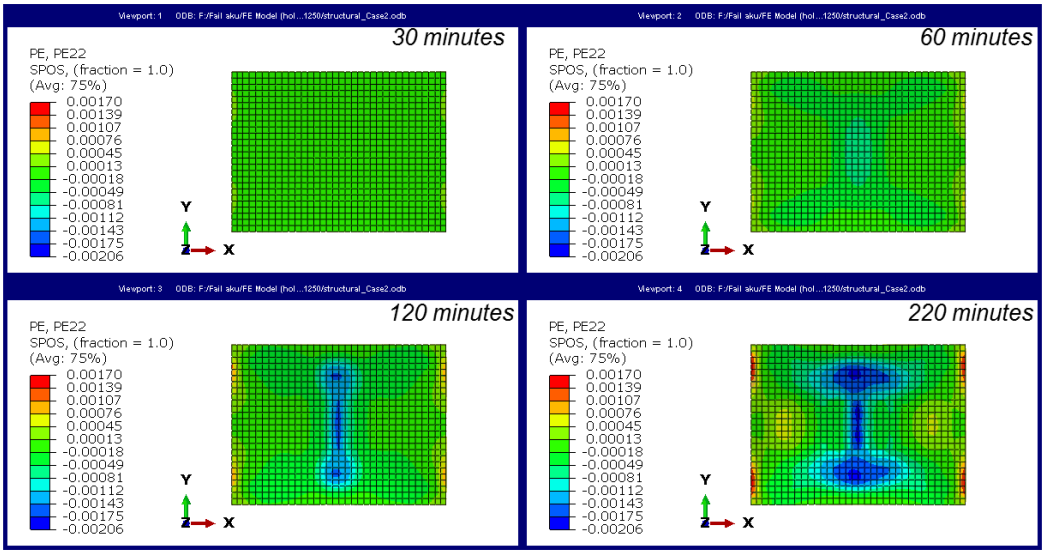

Figure 5.40: Plastic strain in Y-direction at top section of concrete (surface unexposed to fire) at 30 minutes, 60 minutes, 120 minutes, and 220 minutes of exposure for slab tested by Zhang et al. (2014)

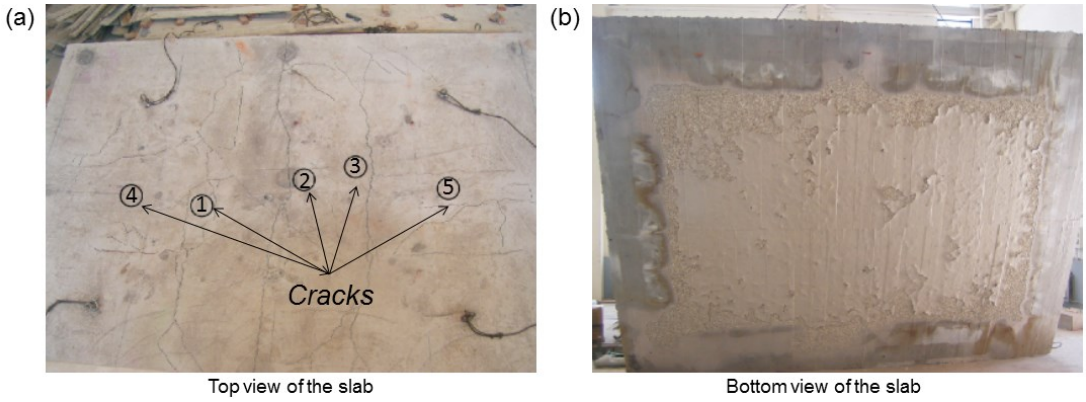

Figure 5.41: (a) Top view of slab and (b) bottom view of slab after the fire test reproduced from Zhang et al. (2014)

Maximum reinforcing steels mechanical strain defined in the material model was 15%. Beyond 15%, linear descending branch was defined in the stress-strain formulation of the material model to represent rupturing of the reinforcement. Reinforcing steel totally lost its strength at 20% mechanical strain. The maximum plastic strain predicted for modelling Zhang et al. (2014) slab in bottom reinforcement was 0.14%. In contrast,

the predicted plastic strain at the top section of the slab (in concrete) also during 220 minutes of exposure was 3.81%. No top reinforcements were provided at centre of the slab where these values of plastic strain are discussed here. Evolution of plastic strains in reinforcing steels with time in elements along centre line of the slab is shown in Figure 5.42 and Figure 5.43. Plastic strain in elements along longitudinal direction of the slab are shown in Figure 5.42 while Figure 5.43 shows the strain in transverse elements, also along the slab's centre line.

With maximum plastic strain in reinforcing steels predicted as 0.14%, which is far less than the one calculated for Slab 1 i.e. 5.91% (note that both models were developed with fracture energy, G_f = 1250 N/m), which explains why no sign of runaway deflection were found here. For model heated to *Case 1 Temperature*, the maximum calculated plastic strain was 1.20% (see 'base case' model developed using explicit dynamic approach in Figure 5.29)

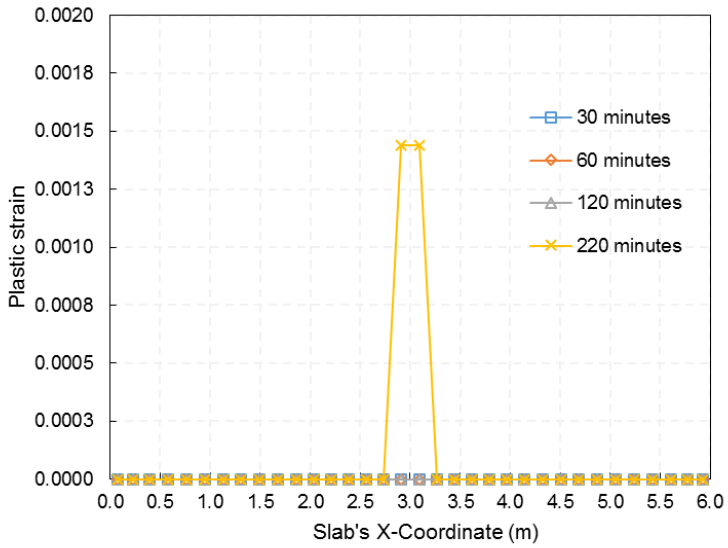

Figure 5.42: Evolution of plastic strain with time in bottom longitudinal (spanning along X-axis) reinforcing steels near centre of the slab predicted for slab tested by Zhang et al. (2014)

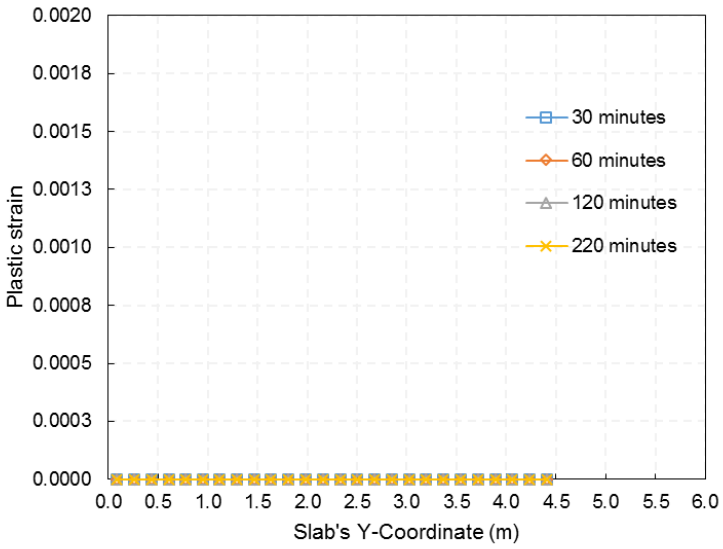

Figure 5.43: Evolution of plastic strain with time in bottom transverse (spanning along Y-axis) reinforcing steels near centre of the slab predicted for slab tested by Zhang et al. (2014)

5.4.2.4 Tensile membrane action

Principal membrane forces in the slab at 15 mins, 120 mins, and 220 mins of fire exposure are shown in Figure 5.44. Note that the plotted membrane forces in the figure are based on model developed with F_t = 2.99 MPa, G_f = 1250 N/m, coefficient of thermal expansion (CTE) based on recommendation from Eurocode 2 (CEN, 2004), and heated with temperatures from *Case 2 Temperature*. Note that similar model for presenting the state of plastic strain discussed in the previous section is selected here. Formation of tensile net can be clearly visualised at the central area of the slab. This confirmed that the slab retained its integrity by mobilising tensile membrane action.

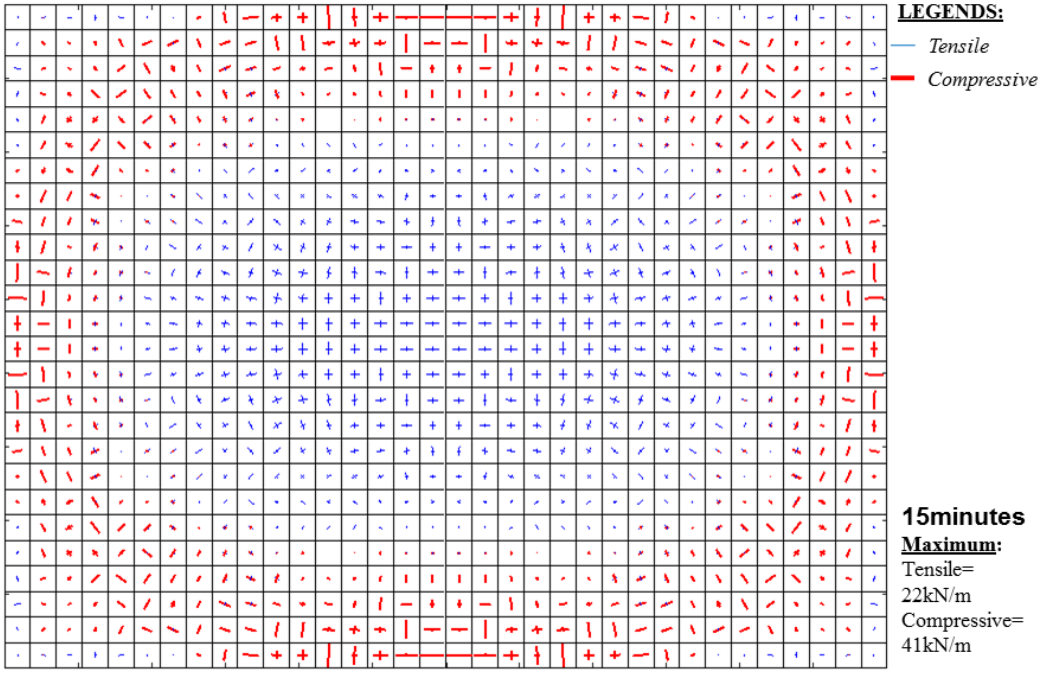

Figure 5.44: Principal membrane forces at 15 minutes of fire exposure for slab tested by Zhang et al. (2014)

Maximum tensile force calculated at 15 mins, 120 mins, and 220 mins were 22 kN/m, 134 kN/m, and 144 kN/m width of the slab, respectively. At 120 minutes of exposure, at central area of slab where tensile net formed, a few elements demonstrated a combination of tensile force and compressive force (see Figure 5.45). This behaviour however, does not mean that the slab demonstrated compressive force at the central section of the slab. It was rather the model trying to find equilibrium condition while it was suspected that concrete tensile cracking at the surface unexposed to fire has initiated. In this process, some numerical inconsistency occurred as the model attempted to find the equilibrium condition. Note that, smeared cracking approach was implemented in the model, meaning cracks were uniformly distributed across an element therefore it is slightly controversial to specifically point the exact location as where the crack actually opened.

Stress in reinforcing steel spanning along X-direction (longitudinal) in an element near central of the slab at 120 minutes of exposure was calculated as 223 MPa (in tension) with temperature predicted as 454 °C. Steel material model defined for the model

provides ultimate strength of 461 MPa when temperature in the reinforcement attained 454 °C. This indicates that only 49% of the steel strength was utilised at this point of time. 49% of steel strength corresponding to 139 kN/m of force calculated from steel only (ignoring concrete strength). With maximum membrane force calculated as 134 kN/m width of slab (see Figure 5.45), it further verified the predicted value and consequently confirmed that only steel provides the required strength in preserving the load carrying capacity of the slab.

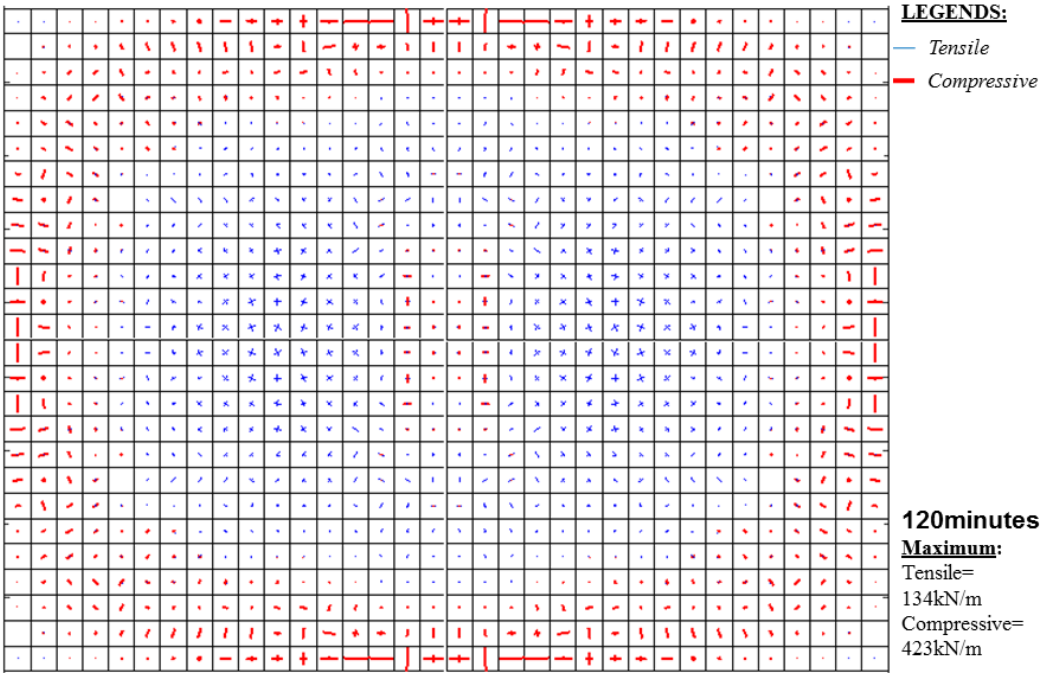

Figure 5.45: Principal membrane forces at 120 minutes of fire exposure for slab tested by Zhang et al. (2014)

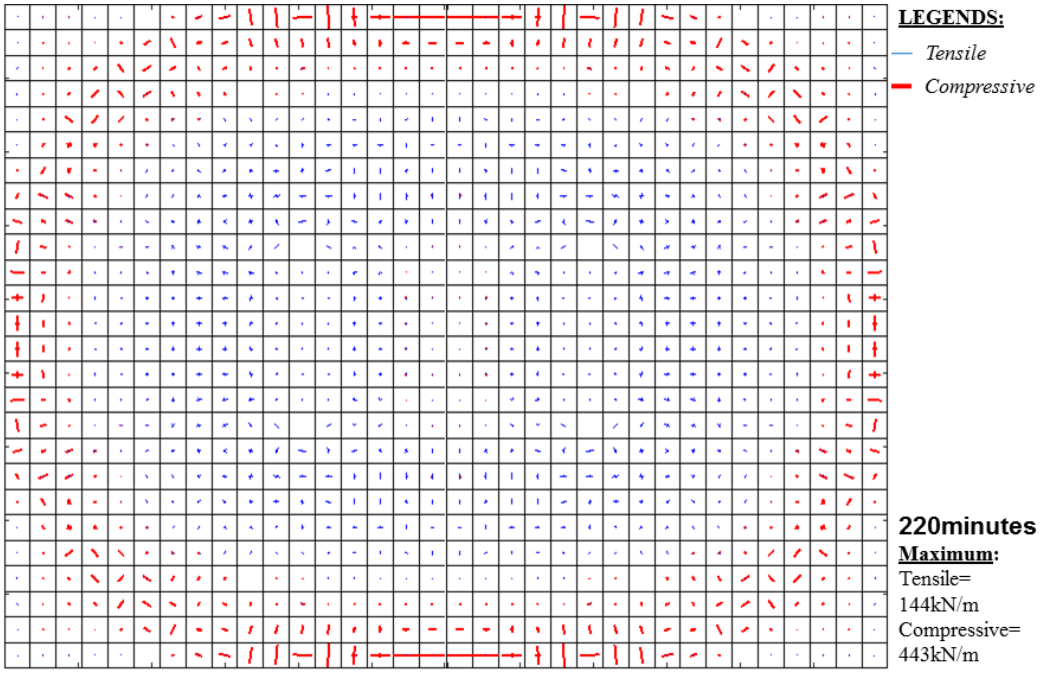

Figure 5.46: Principal membrane forces at 220 minutes of fire exposure for slab tested by Zhang et al. (2014)

5.4.2.5 Summary

Aspect of validating finite element model against experimental results for the case of the slab tested by Zhang et al. (2014) is presented in the current section. Influence of varying the input mechanical properties to the predicted mid-span deflection is presented. In addition, structural performance of the slab under exposure to fire from below is presented and discussed.

Table 5.10 shows summary of structural fire resistance rating for the slab under consideration. The slab heated to *Case 2 Temperature* was found to be more representative of the slab tested by Zhang et al. (2014), with the slab satisfying fire resistance rating specified by both Eurocode 2 (CEN, 2004) and International Building Code (International Code Council, 2009), respectively. Note that slab heated to *Case 2 Temperature* was assumed as more representative to the tested slab due to both predictions of temperature and mid-span deflection matching the test results reported by (Zhang et al., 2014) reasonably well. If tensile strain in reinforcing steels of 2% was

set as the performance indicator, both models from *Case 1 Temperature* and *Case 2 Temperature* satisfy the criteria up to 220 minutes of fire exposure.

Findings from modelling the current slab suggests that fire resistance rating recommended by both Eurocode 2 (CEN, 2004) and International Building Code (International Code Council, 2009) are conservative with regard to structural response of the slab under exposure to ISO 834 (ISO, 1999) fire from below.

Table 5.10: Summary of structural fire resistance rating for slab tested by Zhang et al. (2014)

Fire resistance criterion	*L/20* (BSI, 1987)	Tensile strain in reinforcing steels: 2% (Wang et al., 2013b)	Eurocode 2 (CEN, 2004)	International Building Code (International Code Council, 2009)
Test	175 mins	-	90 mins	90 mins
Case 1 Temperature	37 mins	> 220 mins		
Case 2 Temperature	137 mins	> 220 mins		

5.4.3 Slab 3

5.4.3.1 Base case analysis

In contrast to the previously modelled slabs, the slab presented in this section is unique in a sense that it was loaded in both out-plane and in-plane. The selected candidate, S4 as described by Wang et al. (2016) represents a slab with superimposed (out-plane) load of 2 kPa and an in-plane uniaxial load of 2 MPa. In the test, the in-plane load was applied to a pre-determined value, which was 2 MPa in this case and thereafter the load was kept constant during the fire test (Wang et al., 2016). In addition, the slab behaviour during cooling stage was also reported.

In the FE model, both out-plane and in-plane load were introduced in a separate step from the temperature load step. Both mechanical out-plane and in-plane load were introduced in the first step and the load were kept constant for the following steps. In the steps that follow, temperatures were introduced into the slab. Using similar strategy

for modelling the previous slabs, two (2) temperature load cases were defined namely *Case 1 Temperature* and *Case 2 Temperature*.

No premature termination of analysis was found for modelling the current slab here. Maximum plastic strain at the surface unexposed to fire calculated for *Case 1 Temperature* and *Case 2 Temperature* model were 1.70% and 1.28%, respectively. Note that, it was found previously for modelling Slab 1 and Slab 2 that the premature termination of analysis occurred when longitudinal plastic strain at the unexposed surface reached 1.62% to 1.70%. A slightly contradicting result was found in the current section where no premature termination of analysis occurred for base case model, heated to *Case 1 Temperature* although the concrete plastic strain has reached 1.70%. Since the value was very close to values reported for the previous results from modelling Slab 1 and Slab 2, it is unfair to claim that no numerical instability problems occurred at all for the current slab even though no termination of analysis occurred.

In addition, it is noteworthy that the slab presented here has been intentionally designed with high reinforcement ratio (Wang et al., 2016). Within the experimental scope performed by the authors, higher reinforcement ratio than the required amount of reinforcement, designed in accordance to Chinese design standard was provided for the current slab. In this regard, the recommended amount of reinforcement was reported as 251 mm^2/m in each direction but the provided reinforcement for the slab under consideration (referred as S4 in Wang et al. (2016)) was 502 mm^2/m, which is

twice the required reinforcement designed following Chinese design standard recommendation.

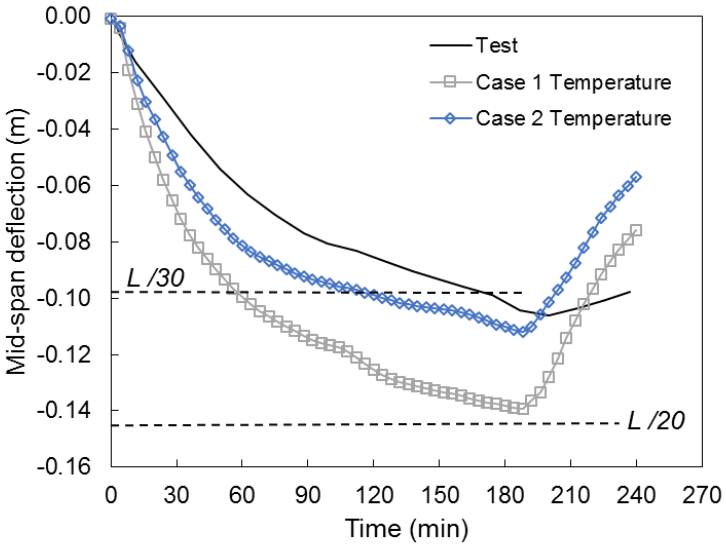

Figure 5.47: Comparison of mid-span deflection between model prediction and test results (Wang et al., 2016)

5.4.3.2 Sensitivity analysis

For the purpose of sensitivity studies looking at the influence of input mechanical parameters (as shown in Figure 5.48), simulation was carried out until 240 minutes of fire exposure only. Note that the test results reported by Wang et al. (2016) presents results of up to 400 minutes of fire test (heating-cooling cycle). Rationale of this decision is due to preliminary investigation, which indicated that the developed finite element model was not able to capture the deflection trend measured in the test during cooling stage. Therefore, it was decided to only model the slab up to 240 minutes only, which include 180 minutes of heating plus 60 minutes of cooling. Note that 60 minutes of cooling period was still considered in the analysis.

Figure 5.48(b) and Figure 5.48(e) demonstrate the differences in deformation behaviour during fire decaying stage when different thermal expansion properties were defined in the model. In contrast to varying concrete tensile strength (F_t) and fracture

energy (G_f), varying thermal expansion properties affect the deformation behaviour during cooling stage significantly.

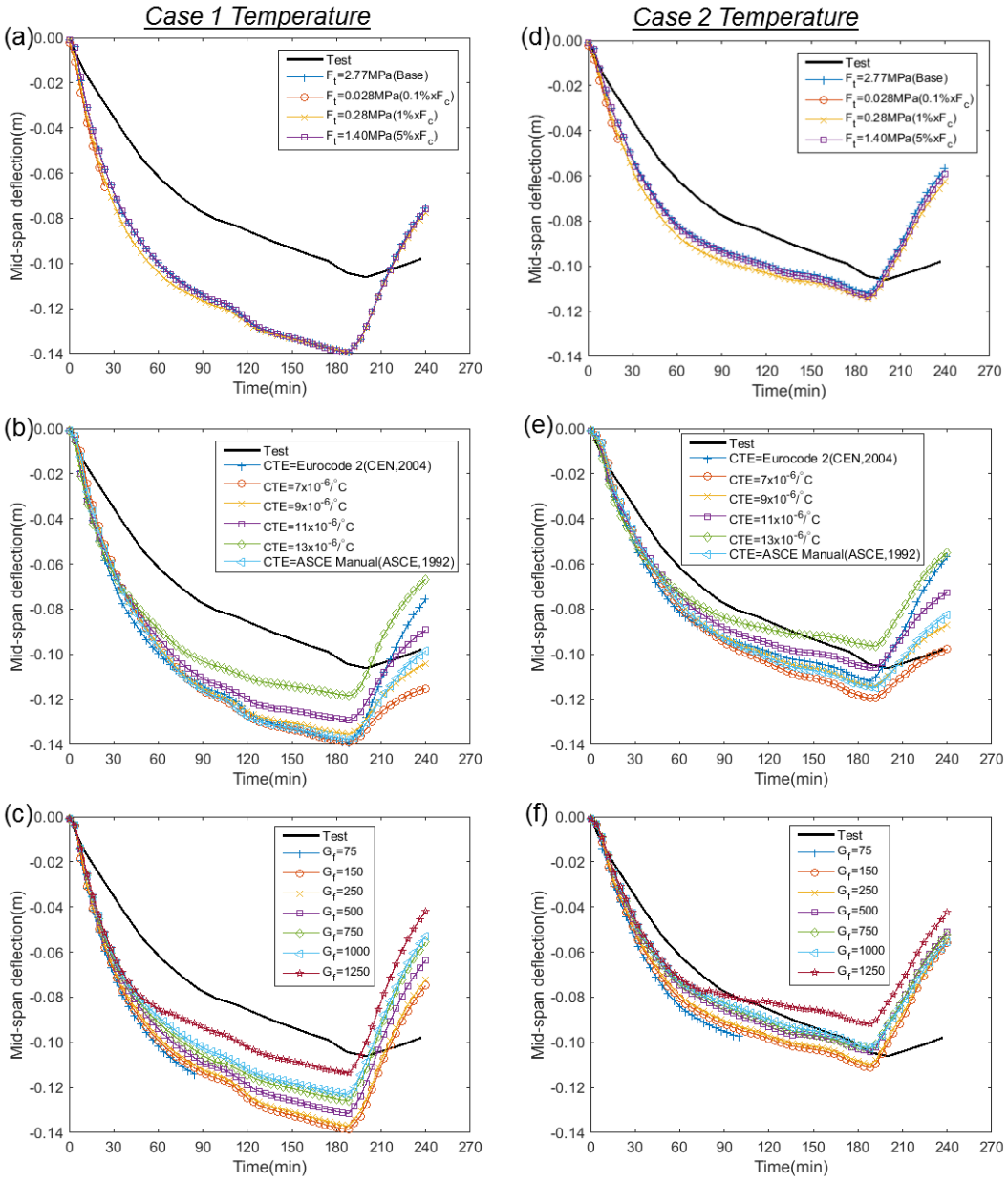

Figure 5.48: Mid-span deflection predicted with various input parameters for '*Case 1 Temperature*': (a) concrete tensile strength, F_t, (b) coefficient of thermal expansion, (c) fracture energy, G_f and for '*Case 2 Temperature*': (d) concrete tensile strength, F_t, (e) coefficient of thermal expansion, and (f) fracture energy, G_f for slab tested by Wang et al. (2016)

To accurately capture expansion behaviour of concrete during heating-cooling cycle within the context of finite element modelling, it is crucial to understand the irrecoverable expansion of concrete after the concrete is heated for the first time. Transient creep strain is described by Anderberg and Thelandersson (1976) as irrecoverable and occurs only under the first heating. By definition, transient creep strain is the net strain component between a sample loaded under steady state test and transient test. For steady state test, samples are heated to specified temperatures and then loaded. Load is increased while temperatures are kept constant. In contrast, for transient test, the samples are loaded to a specified magnitude and then exposed to heating. The load is kept constant throughout the heating period.

Formulation of concrete material model in accordance to Eurocode 2 (CEN, 2004) has implicitly considered this transient creep strain. Although included implicitly, results presented in this section demonstrate that mid-span deflections during cooling stage diverged from the trend reported from test results (Wang et al., 2016). Stress-temperature paths in structural elements are complex and these paths induce different effects in terms of transient creep strain (Gernay, 2012). Gernay (2012) claims that implicit transient creep strain concept only produce reliable predictions for simple cases, when temperature increases and stress are constant, a situation which is not common even for simple element during heating only. This will be even worse for response prediction during cooling stage. Presented mid-span deflections in this section seem to align with the idea put forward by Gernay (2012). Note that the slab modelled in this section were loaded both out-plane and in-plane, prior to being subjected to complex mechanical stresses.

The behaviour described above further highlights the complexities in understanding deformation behaviour of reinforced concrete slabs under fire exposures. It also explains why research on characterising strain behaviour of concrete materials is a topic of research interest within the structural fire engineering community. This has been explained and discussed previously in Chapter 2. Even though it is acknowledged that this aspect is very important in predicting the structural behaviour of fire exposed concrete elements, current research in hand will not attempt to further investigate this

behaviour. The mid-span deflection plots during fire decaying stage are shown simply for comparison with the test results only as the deflection behaviour during cooling stage was reported by Wang et al. (2016) in their paper.

In general, all models developed for *Case 2 Temperature* predicts mid-span deflection reasonably well in comparison to the reported results from the test. This applies to both magnitude and trend. Slab deflects rapidly during the early stage of heating and this behaviour is due to thermal bowing. After certain period of time, the rate of deflection seems to reduce and slabs deflect relatively less in terms of rate of deflection. Gernay (2012) describes two-way slabs deflect in three (3) phases. First phase demonstrates slabs deflect rapidly as a result of thermal bowing and in the second stage, slabs will deflect gradually when temperatures have penetrated into the slab's depth and the effect of temperature non-linearity became less significant. Third phase will occur when the slabs deflect vertically in a rapid manner again due to steel rebar beginning to significantly lose its strength.

From a different perspective, the gradual deflection (described as second phase above) occurs due to the slab mobilising tensile membrane action. A compressive ring surrounds formation of tensile net at central of the slab, which preserve the structural integrity of the slab. At central area of the slab where the tensile net formed, concrete does not provide significant contribution to the slab's integrity due to very low tensile strength in it. Tensile strength is provided by steel reinforcement. This explains why, as soon as strength in steel rebar degrades significantly and is not enough to provide load bearing capacity for the slab, the slab will deflect vertically in a rapid manner again (described as phase three by Gernay (2012)).

5.4.3.3 Definition of damage parameters

Simulation of full 400 minutes of fire test was also conducted for a limited number of cases, for the sake of comparison and validation only. Both slabs loaded (temperature load) with *Case 1 Temperature* and *Case 2 Temperature* were modelled. The predicted mid-span deflections are shown in Figure 5.50, while Figure 5.51 shows the predicted

temperatures in the reinforcing steel from both *Case 1 Temperature* and *Case 2 Temperature* plotted together with the temperatures reported from Wang et al. (2016).

Concrete Damage Plasticity (CDM) model available in ABAQUS (ABAQUS, 2012) and adopted in the current study offers modelling concrete behaviour that captures both plasticity and damage behaviour of concrete during loading and unloading. This behaviour is important in particular for modelling concrete elements under cyclic loading. Damage is represented by a scalar in the range of 0 to 1. Tensile damage and compressive damage are denoted as d_t and d_c, respectively (ABAQUS, 2012). Stiffness is degrading at 100% during unloading whenever scalar is defined as 1 while full stiffness recovery is defined whenever damage scalar is defined as 0 (ABAQUS, 2012). Stiffness degradation is idealised with the reduction of elastic modulus upon reloading of the concrete elements.

Implementation of the damage parameters within finite element is not straightforward. It is indeed a field of research by itself. Lubliner et al. (1989), among the pioneers in this field introduced a relatively simple approach where this damage parameter is introduced only in the softening branch of the stress-strain curve. While it is possible to also introduce this damage parameter in the strain hardening branch within the stress-strain curve, it is worth to mention that the computational resources required are tremendous, in addition to the difficulties in the analysis to obtain a converged solution during solving the stiffness matrix.

Moreover, solving the analysis within finite element analysis even with damage parameter introduced during the strain softening branch is already difficult, given the highly nonlinear problems of concrete behaviour at elevated temperatures. This will be further discussed in the following paragraph with reference to mid-span deflections predicted with and without damage parameters (shown in Figure 5.50). Specifically, in the prediction for mid-span deflection presented here, models are developed considering both with and without damage parameters entered to study whether this has any influence to the predicted response.

Damage parameters proposed by Lubliner et al. (1989) were adopted for calculating the scalar damage in compression (d_c) and the typical stress-strain curve produced at 20 °C is presented in Figure 5.49. Note that in the figure, linear descending branch was defined. No damage was found in the concrete at peak strength, and the damage reduced linearly until 0.99 (only 1% stiffness left) at failure strain. The damage parameter at failure strain was approximated from Lubliner et al. (1989) and is not necessarily the same for stress-strain concrete at other temperatures. The selected values are such that no negative values and/or decreasing plastic strain occur during conversion from crushing/cracking to plastic strain (ABAQUS, 2012), an aspect which is built-in in ABAQUS (ABAQUS, 2012).

For modelling tensile behaviour, damage parameter, d_t was simply defined as 0.5 at failure strain for concrete behaviour both at ambient and elevated temperatures. Within the context of modelling current slab (i.e. (Wang et al., 2016)), higher values are possible. However, the numerical stability issues were too severe and therefore a value of 0.5 (50% stiffness degradation) was simply adopted throughout. Note that a unique tensile damage parameter, d_t of 0.5 for the concrete tensile behaviour at different temperatures is possible in the current model and the condition stated previously i.e. no decreasing plastic strain during conversion from crushing/cracking to plastic strain (ABAQUS, 2012) was satisfied.

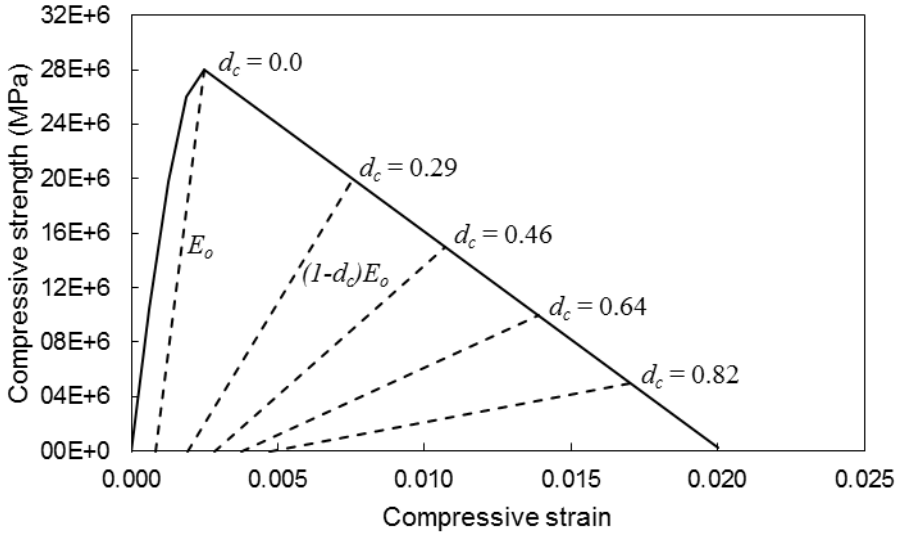

Figure 5.49: Typical stress-strain curve for concrete at ambient temperature conditions under compression with damage parameter inputted

Model developed with and without damage parameters entered produced mid-span deflection with extremely minimal differences. In other words, defining damage parameters did not influence the prediction for mid-span deflection, at least during heating stage. However, it must be also emphasized here that the damage parameters were only defined during strain softening for concrete in compression. The prediction is potentially different if the damage parameter was defined within strain hardening branch (region between the end of elastic strain and peak strain). With the exception of the model discussed here, all other models presented in this thesis were developed without damage parameters defined. It was hypothesized earlier that this would not affect the response prediction (or specifically mid-span deflection), which was proven here in the current section. Moreover, most FE models presented in other chapters of this thesis are only developed for heating stage only.

Referring to Figure 5.50, prediction of mid-span deflection during heating stage matches reasonably well with the test result especially for *Case 2 Temperature*. Both predictions from *Case 1 Temperature* and *Case 2 Temperature* produced trends of mid-span deflection that agree reasonably well with the test results. Unfortunately, deflection recovery during cooling stage was excessively predicted for both

temperature load cases. For this particular model, facture energy was defined as 750 N/m. Although the value is quite high, it was necessary due to numerical instability in addition to the long period required for each of the simulation to complete. Note that total duration of heating-cooling cycle in the model was 400 minutes (24000 s) with maximum time step size limited to 30 seconds for accuracy.

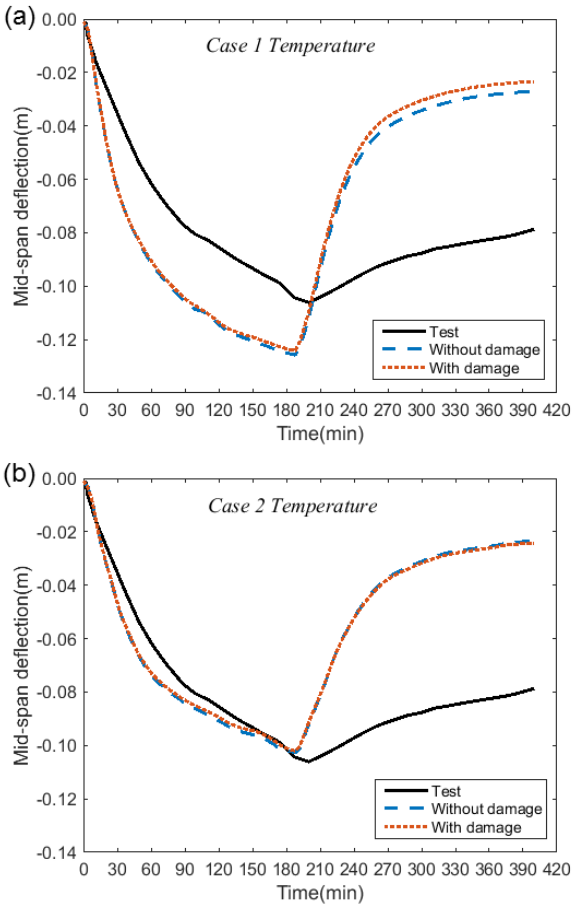

Figure 5.50: Predicted mid-span deflection with and without damage parameter defined for (a) *Case 1 Temperature* and (b) *Case 2 Temperature*

Solid line and dotted line in plot shown in Figure 5.51 represent bottom rebar temperatures for the slab loaded with *Case 1 Temperature* and *Case 2 Temperature*, respectively. Other curves with markers (6 of them) represent measured and reported rebar temperatures (Wang et al., 2016) recorded at different locations on the slab's plan. From all the curves shown, predicted and measured reinforcement temperatures were found to be in a reasonably good agreement. From *Case 1 Temperature* analysis,

maximum difference between predicted reinforcing steel temperatures and average measured reinforcing steel temperatures was 65 °C throughout 180 minutes of heating time while only 25 °C was found for heat transfer analysis in *Case 2 Temperature*.

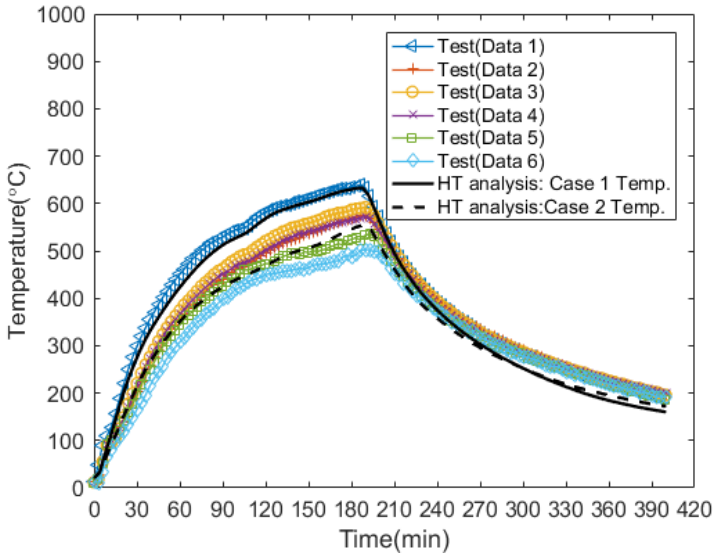

Figure 5.51: Predicted temperature in rebar compared with the measured temperatures (Wang et al., 2016)

Reinforcing steel temperatures predicted from *Case 2 Temperature* match with the test results best. This confirms that prediction of temperature within the slab's depth using Eurocode 2 (CEN, 2004) material thermal properties is sufficient to perform heat transfer analysis for concrete elements. It also further indicates that the challenges in performing heat transfer analysis for furnace testing of concrete elements lie in defining boundary interface where concrete exposed surface interact with fire environment and/or ambient (Maluk, 2014). Note that the difference between *Case 1 Temperature* and *Case 2 Temperature* is the manner in which temperature at the exposed surface is calculated.

The main issue in modelling concrete material behaviour during cooling stage is the consideration on whether concrete recovers its strength and stiffness when temperature decreases or there is no strength recovery at all. For steel, strength and stiffness are recovered as soon as temperature decreases completely or partially depending on type

of steel and the maximum reached temperatures (Kirby et al., 1986). Similar phenomena however is not happening for concrete. Concrete not only doesn't recover its strength during cooling, but there is also additional loss of strength during cooling from maximum temperature to ambient temperature (Li and Franssen, 2011). Eurocode 4 (CEN, 2005) provides recommendation on treating the degradation of concrete material model during cooling stage. Concrete is assumed to have with some residual strength, meaning some of the initial strength is not recovered after it was heated to a certain temperature and cooled down.

Defining the behaviour mentioned above into ABAQUS (ABAQUS, 2012) requires special input procedures where sub-routine needs to be specified. However, this is beyond the scope of the current investigation. Scope of work in this thesis will not attempt to explore the residual behaviour of concrete material upon heating-cooling cycle. It is worth to mention that residual strength of concrete upon heating-cooling cycle is a field of research by itself, therefore requiring a long section dedicated for discussion of the topic.

5.4.3.4 Plastic strain in concrete and reinforcement

Similar model presented in the previous Section 5.4.3.3 was selected here for showing the state of plastic strain in both concrete and reinforcing steels. The slab was heated to *Case 2 Temperature* and fracture energy was defined as 750 N/m.

To further understand the behaviour of the slabs under exposure to ISO 834 (ISO, 1999) fire, contour plots for plastic strain in concrete section at fire exposed and unexposed surface are shown in Figure 5.52, Figure 5.53, Figure 5.54, and Figure 5.55. Plastic strains in exposed surface for longitudinal and transverse direction are presented in Figure 5.52 and Figure 5.53 respectively. Figure 5.54 presents longitudinal plastic strain in concrete section at top (unexposed surface) while Figure 5.55 shows the plastic strain in concrete section at unexposed surface along transverse direction. In the plots, the selected duration of exposure for showing the state of plastic strain are 30 minutes, 60 minutes, 120 minutes, and 180 minutes. In general, plastic strain in bottom section of the concrete, both along X and Y axis are in the state of

compression. On the other hand, a combination of tensile and compressive plastic strains are found in the top section of the concrete. Note that, uniaxial in-plane load was defined in West-East direction of the slab's plan view. Maximum tensile plastic strain and compressive plastic strain were predicted as 1.94% and 0.61% respectively, throughout 180 minutes of heating period.

Figure 5.56 shows the photo taken when the test finished and sample was lifted from the furnace. Top view i.e. unexposed surface and bottom view i.e. fire exposed surface are shown in Figure 5.56(a) and Figure 5.56(b), respectively. Wang et al. (2016) reported that cracks were found parallel to the direction of applied in-plane load. They state that the development of mechanical strain parallel to the lateral restraint has caused additional tensile strain developed perpendicular to the lateral in-plane load. This behaviour is also due to the effect of passion ratio (Wang et al., 2016).

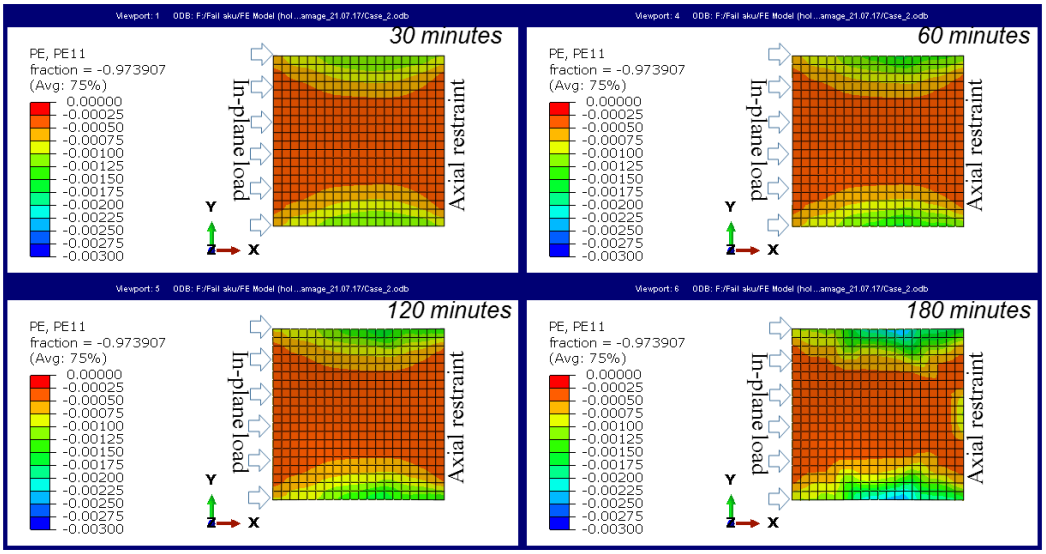

Figure 5.52: Plastic strain in X-direction at bottom section of concrete (fire exposed surface) at 30 minutes, 60 minutes, 120 minutes, and 180 minutes of exposure for slab tested by Wang et al. (2016)

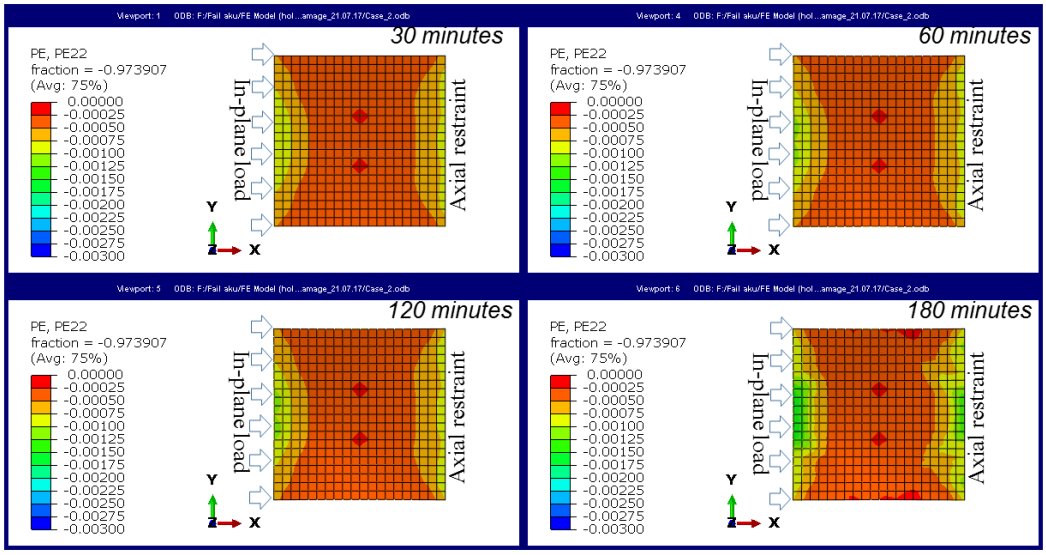

Figure 5.53: Plastic strain in Y-direction at bottom section of concrete (fire exposed surface) at 30 minutes, 60 minutes, 120 minutes, and 180 minutes of exposure for slab tested by Wang et al. (2016)

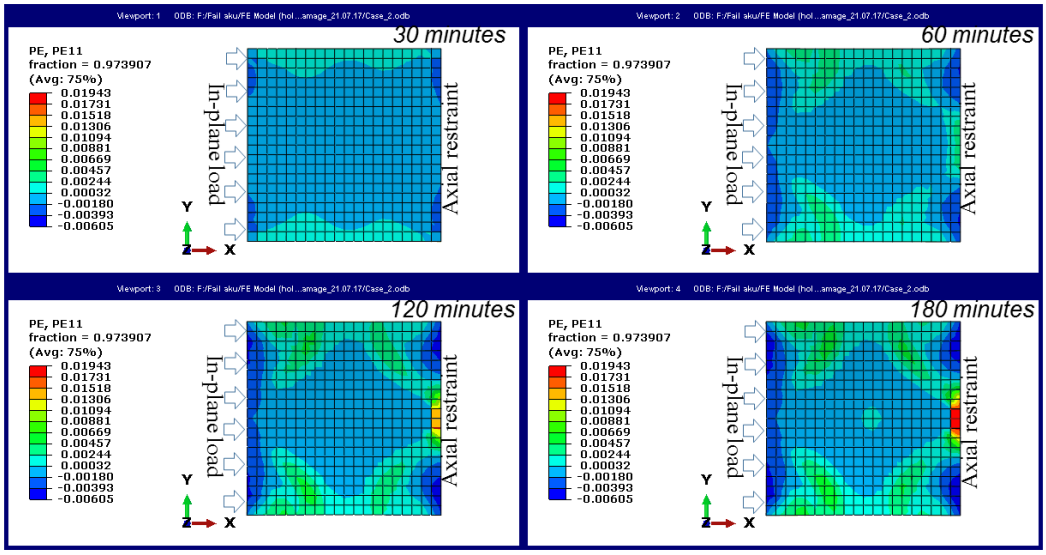

Figure 5.54: Plastic strain in X-direction at top section of concrete (surface unexposed to fire) at 30 minutes, 60 minutes, 120 minutes, and 180 minutes of exposure for slab tested by Wang et al. (2016)

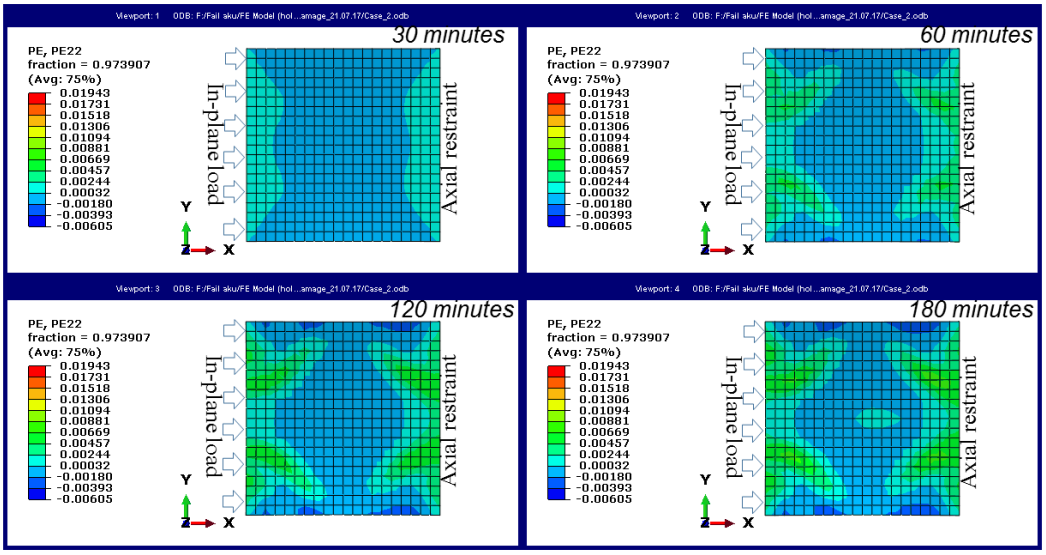

Figure 5.55: Plastic strain in Y-direction at top section of concrete (surface unexposed to fire) at 30 minutes, 60 minutes, 120 minutes, and 180 minutes of exposure for slab tested by Wang et al. (2016)

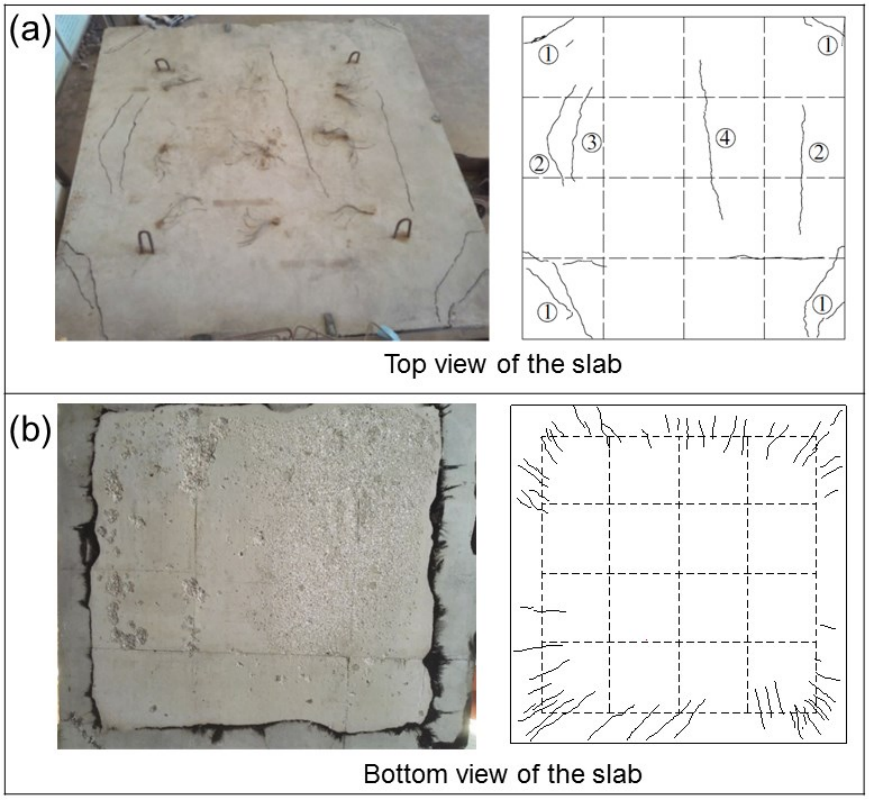

Figure 5.56: (a) Top view of slab and (b) bottom view of slab after the fire test reproduced from Wang et al. (2016)

Evolutions of plastic strain with time in reinforcing steels in elements along centre line of the slab are presented in Figure 5.57 and Figure 5.58 below. Figure 5.57 shows the plastic strain in longitudinal steel, spanning along horizontal axis (X-axis) while Figure 5.58 shows the plastic strain in transverse steel, spanning along vertical axis (Y-axis) of the slab. Interestingly, transverse steels demonstrate higher plastic strain than the reinforcing steels spanning along longitudinal direction. Note that, the uniaxial in-plane load was introduced in longitudinal (West-East) direction of the slab's plan view. The predicted strains are mostly in tension, with central of the slabs demonstrating the highest plastic strain value, predicted as 0.2%.

These findings align with the reported test results where it was reported that cracks were parallel to the applied in-plane load and suggested that tensile strain perpendicular to the lateral restraint (in-plane load) caused these cracks opening. In

the test, the authors (Wang et al., 2016) claim that no cracks ran for the full depth of the slab's specimen. This was believed to be due to relatively higher reinforcement ratio provided. The slab was designed in accordance to Chinese design standard. Other slab specimens were designed and casted with reinforcement of 251 mm^2/m width of the slabs in each direction while for the current slab under consideration, the provided reinforcement was 502 mm^2/m in each direction. The high reinforcement ratio provided was intentionally to investigate the influence of ratio of reinforcement to structural fire performance of the slabs.

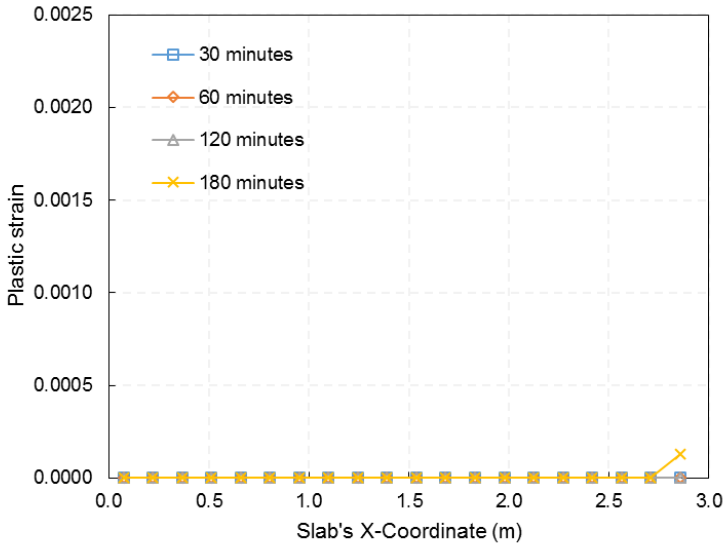

Figure 5.57: Evolution of plastic strain with time in bottom longitudinal (spanning along X-axis) reinforcing steels near centre of the slab predicted for slab tested by Wang et al. (2016)

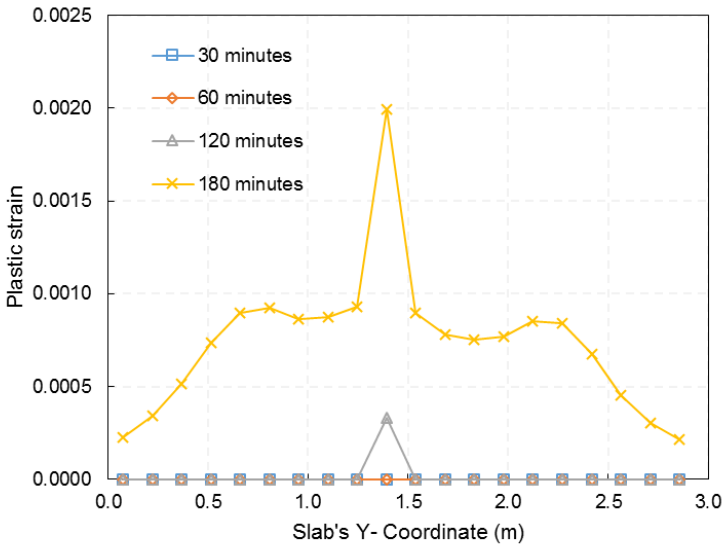

Figure 5.58: Evolution of plastic strain with time in bottom transverse (spanning along Y-axis) reinforcing steels near centre of the slab predicted for slab tested by Wang et al. (2016)

5.4.3.5 Tensile membrane action

Principal membrane traction in slabs at 15 mins, 120 mins, and 180 mins of fire exposure are shown in Figure 5.59, Figure 5.60, and Figure 5.61, respectively to better demonstrate the state of membrane forces in the slabs. The location where the imposed in-plane load of 2 MPa was applied, and the defined axial restraint at slab edges opposite to the in-plane load are also shown in the figure. Using similar model for showing the state of plastic strain presented previously in Section 5.4.3.4, the slab heated to *Case 2 Temperature* was chosen here to demonstrate the state of membrane forces in the slab.

Formation of tensile membrane action was evident as early as 15 minutes of fire exposure. This can be seen in Figure 5.59 below. In the figure, formation of tensile net at the slab's centre shifted slightly towards the axial restraint support, meaning it was moving away from the edge where in-plane load was applied. This behaviour happened due to the manner in which the test was performed and the model was developed and boundary condition was defined. Note that at the location where slab

was restrained axially (at East part, based on plan view of the slab), zero axial movement is allowed (in FE model) whereas at the location where the in-plane load was applied, axial displacement was allowed. This is believed to play a role with regard to the formation of membrane traction in the slab as shown in Figure 5.59.

In the test, at East part of the slab, reaction beam was installed at the edge to provide restraint condition to the slab and from the in-plane load induced at the edge opposite to it (Wang et al., 2016). This reaction beam provides restraint in one way only, meaning it restrained the slab from displacing axially away from slab's centre. In other words, it restrained the slab against the in-plane load. Axial movement towards the slab centre (or inward movement) was allowed, a condition that is contrary to the finite element condition. The set-up of the loading frame is reproduced from Wang et al. (2016) and shown previously in Figure 5.4 in Section 5.2.3.

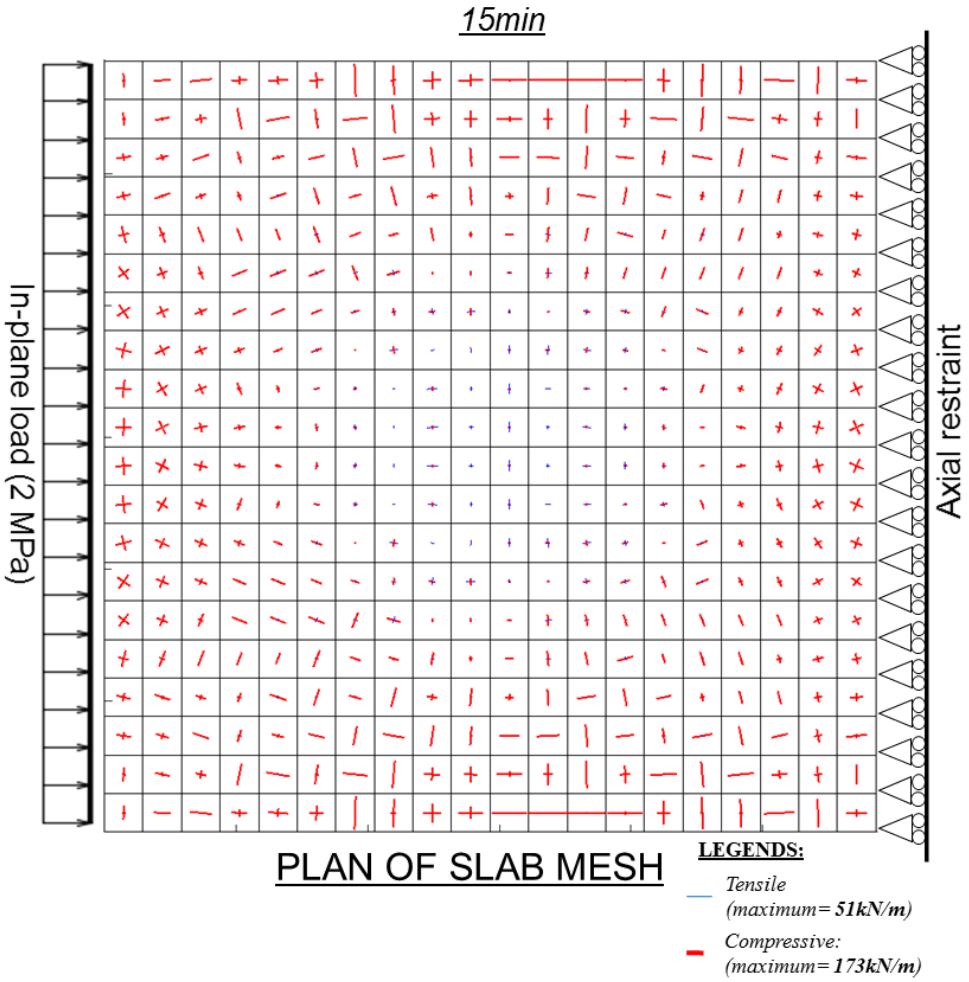

Figure 5.59: Principal membrane forces at 15 minutes of fire exposure for slab tested by Wang et al. (2016)

At the end of heating time i.e. 180 mins, the calculated reinforcing stresses in an element near central of the slab are 89 MPa and 179 MPa for reinforcement spanning along X-axis and Y-axis, respectively. Note that, the in-plane force was applied parallel to X-axis. This implies that reinforcing steels perpendicular to the application of in-plane load is more critical than the steel parallel to the application of in-plane load. Temperature at this point of time in the reinforcing steel was predicted as 546 °C, applicable to both X and Y-direction of the slab. The formulation of steel material model defined in the model provides steel strength of 303 MPa when heated to 546 °C. Therefore, 29% of ultimate strength and 59% of ultimate strength have been

utilised for steel parallel and perpendicular to the application in-plane load, respectively.

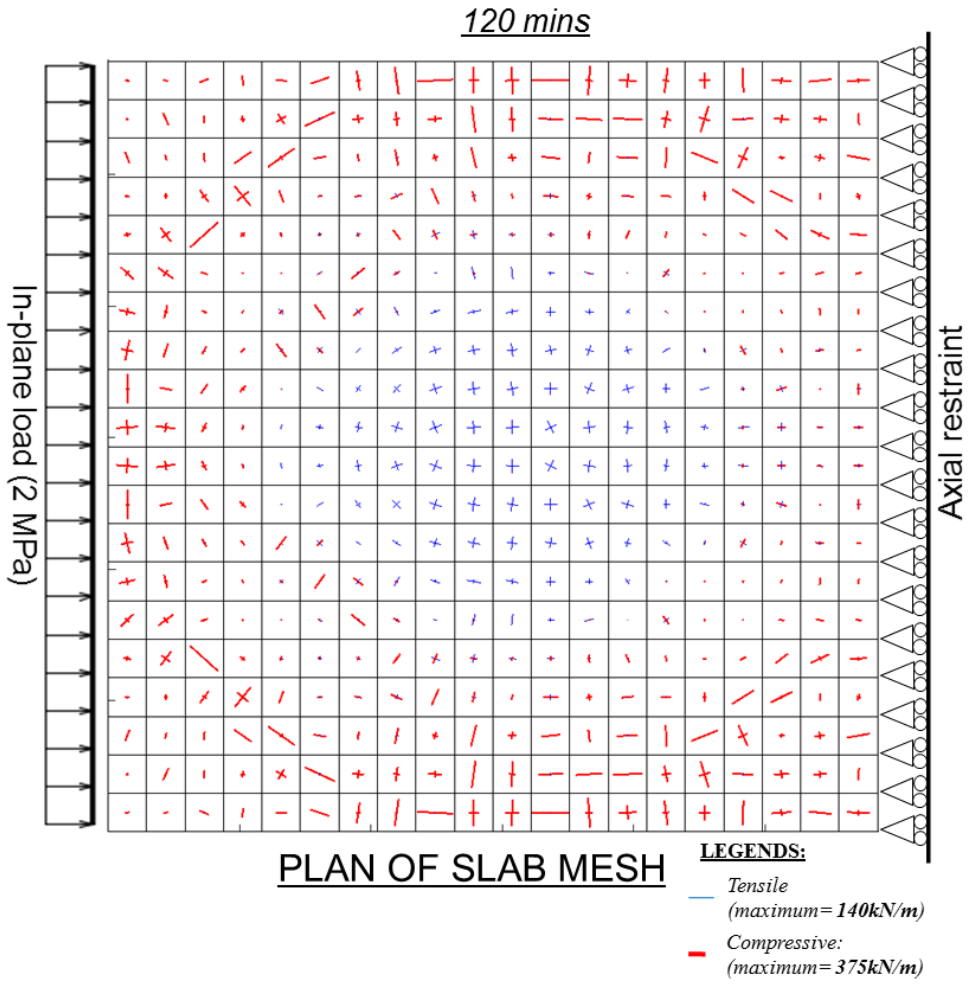

Figure 5.60: Principal membrane forces at 120 minutes of fire exposure for slab tested by Wang et al. (2016)

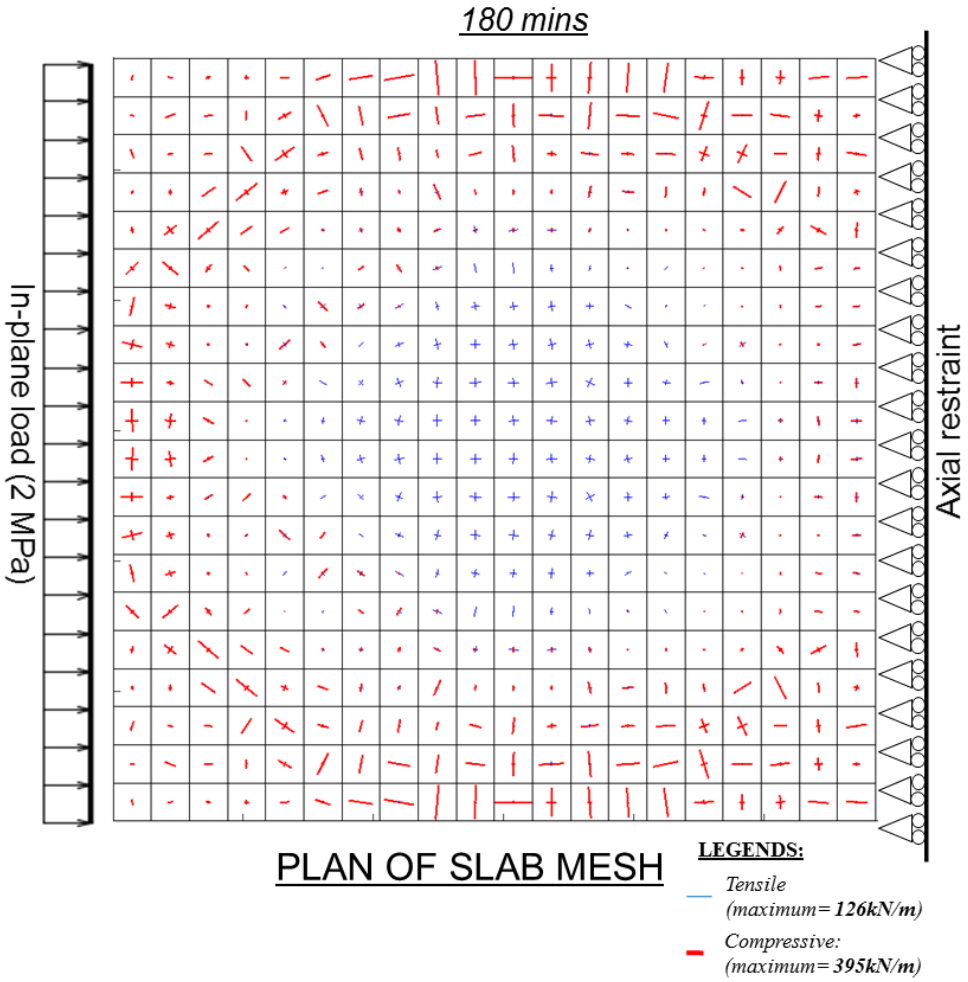

Figure 5.61: Principal membrane forces at 180 minutes of fire exposure for slab tested by Wang et al. (2016)

5.4.3.6 Summary

Table 5.11 provides summary of structural fire resistance rating for the slab under consideration. With slab S4 Wang et al. (2016) selected for the study, the lack of comprehensive understanding in specifying fire resistance rating for two-way slabs under exposure to fire from below is further highlighted. With relatively higher reinforcement ratio as compared to other specimens in the testing scheme (Wang et al., 2016), it might explain why the slab has excellent fire performance where more than 180 minutes of fire performance was predicted when $L/20$ (BSI, 1987) and limiting steel tensile strain of 2% (Wang et al., 2013b) are used as the indicator. On

the other hand, only 90 minutes and 60 minutes were specified when geometrical configuration of the slab follows recommendation from Eurocode 2 (CEN, 2004) and International Building Code (International Code Council, 2009), respectively. Holistic understanding on the realistic behaviour of two-way reinforced concrete slabs under exposure to fire is required to provide better fire resistance rating for these kinds of slabs.

Table 5.11: Summary of structural fire resistance rating for slab tested by Wang et al. (2016)

Fire resistance criterion	*L/20* (BSI, 1987)	Tensile strain in reinforcing steels: 2% (Wang et al., 2013b)	Eurocode 2 (CEN, 2004)	International Building Code (International Code Council, 2009)
Test	> 180 mins	-	90 mins	60 mins
Case 1 Temperature	> 180 mins	> 180 mins		
Case 2 Temperature	> 180 mins	> 180 mins		

5.5 Overall summary and conclusions

Finite element models of two-way reinforced concrete slabs exposed to fires have been presented in the current chapter. Three (3) tests on two-way reinforced concrete slabs exposed to (nominal) ISO 834 (ISO, 1999) fires were selected for assessment of the finite element modelling capability, when modelled applying the Eurocode 2 (CEN, 2004) material models for concrete and reinforcing steel in an attempt to validate the models against experimental results. Further to this, the sensitivity of the predictive performance of the finite element models to various input mechanical material properties was examined. Several conclusions can be drawn on this basis:

- The accuracy of input temperatures is crucial for agreement between finite element models and experimental results. Defining an accurate boundary condition at the surface interacting with air and/or the fire environment is the most challenging aspect in performing a heat transfer analysis for concrete slabs tested in furnace. Due to this, one has to be certain on the actual heating condition during experiments for instance; (1) proper measurement and recording of gas temperatures, (2) whether furnace dimension and wall lining has any potential influence to the heat transfer process (3) actual and exact location of thermocouples that is claimed to be at the 'fire exposed' surface. Correctly identifying the abovementioned factors will determine whether beneficial comparison can be made between heat transfer analysis results and measured temperatures.
- In line with the above, accurately placing and reporting thermocouple locations within a concrete slab's depth is crucial for accurate model/test comparisons, particularly at locations closer to the heat face where thermal gradients are steepest, and especially during the first 60 minutes of fire exposure.
- Predicting deformation behaviour of concrete slabs exposed to severe heating from below during cooling stage remains a challenge from a numerical modelling perspective. Better understanding, which are currently lacking on two aspects; (1) concrete strength and stiffness degradation and recovery, and (2) complex strain behaviour; expansion and contraction (both thermal and mechanical) are crucial for credible prediction of response for concrete slabs during heating-cooling cycle.

- The results in this chapter concur with previous research suggesting that reinforcing steels along longer spans are more stressed during exposure to fire as compared with shorter spans, as is typical for design at ambient temperatures. As such, cracks typically propagate along the shorter span.
- From finite element models presented in this chapter, along with comparison with the test results, it is suggested that for two-way reinforced concrete slabs exposed to fire from below, critical location for concrete cracks is at the top surface of the slabs (unexposed surface). Results from the study demonstrate that relatively higher plastic strain occur at slab's top surface, with the absence of top reinforcing steels. This indicates that provision of top reinforcing steels might be beneficial for the design of simply supported rectangular slab exposed to fires.
- From investigation in this chapter, it was found that excessive strain in reinforcing steels can be used as an indicator of the slabs structural performance under exposure to fires. From the three slab models, Slab 1 shows runaway type of deflection, triggered during 158 minutes of exposure with plastic strain in the reinforcing steels predicted as 1.82%. No sign of runaway deflection for the other two slabs were evident, with maximum plastic strain in reinforcing steels at the end of heating time predicted as 0.14% (during 220 minutes of exposure) and 0.2% (during 180 minutes of exposure) for Slab 2 and Slab 3, respectively. However, it is also acknowledged that more experimental results, which are unfortunately lacking within literature are required for validation.
- Previous studies by Wang et al. (2013b) stated that 2% reinforcing steel mechanical strain is critical. With plastic strain of 1.82% found to be critical in the current study, it is therefore suggested that limiting mechanical strain of 2% can be used as an indicator on the slab's performance when heated from below.

Chapter 6:

Parametric studies on two-way reinforced concrete slabs exposed to severe heating from below

6.1 Introduction

Chapter 3 and Chapter 4 have presented aspect of finite element model and structural behaviour of one-way reinforced concrete slabs under exposure to fires. To further investigate structural behaviour of reinforced concrete slabs under exposure to fires, this chapter extends the previous investigation on one-way slabs to two-way slabs. With similar motivation, careful examination into the behaviour of two-way slabs exposed to ISO 834 (ISO, 1999) fires for three hours is presented.

Aspects of restraint conditions at supports, fire scenario, as well as geometrical configuration of the slabs i.e. span-to-depth ratio and aspect ratio are interrogated with the intention to improve understanding on the structural behaviour of the slabs under exposure to fires and provide guidance to modellers and designers.

Axial restraint at the slab boundary has a significant effect on the structural performance of fire exposed concrete slabs. However, whether the effect is beneficial or detrimental is still a matter of research and depends on a range of factors. Deeny (2010) investigated the behaviour of two-way concrete slabs exposed to ISO 834 (ISO, 1999) fires under different boundary conditions. Typical boundary conditions i.e. simple support, pinned, and fixed supports were applied in this study. The study concluded that the possible location of reinforcement rupture depends on the defined boundary condition. The critical location for reinforcement rupture for unrestrained slabs was in the top reinforcement layer at the slab centre. For slabs with both translational and rotational restraint condition at supports, the critical location is in the top layer at slab edge (Deeny, 2010).

The abovementioned studies however, did not investigate the effect of varying the degree of restraint. Actual and realistic degree of restraining forces at supports is difficult to measure as it depends on the stiffness of the surrounding elements of the concrete slabs. However, it is important to understand on how degree of restraint at supports affect the structural response (in this context it refers to the predicted mid-span deflection and mechanical strain in reinforcing steels) of two-way reinforced

concrete slabs under exposure to severe heating from below and consequently prescribing fire resistance rating for the slabs.

6.2 Description of selected slab for parametric studies

Validated finite element model of the slab described by Wang et al. (2016) is selected for parametric studies. In the test, the slab was exposed to fires from below with clear plan dimension of furnace wall of 2560×2560 mm. Slab's vertical supports were provided at 2930 mm c/c in each direction. Only bottom reinforcement was provided, spanning in both direction i.e. X and Y. 8 mm diameter reinforcing steel spaced at 100 mm c/c were provided. In addition to superimposed mechanical load of 2 kPa, uniaxial in-plane load was also introduced during the test with magnitude of 2 MPa.

However, for the purpose of parametric studies in this chapter, no initial in-plane load is considered and reinforcing steels were arranged at 200 mm in each direction. Note that, Wang et al. (2016) described in their studies that the tested slab should have had reinforcing steels arranged at 200 mm centre instead of 100 mm centre. The reinforcement was arranged at 100 mm centre (referring to specimen selected for validation presented in the previous Chapter 5 and described above) simply because they wanted to investigate the slabs performance with slightly high reinforcement ratio (Wang et al., 2016). Therefore, for the study in the current section, reinforcing steels will be defined at 200 mm centre.

For the purpose of consistency of slab configuration, and in order to suit all the design requirements for the parametric studies, some modification to the slab details are made. For simplicity, fire exposed length was assumed as 2930 mm in each span direction, even though the reported furnace wall-to-wall dimension was reported as 2560 mm (Wang et al., 2016). With slab was vertically supported at 2930 mm c/c and the manner in which the test was set up (see description in Chapter 5), it is of the author's opinion that heat transfer within slab not only occurring at 2560 mm length, but potentially larger than that. Moreover, the occurrence of in-plane heat transfer along the slab, which was not taken into consideration in the current study (thermal analysis) has made the assumption that the slab model was only exposed to 2560 mm length of fire

was not appropriate. The slab is assumed to be heated to ISO 834 (ISO, 1999) fire for three hours. It is possible to model the slabs for heating of more than three (3) hours however this was not done considering constraints on time and computational resources. High nonlinear problems involved in the current study means it takes long time for the analysis to finish for each of the cases (model) investigated. In addition, the slabs was initially designed to have 90 minutes of fire resistance in accordance to Chinese design standard.

Both top and bottom reinforcement are provided for the parametric studies. Rigid supports at slab edges requires the slab to have top reinforcement near support to resist hogging moment. Therefore, maintaining actual slab's test details and configuration (having only bottom reinforcement) would not be realistic within the context of structural design of the slab both at ambient and fire limit state. Figure 6.1 shows details of the selected slab for the parametric studies presented in the following sections. Table 6.1 and Table 6.2 summary the slab's data and slab properties for FEM input respectively.

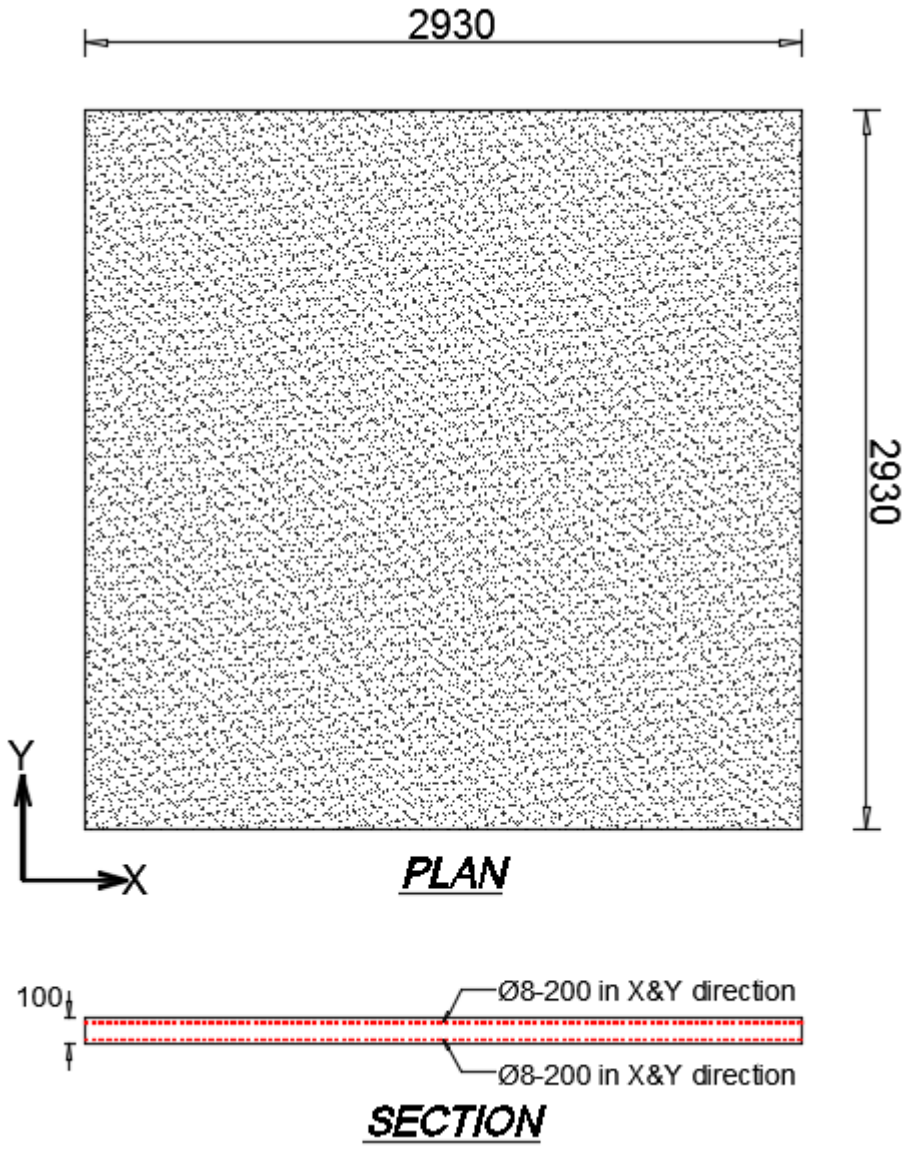

Figure 6.1: Configuration of slab for parametric studies in this chapter

Table 6.1: Slab data

Span & assumed fire exposed length (mm)	Thickness (mm)	Cover (mm)	Fire resistance rating (min)	Reinforcement (mm)	Imposed Load (kPa)
2930	100	15	90*	8Ø-200	2.0

**In accordance with Chinese design standard*

Table 6.2: Slab properties for FEM input

F_c (MPa)	F_t (MPa)	F_y (MPa)	Coefficient of thermal expansion, CTE	Aggregates
28	2.77*	475	EC2	Siliceous

** based on* $0.3F_c^{2/3}$ *(CEB-FIP, 2010)*

6.3 Finite element model

Finite element formulation details are similar to what have been adopted and presented for modelling one-way slabs in previous Chapter 3 and Chapter 4 thus they will not be repeated here. In modelling post-cracking behaviour for concrete, fracture energy of 750 N/m is assumed in the models. The selected value is assumed as appropriate judging from the extensive sensitivity studies presented previously in Chapter 5.

6.4 Criteria for assessing slab's performance

For the purpose of defining fire performance of the slabs investigated in the current chapter, two (2) criteria are adopted; (1) limiting deflection criteria of either $L/20$ or $L/30$ (BSI, 1987), whichever is relevant, and (2) critical tensile strain in reinforcing steels of 2% as presented by Wang et al. (2013). The limiting deflection criteria above are added in each deflection plot for comparison with the model predictions. Slabs structural fire resistance recommended from prescriptive design code; Eurocode 2 (CEN, 2004) as well as International Building Code (International Code Council, 2009) are also included and discussed whenever relevant.

6.5 Fire scenario

In this section, studies looking at the effect of different fire scenario to the predicted mid-span deflection of the slab is presented. Hydrocarbon fire (HCM) (CEN, 2002a), Slow heating curve (CEN, 1999), and Parametric fire curve (CEN, 2002a) were selected to provide severe heating, slow heating, and heating with cooling phase respectively. Slab exposed to ISO 834 (ISO, 1999) was also modelled and included.

In deriving the Parametric fire curve (CEN, 2004), fire compartment size was assumed as 2.93 × 2.93 × 3 m height. Fire load density related to floor area was assumed as 948 MJ/m^2, which is recommended for dwelling occupancy classes, specified in Table E.4 Eurocode 1: Actions on structures- Part 1-2: General actions- Actions on structures exposed to fires (CEN, 2002a) with medium fire growth rate. Two (2) Parametric fire curves (CEN, 2004) were defined. First case, denoted as Parametric 1 was defined to simulate faster and hotter fires while second case, which is denoted as Parametric 2, defined to simulate longer and colder fires. Total area of vertical openings are 4.50 m^2 and 2.25 m^2 for Parametric 1 and Parametric 2 respectively. All the defined fire curves are shown in Figure 6.2.

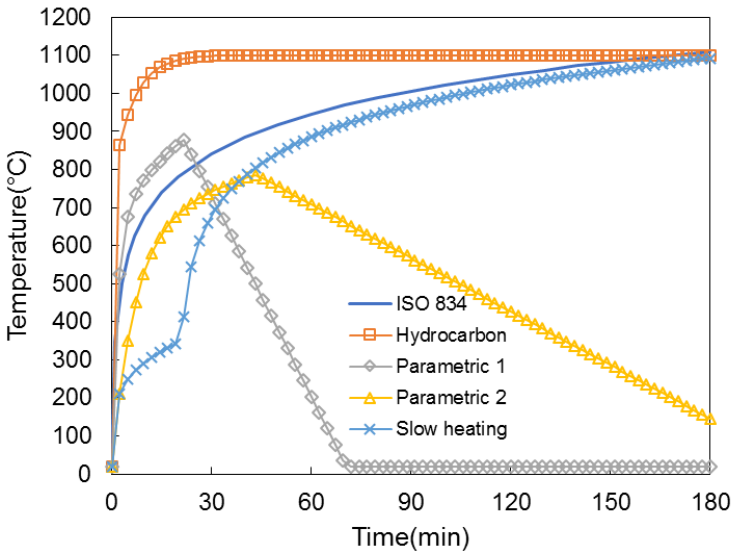

Figure 6.2: Selected design fire curve

The predicted mid-span deflections for the slabs heated with the previously simulated fire environment are shown in Figure 6.3. The slab heated to Hydrocarbon (CEN, 2004) produced the greatest mid-span deflection. This is mainly due to relatively more steep thermal gradients for the case of slab heated to Hydrocarbon (CEN, 2002a) fire as compared to slabs exposed to other fire scenario for instance ISO 834 (ISO, 1999).

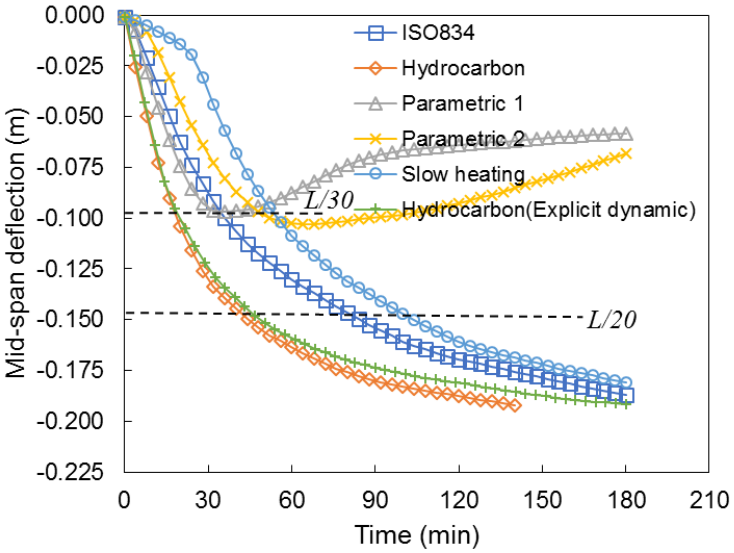

Figure 6.3: Predicted mid-span deflections for the two-way sab considered in the current chapter with different assumed design fire curves

Premature termination of analysis found for the model heated to Hydrocarbon (CEN, 2004) fires and this occurred at approximately 140 minutes of fire exposure. The slab was then re-modelled using explicit dynamic approach to further identify if there was any sign of failure for the slab when the termination occurred. No sign of runaway type of deflection (see Figure 6.3), which led the author to conclude that this was purely numerical instability problems rather than integrity failure of the slab. Numerical instability in this context refers to the failure of analysis to obtain converge solution due to tensile plastic strain in concrete reached a certain value; an aspect which was extensively discussed in the previous Chapter 5, thus it will not be repeated here.

From Figure 6.3, it can be concluded that all the slabs satisfied 180 minutes of fire resistance requirements if integrity of slab is set as the structural performance indicator. Judging from the trend of mid-span deflection predicted for all the fire scenario cases, the slabs demonstrate good structural fire performance of up to 180 minutes of fire exposure with no sign of the slabs losing their load carrying capacity. The slabs are claimed as retained their load carrying capacity because there was no sign of runaway deflection observed in the figure.

However, if critical reinforcing steel temperature as stipulated in ASTM (2015) was set as the performance indicator, slab heated to Hydrocarbon fire (CEN, 2004), ISO 834 (ISO, 1999), and Slow heating (CEN, 1999) would have failed during 44 mins, 78 mins, and 96 mins respectively. Whereas, if limiting temperature at the surface un-exposed to fires was set as the performance indicator, similar slab models would have failed during 97 mins, 132 mins, and 131 mins for the slab heated to Hydrocarbon (CEN, 2004), ISO 834 (ISO, 1999), and Slow Heating (CEN, 1999) fire curves respectively.

Points mentioned above highlight the variation of acceptance criteria for the structural performance of two-way reinforced concrete slabs under exposure to fire from below, which then resulting inconsistencies in reporting performance of the slabs. If temperature domain is set as the indicator, no consistent criteria are observed. For instance, slab exposed to Hydrocarbon (CEN, 2002a) fire failed during 44 minutes and 97 minutes of exposure for 'critical' reinforcing steel temperature and limiting temperature at the surface un-exposed to fire respectively. Although it is acknowledged that the limiting temperature at the un-exposed surface is satisfying an insulation criteria rather than structural criteria.

6.5.1 Summary

Table 6.3 shows summary of fire resistance rating for slabs exposed to varying fire scenario. Limiting deflection criteria (BSI, 1987) and limiting tensile strain of 2% (Wang et al., 2013) are included as the performance indicator.

With all the slabs were simply supported, tensile strain in reinforcing steels never reached a value of 2% throughout 180 minutes of fire exposure. Slabs exposed to Hydrocarbon (CEN, 2002a) failed the earliest (at 42 minutes) if limiting deflection criteria of $L/20$ (BSI, 1987) is used. Given the fact that all the slabs model did not show any sign of runaway deflection, and consequently no sign of the slabs were losing their load carrying capacity, it seems that limiting deflection criteria recommended by BS 476-20:1987 (BSI, 1987) does not have any physical meaning on the slabs

performance under exposure to severe heating from below but merely provides a conservative estimate on the fire resistance for the slabs.

Table 6.3: Summary of fire resistance rating for slabs exposed to different fire scenario

Fire resistance criterion	*L/20* (BSI, 1987)	Tensile strain in reinforcing steels: 2% (Wang et al., 2013)	Eurocode 2 (CEN, 2004)	International Building Code (International Code Council, 2009)
ISO 834	80 mins	>180 mins	90 mins	90 mins
Hydrocarbon	42 mins	>180 mins*		
Parametric 1	>180 mins	>180 mins		
Parametric 2	>180 mins	>180 mins		
Slow heating	100 mins	>180 mins		

**From explicit dynamic analysis*

6.6 Restraint condition at supports

Boundary condition at support is known to have an influence on the deformation behaviour of fire exposed concrete elements (Gillie, 2009; Lim et al., 2004). Within the structural fire engineering community, it is generally accepted that restraint at support improves structural fire performance of a concrete slab (Buchanan and Abu, 2017). However, there is little clear evidence to demonstrate this, as the understanding on the behaviour of concrete slabs under exposure to fires remains limited. More specifically, if it is true that degree of restraint does help improve structural fire performance of a fire exposed concrete elements, the next question would be what degree of restrain is beneficial to the fire resistance of the slabs. This section presents studies looking at the influence of restraint condition to the structural behaviour of slabs exposed to ISO 834 (ISO, 1999) for 3 hours.

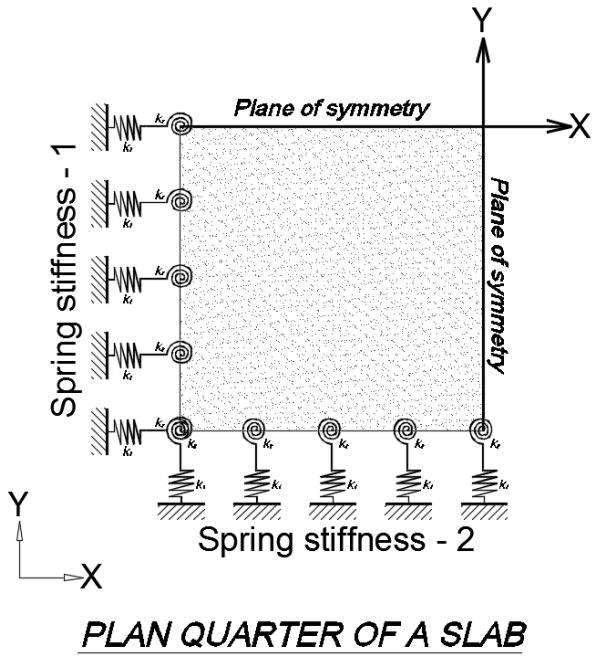

Figure 6.4: Idealisation of restraint condition of a quarter of a slab

Figure 6.4 shows graphical illustration on the defined support restraint condition in the finite element models. Finite translational and rotational spring stiffness were modelled and compared with the mid-span deflection predicted for the case of simply supported slabs and slabs with full restraint condition. The term 'full restraint' however, can be either translational only or rotational only or both, all of which are presented separately in the sections that follow.

The following section presents structural behaviour of slabs with only translational restraint conditions and followed by slabs with only rotational restraint condition. Finally, Section 6.6.3 presents studies looking at more realistic boundary conditions where translational and rotational stiffness act simultaneously.

6.6.1 Translational spring stiffness

In this section, since two-way slab is presented, influence of axial restraint applied as uniaxial and biaxial were specified to look at their effect on the predicted mid-span deflection and strain in reinforcing steels under the influence of finite axial stiffness at supports. In addition to varying the values of elastic axial stiffness, the influence of

combination of finite axial spring stiffness and perfectly axially restraint (pinned) at slab edges was also investigated. These are summarised in Table 6.4 below.

The defined axial stiffness in the slabs is simply an arbitrary value to model slabs with intermediate restraint at supports. The selected value is 7.82×10^8 N/m. Table 6.4 summaries the defined axial stiffness values and location (refer Figure 6.4 for the location of 'stiffness-1' and 'stiffness-2'). In all the restraint conditions modelled, the axial restraint was defined to act at the slab's mid-depth. Indeed it is acknowledged that axial restraint defined at different location within slab's depth (at support) has influence on the predicted response for a fire exposed concrete slabs especially for the case of one-way slabs as studied by Lim (2003). However, in the current study this aspect was not investigated as it is slightly more difficult to get a credible response prediction because shell elements were adopted.

Table 6.4: Summary of the defined translational restraint conditions in the various analyses

Case	Translational stiffness -1 (N/m)	Translational stiffness -2 (N/m)	Notes on **translational** spring stiffness
1	0	0	Zero stiffness (simply supported)
2	7.82×10^8	0	Uniaxial: ($1.00k_t$) + (Free)
3	7.82×10^8	7.82×10^8	Biaxial: ($1.00\times k_t$) + ($1.00\times k_t$)
4	3.91×10^8	3.91×10^8	Biaxial: ($0.50\times k_t$) + ($0.50\times k_t$)
5	7.82×10^7	7.82×10^7	Biaxial: ($0.10\times k_t$) + ($0.10\times k_t$)
6	7.82×10^6	7.82×10^6	Biaxial: ($0.01\times k_t$) + ($0.01\times k_t$)
7	7.82×10^8	∞	Biaxial: ($1.00k_t$) + (infinity)
8	∞	∞	Biaxial: (infinity) + (infinity)

Predicted mid-span deflection for slabs with varying degrees of axial spring stiffness are shown in Figure 6.5. Degree of axial restraint acting at the slab's mid-depth has very minimal influence on the predicted mid-span deflection. For each of the different cases investigated, the difference between the highest and lowest fire resistance rating found based on limiting mid-span deflection as specified in BS 476-20:1987 (BSI, 1987) was found as 8 minutes only; this is summarised in Table 6.7 shown later in Section 6.6.4.

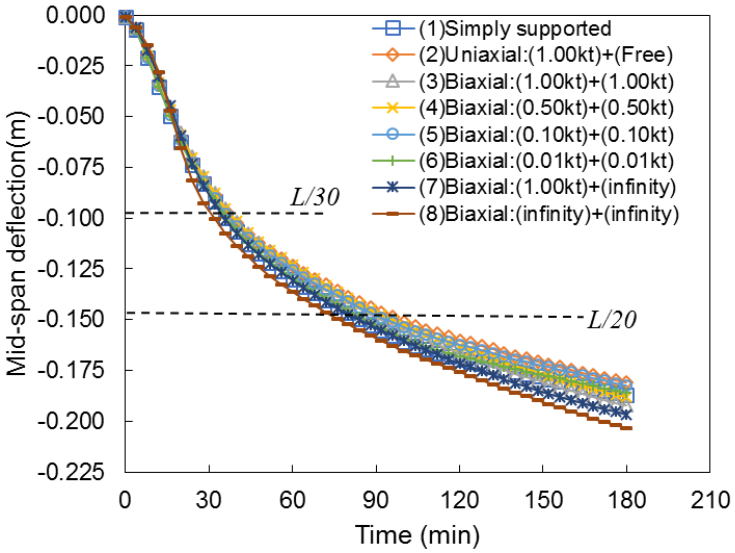

Figure 6.5: Predicted mid-span deflection for slab with varying degree of translational restraint

6.6.2 Rotational spring stiffness

Defining a proper value for the degree rotational stiffness in finite element modelling of two-way slabs is slightly more difficult than defining the same for one-way slabs. This is because the manner in which slab deflects is different for two-way slab. Yield line theory is typically adopted in approximating bending moment in the slabs as opposed to simple bending formula for one-way slabs.

As such, degree of rotational stiffness for the investigation in this section is simply approximated as equal to flexural rigidity of a plate based on the well-known *Kirchhoff-Love* plate theory. This relationship is shown below. In this approximation, no transformed section is assumed in calculating the flexural rigidity. Young's modulus of concrete is simply adopted. This is because an area of a section is not required in applying Equation 6.1 below. In the equation, D is the flexural rigidity, E is Young's modulus, H is plate thickness, and v is the Poisson ratio.

It must be emphasized here that the approximated value is not intended to represent the actual value for the rotational stiffness of the slab. It is simply a reasonable value

to be inputted into the finite element model to define a finite rotational stiffness at the slab edges. Therefore, the selected value cannot be assumed as an actual rotational/bending stiffness that the slab might experience if it is formed as part of reinforced concrete building frames. The intention for this study is simply to look at the response of two-way slabs with intermediate support stiffness and comparing the results with the prediction from slabs with simple supports as well as slabs with full rotational restraint at supports.

Moment of inertia calculated based on 'un-cracked' concrete section is 2.796×10^{-4} m^4 while calculated based on the assumption of 'cracked' concrete section is 1.19×10^{-4} m^4. If rotational stiffness is assumed as bending stiffness as in Chapter 4 (in this section the slab will have to be assumed and simplified as behaving as one-way slabs and deflect in single curvature), then the rotational stiffness will be equal to 6.82×10^5 N.m/rad and 1.59×10^6 N.m/rad for the case 'cracked' and 'un-cracked' concrete section respectively. As comparison, the rotational stiffness approximated based on classical *Kirchhoff-Love* plate theory is 1.45×10^6 N.m/rad (note that the value is calculated based on solely concrete's Young's modulus).

$$D = \frac{EH^3}{12(1-v^2)} \qquad \text{Equation 6.1}$$

Table 6.5 shows the summary of the defined rotational restraint condition on the slabs. Note that, in all the cases slabs were allowed to displace axially (translational). The predicted mid-span deflections for all restraint cases are shown in Figure 6.6. In contrast to the mid-span deflection for the case slabs with varying degree of translational stiffness, here the predicted mid-span deflection demonstrates significant variation in term of magnitude for slabs with different degree of rotational spring stiffness at supports. Simply supported slab predicts the greatest value for mid-span deflection throughout duration of fire exposure and the deflection reduces significantly with the increase in the degree of rotational spring stiffness.

Table 6.5: Summary of the defined rotational restraint

Case	Rotational stiffness -1 (Nm/rad)	Rotational stiffness -2 (Nm/rad)	Notes on **rotational** spring stiffness
1	0	0	Zero stiffness (simply supported)
2	1.45×10^6	0	Uniaxial: ($1.00k_r$) + (Free)
3	1.45×10^6	1.45×10^6	Biaxial: ($1.00\times k_r$) + ($1.00\times k_r$)
4	7.25×10^5	7.25×10^5	Biaxial: ($0.50\times k_r$) + ($0.50\times k_r$)
5	1.45×10^5	1.45×10^5	Biaxial: ($0.10\times k_r$) + ($0.10\times k_r$)
6	1.45×10^4	1.45×10^4	Biaxial: ($0.01\times k_r$) + ($0.01\times k_r$)
7	1.45×10^6	∞	Biaxial: ($1.00k_r$) + (infinity)
8	∞	∞	Biaxial: (infinity) + (infinity)

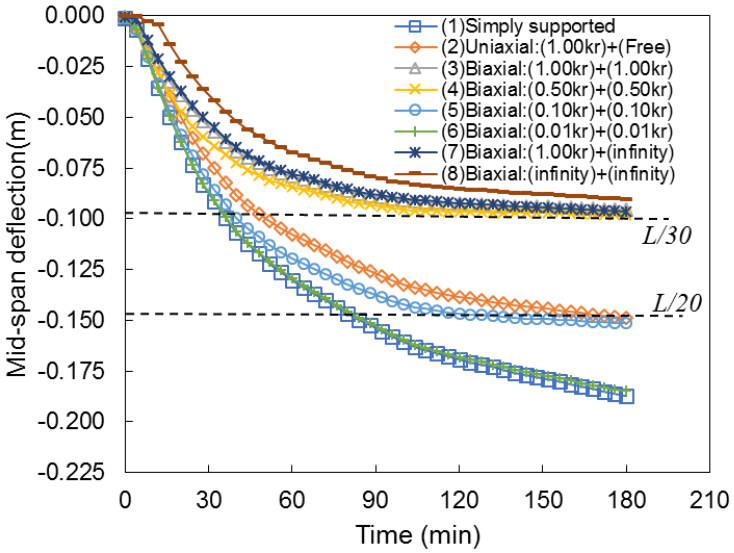

Figure 6.6: Predicted mid-span deflection for slabs with varying degrees of rotational restraint

6.6.3 Combination of translational and rotational spring stiffness

A more realistic restraint condition at the slab boundary for a cast in-place concrete slab is a combination of both translational and rotational restraint existing simultaneously. However, as mentioned in the previous section, approximating a realistic value for the restraint stiffness is another challenge. The current study only looks at the structural behaviour of a two-way reinforced concrete slabs with finite restraint stiffness at supports, and it is not the intention to realistically replicate the actual restraint stiffness that the slabs might experience in a reinforced concrete frame

structure. Table 6.6 lists the magnitude of both translational and rotational restraint stiffness defined in the model for the investigation.

Table 6.6: Summary of the defined combination of translational and rotational restraint

Case	Translational stiffness -1 (N/m)	Rotational stiffness -1 (Nm/rad)	Translational stiffness -2 (N/m)	Rotational stiffness -2 (Nm/rad)	Notes on **combination of translational and rotational** spring stiffness
1	0	0	0	0	Zero stiffness (simply supported)
2	7.82×10^8	1.45×10^6	0	0	Uniaxial ($1.00k_{tr}$) + (Free)
3	7.82×10^8	1.45×10^6	7.82×10^8	1.45×10^6	Biaxial: ($1.00\times k_{tr}$) + ($1.00\times k_{tr}$)
4	3.91×10^8	7.25×10^5	3.91×10^8	7.25×10^5	Biaxial: ($0.50\times k_{tr}$) + ($0.50\times k_{tr}$)
5	7.82×10^7	1.45×10^5	7.82×10^7	1.45×10^5	Biaxial: ($0.10\times k_{tr}$) + ($0.10\times k_{tr}$)
6	7.82×10^6	1.45×10^4	7.82×10^6	1.45×10^4	Biaxial: ($0.01\times k_{tr}$) + ($0.01\times k_{tr}$)
7	7.82×10^8	1.45×10^6	∞	∞	Biaxial: ($1.00k_{tr}$) + (infinity)
8	∞	∞	∞	∞	Biaxial: (infinity) + (infinity)

Figure 6.7 shows the predicted mid-span deflection for slabs with varying degree of restraint stiffness. Similar strategy in the previous Section 6.6.2, simply supported slab case and slab restraint in a uniaxial manner are also included to investigate the structural response of the slabs with different configuration of restraint conditions.

In general, the higher the rotational restraint defined, the lower the mid-span deflection predicted. But there was no trend can be observed (see Figure 6.7) with regard to whether the deflection is increasing or decreasing when the restraint stiffness was increased. At 180 minutes of exposure, the predicted mid-span deflection for slab with restraint defined at $1.00k_{tr}$ is 169 mm while for the slab restraint defined at $0.50k_{tr}$, the predicted mid-span deflection was 163 mm, which is slightly lower.

This findings highlight how importance it is to not only consider the limiting mid-span deflection criteria in assessing the structural fire resistance of two-way reinforced concrete slabs. Slabs failed limiting deflection criteria (BSI, 1987) at 137 mins and 144 mins for slab with restraint at $1.00k_{tr}$ and 0.50ktr respectively. From a different perspective, slab with $1.00k_{tr}$ and $0.50k_{tr}$ failed limiting tensile strain (Wang et al., 2013) criteria at 93 mins and 130 mins respectively.

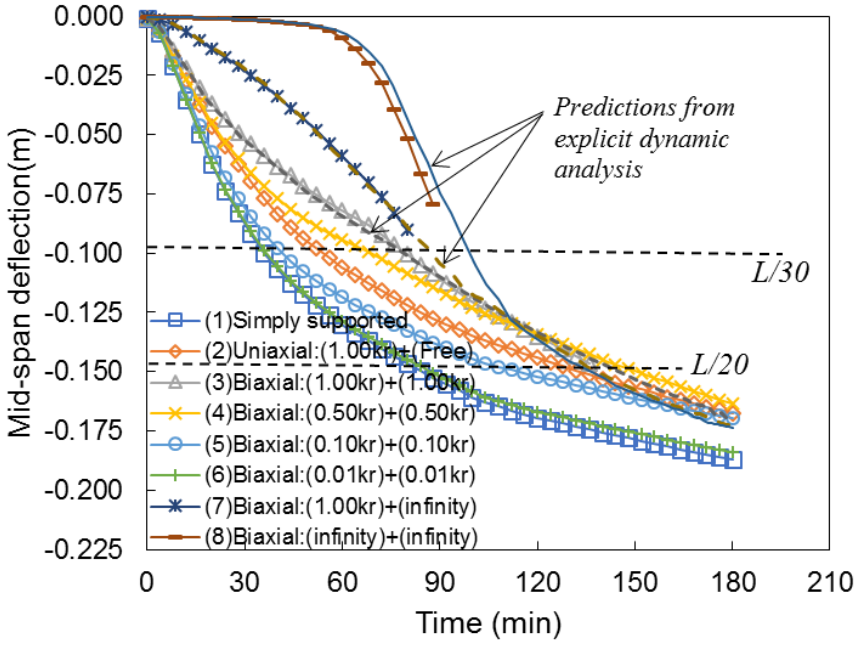

Figure 6.7: Predicted mid-span deflections for slabs with varying degrees of combinations of translational and rotational restraint

6.6.4 Summary

The presence of restraint at support generally improves fire resistance of two-way reinforced concrete slabs exposed to severe heating from below if limiting mid-span deflection is set as the performance indicator. However, no straightforward fire resistance rating can be provided if limiting tensile strain in reinforcing steels is specified as the performance indicator. This is because, presence of restraint (both translational and rotational) reduce the magnitude of mid-span deflection but at the same time increasing mechanical strain in the reinforcing steels. Although this is the case, the use of combination criteria (both limiting deflection and limiting reinforcing steel's tensile strain) gives more comprehensive insight into specifying fire resistance rating for two-way reinforced concrete slabs exposed to severe heating from below.

Table 6.7: Summary of fire resistance rating for slabs with varying restraint condition at supports

	#	Fire resistance criterion	*L/20* (BSI, 1987)	Tensile strain in reinforcing steels: 2% (Wang et al., 2013)	Eurocode 2 (CEN, 2004)	International Building Code (International Code Council, 2009)
Translational restraint	*1*	*Simply supported*	80 mins	>180 mins	90 mins	90 mins
	2	*Uniaxial:(1.00kt)+(Free)*	93 mins	>180 mins		
	3	*Biaxial:(1.00k_t)+(1.00k_t)*	87 mins	>180 mins		
	4	*Biaxial:(0.50k_t)+(0.50k_t)*	90 mins	>180 mins		
	5	*Biaxial:(0.10k_t)+(0.10k_t)*	89 mins	>180 mins		
	6	*Biaxial:(0.01k_t)+(0.01k_t)*	81 mins	>180 mins		
	7	*Biaxial:(1.00k_t)+(infinity)*	79 mins	>180 mins		
	8	*Biaxial:(Full)+(Full)*	72 mins	154 mins		
Rotational restraint	*1*	*Simply supported*	80 mins	>180 mins		
	2	*Uniaxial:(1.00k_r)+(Free)*	164 mins	25 mins		
	3	*Biaxial:(1.00k_r)+(1.00k_r)*	>180 mins	31 mins		
	4	*Biaxial:(0.50k_r)+(0.50k_r)*	>180 mins	57 mins		
	5	*Biaxial:(0.10k_r)+(0.10k_r)*	120 mins	>180 mins		
	6	*Biaxial:(0.01k_r)+(0.01k_r)*	80 mins	>180 mins		
	7	*Biaxial:(1.00k_r)+(infinity)*	>180 mins	15 mins		
	8	*Biaxial:(Full)+(Full)*	>180 mins	22 mins		
Combined trans. & rota. restraint	*1*	*Simply supported*	80 mins	>180 mins		
	2	*Uniaxial:(1.00k_{tr})+(Free)*	124 mins	52 mins		
	3	*Biaxial:(1.00k_{tr})+(1.00k_{tr})*	137 mins	93 mins		
	4	*Biaxial:(0.50k_{tr})+(0.50k_{tr})*	144 mins	130 mins		
	5	*Biaxial:(0.10k_{tr})+(0.10k_{tr})*	107 mins	>180 mins		
	6	*Biaxial:(0.01k_{tr})+(0.01k_{tr})*	83 mins	>180 mins		
	7	*Biaxial:(1.00k_{tr})+(infinity)*	137 mins*	86 mins*		
	8	*Biaxial:(Full)+(Full)*	132 mins*	103 mins*		

**From explicit dynamic analysis*

6.6.5 Recommendation for best practice guidance

Studies performed in the current section confirmed that the presence of restraint, both translational and rotational improves structural integrity of two-way slabs with regard to limiting mid-span deflection. Although reinforcing steel's tensile strain increase with the increase in restraint stiffness (especially rotational stiffness), the benefits of restraint to the specified fire resistance rating is still observed based on investigation in the current chapter.

From the design perspective, it is therefore suggested that limiting deflection criteria would not give an economical design for the case of simply supported two-way slabs exposed to severe heating from below. Limiting deflection criteria based on BS 476-20:1987 (BSI, 1987) gives very conservative fire resistance rating for simply supported slabs. Combination of limiting deflection criteria (BSI, 1987) and limiting tensile strain (Wang et al., 2013) shall always be used simultaneously to give a comprehensive insight into specifying fire rating for the slabs.

6.7 Curtailment of top reinforcement

Top reinforcement in cast in-situ reinforced concrete slab construction is often curtailed at certain lengths for economic reasons. This section investigates the effects of curtailment of top reinforcement on the structural behaviour of two-way slabs exposed to ISO 834 (ISO, 1999) fires. Buchanan and Abu (2017) suggested special treatment for curtailment of top reinforcement for a fire exposed flexural elements. Top reinforcing steels should be extended for 15% to 20% extra (Buchanan and Abu, 2017). However, the authors refer to beams and/or one-way slabs. In addition, no specific guidance is given on how to design this 'additional' length of top reinforcement. With the above background, this section explores the influence of different curtailment lengths on the predicted mid-span deflection as well as strain in the steel reinforcement. Slab with rigid supports (Section 6.7.1) and intermediate spring stiffness (Section 6.7.2) are presented.

6.7.1 Rigid support

Provision of top reinforcement's length is in the ratio of span (L) of the slab, these being $0.125L$, $0.250L$, and $0.375L$. Full length of top reinforcement (doubly reinforced slab) is also included. Figure 6.8 shows the predicted mid-span deflection for the case of slabs with varying length of top reinforcing steels. All the slabs were modelled with rigid supports.

With regard to mid-span deflection, provision of different length of top reinforcement does not have significant influence on the prediction of mid-span deflection. Very

minimal difference in fire resistance rating is provided for each of the different cases investigated; a summary on this is provided and shown later in Table 6.8 in Section 6.7.3. Understanding the influence of curtailment's length for the case of two-way slabs is slightly more complicated as compared to one-way slabs. With one-way slabs bend in single curvature, evolution of bending moment diagram with time can be easily interpreted with regard to the requirements for length of top reinforcement. In contrast, two-way slabs bend in double curvature and yield line theory is commonly adopted in approximating the requirements for location and total length of reinforcing steels. As such, author cannot make any conclusion from the limited results presented in the current section.

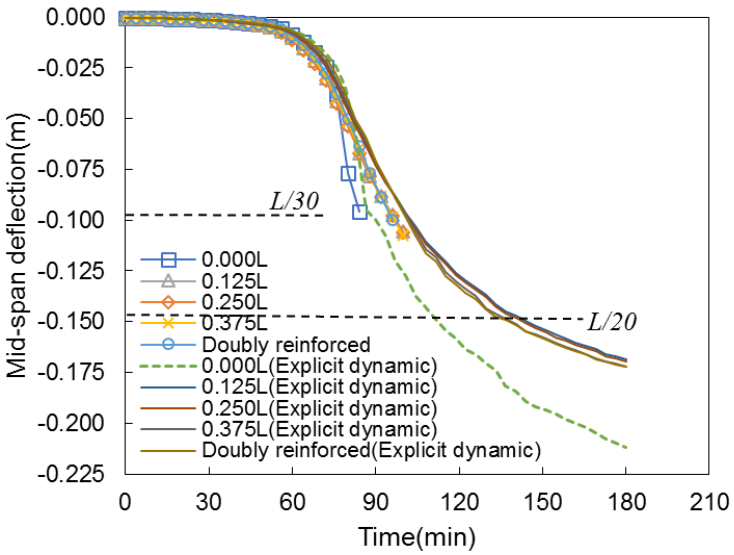

Figure 6.8: Predicted mid-span deflection for slab with different curtailment length of top reinforcement: rigid support

6.7.2 Intermediate stiffness

Figure 6.9 shows the predicted mid-span deflection for the case slabs modelled with varying length of top reinforcing steels. In this section, intermediate spring stiffness is defined at slab's supports. With translational and rotational spring stiffness defined at 7.82×10^{8} N/m and 1.45×10^{6} Nm/rad respectively, there is no noticeable difference in the predicted mid-span deflection for all the modelled slabs with varying length of top

reinforcement. However, no variation in the value of rotational spring stiffness is investigated in this section. This is because designing two-way slab typically based on plate theory rather than simple flexural theory. This means the understanding on the behaviour is more complex and requires a long section dedicated for discussion on the topic. Therefore, it was decided to limit the study to only single value of spring stiffness (both translational and rotational), and specified as 'intermediate stiffness' in the current section.

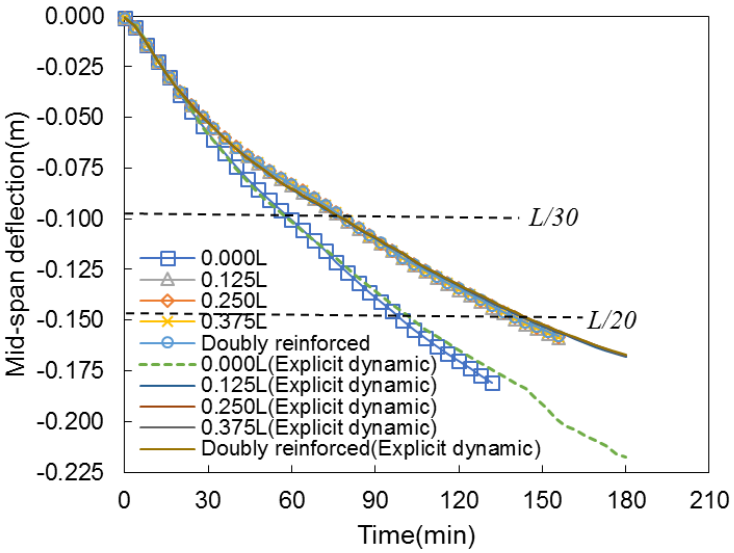

Figure 6.9: Predicted mid-span deflection for slab with different curtailment length of top reinforcement: finite spring stiffness at support

Without top reinforcing steels (see Figure 6.9), the trend of deflection is different from the rest of the models (i.e. defined with 0.125L, 0.250L, 0.375L, and doubly reinforced). From the results, it was found that the absence of top reinforcing steels would not guarantee that the slab would collapse, at least for the case of two-way slabs investigated in the current section. However, it is not fair to claim that the top reinforcing steels is not needed based on limited information available in the current study. Among others, realistic modelling on concrete cracking behaviour (e.g. discrete cracks) is required in order to get better results with regard to concrete cracking/crushing behaviour at the top section of the slabs.

6.7.3 Summary

Table 6.8 lists summary of the approximated fire resistance rating for slabs with varying length of top reinforcement. Both slabs with rigid supports and intermediate spring stiffness are included in the table.

In general, no significant variation on the fire resistance rating predicted for slabs with varying length of top reinforcing steels with the exception of slabs modelled without top reinforcing steels. Both limiting deflection criteria (BSI, 1987) and limiting tensile strain (Wang et al., 2013) give very minimal differences (see Table 6.8) on fire resistance rating for slabs with different length of top reinforcement. Therefore, for the case of two-way slabs, it can be concluded that varying the length of top reinforcing steels has very minimal effects on the fire resistance of the slabs.

Table 6.8: Summary of fire resistance rating for slabs with varying top reinforcement's curtailment's length

	#	Fire resistance criterion	*L/20* (BSI, 1987)	Tensile strain in reinforcing steels: 2% (Wang et al., 2013)	Eurocode 2 (CEN, 2004)	International Building Code (International Code Council, 2009)
Rigid support	*1*	*0.000L*	110 mins*	141 mins*	90 mins	90 mins
	2	*0.125L*	140 mins*	115 mins*		
	3	*0.250L*	138 mins*	115 mins*		
	4	*0.375L*	135 mins*	115 mins*		
	5	*1.000L*	133 mins*	113 mins*		
Inter. support stiffness	*1*	*0.000L*	100 mins*	154 mins*		
	2	*0.125L*	140 mins*	121 mins*		
	3	*0.250L*	141 mins*	122 mins*		
	4	*0.375L*	140 mins*	122 mins*		
	5	*1.000L*	141 mins*	122 mins*		

**From explicit dynamic analysis*

6.7.4 Recommendation for best practice guidance

Findings from the study in the current section suggest that no special treatment is required on provision of top reinforcing steels for the design of two-way slabs under exposure to severe heating from below. Different findings found for one-way slabs

presented in Chapter 4, where length of top reinforcing steels has significant influence on the structural response of the slabs when heated from below.

6.8 Span-to-depth ratio

One of the important steps in designing reinforced concrete slabs both at ambient and elevated temperatures is determining the optimum thickness for the slabs. The selected thickness has to satisfy the design objectives i.e. providing enough flexural capacity, deflection criteria, as well as shear capacity.

Sufficient amount of information are available in textbook as well as the old prescription design code of practice for instance BS 8110-1:1997 (BSI, 1997) to guide designers in selecting the suitable slab's thickness to cater for the required flexural capacity and also deflection criteria. Deflection criteria generally specified based on the limiting span-to-depth ratio. Unfortunately, all of these are only applicable for the design at ambient temperature. There is no similar information available for designing the slab for structural fire resistance either in textbook or design code. One of the reasons behind this is the common assumption that protecting steel reinforcement against certain 'critical' temperatures is sufficient for the structural fire design strategy for most cast in-place reinforced concrete buildings. Protecting the steel reinforcement against high temperature means greater concrete cover and consequently thicker slabs. However, better understanding is required, beyond the common practice mentioned above. In addition, it is well accepted within structural fire engineering community that two-way slab retains its load carrying capacity by utilizing tensile membrane action, which further confirmed that the approach of only protecting reinforcing steels against certain 'critical' temperature is not a comprehensive approach in treating the problems.

Against the background mentioned above, this section presents studies looking at the aspect of varying span-to-depth ratio in designing two-way reinforced concrete slabs based on the applicable Eurocodes for ambient temperature structural design (CEN, 2014, 2005, 2004).

Assuming a slab design is required for a hotel bedroom occupancy class (i.e. subcategory A3 from Table NA.2, UK National Annex to Eurocode 1: Actions on structures (CEN, 2002b)), which also means the slab has to support 2 kPa of superimposed load, a study is then conducted to check whether varying the slab's thickness (consequently span-to-depth ratio) will improve the slab's structural fire performance based on limiting deflection criteria (BSI, 1987) as well as limiting tensile strain criteria i.e. 2% (Wang et al., 2013) or otherwise. Table 6.9 lists the selected span-to-depth ratio and their relevant design input data. The structural fire performance of the slabs with simple support, rigid support, and support with intermediate spring stiffness are evaluated and presented individually in the following sections.

Table 6.9: Selected span-depth ratios and their relevant design input data

Case	Span, L (mm)	Thickness, h (mm)	Axis distance (mm)	Eff. depth, d (mm)	Span/ d	Dead Load (N/m^2)	Live Load (N/m^2)	Design $Load_{ult}$ ($1.35G_k+1.5Q_k$) (N/m^2)	Design $Load_{fire}$ ($1.0G_k+0.5Q_k$) (N/m^2)
1	2930	100	19	81	36.2	2256	2000	6046	3256
2	2930	125	19	106	27.6	2820	2000	6807	3820
3	2930	150	19	131	22.4	3384	2000	7568	4384

6.8.1 Simply supported

Table 6.10 presents summary of design results for slabs with different span-to-depth ratio. All slabs are simply supported. The chosen area of steel reinforcement for all the cases are exactly the steel area required i.e. $A_{s\ provided} = A_{s\ required}$. This is done to ensure consistency in comparing the predicted mid-span deflection for the slabs with varying span-to-depth ratio. Figure 6.10 shows the predicted mid-span deflection for simply supported slab with varying span-to-depth ratio.

Table 6.10: Selected span-to-depth ratios and their relevant design results for simply supported case

Case	Span, L (mm)	Thickness, h (mm)	Ø reinforcing steel (mm)	*BM coef.	Design moment$_{ult}$ (kNm)	z (mm)	A_s required (mm^2/m)	A_s (%)
1	2930	100	4	0.062	3.22	0.95d	101	0.10
2	2930	125	4	0.062	3.62	0.95d	87	0.07
3	2930	150	4	0.062	4.03	0.95d	78	0.05

** The widely used bending moment coefficient for simply supported slab based on tabulated data in BS 8110-1:1997 (BSI, 1997)*

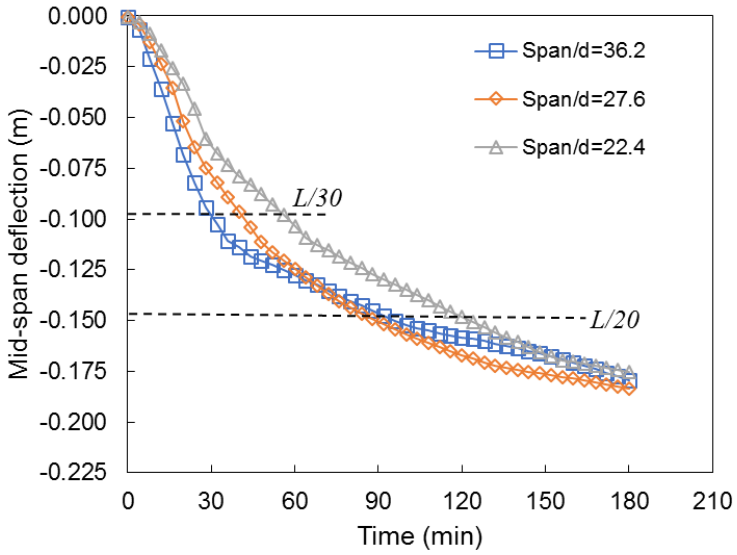

Figure 6.10: Predicted mid-span deflection for simply supported slabs with different span-to-depth ratio

It is suspected that the mechanism of tensile membrane action is potentially more beneficial and efficient for thinner slabs rather than thicker slabs. As the term 'membrane' implies, membrane effect is more effective for thin plate elements. In other words, the thicker the element gets, the membrane effects lessen and the slab resists both mechanical and fire load through flexural behaviour rather than membrane behaviour. Note that the investigation for the case of one-way slabs in Chapter 4 presented contradictory outcomes to the current findings therefore it is suggested

thinner slabs have better structural fire performance than thicker slabs, at least for the case of simply supported two-way slabs exposed to ISO 834 (ISO, 1999).

6.8.2 Continuous

Further to the study presented in the previous section, this section presents similar studies, extended in looking at the aspect of continuity at support to the structural fire performance of the slab with varying span-to-depth ratio. The term 'continuous' is used to distinguish motivation behind the studies presented in Section 6.8.1 and in this section i.e. Section 6.8.2. Continuity generally introduces some degree of restraint at the slab's support due to the existence of adjacent element to the element under consideration. The degree of restraint (or fixity) at the support however, is difficult to approximate and realistically modelling full frame behaviour is still the best way to understand actual full frame behaviour of reinforced concrete structures exposed to fires.

Studies looking at the aspect of continuity and span-to-depth ratio in this section is divided into two (2) subsection namely; (1) Rigid supports and (2) Intermediate support stiffness. Details regarding slab's configuration, design input data, and design results are presented separately in the respective subsection. These also include explanation on approach to the problems in ensuring the methodology can be related to the actual practice within design offices.

6.8.2.1 Rigid supports

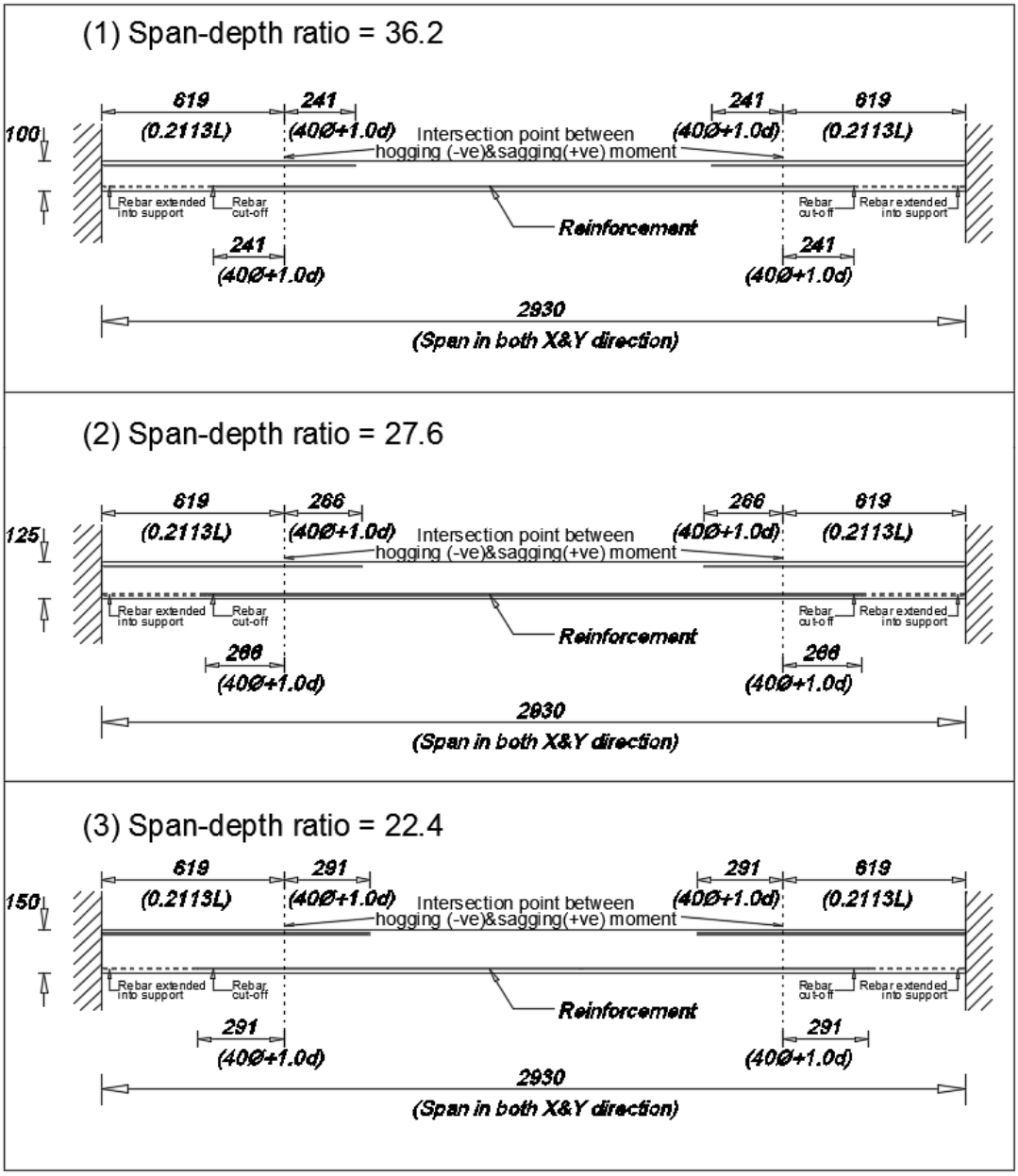

Figure 6.11: Arrangement of reinforcements for slabs with different span-to-depth ratio

Figure 6.11 shows the detail arrangements of reinforcement for the selected span-to-depth ratio. The slabs were designed in accordance to relevant Eurocode (CEN, 2014,

2005, 2004). Design moments for all cases were calculated with the assumption slabs have continuity at supports; aligned with the tabulation of coefficient in BS 8110-1:1997 (BSI, 1997). Also, note that the provision of the details in the figure applicable to slab spanning both in X, and Y-direction.

Table 6.11 and Table 6.12 show the relevant design results for slab with varying span-to-depth ratio and rigid support condition. Table 6.11 presents the approximation of reinforcement for resisting sagging moment at mid-span while Table 6.12 presents similar outcome for the slab to resist hogging moment.

Table 6.11: Selected span-to-depth ratio and their relevant design results for continuous slab case: *sagging moment (at mid-span)*

Case	Span, *L* (mm)	Thickness, *h* (mm)	Ø reinforcing steel (mm)	*BM coeff.	Design *sagging* $moment_{ult}$ (kNm)	*z* (mm)	A_s required (mm^2/m)	A_s (%)
1	2930	100	4	0.024	1.25	0.95*d*	40	0.04
2	2930	125	4	0.024	1.40	0.95*d*	44	0.04
3	2930	150	4	0.024	1.56	0.95*d*	49	0.05

** The widely used bending moment coefficient for slabs based on tabulated data in BS 8110-1:1997 (BSI, 1997)*

Table 6.12: Selected span-to-depth ratio and their relevant design results for continuous slab case: *hogging moment (at support)*

Case	Span, *L* (mm)	Thickness, *h* (mm)	Ø reinforcing steel (mm)	*BM coeff.	Design *hogging* $moment_{ult}$ (kNm)	*z* (mm)	A_s required (mm^2/m)	A_s (%)
1	2930	100	4	0.032	1.66	0.95*d*	52	0.05
2	2930	125	4	0.032	1.87	0.95*d*	59	0.06
3	2930	150	4	0.032	2.08	0.95*d*	65	0.07

** The widely used bending moment coefficient for slabs based on tabulated data in BS 8110-1:1997 (BSI, 1997)*

Contrary to the findings from the previous Section 6.8.1, here slab with lower span-to-depth ratio (thicker) demonstrate better structural fire performance if mid-span

deflection is set as the criteria. This can be seen in the predicted mid-span deflection shown in Figure 6.12. With slabs have rigid support condition, snap trough occurred when the slabs transitioned from compressive membrane behaviour to tensile membrane behaviour. This is demonstrated for the case slab with span-to-depth ratio= 36.2 (see Figure 6.12). The findings suggest that for the case slabs with varying span-to-depth ratio and rigidly supported, snap trough occurred earlier for slabs with higher span-to-depth ratio.

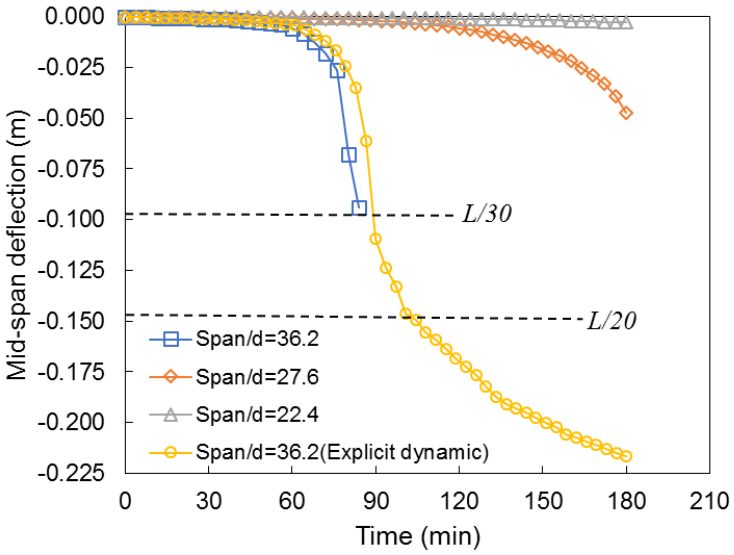

Figure 6.12: Predicted mid-span deflection for rigid supported slab with different span-to-depth ratio

6.8.2.2 Intermediate support stiffness

Similar studies presented in previous Section 6.8.2.1 are repeated here. However, instead of rigid condition at support, slabs are modelled with finite spring stiffness both for translational and rotational restraint. For each of the span-to-depth ratio, elastic axial and rotational stiffness are simply calculated with the assumption of un-cracked concrete section. With un-cracked concrete section assumed, the predicted response is relatively similar to the predicted response for the case slab modelled with rigid supports. Therefore, it was decided to model the slab with 10% of the calculated axial and rotational spring stiffness to reduce the support's stiffness value.

Summary of the calculated spring stiffness are shown in Table 6.13. Note that the estimated stiffness values are not comparable to the one estimated from the studies in Section 0 as the amount of reinforcement is not the same. In approximating the area of steel reinforcement, similar bending moment values calculated in the previous Section 6.8.2.1 are adopted and these are also shown in Table 6.13.

Table 6.13: Summary of the calculated elastic spring stiffness

Slab thick. (mm)	Span/ depth	$A_{s(top)}$ (mm^2/m)	$A_{s(bottom)}$, (mm^2/m)	Transformed section (m^2)	*N.A (mm)	$I_{un\text{-}crack}$ (m^4)	*EI/L* (Nm/rad)	*AE/L* (N/m)
100	36.2	52	40	0.296279	50.06	2.4548×10^{-4}	1.399×10^{6}	1.689×10^{9}
125	27.6	59	44	0.369924	62.58	4.8384×10^{-4}	2.758×10^{6}	2.108×10^{9}
150	22.4	65	49	0.443565	75.09	8.3681×10^{-4}	4.770×10^{6}	2.528×10^{9}

**Measured from bottom of slab*

Mid-span deflection predicted for slabs with varying span-to-depth ratio and intermediate spring stiffness at supports are shown in Figure 6.13. Higher span-to-depth ratio means greater mid-span deflection as well as higher tensile strain in the reinforcing steels (see summary in Table 6.14). Again, as has been discussed in the earlier section of this chapter, both criteria i.e. limiting mid-span deflection (BSI, 1987) and limiting reinforcing steel's tensile strain (Wang et al., 2013) have to be used in order to determine fire resistance rating for the slabs.

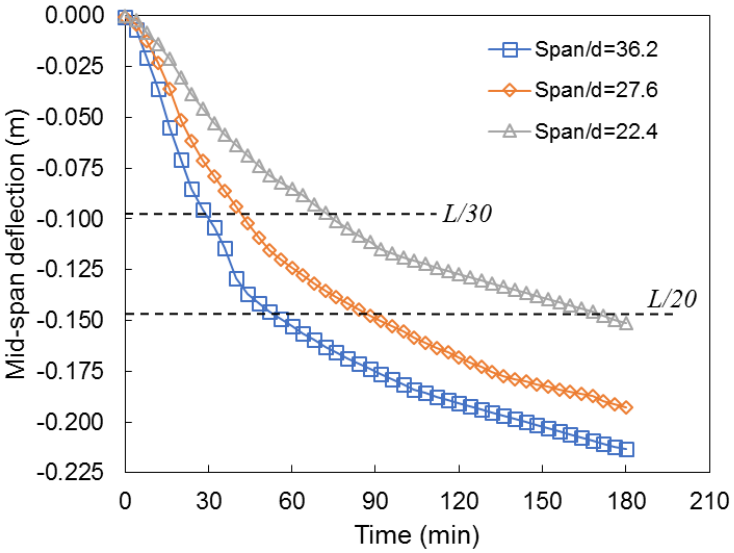

Figure 6.13: Predicted mid-span deflection for slab with different span-to-depth ratio and intermediate spring stiffness at supports

6.8.3 Summary

Studies looking at the effect of varying span-to-depth ratio to the structural response of two-way slabs under exposure to ISO 834 (ISO, 1999) have been presented in the current section. Table 6.14 summaries the estimated fire resistance rating for the slabs based on limiting mid-span deflection (BSI, 1987) criteria as well as limiting tensile strain in reinforcing steels (Wang et al., 2013).

Overall trend of mid-span deflection for simply supported slabs with varying span-to-depth ratio indicates that slab with higher span-to-depth ratio behaves better with tensile membrane actions efficiently preserved the load carrying capacity of the slabs. In contrast, slabs with rigid and intermediate spring stiffness at support demonstrate that lower span-depth-ratio slabs have better fire resistance rating when both criteria i.e. limiting mid-span deflection (BSI, 1987) and limiting reinforcing steel's tensile strain (Wang et al., 2013) are used as the indicator.

Table 6.14: Summary of fire resistance rating for slabs with varying span-to-depth ratio

	#	Fire resistance criterion	*L/20* (BSI, 1987)	Tensile strain in reinforcing steels: 2% (Wang et al., 2013)	Eurocode 2 (CEN, 2004)	International Building Code (International Code Council, 2009)
Simple support	*1*	*Span/d= 36.2*	91 mins	>180 mins	90 mins	90 mins
	2	*Span/d= 27.6*	84 mins	>180 mins		
	3	*Span/d= 22.4*	118 mins	>180 mins		
Rigid support	*1*	*Span/d= 36.2*	101 mins*	>180 mins		
	2	*Span/d= 27.6*	>180 mins	>180 mins		
	3	*Span/d= 22.4*	>180 mins	>180 mins		
Inter. support stiffness	*1*	*Span/d= 36.2*	53 mins	118 mins		
	2	*Span/d= 27.6*	87 mins	>180 mins		
	3	*Span/d= 22.4*	170 mins	>180 mins		

**From explicit dynamic analysis*

6.8.4 Recommendation for best practice guidance

For the case of simply supported two-way slabs exposed to severe heating from below, slabs with higher span-to-depth ratio (thinner slabs) mobilised tensile membrane action efficiently as compared to its lower span-to-depth ratio counterparts. As such, whenever possible, selection of higher span-to-depth ratio is recommended. For the case of slabs with rigid and intermediate spring stiffness at supports, lower span-to-depth ratio slabs tend to behave better.

6.9 Aspect ratio

One-way slab is defined when ratio of its longer dimension (l_y) to its shorter dimension (l_x) is greater than two. With the above ratio is equal or less than two, the slab is classified as two-way slabs. For cast in-situ concrete frame construction, slabs can be designed as one-way or two-way category depending on several criteria for instance the locations of supporting columns as well as beams. Commonly one-way condition exists at corridors or hallways while two-way slabs condition typically exists for designing bedrooms, offices etc.

In preparing a design scheme for a cast in-situ concrete building frame, determination of either one-way or two-way slabs is up to the discretion of the designer, with practicality and economic being the determining factor. In other words, two-way slabs can be turned into one-way slabs by simply introducing secondary beams to shorten the slab's span. Whether this is a wise decision to make is another issue that need further discussion.

In this section, the effect of varying slab's aspect ratio to the structural performance of reinforced concrete slabs exposed to ISO 834 (ISO, 1999) fires is investigated. Ratio of 1 ($l_y/l_{lx} = 1.0$) i.e. square slabs and up to 1.8 ($l_y/l_{lx} = 1.8$) are investigated. These are summarised in Table 6.15. The selected aspect ratios are studied for slabs with simple supports.

Influence of aspect ratio to the structural fire resistance of two-way concrete slabs has been previously investigated by Lim (2003) and Deeny (2010). Both authors concluded that slabs with aspect ratio closest to 1 (square slabs) has better fire resistance than their rectangular counterparts. Greatest enhancement on strength is achieved when the slab's aspect ratio equals to 1 (square slabs) due the effect of double curvature (Lim, 2003). However, the studies were performed with reinforcements in the slabs were similar in all cases (variation of aspect ratio). Designing the slabs in accordance to the relevant design codes was disregarded. Therefore, studies in this section will focus on the influence of aspect ratio to the structural fire resistance of reinforced concrete two-way slabs, with the slabs designed in accordance to relevant Eurocodes (CEN, 2014, 2005) and British Standards (BSI, 1997).

Table 6.15: Selected aspect ratios and their relevant design input data

Case	Shorter span, L_x (mm)	Longer span, L_y (mm)	Aspect ratio	Thick. (mm)	Eff. depth, d (mm)	Dead Load (N/m^2)	Live Load (N/m^2)	Design $Load_{ult}$ ($1.35G_k+1.5Q_k$) (N/m^2)	Design $Load_{fire}$ ($1.0G_k+0.5Q_k$) (N/m^2)
1	2930	2930	1.0	100	81	2256	2000	6046	3256
2	2930	3516	1.2	100	81	2256	2000	6046	3256
3	2930	4102	1.4	100	81	2256	2000	6046	3256
4	2930	4688	1.6	100	81	2256	2000	6046	3256
5	2930	5274	1.8	100	81	2256	2000	6046	3256

6.9.1 Simply supported case

Table 6.16 shows summary of the selected aspect ratio and their corresponding design outputs and Figure 6.14 shows the predicted mid-span deflection for simply supported slabs with varying aspect ratio. Referring to mid-span deflection presented in Figure 6.14, square slab demonstrates the best trend with regard to integrity. No sign of runaway type of deflection throughout the simulation as compared to rectangular slabs. The higher the aspect ratio, the earlier for the slabs experiencing integrity failures. In this context, integrity failure refers to runaway type of deflection.

As simply supported slabs sustaining large vertical deflection through membrane action, it seems that mobilisation of tensile membrane actions is better with square slabs as opposed to rectangular slabs. If this is to be translated into practices in the structural fire engineering, whenever possible, slabs have to be designed with the smallest aspect ratio possible.

Table 6.16: Selected span-to-depth ratios and their relevant design results for slab with simple support

Case	Ø reinforcing steel (mm)	*BM coeff. a_{sx}	*BM coeff. a_{sy}	Design moment$_{ult}$: M_{sx} (kNm)	Design moment$_{ult}$: M_{sy} (kNm)	z (mm)	A_{sx} required (mm^2/m)	A_{sx} (%)	z (mm)	A_{sy} required (mm^2/m)	A_{sy} (%)
1	4	0.062	0.062	3.22	3.22	0.95d	101	0.10	0.95d	101	0.10
2	4	0.084	0.059	4.36	3.06	0.95d	137	0.14	0.95d	96	0.10
3	4	0.099	0.051	5.14	2.65	0.95d	162	0.16	0.95d	83	0.08
4	4	0.108	0.042	5.61	2.18	0.95d	176	0.18	0.95d	69	0.07
5	4	0.114	0.035	5.92	1.82	0.95d	186	0.19	0.95d	57	0.06

** The widely used bending moment coefficient for simply supported slabs based on tabulated data in BS 8110-1:1997 (BSI, 1997)*

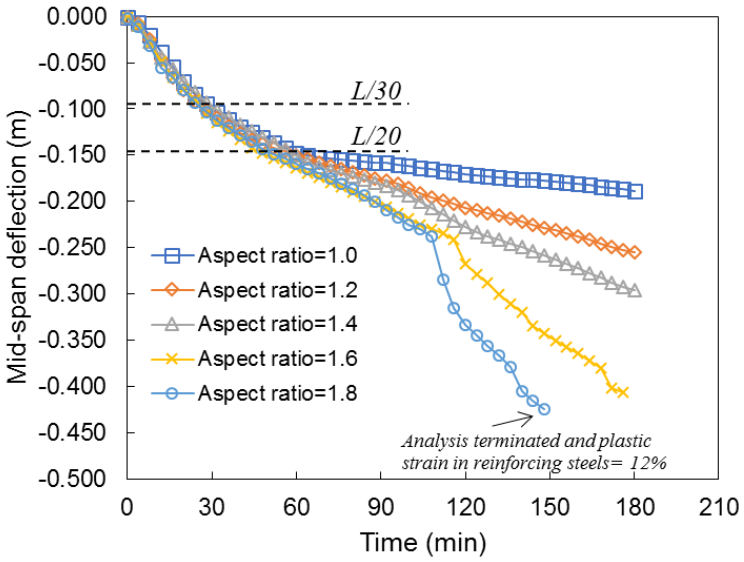

Figure 6.14: Predicted mid-span deflection for simply supported slabs with varying aspect ratios

6.9.2 Summary

The effect of varying aspect ratio to the structural response of two-way reinforced concrete slabs exposed to severe heating from below is investigated in the current section. Table 6.17 presents summary of the estimated fire resistance rating for the

slabs based on limiting mid-span deflection criteria (BSI, 1987) and limiting reinforcing steel's tensile strain (Wang et al., 2013).

Although no significant variation of fire resistance rating for slabs with different aspect ratio is provided when limiting deflection is set as the criteria (minimum fire resistance is 47 mins while the maximum rating is 60 mins), this is not the case when limiting tensile strain is used as the performance indicator (see Table 6.17). High tensile strain in reinforcing steels for slabs with greater aspect ratio translates to runaway deflection as demonstrated in the previous Figure 6.14. More than 180 minutes of fire resistance rating is provided for slab with aspect ratio equals to 1 (square slabs) while only 18 minutes of fire resistance can be specified if limiting tensile strain in reinforcing steels was set as the performance indicator.

Table 6.17: Summary of fire resistance rating for slabs with varying aspect ratio

	#	Fire resistance criterion	*L/20* (BSI, 1987)	Tensile strain in reinforcing steels: 2% (Wang et al., 2013)	Eurocode 2 (CEN, 2004)	International Building Code (International Code Council, 2009)
Simple support	*1*	*Aspect ratio= 1.0*	60 mins	>180 mins	90 mins	90 mins
	2	*Aspect ratio= 1.2*	57 mins	99 mins		
	3	*Aspect ratio= 1.4*	58 mins	101 mins		
	4	*Aspect ratio= 1.6*	47 mins	88 mins		
	5	*Aspect ratio= 1.8*	50 mins	18 mins		

6.9.3 Recommendation for best practice guidance

In designing simply supported two-way slabs for fire, selection of lower aspect ratio is recommended. Based on investigation in the current section, slabs with lower aspect ratio has better load carrying capacity, judging from the trend of mid-span deflection as well as the predicted tensile strain in reinforcing steels.

6.10 Overall summary and conclusion

Structural behaviour of two-way reinforced concrete slabs exposed to ISO 834 (ISO, 1999) fires for three (3) hours is investigated in the current chapter. Influence of parameters such as fire scenario, restraint condition at supports, span-to-depth ratio as well as aspect ratio to the structural performance of the slabs are investigated. Specific findings from the study in this chapter are listed below:

- Investigation on the structural behaviour of two-way reinforced concrete slabs exposed to varying fire scenario further highlight the inconsistencies in defining slab's performance acceptance criteria when temperature domain is used as the indicator. FE model for the slab exposed to Hydrocarbon (CEN, 2002a) fire indicates that the slab failed insulation criteria (temperature at the un-exposed surface exceeding 139 °C) during 97 minutes of exposure and failed load bearing capacity criteria (critical reinforcement temperature of 593 °C) during 44 minutes of exposure. On the other hand, overall trend and magnitude of mid-span deflection indicates the slab survived 180 minutes of exposure
- No definitive conclusion can be drawn on the effect of varying the degree of support restraint stiffness to structural fire response of two-way reinforced concrete slabs studied in the current chapter. Plastic strain in reinforcing steels tend to be higher as the support restraint stiffness increased. This applicable to both translational and rotational stiffness
- Curtailment of top reinforcement does not seem to have noticeable effect to the predicted mid-span deflection. Therefore, provision of top reinforcement's length in accordance to the relevant Eurocode (CEN, 2014) is sufficient for the case of two-way reinforced concrete slabs exposed to ISO 834 (ISO, 1999) fire from below
- With regard to variation of span-to-depth ratio, simply supported slabs with higher span-to-depth ratio (thinner slabs) have better structural fire performance than slabs with lower span-to-depth ratio. Mobilisation of membrane action is found to be more efficient in thinner slabs as compared to slabs with relatively lower span-to-depth ratio (thicker slabs).

- For simply supported two-way slabs, an aspect ratio closest to 1 (square slabs) is recommended. Mobilisation of tensile membrane action is more efficient for square slabs and the predicted tensile strain in reinforcing steels is also small for square slabs as opposed to slabs with aspect ratio greater than 1
- Limiting deflection criteria recommended in BS 476-20:1987 (BSI, 1987) does not give a realistic acceptance criteria for structural behaviour of two-way reinforced concrete slabs under exposure to fires. Magnitude of deflection typically depending on the degree of restraint at supports, with simply supported slabs resulting higher vertical displacement rather than slabs with certain degree of stiffness at supports, which in general resulting very low vertical displacement. In contrast, reinforcing steel's plastic strain tend to be higher for slabs with restraint at support as compared to simply supported slabs

Chapter 7:

Conclusions, recommendations, and further work

7.1 Summary

The work presented in this thesis has been carried out to develop a deeper understanding of the structural behaviour of both one-way and two-way spanning reinforced concrete slabs under exposure to severe heating from below (i.e. fire), and to provide best practice recommendations to structural fire modellers seeking to undertake performance-based structural fire engineering design of concrete buildings. The main goal is to provide inputs and guidance for designing the slabs within structural fire engineering practices through the use of finite element modelling approaches.

None of the research presented in this thesis has considered the potential impacts of spalling on the structural response of fire-exposed reinforced concrete slabs. This is due to the fact that it is not, at present, possible to credibly model heat-induced spalling of concrete, nor to predict the extent of spalling which might be likely for a given concrete mix under a given heating scenario (Maluk, 2014). The research presented in this thesis has therefore been performed under the assumption of a non-spalling concrete mix, either due to concrete mix properties or owing to the addition of a suitable quantity and type of polypropylene anti-spalling fibres.

Current knowledge on the structural fire engineering of reinforced concrete building structures has been reviewed; and the importance of developing a better understanding of how reinforced concrete structures behave during fires has been highlighted, together with a review of the methods currently used for designing such slabs to have adequate ‘fire resistance’.

Available full-scale experimental fire tests on reinforced concrete slabs within the literature have been presented and discussed. The variations between reported results from different testing laboratories are discussed with regard to the applicability and usefulness of these test data for validation of structural fire finite element models. This will serve for future improvements of similar tests as well as for the benefits of subsequent data collected to the structural fire engineering community. In addition, the sensitivity of the predictive performance of finite element models to thermal and

mechanical input data has been interrogated to better understand the respective influences and applicability of the common material thermal and mechanical input parameters, within reasonable ranges, for the predictive performance and variation of response of finite element models for reinforced concrete slabs under a range of support and restraint conditions.

The later chapters of the thesis focus on developing a deeper understanding of the structural behaviour of both one-way and two-way slabs under exposure to severe heating from below with respect to parameters such as heating scenario, support and restraint conditions, reinforcement curtailment lengths, span-to-depth ratios, and aspect ratios. These parameters are considered individually with a view to better understanding the factors that may be critical for modelling and assessing the acceptability of particular concrete design solutions as regards their structural response during fire.

The following sections outline the key conclusions from the work presented in this thesis, under the specific headings: (7.2) Experimental data for model validation, (7.3) Experimental validation of thermal analysis by finite element methods, (7.4) Sensitivity of finite element model predictions to thermal and mechanical input parameters, and (7.5) Design recommendations for reinforced concrete slabs subjected to severe heating from below (including both one-way spanning and two-way spanning slabs). This chapter ends with a brief summary of recommendations for future research, based on the outcomes of the current thesis.

7.2 Experimental data for model validation

The availability of high quality/fidelity experimental fire test data on reinforced concrete slabs (and physically realistic reinforced concrete structural elements and systems in general) is rather limited. Additional experiments are required to provide much-needed data for validation of available finite element models and modelling techniques. In contrast to structural steel elements and building systems, reinforced concrete poses considerably more complex material behaviour in most cases, both at

ambient and at elevated temperatures. Therefore, it is important to have more high quality test data for the benefit of structural fire engineering community.

Measurement of temperature at the surface exposed to fires is crucial with regard to how these readings are taken and consequently reported. Alternatively, measurement of heat fluxes at the surface exposed to fire could potentially provide better 'raw' data to finite element modellers attempting to model heat transfer in concrete.

Extensive modelling and validating of finite element model for the slabs tested by Cooke (2001); Lim and Wade (2002); Rickard et al. (2015); Wang et al. (2016); Zhang et al. (2014) and presented in the current work have led the author to conclude that measurement of reinforcing steel strains would provide the most important data for validating structural finite element models. Claiming that the modelled slabs have failed due to high magnitude of deflection is not necessarily a rational basis for defining 'fire resistance'. Therefore, measurement of reinforcing steel strain at both the top and bottom of the slabs will potentially benefit finite element modellers with regard to validating their model and defining 'failure' for the slabs. It should be noted that accurately measuring steel strains at high temperature is extremely challenging, and development of robust and economical high temperature strain sensors is a key research need in structural fire engineering research.

Performing full scale fire tests of reinforced concrete slabs with restraint at supports remains a challenging task. Only Lin et al. (1989), and more recently Wang et al. (2016), have tested two-way slabs with certain degrees of restraint at the supports, and no other tests appear to have been carried out in the years between these two tests (to the author's knowledge).

7.3 Experimental validation of thermal analysis by finite element methods

It was demonstrated in Chapter 3 (Section 3.6.1) and Chapter 5 (Section 5.3.1, Section 5.3.2, and Section 5.3.3) that considerable differences exist between the predictions of the finite element heat transfer models and the available experimental test data from furnace tests on reinforced concrete slabs. In particular, it appears that properly

reproducing furnace test thermal environments in numerical heat transfer models is a complex problem with a number of important unknowns that are not adequately captured using the recommendations of Eurocode 1 (CEN, 2002a). In contrast, heat transfer by thermal conduction within concrete elements is relatively well captured in available finite element heat transfer models – aside from not capturing the observed thermal plateau in concrete at temperatures in the region of 100 ºC, which is unlikely to be important for capturing the structural fire response in any case.

The modelling presented in this thesis clearly shows that different furnaces impose different thermal exposures on the tested elements, even when the nominal heating of the gas phase within the furnace chamber follows the same standard temperature versus time curve. This has been observed by previous authors (Sanad et al., 2000) and suggests that validation of structural fire models using furnace tests data should be undertaken using the surface temperature of the structural element as the thermal boundary condition for subsequent thermal and structural analysis, rather than the gas phase temperature (either prescribed or measured). This issue is discussed in more detail in Chapter 3 and Chapter 5 of this thesis.

Significant variation of reported temperatures (from fire tests) was observed at the fire exposed surfaces of tested concrete elements, even though the design fires (for instance ISO 834 (ISO, 1999)) were nominally identical. Consistency in the manner in which the severity of heating is produced for the tested specimens is therefore very important to assist the development of numerical heat transfer models.

7.4 Sensitivity of finite element model predictions to thermal and mechanical input parameters

Chapter 3 illustrates the sensitivity of finite element model predictions to various model input parameters. It has been demonstrated via the various analyses presented that varying thermal conductivity within the bounds permitted by Eurocode 2 (CEN, 2004), or the initial moisture content of concrete within physically realistic ranges, does not significantly affect the predicted temperatures or mid-span deflection of simply-supported one-way spanning reinforced concrete slabs, although varying the

initial concrete moisture content has a more pronounced influence on the predictive performance of the models as compared with the thermal conductivity values, all of which is based on models developed by applying material thermal properties recommended by the Structural Eurocodes (CEN, 2005, 2004) which are widely applied within the structural fire engineering community.

With 0% moisture (dry) and 6% moisture, the maximum predicted temperature difference anywhere in the slab was 67 °C through 180 minutes of heating. The provision of lower and upper limit of thermal conductivity values in Eurocode 2 (CEN, 2004) gave a maximum difference in temperature prediction of 47 °C through 180 minutes for the Cooke (2001) slab analysis. Slab heated to temperatures predicted from model assuming 0% moisture (dry concrete) experienced runaway deflection 17 minutes earlier than a similar slab heated with temperatures predicted from model developed with the assumption of 6% moisture in the concrete.

Varying the thermal conductivity values of either upper or lower limit as recommended in Eurocode 2 (CEN, 2004) has no noticeable effect on the deflection behaviour of the slabs. Based on detailed investigations presented in both Chapter 3 and Chapter 5, it is the author's opinion that varying thermal input parameters for the case of two-way slabs would not be any different than the results for one-way slabs; although note that sensitivity studies for thermal input parameters were not performed for two-way slabs due to time and space limitations. However, the sensitivity of temperature inputs to the predictive performance of structural finite element models was studied with the definition of *Case 1 Temperature* and *Case 2 Temperature* (refer Chapter 5).

The concrete thermal expansion properties recommended in the Eurocodes (CEN, 2005, 2004) for both siliceous and calcareous aggregate concrete mixes were found to generally produce the greatest predictions for mid-span deflection, again for the simply-supported, one-way spanning case. As such, models developed with concrete thermal expansion properties recommended by Eurocodes (CEN, 2005, 2004) tend to fail by a limiting deflection criterion of $L/20$ (BSI, 1987) earlier than models developed with other thermal expansion properties, within the range investigated in

the current thesis. For instance, model developed with thermal expansion properties recommended from Structural Fire Protection: Manual of Practice by American Society of Civil Engineers (ASCE, 1992) failed the limiting mid-span deflection criteria (BSI, 1987) at 103 minutes of exposure to ISO 834 (ISO, 1999) fire while model developed with thermal expansion properties as recommended from Eurocodes (CEN, 2005, 2004) failed the criteria at 78 minutes of exposure when modelling slab tested by Cooke (2001) Therefore, design based on mid-span deflections as the fire resistance criterion potentially results in uneconomic design if thermal expansion criteria based on the Eurocodes (CEN, 2005, 2004) are adopted. The influence of varying concrete thermal expansion properties for slabs with restraint at supports potentially different than those with simple supports (applicable to both one-way and two-way slabs). This aspect however, was not investigated in the current work. Therefore, no firm conclusions on this issue can be made.

One challenging aspect of developing finite element models for fire exposed concrete elements and structures lies in adequately defining the tensile and cracking behaviour of concrete. Modelling cracking (or tensile response) in concrete can significantly influence the amount of computational resources required to solve the stiffness matrix in finite element analyses, and consequently can determine whether an analysis is feasible within a reasonable period of time. Defining higher fracture energies, longer stress-free crack displacement lengths, or greater tensile strain limits, all of which refer to the manner in which concrete tensile cracking behaviour is defined in the FE models, will significantly improve both the numerical stability and quantity of computational resources required in performing the analysis. The setback of this method however, as demonstrated in Section 3.7.15 and Section 3.7.2.4 and Section 5.4.1.2, Section 5.4.2.2, and Section 5.4.3.2, is that vertical deflections tend to be under predicted and this sacrifices a certain degree of accuracy in the results. More importantly, it must be emphasized that fracture energy is a material property, which cannot be changed simply to improve numerical stability.

For example, concrete with a characteristic compressive strength of 30 MPa and heated to 500 °C, the stress-free crack displacement widths are approximated as 0.517 mm

and 4.310 mm for fracture energies equal to 150 N/m and 1250 N/m respectively. With regard to the predicted mid-span deflection, the occurrence of runaway deflections delayed at approximately 65 minutes, based on comparison for models developed with fracture energies equal to 150 N/m and 1250 N/m, respectively. While there is no specific guidance on what is the appropriate value for widths of the stress-free crack displacements, it is up to the discretion of the modeller to choose the value. But it must be bear in mind that the use of higher fracture energies will under predict the mid-span deflection, and consequently resulting better fire resistance rating if limiting deflection criteria (BSI, 1987) is set as the performance indicator. All of these conclusions are based on modelling concrete cracking using a smeared cracking approach, as is typical within the structural fire engineering community and as described in Section 3.4.3.

The research in this thesis has also explored the predicted responses from various currently available commercially available finite element software packages; these being SAFIR and LS-Dyna, in addition to ABAQUS, in order to check the variation of response prediction if different finite element softwares are used. With identical thermal and mechanical property inputs (e.g. concrete compressive strength, concrete tensile strength, coefficient of thermal expansion, reinforcing steel yield strength, elastic modulus, as well as reinforcing steel thermal and mechanical properties), it was found that the predicted mid-span deflections are reasonably similar for all software packages, both in term of trend and magnitude, and for both implicit and explicit dynamic analyses (with the exception that explicit dynamic analyses are less prone to numerical instability problems leading to premature termination of the analyses).

Based on all of the points discussed above, it can be concluded that the key issues in modelling the response of reinforced concrete slabs under exposure to severe heating from below lies at defining an accurate temperature load inputs into the models, in order to get a credible response predictions when comparing results from finite element models against experimental test results. Specific recommendations are given in the following sections.

7.5 Recommendations for analysis and design of reinforced concrete slabs subjected to heating from below

The following two sections set out, based on the body of work presented in this thesis, a series of best-practice recommendations for the structural fire analysis and design of reinforced concrete one-way and two-way spanning slabs by finite element analysis.

7.5.1 One-way spanning slabs

Predictive performance of finite element model is sensitive to the defined concrete tensile strength especially for slabs with relatively lower span-to-depth ratio. For instance, modelling slab tested by Rickard et al. (2015) where the span-to-depth ratio= 18.8 in this case, the model could not capture high rate of mid-span deflection during the early stage of heating as witnessed from the test. As it is well known within structural fire engineering community that the high rate of vertical deflection during the early stage of heating is due to thermal bowing of the slabs, investigation in the current thesis (see Chapter 3) suggests that the low rate of mid-span deflection is also interrelated with the tensile crack opening at the slab's mid-depth in an element near central of the slabs. In other words, the inability of the model to produce the tensile crack opening (as a result of thermal bowing) has caused the slab to deflect in a relatively lower rate. The discussion above is suggested based on model developed with concrete tensile (F_t) defined as 10% of the characteristic concrete compressive strength (F_c).

Under a combination of gravity and temperature load, stresses at both the top and bottom of the slabs are compressive, while at mid-depth concrete is in tension. This challenges the applicability of direct use of the classical sectional analysis for the structural design of fire exposed one-way concrete slabs. Whenever possible, finite element analysis should be undertaken. This is due to simple calculation based on classical sectional analysis being crude given the level of complexity of the behaviour of reinforced concrete slabs under exposure to severe heating from below.

Provision of a given length of top steel reinforcement in accordance with the relevant Eurocode (CEN, 2014) and British Standard (BSI, 1997) is generally sufficient for resisting the increase in hogging moment as a result of fire exposure from below. However, depending on the degree of support stiffness, plastic hinges may form at the location where top reinforcement is curtailed. Whenever top reinforcement runs for full length of the slabs i.e. doubly reinforced sections, plastic hinges typically occurred at locations close to supports, but required higher reaction moments to initiate. This further highlights the importance of better understanding the influence of restraint at supports for fire exposed reinforced concrete slabs.

Findings from the current work also suggest that the provision of an additional 15% to 20% length of top reinforcing steel, as recommended by Buchanan and Abu (2017), is likely to be sufficient to cater for the shifting of moment from sagging to hogging as a result of thermal exposure from below, provided detailed studies are performed beforehand to ensure that the chance of plastic hinge formation (as described in the previous paragraph) is minimal. However, having reinforcing steel run for the full span length (i.e. doubly reinforced section) is recommended, based on the current study as it has the least chances for plastic hinges to form. Plastic hinges formation means concrete at the location where the hinges formed has crushed and/or cracked and the reinforcing steel has yielded, which is not an ideal condition for a structural element to continue serving its design purpose.

For simply supported slabs, if load bearing capacity and integrity are set as the structural fire performance criteria, varying the slab's span-to-depth ratio would not influence the fire resistance rating. However, if mid-span deflection is set as the criteria, it was found that thinner slabs (i.e. higher span-to-depth ratios) produce greater deflections compared to their thicker counterparts, and consequently have less 'fire resistance' based on a deflection criterion (further highlighting the inadequacy of deflection criteria for rationally assessing fire resistance ratings).

7.5.2 Two-way spanning slabs

For the case of two-way slabs, findings from the studies presented in Chapter 5 concur with previous research (Bailey and Toh, 2007) suggesting that reinforcing steels along longer spans are more stressed during exposure to fire as compared with shorter spans, as is typical at ambient temperatures. As such, cracks typically propagate along the shorter span during fire. In addition to this, a thorough investigation was presented in Chapter 5 which also suggests that the first crack will occur at the surface which is un-exposed to fire, rather than at the surface exposed to fire. Higher stresses (along the longer span) occur at the un-exposed surface as compared to soffit of the slabs (i.e. the fire exposed surface). Therefore, provision of top reinforcing steels the centre of slabs, for the case of simply supported slabs might be beneficial to delay the tensile cracking in the concrete. Such reinforcement would not typically be needed for ambient temperature design and would represent a structural fire-specific design measure.

Investigation into the structural behaviour of the slabs exposed to varying fire scenarios further highlighted the inconsistencies in defining slabs' performance acceptance criteria when a temperature domain is used as the indicator. The finite element model for the slab exposed to a Hydrocarbon (CEN, 2002a) fire indicated that the slab failed by the insulation criterion (i.e. temperature at the un-exposed surface exceeding 139 °C) after 97 minutes of exposure and failed by load bearing capacity criterion (critical reinforcement temperature of 593 °C) after 44 minutes of exposure. On the other hand, the overall trend and magnitude of mid-span deflection indicates the slab comfortably survived 180 minutes of exposure if neither of these prescriptive acceptance criteria are applied. The question of appropriate acceptance criteria for performance-based design of reinforced concrete slabs is a key future research need if performance-based structural fire design of concrete structures is ever likely to become a reality.

Membrane action mechanism in preserving the load carrying capacity works more efficiently for thinner slabs (i.e. greater span-to-depth ratios) than for thicker slabs; for slabs with simple supports. As a result, better structural performance is found for slabs

with higher span-to-depth ratios if a limiting deflection criterion, as well limiting tensile strain (total mechanical strain) of 2% (Wang et al., 2013), is adopted.

No explicit conclusions can be drawn on the effects of varying the degree of support restraint stiffness on structural fire response of two-way reinforced concrete slabs studied in Chapter 6 of the thesis. Plastic strain in reinforcing steels tended to be higher as the support restraint stiffness increased. This is applicable to both translational and rotational stiffness. On the other hand, mid-span deflections decreased as both translational and rotational restraint increased. However, for slabs with relatively higher restraint stiffness, snap through behaviour was observed. Snap through could lead to catenary mode and high axial tensile forces generated in the slabs (Lim, 2003). If slab's support is not designed to cater for the generated tensile forces then collapse will trigger.

With regard to varying slab's aspect ratio, findings from the studies presented herein concur with the previously reported work by Deeny (2010) and Lim (2003) where slabs with smaller aspect ratios have better structural performance under exposure to severe heating from below. This is due to strength enhancement provided by the slabs due to double curvature bending. Mobilisation of tensile membrane action is more efficient for square slabs and the predicted tensile strain in reinforcing steels is also smaller for square slabs, as opposed to slabs with aspect ratios greater than one.

No definitive conclusions can be drawn on the influence of top reinforcing steels curtailment's length investigated for the case of two-way slabs. The effect of varying the length of top reinforcing steel on the predicted mid-span deflection was minor. This is likely due to yield line mechanism for the case of two-way slabs, which is more complicated to understand as compared to simple flexural mechanism for the case of one-way slabs. More in-depth study (both at experimental and numerical level) are required before any conclusion can be drawn and to provide recommendation on the best practice guidance. At the numerical level, modelling concrete cracks using discrete crack approach potentially able to better capture the influence of varying the length of top reinforcing steels to the slab's structural behaviour as it models concrete

crack closest to reality (Deeny, 2010). Crack paths may be pre-determine where in this case, the crack line shall be specified to occur at the yield line of the slabs.

7.5.3 Acceptance criteria

Both limiting plastic strain in reinforcing steels of 2% as well as limiting deflection criteria of $L/20$ (BSI, 1987) should be used together to give more comprehensive assessment on the structural performance of one-way reinforced concrete slabs exposed to severe heating from below, and consequently providing more accurate fire resistance rating for the slabs. Validation of finite element models presented in Chapter 3 of the thesis suggests that runaway deflection triggered and followed by rupture of reinforcing steels near mid-span and this occurred (rupture of reinforcing steels) when plastic strain (in tensile) reached a value of 2%. Conclusion made here however, based on modelling the concrete tensile behaviour using smeared cracking approach. It is acknowledged that in reality, cracks in concrete is localised in nature rather than smeared (uniformly distributed in an element as assumed in the current study).

In performing structural design for both one-way and two-way spanning slabs under exposure to severe heating from below in accordance to performance-based structural fire design code, it is recommended that tensile plastic strain in reinforcing steels should be limited to 2% in order for the design to be claimed as safe. For the case of simply supported slabs (both one-way and two-way), limiting mid-span deflection of $L/20$ (BSI, 1987) shall also be used together with limiting tensile plastic strain of 2%, depending on whichever occurs first.

7.6 Recommendations for further research

In parallel to advancements in computational methods, experiments and modelling on full frame reinforced concrete structures when exposed to fire is urgently required for a better understanding of the realistic behaviour of reinforced concrete structures under exposure to unwanted fires. The computational studies presented in this thesis have highlighted the significance of the degree of rotational support stiffness for the

structural fire response and consequently attempt to define failure of one-way and two-way spanning reinforced concrete slabs.

Although numerical studies on full frame behaviour exist within the technical literature (Huang, 2010; Law, 2010), these studies typically involve certain levels of simplification such as high fracture energy (i.e. 1250 N/m (Law, 2010)) being assumed to reduce the computational resources required. Finite element modellers face difficulties in obtaining a stable analysis, without premature termination of analysis in modelling even an isolated, single element. Indeed, this issue is not something that is unusual (Buchanan, 2008). As such, modelling a full frame behaviour is very challenging without considerable simplifications.

As an alternative, the use of an explicit dynamic approach in performing the finite element modelling is recommended. However, a solid knowledge and understanding on how explicit dynamic solutions work is crucial before one can interpret the results from models developed using an explicit dynamic approach. No stability condition (i.e. no convergence in solving the nonlinear equations) is required in order for the analysis to perform its calculations, which also means the model will always produce results. Whether the results are accurate or not is a complex issue, which is why the modeller needs to have a good understanding on how solution is obtained from an explicit dynamic analysis scheme. The nonlinear equation formulated is based on dynamic equilibrium, which could possibly imposing *hourglassing* (see Chapter 3). *Hourglass* is a zero energy deformation in an element occurred in explicit dynamic analysis which signals that the response prediction no longer have any scientific meaning.

The extreme scarcity of available of realistic full-scale structural element fire tests, sub-frame fire tests, as well full frame fire tests in reinforced concrete structures presents a serious impediment to demonstrating a credible ability to computationally model the response of a real reinforced concrete structure during fire. Additional tests are needed to make further progress and improve knowledge on the response of reinforced concrete structures under exposure to fires. Full-frame test with varying

scenario such as; (1) fire occurrence in single floor versus multiple floors, (2) fire in a large floor area, which could possible remove the requirement for compartmentation to contain fire in a building, as well as (3) building design configuration for instance flat slab building versus conventional beam-column construction will provide the much needed data for finite element model validation. In the context of element fire tests, it would be interesting and beneficial to have tests on multiple span rather single span beams and/or slabs.

Finally, it is noteworthy that the work presented in this thesis has not, in general, explicitly considered the response of reinforced concrete structures on cooling. This is important aspect of structural response is particularly important in performance-based design when burnout fires are explicitly considered as part of the design process. Section 5.4.3 demonstrated (however briefly) that the response of concrete slabs on cooling was not well captured by the models developed in this thesis, and a great deal of additional research is needed to better understand both the material properties of concrete, under load, during cooling after heating to elevated temperature, and the consequent structural response of concrete structures during burnout fire scenarios. The residual mechanical properties of concrete also warrant additional research, so that post-fire evaluation of concrete structures can be undertaken with confidence.

References

ABAQUS (2012) *Abaqus analysis user's manual*. Dassault Systemes.

Abu, A., Burgess, I. & Plank, R. (2013) Tensile Membrane Action of Thin Slabs Exposed to Thermal Gradients. *Journal of Engineering Mechanics*. 139 (11), 1497–1507.

Ali, F., Nadjai, A. & Tair, A.A. (2009) Experimental and Numerical Study on Performance of Concrete Slabs Subjected to Severe Fire. *9th International IAFSS Symposium*. 9 (January), 1255–1266.

Anderberg, Y. (1986) Modelling steel behaviour. *(LUTVDG/TVBB--3028--SE;Vol.3028)*.

Anderberg, Y., Forsen, N.E. & Aasen, B. (1986) Measured And Predicted Behaviour Of Steel Beams And Columns In Fire. In: *First International Symposium on Fire Safety Science*. 1986 pp. 259–269.

Anderberg, Y. & Thelandersson, S. (1976) Stress and deformation characteristics of concrete at high temperature: 2. Experimental investigation and material behaviour model. *Bulletin No. 54*.p.86.

ASCE (1992) *Structural Fire Protection* T. T. Lie (ed.). (78).

ASTM (1985) *Standard methods of fire tests of building constructions and materials*.

ASTM (2015) Standard Test Methods for Fire Tests of Building Construction and Materials. *ASTM International*.

Baharudin, E., Bisby, L. & Stratford, T. (2016) Modelling the Response of Simply-Supported Two-Way Reinforced Concrete Slabs Exposed to Fire. *Key Engineering Materials*. (711)588–595.

Bailey, C. (2002) Holistic behaviour of concrete buildings in fire. In: *Proceedings of the ICE - Structures and Buildings*. 2002 pp. 199–212.

Bailey, C.., Burgess, I.. . & Plank, R.. (1996) Computer simulation of a full-scale structural fire test. *The Structural Engineer*. 74 (6), 93–100.

Bailey, C. & Toh, W.S. (2007) Small-scale concrete slab tests at ambient and elevated temperatures. *Engineering Structures*. 29 (10), 2775–2791.

Bailey, C.G. (2004) Membrane action of slab/beam composite floor systems in fire. *Engineering Structures*. 26 (12), 1691–1703.

Bailey, C.G. & Ellobody, E. (2009) Fire tests on bonded post-tensioned concrete slabs. *Engineering Structures*. 31 (3), 686–696.

Baker, G. (1996) The effect of exposure to elevated temperatures on the fracture energy of plain concrete. *Materials and Structures*. 29 (July), 383–388.

Bamonte, P. & Felicetti, R. (2012) High-temperature behaviour of concrete in tension. *Structural Engineering International*. 22 (4), 493–499.

Banerjee, D. (2012) *A Study of Thermal Behavior of a Composite Floor System in Standard Fire Resistance Tests*. (October).

Bazant, Z.P. & Prat, P.C. (1988) Effect of Temperature and Humidity on Fracture Energy of Concrete. *ACI Materials Journal*.85 (4) pp.262–271.

Beitel, J. & Iwankiw, N. (2005) Historical Survey of Multi-Story Building Collapses Due to Fire. *Fire Protection Engineering*. 27.

Bisby, L., Gales, J. & Maluk, C. (2013) A contemporary review of large-scale non-standard structural fire testing. *Fire Science Reviews*. 2 (1), 1–27.

British Steel (1998) The Behaviour of a Multi-Storey Steel Framed Building Subjected to Fire Attack. *British Steel*. p.332.

BSI (1987) *BS 476-20:1987: Fire tests on building materials and structures*.

BSI (1997) *Structural use of concrete - Part 1: Code of practice for design and construction*.

Buch, N. & Jahangirnejad, S. (2008) *Quantifying coefficient of thermal expansion values of typical hydraulic cement concrete paving mixtures*. (January).

Buchanan, A. (2008) The challenges of predicting structural performance in fires. In: *Fire Safety Science*. 2008 pp. 79–90.

Buchanan, A.H. & Abu, A.K. (2017) *Structural design for fire safety*. Second edi. Chichester, John Wiley & Sons Ltd.

Building Research Board (1951) *The thermal expansion of concrete*.

CEB (1996) *RC elements under cyclic loading*. London, Thomas Telford.

CEB-FIP (2010) *CEB-FIP Model code 2010 Volume 1*.

CEN (1999) *BS EN 1363-2:1999 Fire resistance tests - Part 2: Alternative and additional*.

CEN (2005a) *Eurocode - Basis of structural design*.

CEN (2002a) *Eurocode 1: Actions on structures - Part 1-2: General actions - Actions on structures exposed to fire*.

CEN (2004) *Eurocode 2 : Design of Concrete Structures - Part 1-2: General rules - Structural fire design*.

CEN (2014) *Eurocode 2 — Design of concrete structures - Part 1-1: General rules and rules for buildings*.

CEN (2001) *Eurocode 3: Design of steel structures-Part 1.2: General rules-Structural fire design*.

CEN (2005b) *Eurocode 4 - Design of composite steel and concrete structures*.

CEN (2002b) *UK National Annex to Eurocode 1 : Actions on structures —Part 1-1: General actions- Densities, self weight, imposed loads for buildings*.

Chen, J., Young, B. & Uy, B. (2006) Behavior of high strength structural steel at elevated temperatures. *Journal of Structural Engineering*. 132 (12), 1948–1954.

Cooke, G.M.E. (2001) Behaviour of precast concrete floor slabs exposed to standardised fires. *Fire Safety Journal*. 36 (5), 459–475.

Cooke, G.M.E. & Latham, D.J. (1987) The inherent fire resistance of a loaded steel framework. *Steel Construction Today*.1.2 pp.49–58.

Dahlblom, O. & Ottosen, N.S. (1990) Smeared crack analysis using generalized fictitious crack model. *Journal of Engineering Mechanics*. 116 (1), 55–76.

Deeny, S. (2010) *The implifications of compartment fire non-uniformity for the membrane action of reinforced concrete slabs*. The University of Edinburgh.

Elghazouli, a. Y., Izzuddin, B. a. & Richardson, a. J. (2000) Numerical modelling of the structural fire behaviour of composite buildings. *Fire Safety Journal*. 35 (4), 279–297.

Ellobody, E. & Bailey, C. (2009) Modelling of unbonded post-tensioned concrete slabs under fire conditions. *Fire Safety Journal*. 44 (2), 159–167.

Feenstra, P.H. & De Borst, R. (1996) A composite plasticity model for concrete. *International Journal of Solids and Structures*. 33 (5), 707–730.

Forth, J.P., Brooks, J.J. & Bingel, P.R. (2003) Movement in a seven storey reinforced concrete frame. *Structures&Buildings*. 156 (2), 131–140.

Fox, D.C.A. (2013) *The Fire Performance of Restrained Polymer-Fibre-Reinforced Concrete Composite Slabs*. The University of Edinburgh.

Gales, J.A. (2013) *Unbonded post-tensioned concrete structures in fire*. The University of Edinburgh.

Gao, W.Y., Dai, J.-G., Teng, J.G. & Chen, G.M. (2013) Finite element modeling of reinforced concrete beams exposed to fire. *Engineering Structures*. (52)488–501.

Gernay, T. (2012) *A multiaxial constitutive model for concrete in the fire situation including transient creep and cooling down phases*. University of Liege.

Gillie, M. (2009) Analysis of heated structures: Nature and modelling benchmarks. *Fire Safety Journal*. (44)673–680.

Gillie, M., Stratford, T. & Chen, J.-F. (2012) Behaviour of a concrete structure in a real compartment fire. *Proceedings of the ICE - Structures and Buildings*. (165)421–433.

Gillie, M., Usmani, A. & Rotter, M. (2004) Bending and membrane action in concrete slabs. *Fire and Materials*. 28 (24), 139–157.

Gillie, M., Usmani, A., Rotter, M. & O'Connor, M. (2001) Modelling of heated composite floor slabs with reference to the Cardington experiments. *Fire Safety Journal*. 36 (8), 745–767.

Gillie, M., Usmani, a. S. & Rotter, J.M. (2001) A structural analysis of the first Cardington test. *Journal of Constructional Steel Research*. 57 (6), 581–601.

Guo, S. & Bailey, C.G. (2011) Experimental behaviour of composite slabs during the heating and cooling fire stages. *Engineering Structures*. 33 (2), 563–571.

Gustaferro, A.H. (1976) *Design of reinforced and prestressed concrete structures for fire resistance*.

Hillerborg, A., Modeer, M. & Petersson, P.E. (1976) Analysis of crack formation and crack growth in concrete by means of fracture mechanics and finite elements. *Cement and Concrete Research*. 6 (6), 773–781.

Hoek, E. & Brown, E.T. (1980) Empirical Strength Criterion for Rock Masses. *Journal of the Geotechnical Engineering Division*. 106 (9) pp.1013–1035.

Huang, Z. (2010a) Modelling of reinforced concrete structures in fire. *Proceedings of the ICE - Engineering and Computational Mechanics*. 163 (March), 43–53.

Huang, Z. (2010b) The behaviour of reinforced concrete slabs in fire. *Fire Safety Journal*. 45 (5), 271–282.

Huang, Z., Burgess, I.W. & Plank, R.J. (2003a) Modeling Membrane Action of Concrete Slabs in Composite Buildings in Fire. I: Theoretical Development. *Journal of Structural Engineering*. 129 (8), 1103–1112.

Huang, Z., Burgess, I.W. & Plank, R.J. (2003b) Modeling Membrane Action of Concrete Slabs in Composite Buildings in Fire. II: Validations. *Journal of Structural Engineering*. 129 (8), 1103–1112.

Huang, Z., Burgess, I.W. & Plank, R.J. (2001) Non-linear structural modelling of a fire test subject to high restraint. *Fire Safety Journal*. 36 (8), 795–814.

International Code Council (2009) *International Building Code (IBC)*.

ISO (1999) *ISO 834-1: Fire resistance tests - Elements of building construction - Part 1: General requirements*.

Issen, L.., Gustaferro, A.. & Carlson, C.. (1970) *Fire Tests of Concrete Members : An Improved Method for Estimating Thermal Restraint Forces*.

K.W.Poh (2001) Stress-strain-temperature relationship for structural steel. *Journal of Materials in Civil Engineering*. 13 (October), 371–379.

Khazaeinejad, P. (2015) *Fundamental solutions for beams, plates, and shells under thermomechanical actions*. University of Edinburgh.

Khoury, G.., Grainger, B.. & Sullivan, P.J.. (1985) Strain of concrete during first heating to 600C under load. *Magazine of Concrete Research*. 37 (133), 195–215.

Kirby, B.R., Lapwood, D.G. & Thomson, G. (1986) *The reinstatement of fire damaged steel and iron framed structures*.

Kirby, B.R. & Preston, R.R. (1988) High temperature properties of hot-rolled, structural steels for use in fire engineering design studies. *Fire Safety Journal*. 13 (1) pp.27–37.

Kodur, V. (2014) *Review Article: Properties of Concrete at Elevated Temperatures*. 2014 pp.1–15.

Kodur, V., Dwaikat, M. & Fike, R. (2010) High temperature properties of steel for fire resistance modeling of structures. *Journal of Materials in Civil Engineering*. 22 (May), 423–434.

Kotsovinos, P. (2013) *Analysis of the structural response of tall buildings under multifloor and travelling fires*.

Lakhani, H., Sharma, A. & Hofmann, J. (2016) *Coupled thermo-mechanical inelastic analysis of reinforced concrete flexural members subjected to fire loads*.

Lange, D. & Boström, L. (2017) A round robin study on modelling the fire resistance of a loaded steel beam. *Fire Safety Journal*. 92 (May), 64–76.

Law, A.H. (2010) *The assessment and response of concrete structures subject to fire*. The University of Edinburgh.

Law, M. (1981) Designing fire safety for steel-recent work. In: *ASCE Spring Convention*. 1981 p.

Lee, J. & Fenves, G. (1998) Plastic-damage model for cyclic loading of concrete structures. *Journal of engineering mechanics*. 124 (8), 892–900.

Li, Y.-H. & Franssen, J.-M. (2011) Test results and model for the residual compressive strenght of concrete after a fire. *Journal of Structural Fire Engineering*. 2 (1), 29–44.

Lie, T.T. & Williams-Leir, G. (1979) Factors affecting temperature of fire-exposed concrete slabs. *Fire and Materials*. 3 (2), 74–79.

Lim, L. (2003) *Membrane action in fire exposed concrete floor systems*. The University of Canterbury.

Lim, L., Buchanan, A., Moss, P. & Franssen, J. (2004a) Computer Modeling of Restrained Reinforced Concrete Slabs in Fire Conditions. *Journal of Structural Engineering*. 130 (12), 1964–1971.

Lim, L., Buchanan, A., Moss, P. & Franssen, J.-M. (2004b) Numerical modelling of two-way reinforced concrete slabs in fire. *Engineering Structures*. 26 (8), 1081–1091.

Lim, L. & Wade, C. (2002) *Experimental Fire Tests of Two-Way Concrete Slabs*.

Lin, F.B., Bazant, Z.P., Chern, J.C. & Marchertas, A.H. (1987) Concrete model with normality and sequential identification. *Computers and Structures*. 26 (6) pp.1011–1025.

Lin, T.D. & Abrams, M.S. (1981) Simulation of Realistic Thermal Restraint During Fire Tests of Floor and Roof Assemblies. *PCA R&D Publication No. SP80-1*.

Lin, T.D., Zwiers, R.I., Shirley, S.T. & Burg, R.G. (1989) Fire test of concrete slab reinforced with epoxy-coated bars. *ACI Structural Journal*.86 (2).

Livermoore Software Technology Corporation (2012) *LS-Dyna keyword user's manual*.II (February).

Lubliner, J., Oliver, J., Oller, S. & Onate, E. (1989) A plastic-damage model for concrete. *International Journal of Solids and Structures*. 25 (3), 299–326.

Malhotra, H.. (1978) Some noteworthy fires in concrete structures. In: *Proceedings of The Congress-Federation Internationale De La Precontrainte*. 1978 London. pp. 86–98.

Maluk, C. (2014) *Development and Application of a Novel Test Method for Studying the Fire Behaviour of CFRP Prestressed Concrete Structural Elements*. The University of Edinburgh.

Maluk, C., Law, A. & Torero, J.L. (2016) Thermal boundary conditions when fire testing concrete. In: *Proceedings of the Ninth International Conference Structures in Fire*. 2016 pp. 209–216.

Meacham, B., Park, H., Engelhardt, M., Kirk, A., et al. (2010) Fire and Collapse , Faculty of Architecture Building , Delft University of Technology : Data Collection and Preliminary Analyses. In: *8th International Conference on Performance Based Codes and Safety Design Methods*.

Morris, W., Read, R. & Cooke, G. (1988) *Guidelines for the construction of fire-resisting structural elements*. BRE Press.

Ndon, U.J. & Bergeson, K.. (1995) Thermal expansion of concretes: case. *Journal of Materials in Civil Engineering*. (7), 246–251.

Nielsen, C. V. & Bicanic, N. (2003) Residual fracture energy of high-performance and normal concrete subject to high temperatures. *Materials and Structures*. (36)515–521.

Outinen, J. (2006) Mechanical properties of structural steels at elevated temperatures and after cooling down. *Fire and materialsconference, San Francisco, USA*. (February 2006).

Papaioannou, K. (1986) The conflagration of two large department stores in the centre of athens. *Fire and Materials*. 10 (3–4) pp.171–177.

Purkiss, J. & Li, L. (2013) *Fire Safety Engineering Design of Structures*. 3rd edition. CRC Press.

Rickard, I., Maluk, C., Bisby, L. & Deeny, S. (2015) Predictive Testing for Heat-Induced Spalling of Concrete. *IABSE Conference Geneva, Structural Engineering: Providing Solutions to Global Challenges*. 929–936.

Salse, E.A.B. & Gustaferro, A.H. (1971) Structural capacity of concrete beams during fires as affected by restraint and continuity. In: International Council for Building Research (ed.). *5th CIB Congress*. 1971 Rotterdam. pp. 199–204.

Sanad, A.M., Lamont, S., Usmani, A.S. & Rotter, J.M. (2000) Structural behaviour in fire compartment under different heating regimes-Part 2: (Slab mean temperatures). *Fire Safety Journal*. 35 (2), 117–130.

Schneider, U. (1988) Concrete at high temperatures – A general review. *Fire Safety Journal*. 1355–68.

Selvaggio, S.. & Carlson, C.. (1967) *Restraint in fire tests of concrete floors and roofs*.39.

Usmani, A.S. & Cameron, N.J.K. (2004) Limit capacity of laterally restrained reinforced concrete floor slabs in fire. *Cement and Concrete Composites*. 26 (2), 127–140.

Vecchio, F.J. & Tang, K. (1990) Membrane action in reinforced concrete slabs. *Canadian Journal of Civil Engineering*. 17 (5) pp.686–697.

Vollum, R.L., Moss, R.M. & Hossain, T.R. (2002) Slab deflections in the Cardington in-situ concrete frame building. *Magazine of Concrete Research*. 54 (1), 23–34.

Wang, G. (2006) *Performance of reinforced concrete flat slabs exposed to fire*. The University of Canterbury.

Wang, Y., Dong, Y., Yuan, G. & Zou, C. (2015) New Failure Criterion to Determine the Load Carrying Capacity of Two-Way Reinforced Concrete Slabs. *Advances in Structural Engineering*. 18 (2), 221–235.

Wang, Y., Dong, Y.L., Li, B. & Zhou, G.C. (2013a) A fire test on continuous reinforced concrete slabs in a full-scale multi-story steel-framed building. *Fire Safety Journal*. (61)232–242.

Wang, Y., Dong, Y.L., Li, B. & Zhou, G.C. (2013b) A fire test on continuous reinforced concrete slabs in a full-scale multi-story steel-framed building. *Fire Safety Journal*. (61)232–242.

Wang, Y., Dong, Y.L. & Zhou, G.C. (2013) Nonlinear numerical modeling of two-way reinforced concrete slabs subjected to fire. *Computers and Structures*. (119)23–36.

Wang, Y., Yuan, G., Huang, Z., Lyv, J., et al. (2016) Experimental study on the fire behaviour of reinforced concrete slabs under combined uni-axial in-plane and out-of-plane loads. *Engineering Structures*. (128)316–332.

Yu, J., Yu, K. & Lu, Z. (2012) Residual fracture properties of concrete subjected to elevated temperatures. *Materials and Structures*. 45 (8), 1155–1165.

Zhang, B. & Bicanic, N. (2001) Fracture energy of high performance concrete at temperatures up to 450C. *Proceedings of The Fourth International Conference on Fracture Mechanics of Concrete and Concrete Structures*. 461–468.

Zhang, D., Dong, Y. & Fang, Y. (2014) Behaviour of full-scale two-way simply supported concrete slabs in fire. *Magazine of Concrete Research*.66 (16) pp.836–844.